

**Climate change and glacier retreat in
the French Pyrénées: implications for
alpine river ecosystems**

by

KIERAN KHAMIS

A thesis submitted to the University of Birmingham

for the degree of

DOCTOR OF PHILOSOPHY

School of Geography, Earth and Environmental Sciences

College of Life and Environmental Sciences

University of Birmingham

Nov 2013

UNIVERSITY OF
BIRMINGHAM

University of Birmingham Research Archive

e-theses repository

This unpublished thesis/dissertation is copyright of the author and/or third parties. The intellectual property rights of the author or third parties in respect of this work are as defined by The Copyright Designs and Patents Act 1988 or as modified by any successor legislation.

Any use made of information contained in this thesis/dissertation must be in accordance with that legislation and must be properly acknowledged. Further distribution or reproduction in any format is prohibited without the permission of the copyright holder.

Abstract

Climate change disproportionately threatens alpine river ecosystems due to the strong connections between cryosphere, hydrology and physicochemical habitat. Our general understanding of how these systems will respond to warming is, however, based on conceptual models derived from studies undertaken at relatively small spatial scales. This research utilizes: (i) field data collected from five glacierized river basins in the French Pyrénées; (ii) field based experimentation; and (iii) climate/hydrological modelling, to improve understanding of alpine river ecosystem change.

Despite a linear, harsh-begin, physicochemical habitat gradient running from high to low meltwater (snow and ice) contribution, observed benthic macroinvertebrate community level metrics were unimodal (i.e. mid-meltwater peak). Community assembly processes shifted from niche filtering/stochastic (trait convergence) at high meltwater sites, to limiting similarity/stochastic (trait divergence) at low meltwater sites. Benthic macroinvertebrate community structure, feeding interactions and body size spectra were altered when invertebrate predator range expansion was experimentally simulated.

Empirical observation (space for time substitution) and statistical modelling both suggest an increase in reach scale diversity (alpha) is likely as glacier cover is lost. However, a reduction in habitat heterogeneity is likely to lead to biotic homogenization (reduced beta diversity) as a specialist high meltwater community is replaced by a more generalist community. The need to consolidate monitoring strategies is highlighted and functional trait profiles are suggested as useful bio-monitoring tools for detecting future change.

Acknowledgements

Over the past three and half years I have received support, advice and assistance from many people and organisations to whom I am extremely grateful.

First and foremost I would like to thank my supervisors: Professor Sandy Milner; Professor David Hannah; and Dr Lee Brown (University of Leeds), for their continued support and guidance throughout the writing of this thesis. Despite their lofty titles they never minded getting their hands dirty in the field or carrying a heavy pack which was greatly appreciated.

I thank the Parc National des Pyrénées for permission to work in the study area. Dr. Regis Céréghino (University of Toulouse) for supplying vital ethanol, sharing taxonomic expertise and liaising with the Parc. Claude Trescazes for supplying a seventies static caravan ('the lab') at much reduced rates, giving me vital freezer space beside all the Pain au raisins and keeping the pression flowing after days of rough camping.

I am grateful for the company and field assistance that a number of undergraduates from the University of Birmingham provided. I must give special thanks to Lawrence Bird, Faye Jackson and Robert Senior for their hard work and campstove cooking skills. I am also indebted to Megan Klaar and Deb Finn for field assistance and Rebecca Radcliffe for helping me sort and id the hundreds of Surber samples collected. Richard Johnson deserves a special mention for his logistical and technical support; without his help sourcing equipment, calibrating sensors and designing the mesocosm channels, this research would not have been possible. Mel Bickerton also provided vital support in the laboratory for all things bug related and Gillian Kingston gave useful advice regarding water chemistry analysis.

I also thank Stefan Rimkus and Dr. Simone Fatichi for support and advice regarding TOPKAPI catchment simulations; Simon Wilde for downloading the RCM data; and MeteoFrance for supplying meteorological records, in particular Thomos Buffon who had to put up with my appalling French.

The numerous people in GEES and room 325 who made me feel welcome deserve a mention but there are too many to name! I would, however, like to thank Dr. Phil Blaen for sharing his GIS knowledge (and endless cake supply) and Grace Garner for advice on R and all things hydrological.

The EU provided the funding for this research through an FP7 project (ACQWA) for which I am extremely grateful.

Finally I thank Emma Rixon for always being there and putting up with my late night 'graphing' and my family for always supporting me and enjoying discussions (sometimes heated) about Science, Politics and everything in-between.

Table of contents

1. CHAPTER 1 INTRODUCTION	1
1.1. Research rationale.....	2
1.1.1. <i>Environmental change and alpine river ecosystems</i>	2
1.1.2. <i>Monitoring change in alpine river ecosystems</i>	4
1.1.3. <i>Predicting responses to change in alpine river ecosystems</i>	4
1.1.4. <i>ACQWA project</i>	6
1.2. Research gaps	7
1.3. Research aim and objectives	11
1.4. Thesis structure.....	14
1.5. Chapter summary.....	16
2. CHAPTER 2 STUDY REGION	17
2.1. Study region	18
2.1.1. <i>Geography and topography</i>	18
2.1.2. <i>Climate of the Pyrénées</i>	18
2.1.3. <i>Geology of the Pyrénées</i>	20
2.1.4. <i>Vegetation of the Pyrénées</i>	20
2.2. Glaciers of the Pyrénées.....	21
2.3. Study catchments.....	24
2.3.1. <i>Study region and river basin selection</i>	24
2.3.2. <i>Taillon-Gabiétous basin</i>	28
2.3.3. <i>Ossoue basin</i>	32
2.3.4. <i>Vignemale basin</i>	36
2.3.5. <i>Tromouse basin</i>	40
2.3.6. <i>Néous basin</i>	43
2.4. Chapter Summary.....	46
3. CHAPTER 3 THE PHYSICOCHEMICAL HABITAT TEMPLATE OF ALPINE GLACIER-FED RIVER SYSTEMS: METHODS FOR MONITORING ENVIRONMENTAL CHANGE.....	47
3.1. Introduction	48
3.2. Methods.....	53
3.2.1. <i>Study region</i>	53
3.2.2. <i>Physicochemical habitat sampling</i>	56
3.2.3. <i>Glacier cover and Glaciation Index (Jacobsen and Dangles)</i>	59
3.2.4. <i>Glaciation Index (Ilg & Castella)</i>	60
3.2.5. <i>Water sources and mixing model</i>	60

3.2.6.	<i>Statistical analysis</i>	62
3.3.	Results.....	64
3.3.1.	<i>Glaciation Index</i>	64
3.3.2.	<i>End-members and hydrograph separation (water sources)</i>	64
3.3.3.	<i>Spatial and temporal patterns in glacier influence</i>	67
3.3.4.	<i>Physicochemical habitat patterns along the glacier influence gradient</i>	72
3.3.5.	<i>Physicochemical habitat – glacier influence relationships</i>	75
3.3.6.	<i>Relationship between methods</i>	87
3.4.	Discussion	89
3.4.1.	<i>Spatial and temporal patterns in methods for measuring glacial influence</i>	89
3.4.2.	<i>Relationship between glacial influence and important biological variables</i> ..	91
3.4.3.	<i>Interaction between glacier influence and habitat characteristics</i>	94
3.4.4.	<i>Concordance between methods for glacier influence</i>	95
3.5.	Conclusions	96
3.6.	Chapter summary.....	98
4.	CHAPTER 4 DISTURBANCE CONCEPTS PREDICT AQUATIC BIODIVERSITY RESPONSE TO ALPINE GLACIER RETREAT	99
4.1.	Introduction	100
4.2.	Methods.....	104
4.2.1.	<i>Field location</i>	104
4.2.2.	<i>River water source contribution and physicochemical data</i>	106
4.2.3.	<i>Biological sampling and processing</i>	107
4.2.4.	<i>Data analysis</i>	108
4.3.	Results.....	111
4.3.1.	<i>Physicochemical habitat</i>	111
4.3.2.	<i>Taxonomic patterns and diversity</i>	111
4.4.	Discussion	122
4.4.1.	<i>Physicochemical characteristics of the meltwater stress gradient</i>	122
4.4.2.	<i>Assemblage composition and beta diversity</i>	123
4.4.3.	<i>Diversity and abundance patterns along the meltwater stress gradient</i>	124
4.5.	Conclusion.....	128
4.6.	Chapter summary.....	131
5.	CHAPTER 5 BIOLOGICAL TRAITS, FUNCTIONAL DIVERSITY AND COMMUNITY ASSEMBLY PROCESSES IN ALPINE RIVER SYSTEMS	133
5.1.	Introduction	134
5.2.	Methods.....	138
5.2.1.	<i>Field location</i>	138

5.2.2.	<i>Physicochemical data and watersource contribution</i>	140
5.2.3.	<i>Biological sampling and processing</i>	140
5.2.4.	<i>Biological traits</i>	140
5.2.5.	<i>Data analysis</i>	141
5.3.	Results.....	147
5.3.1.	<i>Biological traits</i>	147
5.3.2.	<i>Relationship between traits and habitat patterns</i>	149
5.3.3.	<i>Relationships between traits and meltwater contribution</i>	150
5.3.4.	<i>Functional diversity and meltwater contribution</i>	155
5.4.	Discussion	158
5.4.1.	<i>Biological trait patterns and relationship to meltwater contribution</i>	158
5.4.2.	<i>Functional diversity and meltwater contribution</i>	162
5.5.	Conclusions	165
5.6.	Chapter summary.....	166
6.	CHAPTER 6 THE POTENTIAL IMPLICATIONS OF PREDATOR RANGE EXPANSION IN ALPINE RIVER ECOSYSTEMS: AN EXPERIMENTAL APPROACH USING STREAMSIDE MESOCOSMS	168
6.1.	Introduction	169
6.2.	Methods.....	173
6.2.1.	<i>Study site and experimental channels</i>	173
6.2.2.	<i>Experimental design</i>	175
6.2.3.	<i>Data analysis</i>	177
6.3.	Results.....	181
6.3.1.	<i>Taxonomic composition of channels</i>	181
6.3.2.	<i>Effects of P. grandis on invertebrate abundance and structure</i>	183
6.3.2.	<i>Effects of P. grandis on feeding guild structure</i>	185
6.3.3.	<i>Consumptive and non consumptive effects of P. grandis</i>	187
6.3.4.	<i>Body size spectrum</i>	191
6.4.	Discussion	195
6.4.1.	<i>Impacts of P. grandis on macroinvertebrate abundance and structure</i>	195
6.4.1.	<i>Impacts of P. grandis on feedingguild structure</i>	195
6.4.2.	<i>Consumptive and non consumptive effects of P. grandis</i>	197
6.4.3.	<i>Body size spectrum</i>	200
6.5.	Conclusion.....	201
6.6.	Chapter Summary.....	203

7. CHAPTER 7 HEAT EXCHANGE PROCESSES AND THERMAL DYNAMICS OF A GLACIER FED, ALPINE STREAM	204
7.1. Introduction	205
7.2. Methods.....	208
7.2.1. <i>Field site</i>	208
7.2.2. <i>Data collection</i>	209
7.2.3. <i>Calculation of energy budget</i>	211
7.2.4. <i>Water temperature model</i>	214
7.2.5. <i>Statistical analysis</i>	216
7.3. Results.....	217
7.3.1. <i>Micro-climate, discharge and water temperature patterns</i>	217
7.3.2. <i>Water column and streambed thermal patterns</i>	221
7.3.3. <i>Heat budget</i>	223
7.3.4. <i>Water temperature model</i>	230
7.4. Discussion	233
7.4.1. <i>Thermal dynamics</i>	233
7.4.2. <i>Heat exchange processes</i>	234
7.4.3. <i>Modelled water temperature</i>	237
7.5. Conclusions	238
7.6. Chapter summary.....	239
8. CHAPTER 8 A FUTURE SCENARIO OF WATER SOURCE DYNAMICS, RIVER FLOW AND STREAM WATER TEMPERATURE: IMPLICATIONS FOR BENTHIC COMMUNITIES IN ALPINE GLACIERIZED CATCHMENTS	240
8.1. Introduction	241
8.2. Methods.....	246
8.2.1. <i>Field site</i>	246
8.2.2. <i>Hydro-meteorological variables</i>	248
8.2.3. <i>Regional climate model</i>	249
8.2.4. <i>Bias correction</i>	249
8.2.5. <i>Hydrological model</i>	250
8.2.6. <i>Logistic air-water temperature regression model</i>	253
8.2.7. <i>Calibration and validation of models</i>	255
8.2.8. <i>Ecological implications</i>	256
8.3. Results.....	258
8.3.1. <i>Future temperature and precipitation patterns</i>	258
8.3.2. <i>Calibration and validation of TOPKAPI</i>	262
8.3.3. <i>Climate induced hydrological change</i>	265
8.3.4. <i>Calibration and validation of stream water temperature model</i>	270

8.3.5.	<i>Ecological responses-taxa abundance changes</i>	273
8.4.	Discussion	276
8.4.1.	<i>Catchment model calibration and performance</i>	276
8.4.2.	<i>Changes in climate and hydrology</i>	278
8.4.3.	<i>Stream temperature model and future predictions</i>	279
8.4.4.	<i>Ecological predictions and implications</i>	280
8.5.	Conclusions	283
8.6.	Chapter summary.....	285
9.	CHAPTER 9 SYNTHESIS AND OUTLOOK	286
9.1.	Introduction	287
9.2.	Synthesis	287
9.2.1.	<i>Monitoring for change: the glacial river physicochemical habitat template</i> 288	
9.2.2.	<i>Biodiversity, traits and community assembly</i>	292
9.2.3.	<i>Range expansions and biotic interactions</i>	299
9.2.4.	<i>Stream temperature dynamics and heat exchange</i>	301
9.2.5.	<i>Modelling river ecosystem change in alpine environments</i>	302
9.3.	Further research avenues.....	307
9.4.	Concluding remarks.....	311

APPENDICES

Appendix 3.1.....Rating curves for all gauging stations during the 2010 field season; (a) G4 pre-flood, (b) G4 post-flood (c),T3, (d) T4,(d) O3, (e) Taillon basin outlet. Regression coefficients are displayed in each panel (all curves are of the form: $y = ax^b$).

Appendix 3.2.....Mean hydrograph separation uncertainty estimates for each site during the 2010 and 2011 field seasons. Following Genereux (1998) uncertainty (95% confidence) ,was proportioned between the end members (Melt: Meltwater and GW: Groundwater) and the errors associated with analysis (River). SD is displayed in parentheses.

Appendix 3.3.....Daily mean air temperature and daily total precipitation records for the Gavarnie Meteo France station Highlighted are the spring periods prior to the 2010 and 2011 summer field campaigns.

Appendix 3.4.....Time series of meteorological variable recorded as the AWS located in the Taillon basin with the ‘cold’ Taillon hydrochemistry sampling period highlighted. Net shortwave radiation for (a) 2010 and (b) 2011; air temperature for (c) 2010 and (d) 2011; atmospheric pressure for (e) 2010 and (f) 2011; and precipitation for (g) 2010 and (h) 2011. All records are 15min averages except precipitation which are 15min totals.

Appendix 3.5.....Residuals from the Linear mixed models for (a) minimum water temperature and (b) mean water temperature.

Appendix 4.1.....Study site locations and reach scale physicochemical characteristics (T_w = water temperature, PFAN = Pfankuch Index, SSC = suspended sediment concentration and EC = electrical conductivity). Subscript _s denotes hillslope channels.

Appendix 4.2.....Mantel tests results for regression model residuals and distance between sites(m). The test determines if the Euclidean distance matrices for each variable are correlated and the significance calculated from 999 permutations.

Appendix 4.3.....Analysis of deviance results for geology as an interaction term in the regression models. A significant increase in deviance implies geology is an important explanatory variable.

Appendix 5.1.....Trait list for the most common taxa (n = 51). Coding follows Tachet (2002) except Chironomidae which have been adapted from Snook (2000).

Appendix 5.2.....Correlations (RV coefficients) between all the biological traits recorded. Only significant correlations ($P < 0.05$) are displayed. *P*-values were estimated via a permutation procedure with 999 repeats.

Appendix 5.3.....Logistic regression results for the occurrence of selected traits in response to meltwater proportion. All *P* values are corrected to control for the false discovery rate (FDR) associated with multiple statistical test (* = $P < 0.05$, ** = $P < 0.01$, *** = $P < 0.001$).

Appendix 6.1.....Length – mass regression equations. All equations are in the form $f(x) = \ln A + B \ln x$, where A and B are constants, x body length (mm) and $f(x)$ is body mass (mg).

Appendix 6.2.....Macroinvertebrate abundance (ind m²) recorded in control and treatment mesocosm channels. Functional feeding group (FFG): Gra = grazing algivore; Col = collector/gatherer; Fil = filter feeder; and Pre =predator (* those deemed large bodied predators).

Appendix 6.3.....Mean \pm SE macroinvertebrate drift (ind. 24hr⁻¹) recorded from the control and treatment channels for: (i) date A (10-11 July); (ii) date B (18-19 July); and (iii) date C (26-27 July).

Appendix 8.1.....GAM models based on glacier cover in the catchment and (a) *P. grandis* (b) *Simulium* spp. (c) *Leuctra* spp. (d). *D. latitarsis*, and *Rhithrogena* spp.

Appendix A..... Khamis, K., Hannah, D.M., Hill, M., Brown, L.E., Castella, E., Milner, A.M., 2013. Alpine aquatic ecosystem conservation policy in a changing climate. *Environmental Science & Policy*.

List of figures

- Figure 1.1.** (a) Hypothetical responses of runoff magnitude to changes in glacier volume and (b) melt season flow regimes associated with three stages (A,B,C) along a continuum of glacier retreat (adapted from Milner *et al.* 2009). 3
- Figure 1.2.** The climate–hydrology–ecology cascade for alpine glacierized river basins (after Hannah *et al.* 2007). 5
- Figure 1.3.** Spatiotemporal scale of current understanding (grey shading) and knowledge gaps to be investigated (black shading) for (a) watershed-ecology relationships; and (b) stream water temperature process understanding in alpine river systems In (a) dashed lines represent the scale at which current research has investigated links between ecology and other measure of glacier influence (e.g. distance from glacier); in (b) dashed lines represents studies focused on stream thermal pattern as opposed to processes. 8
- Figure 1.4.** The harsh-benign habitat template for alpine river ecosystems. Adapted from Brown *et al.* (2007b). 10
- Figure 1.5.** Spatiotemporal study scale adopted in the subsequent research chapters. 13
- Figure 1.6.** Thesis structure solid lines represent links between chapters, dotted lines represent the three study scales. Chapter 3-5 large(r)/coarse(r) spatial scale; Chapter 6-7 small(er)/fine(r) spatial scale and Chapter 8 inter-decadal temporal scale. 15
- Figure 2.1.** Map of the Pyrénées with the major peaks highlighted. 19
- Figure 2.2.** Location of all remaining glaciers in the Pyrénées. Numbers correspond to individual glaciers or glaciated massifs with multiple glaciers (see Table 2.1). The grey dashed line represents the French-Spanish border and black circles settlements. The elevation colour ramp is as Figure 2.1. 21
- Figure 2.3.** Study region; Hautes-Pyrénées, France. 25
- Figure 2.4.** Location of the five study basins in the Parc National des Pyrénées. Grey dashed line represents the French-Spanish border, solid black lines the river network and red the basin location. The numbers correspond to the basin name see Table 2.2 for names and basin characteristics. 26
- Figure 2.5.** Hypsometric curves, basin altitude-basin area, for: (a) Taillon-Gabiétous; (b) Vignemale; (c) Ossoue; (d) Tromouse; and (e) Néous. All frequency distributions were constructed from DEMs of 30m resolution 28
- Figure 2.6.** Map of the Taillon–Gabiétous basin displaying the major topographic features, glaciers (grey shading), river network (solid black lines) and watershed (dashed line).

The numbers correspond to the glacier name (1) Glacier des Gabiétous and (2) Glacier du Taillon.	29
Figure 2.7. Digital elevation model of the Taillon-Gabiétous catchment.	30
Figure 2.8. Map displaying the major topographic features, glaciers (grey shading), river network (solid black lines), lakes (black shading) and watershed (dashed line) for the Ossoue basin. The numbers correspond to glacier names: (3) Glacier d'Ossoue, (4) Glacier du Oulettes and (5) Glacier Petit Vignemale.	33
Figure 2.9. Digital elevation model of the Ossoue catchment.	34
Figure 2.10. Map displaying the major topographic features, glaciers (grey shading), river network (solid black lines), lakes (black shading) and watershed (dashed line) for the Vignemale basin. The numbers correspond to glacier names: (4) Glacier du Oulettes and (5) Glacier Petit Vignemale.	37
Figure 2.11. Digital elevation model of the Vignemale catchment.	38
Figure 2.12. Map displaying the major topographic features, glaciers (grey shading), river network (solid black lines), lakes (black shading) and watershed (dashed line) for the Tromouse basin. The number (6) corresponds to glacier names Glacier Munia.	41
Figure 2.13. Digital elevation model of the Cirque de Tromouse catchment.	41
Figure 2.14. Map displaying the major topographic features, glaciers (grey shading), river network (solid black lines), lakes (black shading) and watershed (dashed line) for the Néous basin. The number (7) corresponds to Glacier las Néous.	43
Figure 2.15. Digital elevation model of the Néous catchment.	44
Figure 3.1. Maps of the study basins with sampling sites marked: (a) Taillon – Gabiétous catchment; (b) Ossoue catchment; and (c) Vignemale catchment. River channels (black lines), glacier ice (grey shading), forest (green shading) and lakes (black shading) are also highlighted.	54
Figure 3.2. Mixing plot for all basins, all dates combined. Boxplots represent stream water samples squares and hexagons represent end members (\pm SD). T G (blue) is Taillon-Gabiétous, O (green) is Ossoue and V (yellow) is Vignemale.	66
Figure 3.3. The relationship between distance from the glacier margin and; (a) the proportion of discharge sourced from meltwater (mean \pm SD) and the $GI_{I\&C}$ (mean \pm SD), and (b) the proportion of glacier cover in the catchment and $GI_{I\&D}$	69
Figure 3.4. (a) GI (Ilg & Castella) and (b) meltwater contribution to bulk discharge recorded for all sampling sites and dates.	71

Figure 3.5. PCA ordination of 12 habitat variables for all sample dates. (a) Vector plot displaying the relationship between all habitat variables within the PC1 and PC2 axes. (b) location of all site-sample dates in ordination space defined by the PC1 and PC2. Site labels represent the centroid for all sample dates. Lines link individual sample dates to the site centroid. D denotes the ordination plot scale (i.e. the sub-grid dimension).....	73
Figure 3.6. Surface plot of (a) meltwater porportion (b) glacier cover and (c) $GI_{J\&D}$ in relation to PC_1 and PC_2	74
Figure 3.7. Discharge time series (15 min average) for: Tourettes gauge G4 during (a) 2010 and (b) 2011; Taillon gauge T3 during (c) 2010 and (d) 2011 and Taillon gauge T4 during (e) 2010 and (f) 2011. Precipitation time series (15 min totals) for the Taillon basin during (g) 2010 and (h) 2011. Discharge time series (15 min average) for: (i) Vignemale gaugeV4 during 2011, (j) Vignemale gaugeV2 during 2011 and (k) Ossoue gauge O3 during 2011. (l) Precipitation time series (15 min totals) for the Ossoue basin. *High flow events significantly greater than displayed axis range. ...	76
Figure 3.8. The relationship between mean standardized daily discharge range and (a) glacier cover in the catchment, (b) mean meltwater contribution at gauging site, (c) GI (Jacobsen and Dangles), and (d) GI (Ilg and Castella).....	77
Figure 3.9. Scatterplots for the relationship between: (a) GI and T_{mean} ; (b) GI and T_{min} ; (c) glacier cover and T_{min} ; (d) glacier cover and T_{mean} ; (e) meltwater proportion and T_{mean} ; (f) meltwater proportion and T_{min} . Fitted line for each plot is a LOESS smoother (span = 0.5).....	80
Figure 3.10. Panels represent fitted models for meltwater contribution by stream for: (a) T_{max} (ANCOVA; Meltwater*Stream, $F = 2.91$, $P = 0.04$); (b) T_{min} (ANCOVA; Meltwater*Stream, $F = 4.1$, $P = 0.02$); and (c) T_{mean} (ANCOVA: Meltwater*Stream, $F = 5.2$, $P = 0.003$). Tour = Tourettes, Vign = Vignemale and Oss = Ossoue). Dashed lines represent 95% confidence bands.....	82
Figure 3.11. Boxplots of habitat variables grouped by geology.....	84
Figure 3.12. Panels represent fitted models for (a) meltwater contribution and response variables (PFAN, EC, SSC and pH) by geology and (b) glacier cover in the catchment by geology. Dashed lines represent 95% confidence bands.....	85
Figure 3.13. Scatter plot matrix for all methods for estimating glacier influence. Fitted line for each panel is a LOESS smoother (span = 0.5). Values in upper panel are Pearsons' product moment correlations (all correlations are significant at $P < 0.01$).....	87
Figure 3.14. Relationship between meltwater proportion and $GI_{I\&C}$. The circles represent water temperature (T_{min} °C) with the radius proportional to the scaled (0-1) water temperature. The red and blue boxes highlight samples from Tourettes (G4) and Vignemale (V4) respectively.....	88

Figure 4.1. Location of the study basins within the Gave de Pau drainage. Grey ellipse outlines represent the drainage areas for each basin and stars represent glaciers (not to scale). The broken dashed line is the French – Spanish border.	105
Figure 4.2. Meltwater-habitat relationships for: (a) mean water temperature; (b) suspended sediment concentration (SSC); (c) bed stability (PFAN); (d) chlorophyll <i>a</i> ; (e) pH; and (f) EC. The solid lines are OLS regression fits and dashed lines represent 95% confidence intervals.	112
Figure 4.3. Generalized additive models (GAM's) for the relationship between meltwater contribution to stream flow and: (a) taxonomic richness; (b) total density (ind m ²); (c) EPT richness; (d) evenness; and (e) predator relative abundance (%). (f) Generalized linear model (GLM) of reach scale beta diversity in response to meltwater contribution. Dashed lines represent 95% confidence intervals.	113
Figure 4.4. Relationship between meltwater contribution to streamflow and: (a) Ephemeroptera relative abundance; (b) Trichoptera relative abundance; (c) Plecoptera relative abundance; (d) Diptera relative abundance;(e) <i>Rhyacophila evoluta</i> density (log ₁₀ (x+1)); (f) <i>Baetis alpinus</i> density (log ₁₀ (x+1)); (g) <i>Protonemura</i> spp. density (log ₁₀ (x+1)); and (h) <i>Diamesa latitarsis</i> gr. density (log ₁₀ (x+1)). All lines of best fit represent GAM's, except c and e which are GLM's. Dashed lines represent 95% confidence intervals.	115
Figure 4.5. Three-dimensional graphs displaying the effect of geology on the meltwater-total abundance linear predictor (upper panel) and the meltwater–beta diversity linear predictor (lower panel). Soft rock corresponds to sites underlain by sedimentary lithology and hard rock those underlain by crystalline lithology.	116
Figure 4.6. Three-dimensional graph displaying the effect of geology on the meltwater – <i>R. evoluta</i> density linear predictor. Soft rock corresponds to sites underlain by sedimentary lithology and hard rock those underlain by crystalline lithology.	117
Figure 4.7. NMDS ordination of log ₁₀ (x+1) transformed community data. Rectangles represent meltwater group centroids and ellipses the 95% confidence limits of the group mean. Arrows represent post-hoc vector fit of reach scale physicochemical habitat variables. All vectors are scaled relative to their correlation coefficient; PFAN (R ² = 0.72, P < 0.001), SSC (R ² = 0.44, P < 0.01), pH (R ² = 0.34, P < 0.01), T _w (R ² = 0.45, P < 0.001 and EC (R ² = 0.25, P < 0.05).....	119
Figure 4.8. Theoretical alpine macroinvertebrate community structure responses during the late melt season: (a) the dominant process controlling community characteristics at the reach scale; and (b) hypothetical community responses along the meltwater (environmental harshness) gradient.	130
Figure 5.1. Location of study basins within the Gave de Pau drainage. Grey ellipses represent the drainage areas for each basin and stars represent glaciers. The broken dashed line is the French–Spanish border.	139

- Figure 5.2.** Fuzzy correspondence analysis results: (a) distribution of taxa on axes F1 and F2 in trait space. The taxa are grouped by order and labels represents the group centroid. (b) Bubble plot for all biological trait modalities in F1 and F2 trait space. The size of square represents trait score on the F1 axis, filled squares are positive scores and open squares negative scores. In both panels d denotes the distance associated with each grid sub-division. 148
- Figure 5.3.** (a) Ordination of environmental variables along RLQ axes F1 and F2. (b) Location of sampling sites along RLQ axes F1 and F2 grouped by meltwater contribution; HMC = high meltwater, MMC = mid meltwater and LMC = low meltwater (label represents group centroid). (c) Bubble plot for all biological trait modalities in RLQ axes space, the size of square represents trait score on the F1 axis, filled squares are positive scores and open squares negative scores. In all panels d denotes the distance associated with each grid sub-division. 151
- Figure 5.4.** Logistic regression (GLM) models for meltwater contribution and the proportion of taxa with an affinity to traits identified as significant by fourth corner analysis. Dashed lines represent 95% confidence intervals. 153
- Figure 5.5.** Linear and polynomial regression models of the relationship between: (a) FD_{ric} and meltwater contribution; (b) QE and meltwater contribution; (c) FD_{ric} and indexed taxonomic richness; and (d) QE and indexed taxonomic richness. For a & b dashed lines represent 95% confidence intervals. For c & d the solid lines represent a 1:1 relationship and dashed line represents a linear regression fit. 156
- Figure 5.6.** Relationship between meltwater contribution and: (a) the standardized effect size (SES) for FD_{ric} ($R^2= 0.31$, $P < 0.01$); and (b) SES for QE ($R^2= 0.41$, $P < 0.01$). The solid line represents the regression model's fit and dashed lines the 95% confidence intervals. Standardized effect size (SES) by meltwater contribution group for: (c) FD_{ric} ; and (d) Rao's QE. Filled circles denote mean SES value and whiskers 95% confidence intervals * $P < 0.05$, ** $P < 0.01$; one-tailed Wilcoxon test. 157
- Figure 6.1.** (a) Experimental channels (b) map showing field site and location of experimental channels 174
- Figure 6.2.** Standardized effect size (Cohen's d) for the difference between treatment and control channels for prey density (ind m^2). Whiskers represent the 95% confidence intervals, with significant one-way ANOVA tests highlighted (** $P < 0.01$, * $P < 0.05$ and $\bullet P < 0.1$). 182
- Figure 6.3.** Non-metric dimensional scaling (NMDS) ordination of abundant taxa from experimental channels. Numbers denote channels (1-4 treatment and 5-8 control). Dashed line represents the convex hull for treatment (black) and control channels (grey). 185
- Figure 6.4.** Standardized effect size (Cohen's d) for the difference between treatment and control channels for (a) functional feeding group density (ind m^2) and (b) functional

feeding group relative abundance. Whiskers represent the 95% confidence intervals and significant one-way ANOVA tests are highlighted ($*P < 0.05$ and $\bullet P < 0.1$)...187

Figure 6.5. Drift propensity (emigration/benthic density) of the most abundant taxa recorded from the mesocosm channels during a 24 26-27 July.	190
Figure 6.6. Violin plots for the length (mm) of <i>B. gemellus</i> recorded in the mesocosm channels. The light grey area represents a kernel density function. The black box and line represent a traditional boxplot and the white dot the median length.	192
Figure 6.7. Body mass (log scale) distributions for (a) the control channels and (b) the treatment channels.	193
Figure 6.8. Mean percentage difference (\pm SE) between treatment (not including <i>P. grandis</i>) and control for the number of individuals in each of the five \log_{10} body mass size classes. Mean and SE calculated from all possible pair-wise comparisons between individual treatment and control channels (for each size class $n=16$). Asterisk denotes significance level: $*P < 0.05$ (Kruskal–Wallis test).....	194
Figure 7.1. Study location with study reach and Gavarnie meteorological station highlighted. The map projection of the larger panel is UTM 31	209
Figure 7.2. River discharge and precipitation time-series for: (a) 2010; and (b) 2011. Water column and stream bed temperature recorded for: (c) 2010; and (d) 2011. Air temperature and snowline altitude for: (e) 2010; and (f) 2011.	220
Figure 7.3. Temperature duration curves of the water column and stream bed temperatures for: (a) 2010; and (b) 2011.....	222
Figure 7.4. Daily total ($\text{MJ m}^{-2}\text{d}^{-1}$) net radiation, net shortwave radiation and net longwave radiation in (a) 2010 and (b) 2011, sensible heat in (c) 2010 and (d) 2011, latent heat in (e) 2010 and (f) 2011, bed heat flux in (g) 2010 and (e) 2011, and daily total energy available for the water column in (i) 2010 and (j) 2011.	227
Figure 7.5. Proportion of all energy gains for: (a) the 2010 sampling period; and (b) the 2011 sampling period.	229
Figure 7.6. Modelled water temperature for selected five day periods during early melt season (a) 2010 and (b) 2011; and late melt season (c) 2010 and (d) 2011.....	232
Figure 8.1. Flow diagram displaying scenario modelling framework. Linkages between climate scenarios, simulation/statistical models, and hydrological/habitat/biota output variables.	244

Figure 8.2. Topographic map of the Taillon– Gabiétous study basin with glaciers and extracted river network (top). Location of gauging stations, river temperature stations and automatic weather station (AWS) 1 and AWS 2 (bottom).....	247
Figure 8.3. Relationship between weekly mean air temperature and water temperature at Site T1. Lines represent logistic functions fitted to data for warming and cooling period to account for hysteresis.	254
Figure 8.4. Mean annual cycle of observed and downscaled air temperature and precipitation for AWS 2 (Taillon-Gabiétous basin).....	259
Figure 8.5. The annual proportion of all precipitation that falls as snow (solid state) between 2000 -2080.	260
Figure 8.6. (a) Simulated mean annual average snow fall and snow melt for the control period and 2061-2080 period. (b) Mean annual snow fall by elevation for the control period (green boxes) and the 2061-2080 time slice (yellow boxes).....	261
Figure 8.7. Observed and simulated daily discharge for the calibration period (June 2010 – June 2011) at gauge T3 (basin outlet).....	264
Figure 8.8. Modelled mean annual hydrographs for site T3 for the control period (1991-2010) and future climate periods.....	266
Figure 8.9. One, 3-, 7-, 30-, and 90-day flow minima (a) and maxima (b) simulated for the basin outlet, T3 (mean ± SE), for the 1991-2010 period (observed climate data used for TOPKAPI simulation) and the 2061-2080 period (REMO RCM projection used for TOPKAPI simulation).....	267
Figure 8.10. Modelled mean monthly total meltwater generation in the Taillon-Gabiétous catchment for the control period (1991-2010) and future climate periods.....	269
Figure 8.11. Change in modelled mean monthly snowmelt (a) and ice melt (b) for the Taillon-Gabiétous catchment relative to the control period (1991-2010).	269
Figure 8.12. Predicted glacier thickness for 2020, 2040, 2060 and 2080 based on REMO RCM climate projections. Solid black lines are 100m contours.....	270
Figure 8.13. Modelled mean weekly air temperatures for: (a) Site G1; and (b) Site T1.	272
Figure 8.14. GAM and logarithmic regression predictions of the abundance (log10) of key taxa based on REMO RCM projections (2010 – 2080) at sites (a) T _{snout} , (c) T1, (e) T2 and (g) G4. Relative proportion of the five taxa at sites (b) T _{snout} , (d) T1, (f) T2 and (h) G4.....	275

Figure 9.1. The four methods for quantifying glacial influence framed in the context of the climate-hydrology-ecology process cascade.....	290
Figure 9.2. A conceptual representation of the abiotic and biotic filters that regulate local taxonomic richness and functional divergence across a gradient of glacial influence. The lowest panel depicts functional divergence of the most abundant taxa in the community, with <i>observed</i> (solid lines) representing the actual divergence, and <i>expected</i> (dashed line) representing the predicted divergence under a random colonization scenario (i.e. null model).	295
Figure 9.3. A conceptual outline of (a) alpine stream habitat parameters and (b) taxonomic and functional diversity (divergence) along a gradient of glacial influence. (c) The community assembly processes operating along the glacial influence gradient (importance of each process is depicted by the relative thickness of the box).	297
Figure 9.4. Schematic representation of the changes in water source, habitat heterogeneity and biodiversity as glaciers retreat and disappear. Loss of high meltwater habitats and associated specialist taxa reduces gamma diversity (γ). Habitat conditions become more homogenous and benign leading to an increase in reach scale diversity (α) but a reduction in between site diversity (β).....	298
Figure 9.5. (a) Hypothetical responses of runoff magnitude to changes in glacier volume and (b) smoothed glacial melt season flow regimes associated with four stages along a continuum of glacier retreat. Scenario D represents glacier loss and a future climate scenario (e.g. post 2050).	305
Figure 9.6. A modified conceptual representation of the linkages between climate-hydrology –ecology. The filtering effect of macro-basin characteristic and potential biotic feedback mechanisms are now highlighted.	306

List of tables

Table 2.1. Location, aspect and dimensions of all remaining glaciers in the Pyrénées.	23
Table 2.2. Study basin area, glacier cover and mean elevation (basin number corresponds to Figure 2.4). Thesis chapter in which data collected from the corresponding river basin is presented is also highlighted.....	27
Table 3.1. Sampling periods and corresponding dates.....	57
Table 3.2. Stream/sampling reach physical habitat characteristics.....	58
Table 3.3. Eigen values and physicochemical variable loadings for PC ₁ -PC ₃ of the non-centred PCA analysis for the calculation of GI _{I&C}	64
Table 3.4. Mean Si concentrations, SD and number of samples for meltwater and groundwater end members.....	65
Table 3.5. Values of the four methods for measuring glacier influence. SD is displayed in parentheses for GI _{I & C} and Meltwater (%).	68
Table 3.6. Eigen values and loadings of 12 measured habitat variables for the retained principal components.....	75
Table 3.7. Gauging site characteristics and flow metrics for the 2011 melt season. Ppn corrected range is the average diurnal discharge range for days when total precipitation was less than 3mm. SD is displayed in parentheses.....	78
Table 3.8. Linear Mixed Model results for the relationship between water temperature metrics (response) and methods for quantifying glacier influence (predictor). Both significant and non-significant coefficients are displayed with standard errors. ***P < 0.001, **P < 0.01, ns = not significant.	81
Table 3.9. The t-values of the regression parameter (beta coefficient) from liner mixed models investigating the relationship between method of measuring glacier influence and physicochemical variables. The significance of the term is displayed ($\hat{P} < 0.1$, *P < 0.05, ** P < 0.001 and *** P < 0.001, ns = not significant).....	83
Table 3.10. One way-mixed effect ANOVA testing the difference in physicochemical variables (EC, pH, SSC and PFAN) between sites of different geology. The random effects were multi-levelled with site nested within year to account for repeated measures at each site. ($\hat{P} < 0.05$, ** P < 0.001 and *** P < 0.001, ns = not significant).	84

Table 3.11. Mixed-effect model (site nested in year) results for the interaction between geology and methods for estimating glacier influence (CP = continuous predictor). * $P < 0.05$, ** $P < 0.001$ and *** $P < 0.001$, ns = not significant.	86
Table 4.1. Summary of the GAM and GLM models for the relationship between meltwater (dependant variable) and community/population level responses. ^{ns} denotes no significant relationship between meltwater and the response variable after controlling the False Discovery Rate (FDR) associated with multiple tests (Benjamini & Hochberg 1995).	114
Table 4.2. Spearman rank correlations between taxa abundances and NMDS axis scores. All correlations are significant at $P < 0.05$ after holm's correction for multiple tests. ...	120
Table 4.3. Macroinvertebrate community abundance and diversity (mean \pm 1 SE) for all sites combined, mid-meltwater contribution (MMC) and low-meltwater contribution (LMC) groups combined and each groups considered independently.	121
Table 5.1. List of the biological traits and modalities (categories) used for analysis in this study. Those modalities marked (<i>Resil</i>) represent resilient traits and those marked (<i>Resis</i>) resistant traits in the context of glacier fed streams.	142
Table 5.2. Summary of the results from the separate ordinations and RLQ analysis. Explained variance (%) is displayed in parentheses.	149
Table 5.3. Results of the "4th Corner Method" on the trait-habitat matrix, where HMC = high meltwater contribution group, MMG = mid meltwater group and LMG = low meltwater group. All r values were significant ($P < 0.05$) following a permutation procedure (999 runs) and Bonferroni correction for multiple comparisons.	152
Table 6.1. One-way ANOVA examining the effect of <i>P. grandis</i> (treatment) on the abundance of potential prey taxa. The standardized effect size (Cohen's d) is presented with associated 95% confidence intervals.	184
Table 6.2. Mean abundance (ind m ⁻²) and relative abundance (%) of functional feeding groups in control and treatment channels (SE is displayed in parentheses) and results of one-way ANOVA examining the effect of <i>P. grandis</i> (treatment) on the relative abundance (arcsin sqrt transformed) and actual abundance of functional feeding groups are also displayed.	186
Table 6.3. Diet of <i>P. grandis</i> nymphs in the Tourettes stream (n = 25) and mesocosm channels (n = 8).	188
Table 6.4. Two-way repeated measure, ANOVA results for the effects of predator treatment, time and the interaction of time and treatment on the number <i>Baetis</i> spp. recorded in 24 hr drift samples. The standardized effect size (Cohen's d) is presented with associated 95% confidence intervals.	189

Table 6.5. One-way ANOVA for the effects of predator treatment on the drift propensity (per capita 24 h drift rate) for date C (July 23-24). The standardized effect size (Cohen's <i>d</i>) is presented with associated 95% confidence intervals.	190
Table 6.6. Mean length (\pm SE in parentheses) of the four most abundant taxa recorded in the end point community. Results from student's t-test are complimented by SES (unbiased estimate of Cohen's <i>d</i>) \pm 95% CI.	191
Table 7.1. Meteorological and hydrological variables measured and instrumentation used.	210
Table 7.2. Descriptive statistics for selected hydrometeorological variables over the 2010 (75 days) and 2011 (80 days) monitoring periods. All values are based on 15 minute averages except incoming shortwave radiation (daily totals) and precipitation (seasonal totals). The coefficient of variation is provided in parentheses.	218
Table 7.3. Summary statistics for water column and stream bed temperatures ($^{\circ}$ C) at AWS (lower site). Standard deviations are displayed in parentheses.	223
Table 7.4. Summary statistics for energy fluxes towards (heat gain) and away (heat loss) from the stream channel during summer 2010 and 2011 (SD = standard deviation).	224
Table 7.5. Mean absolute error (MAE $^{\circ}$ C) and root mean square error (RMSE $^{\circ}$ C) calculated for the simulated stream water temperature.	231
Table 8.1. Data sets used for calibration and validation of TOPKAPI and the logistic water temperature regression model.	252
Table 8.2. Predicted seasonal mean change in air temperature and precipitation (relative to 1991-2010) under the A2b scenario for AWS2 (Taillon-Gabiétous basin). Winter = Oct.- March and Summer = April-Sept.	258
Table 8.3. TOPKAPI melt model parameter descriptions and values for 'best-fit' calibration run.	263
Table 8.4. TOPKAPI calibration and validation for the basin outlet, T3 during calibration; and T2 (below the confluence of the Tourrettes and Taillon streams) during validation. Q _o = observed discharge, Q _s simulated discharge, NSE = Nash Sutcliffe coefficient, RMSE = Root mean square error, RMSD = ratio of RMSE to the Stdev.	265
Table 8.5. Flow summary statistics (Mean \pm SD) for the control and future periods. Q _{mean} is mean annual discharge and date max is the mean Julian day when the annual peak flow occurs.	267
Table 8.6. Current and predicted glacier surface areas (km ²) and relative change, for the Glacier du Taillon and Glacier des Gabiétous.	268

Table 8.7. Calibration and validation results for the air–water temperature logistic regression model and associated model efficiency criteria.	271
Table 8.8. Summary statistics of water temperature model results for sites C and D. % frozen represents the proportion of weeks when temperatures are predicted to be below 0 °C.	273
Table 8.9. Taxa predicted to be ‘winners’ (e.g. range expansion and/or higher abundance) and ‘losers’ (range and abundance reduction) under the post 2040, REMO future climate scenario. Winners and losers were classified as taxa with regression coefficient for GCC > ± 1 S D of the mean.	273
Table 8.10. Validation results for the taxa abundance – GCC regression models.	274

List of plates

Plate 2.1. Glacier du Taillon, August, 2011.....	30
Plate 2.2. Glacier des Gabiétous, August, 2010.....	31
Plate 2.3. Confluence of the Tourettes and Taillon streams	31
Plate 2.4. Taillon stream (1850m a.s.l.) roughly 100m above the confluence with the Tourettes stream, July 2011. The automatic weather station (left) and river flow gauging station (right) are in the foreground.	32
Plate 2.5. The Glacier d'Ossoue looking approximately south-east, July 2011.	34
Plate 2.6. Gauging station at the study catchment outlet, Oulettes d'Ossoue stream, June 2011.	35
Plate 2.7. Bedrock cliff roughly 1km downstream from the snout of Glacier d'Ossoue.	35
Plate 2.8. Vignemale massif facing south, September 2010. The Glaciers are highlighted.	38
Plate 2.9. Gave des Oulettes approximately 2.5km from the glacier looking south, June 2010.	39
Plate 2.10. Flood plain below Oulettes de Gaube looking north, August 2011.....	39
Plate 2.11. Glacier Munia looking south, July 2011.	42
Plate 2.12. Gave des Touyeres looking north from the lip of the cirque floor, July 2011. ..	42
Plate 2.13. The Glacier Las Néous taken from Association Moraine Pyrénéenne de Glaciologie (2009).....	44
Plate 2.14. The Gave d'Arrens at the Néous catchment outlet, September 2010.	45
Plate 2.15. The upper Néous catchment looking roughly east towards Pic Balaïtous, July 2011.	45
Plate 6.1. Mesocosm channels and feeder stream in the foreground.	174

CHAPTER 1

Introduction

1.1. Research rationale

1.1.1. *Environmental change and alpine river ecosystems*

High altitude environments are important repositories of both biodiversity (Diaz *et al.* 2003; Brown *et al.* 2009a) and water resources (Beniston 2012). However, climate change disproportionately threatens mountainous regions due to feedbacks between diabatic processes and the surface energy balance, which manifests in an amplification of regional climate signals (Ohmura 2012). Rates of warming over the last century have been significantly greater than in lowland environments, with observations from some sites 2.0 °C greater than the global mean (Beniston *et al.* 1997; Nogues-Bravo *et al.* 2007; Ohmura 2012). During the same period snow cover extent and glacier volumes have decreased for a number of European mountain ranges (Dyrgerov and Meier 2000, Zemp *et al.* 2006, Grunewald and Scheithauer 2010). This trend of warming temperature and associated cryosphere reduction is predicted to continue and accelerate over the coming century (Stahl *et al.* 2008, Stewart 2009).

Cryospheric shrinkage has recently increased concerns regarding both the future of alpine water resources (Barnett *et al.* 2005) and the threats posed to the multiple components of biodiversity (*sensu* Woodward *et al.* 2010, Bellard *et al.* 2012). Milner *et al.* (2009) conceptualised the changing hydrological regime along a continuum of glacier retreat (Figure 1.1), highlighting a shift from a regime characterized by flow buffering during summer (ice melt) to a more unpredictable regime with rainfall/groundwater sources becoming increasingly important during the summer months as glacier ice mass is lost. Yet our understanding of how such hydrological change will influence alpine river ecosystem patterns and processes is still relatively limited (Hannah *et al.* 2007). In particular, improved

process understanding is required to enable accurate and robust prediction of alpine river hydrological and ecological response to a changing climate.

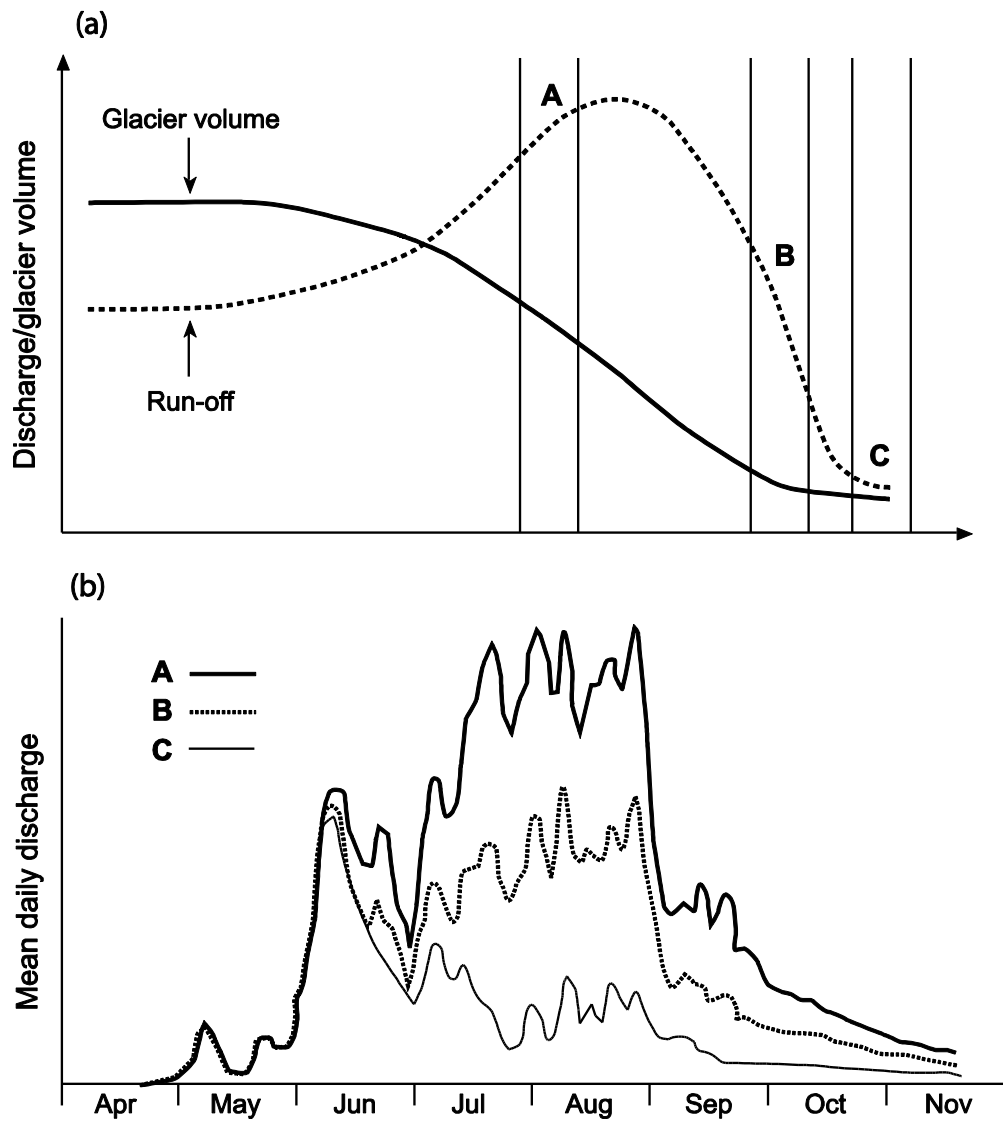


Figure 1.1. (a) Hypothetical responses of runoff magnitude to changes in glacier volume and (b) melt season flow regimes associated with three stages (A,B,C) along a continuum of glacier retreat (adapted from Milner *et al.* 2009).

1.1.2. Monitoring change in alpine river ecosystems

To date multiple approaches have been adopted for monitoring and quantifying glacial influence in alpine river systems. These range from recording glacier cover in the catchment (Füreder 2007; Jacobsen *et al.* 2012) to directly recording water source contributions to bulk discharge, i.e. meltwater:groundwater ratios (Brown *et al.* 2003), and monitoring physicochemical habitat conditions (Castella *et al.* 2001; Ilg & Castella 2006). However, there is a distinct need to consolidate and move forward with more coherent monitoring strategies due to inconsistent approaches (Weekes *et al.* 2012). To do this a rigorous assessment of the relative merits and limitations of each method is required. This becomes particularly important when considering recent calls for the establishment of a global network of monitoring sites, as any such project would need to be based on representative sampling across the range of glacial influence (Milner *et al.* 2009). Without clear guidelines on how to measure glacial influence, inter-site comparisons and meta-analysis is difficult.

1.1.3. Predicting responses to change in alpine river ecosystems

To develop a predictive framework for assessing alpine river ecosystem change a detailed understanding of pattern and process is required, particularly the spatial and temporal scale at which these are represented. Hannah *et al.* (2007) proposed a conceptual process chain linking climate – hydrology – ecology as a framework on which to develop alpine river conservation strategies and model future habitat and biodiversity patterns (Figure 1.2). The idea is that climatic forcing exchange of mass (precipitation) and energy (melt) dictates the cryospheric state, and thus the water source dynamics (i.e. the proportions of flow sourced from snow/ice/groundwater at a given reach and point in time) (Smith *et al.* 2001; Hannah *et al.* 2007). There is a unique physicochemical signal associated with each water source (e.g. glacial meltwater tends to have high turbidity and low water temperature), which can mix in

different proportions to create distinct habitat types (Brown *et al.* 2003). It is this habitat heterogeneity that dictates benthic biodiversity patterns; however, quantification of this approach has been limited (Brown *et al.* 2010b). Therefore, further refinement and testing is required if this framework is to be developed into a predictive tool for alpine river systems.

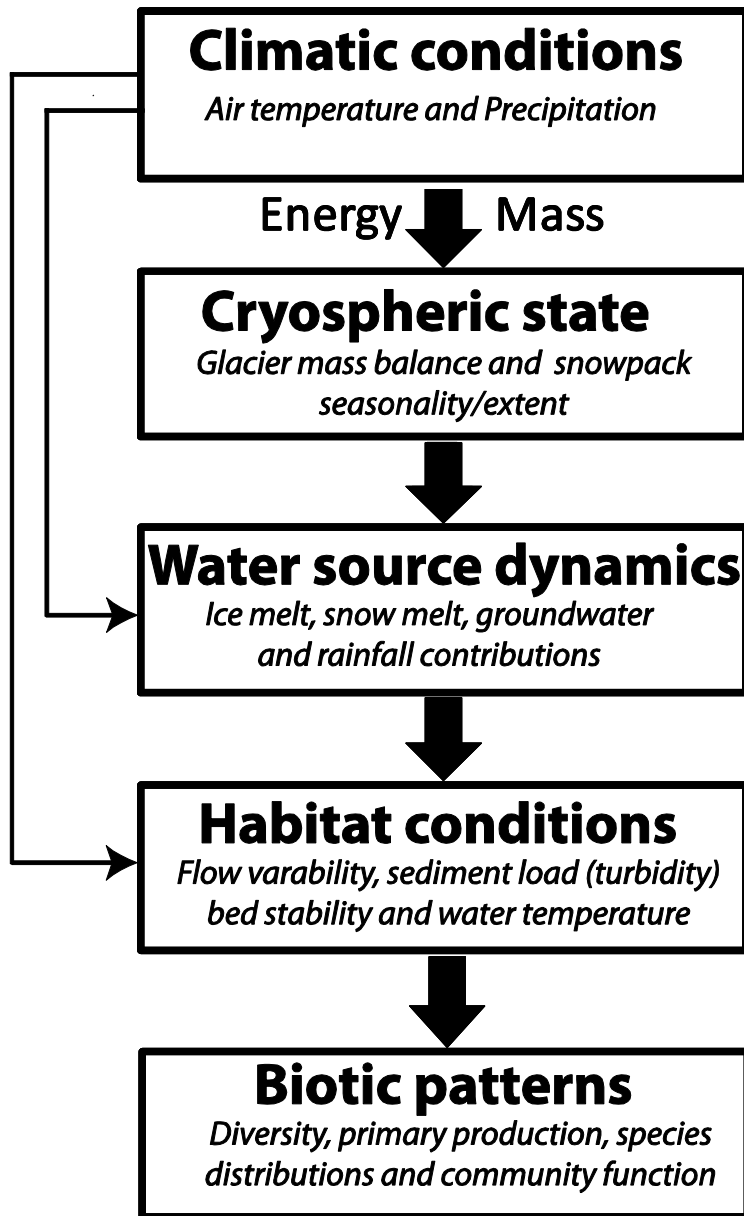


Figure 1.2. The climate–hydrology–ecology cascade for alpine glacierized river basins (after Hannah *et al.* 2007).

The research presented in this thesis focuses on the cascade of processes which link climate to cryosphere to hydrological and ecological patterns and processes. The thesis stems from work undertaken as part of an EU-funded research consortium (see the next section). However, sampling and field experimentation was expanded beyond the consortium goals to address a number of research gaps which are outlined in Section 1.2.

1.1.4. ACQWA project

This thesis is based partly on work that was undertaken as part of the EU-FP7 ACQWA project (Assessing the impacts of Climate on the Quantity and Quality of Water; www.acqwa.ch). This project adopted an inter-disciplinary approach with over 35 partners (climatologists, hydrologists, ecologists and social scientists) to elucidate the impact of climate change on water resources in mountain river systems. The specific ACQWA goals relevant to this thesis are associated with the impacts of climate on running water ecosystems and were as follows:

1. To collect habitat and biodiversity data on test sites to validate predictions from models
2. To develop scenarios for biodiversity changes under climate/ hydrology changes
3. To provide recommendations for conservation strategies of alpine stream ecosystems (see Khamis *et al.* 2013; Appendix A)

The first two objectives listed above directly link with Chapters 4 and 8 respectively.

1.2. Research gaps

Over the last 20 years, a number of studies undertaken in the French Pyrénées by successive teams from the University of Birmingham have advanced significantly our understanding of alpine hydroecology (reviewed in part by Hannah *et al.* 2007). In particular, identifying and quantifying the links between cryosphere – hydrology (water source) - ecology (Smith 1999; Snook 2000; Brown 2005). However, their work has been based on a single glacierized basin, namely the Taillon–Gabiétous, and needs expanding spatially to include other river basins. This would enable identification of patterns and processes that are basin specific and those that can be generalised. Figure 1.3a outlines the spatiotemporal scale on which our understanding of water source-habitat-ecology linkages is based and highlights the scale based research gap to be addressed in this thesis. This will enable reassessment, and if necessary refinement, of current conceptual understanding (Figure 1.4). In a similar vein, Figure 1.3b isolates the scale at which current understanding of alpine stream temperature, a water quality parameter of key biological importance (Webb *et al.* 2008), is based. Here, the temporal scale on which our understanding of heat exchange processes is based is highlighted as a key knowledge gap.

Research into the hydroecological impacts of climate change and cryosphere retreat in alpine river systems has predominately focused on biodiversity patterns at the community and population levels. For example, recent work has assessed both taxonomic (Jacobsen *et al.* 2012) and functional diversity (Ilg & Castella 2006; Brown & Milner 2012) of benthic macroinvertebrate communities. Patterns of individual taxa abundance (Brown *et al.* 2007a; Muhlfield *et al.* 2011) and genetic diversity (Finn *et al.* 2013) have also been investigated. However, work on biotic interactions is limited and has tended to be embedded in systems thinking (Lavandier & Decamps 1984; Clitherow *et al.* 2013) or focused on feeding patterns/interactions of individual taxa (Lavandier & Céréghino 1995; Céréghino 2006). This

knowledge gap is poignant as future scenarios of environmental change are likely to promote altitudinal range expansions of more lowland taxa (Brown *et al.* 2007a), leading to novel interactions. Hence, an understanding of current and likely future interactions is needed to enable more robust predictions of future change to be made. Finally, the predictive potential of the climate cascade framework (Figure 1.2) needs to be quantified (Hannah *et al.* 2007) using future climate scenarios.

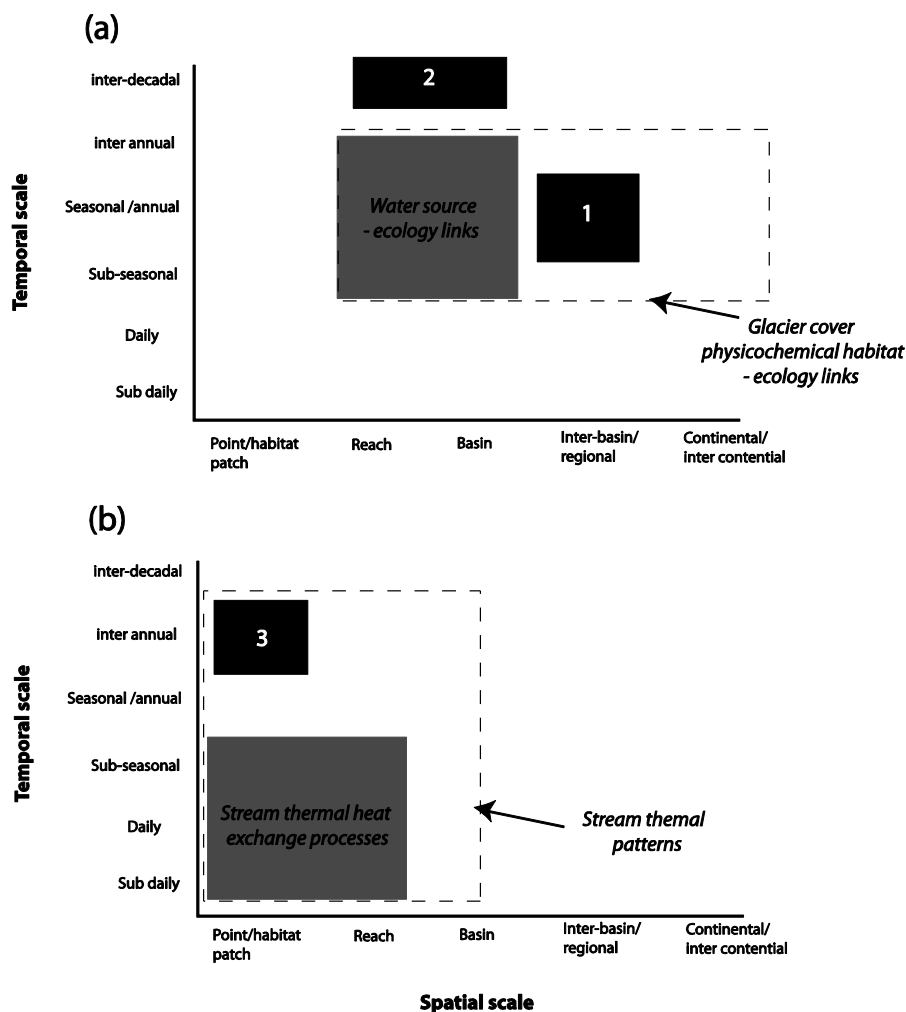


Figure 1.3. Spatiotemporal scale of current understanding (grey shading) and knowledge gaps to be investigated (black shading) for (a) watersource-ecology relationships; and (b) stream water temperature process understanding in alpine river systems. In (a) dashed lines represent the scale at which current research has investigated links between ecology and other measure of glacier influence (e.g. distance from glacier); in (b) dashed lines represents studies focused on stream thermal pattern as opposed to processes.

Following a detailed evaluation of the literature (presented in Chapters 3-8), six broad research gaps were identified:

1. The physicochemical habitat template of alpine river systems has been identified as a key determinant of biotic patterns and, in alpine river systems, is strongly determined by cryospheric processes (Milner *et al.* 2010). However, despite the need for a coherent monitoring framework given the current context of climate change; no rigorous, multi-basin assessment of the multiple methods/approaches for quantifying glacial influence at a given location has been conducted. Furthermore, the potential ‘filtering’ (*sensu* Poff 1997) effect of macroscale basin properties (e.g. bedrock lithology) on the glacial influence – physicochemical habitat relationship has been largely ignored (Weekes *et al.* 2012).

2. While a number of studies have investigated the potential impacts of climate change and cryospheric retreat on biodiversity in alpine river systems (Füreder 2007; Cadbury *et al.* 2011; Jacobsen & Dangles 2012; Jacobsen *et al.* 2012), the quantitative assessments of links between meltwater contribution and biodiversity are scarce (Brown *et al.* 2010b). The few studies that have investigated meltwater-biodiversity relationships were based on single river basins, with the lower portion of the meltwater contribution spectrum not considered (Brown *et al.* 2007a; Mellor 2012). Hence, current conceptual understanding (i.e. alpine harsh-benign habitat template; Figure 1.4) may need refinement when multiple basins or lower meltwater habitats are investigated.

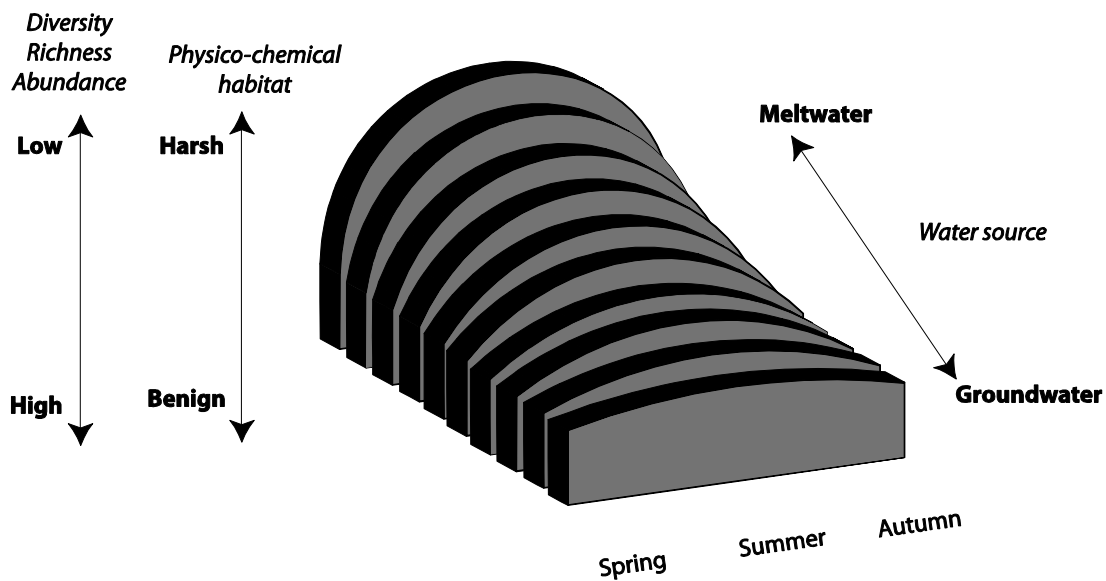


Figure 1.4. The harsh-benign habitat template for alpine river ecosystems. Adapted from Brown *et al.* (2007b)

3. Despite the utility of biological traits for assessing benthic community response to climate change and unravelling community assembly processes (Bonada *et al.* 2007; Poff *et al.* 2010; Brown & Milner 2012) our understanding of habitat – trait and habitat-assembly process, remains limited in alpine river systems (Ilg & Castella 2006; Füreder 2007). Furthermore, the water source (meltwater) habitat template has not been used yet for trait based studies in alpine river systems. This is particularly surprising as the approach can account for both spatial (e.g. tributary attenuation of glacial signal) and temporal (e.g. seasonal evolution of water source dynamics) variations (Malard *et al.* 2000; Hannah *et al.* 2007).

4. Climate change and cryospheric retreat is likely to alter the thermal regimes of alpine river systems (Brown & Hannah 2008; Cadbury *et al.* 2008; Fellman *et al.* 2013). However, to date, few detailed studies of the fundamental processes controlling energy transfer have been carried out in glacier fed rivers, with the exception of Chikita *et al.* (2010) and Magnusson *et al.* (2012a). In neither of these studies were all meteorological variables recorded above or adjacent to the stream channel. Despite the need for longer term monitoring to enable

characterization of year on year variability in heat flux components (Garner *et al.* 2012), both studies were conducted over single summer melt seasons. To date no multi-year studies of heat exchange processes for alpine, glacier-fed streams have been published.

5. Climate induced altitudinal range shifts or expansions have been observed for a variety of species (Pauli *et al.* 2007; Chen *et al.* 2011b). Alpine river systems are particularly sensitive to shifting ranges and distributions due to numerous unique (endemic) taxa, which are often at their range limits (Brown *et al.* 2009a; Engler *et al.* 2011). However, little is known about biotic interactions in alpine streams (Milner *et al.* 2009), in particular how the range expansion of large(r) bodied invertebrate predators may alter community structure through novel trophic/competitive interactions (Gilman *et al.* 2010).

6. Alpine river ecosystems are vulnerable to changes in climate due to the links between cryosphere-physicochemical habitat–hydrology (Hannah *et al.* 2007; Milner *et al.* 2009). Hence, the ability to predict how climatic and hydrological changes will alter benthic habitats and taxa abundances and distributions is important for directing appropriate conservation measures for these threatened ecosystems (Hannah *et al.* 2007). The climate driven process cascade for alpine river ecosystems outlined in Figure 1.1 provides a useful framework for developing hydroecological modelling strategies but has yet to be tested.

1.3. Research aim and objectives

The primarily *aim* of research presented in this thesis is *to improve understanding of how climate-cryosphere interactions shape hydroecological patterns and processes in alpine*

river ecosystems, thus enabling the validation and further development of monitoring strategies and predictive models. As outlined in section 1.1, most research conducted in alpine river systems has focused on pattern, often ignoring process. The research documented in this thesis explores alpine hydroecology at a range of spatiotemporal scales to improve our understanding of coarser/larger (i.e. reach scale between basin) and finer/smaller scale (point/habitat patch scale) pattern and process, thus providing the foundation for inter-decadal predictions of change driven change in alpine river system to be conducted and interpreted. Given the research gaps identified the *specific objectives* of this research were as follows:

1. Identify the relationship between the multiple methods for measuring glacial influence, and their relationship with the physicochemical habitat template, to provide a first roadmap for monitoring alpine hydroecological change (Chapter 3).
2. Assess the mechanisms driving reach-scale community diversity and abundance patterns across multiple alpine glacierized river basins using the water source habitat template (Chapter 4).
3. Investigate the potential implications of glacier retreat for functional (trait) diversity and community assembly processes in alpine river systems (Chapter 5).
4. Elucidate the effect of predation on stream benthic communities in the context of climate change and range expansion (Chapter 6).
5. Quantify the heat-exchange process driving thermal variability at inter-annual seasonal and sub-seasonal scales, and employ a deterministic temperature model as a tool to understand further stream temperature drivers and processes (Chapter 7).

6. Model alpine river ecosystem change in response to a future climate scenario by employing a modified version of the climate cascade (Figure 1.1) research framework (Chapter 8).

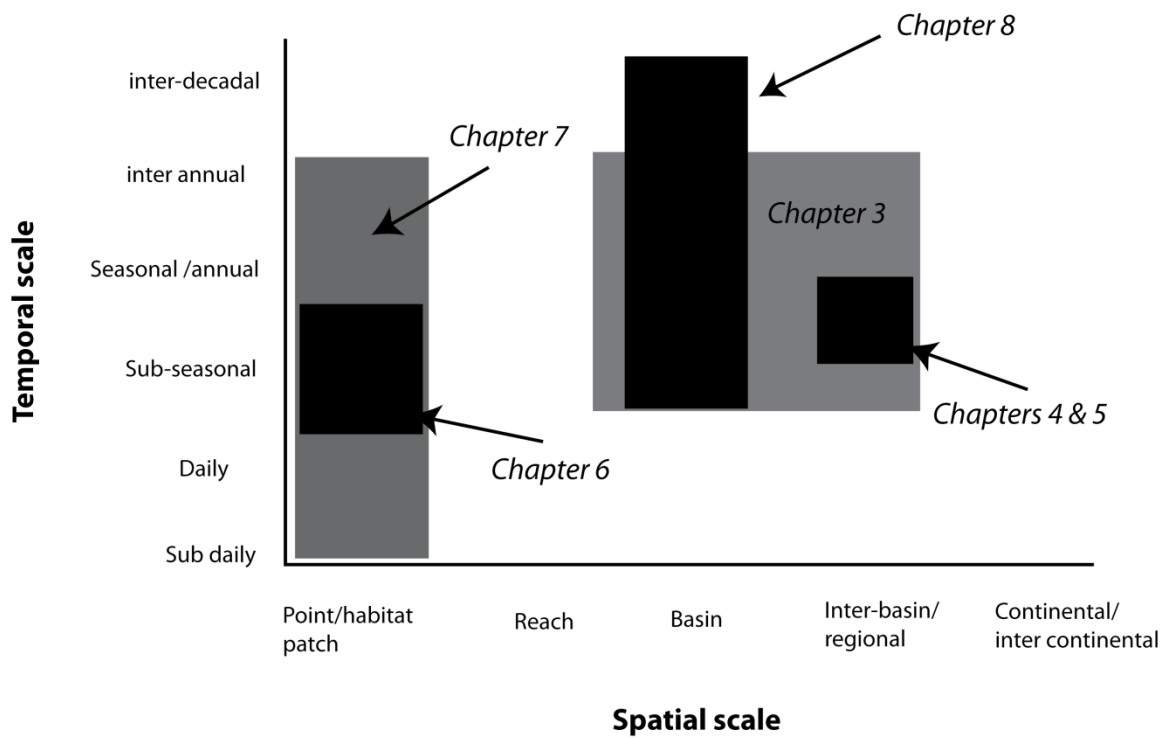


Figure 1.5. Spatiotemporal study scale adopted in the subsequent research chapters.

1.4. Thesis structure

This thesis follows a paper style format with each chapter constituting a methodologically independent piece of research. Therefore, it was appropriate to review the relevant literature in the introduction of each chapter and include a detailed methods section in each. On the occasions when similar methods are adopted, the reader is referred to the relevant chapter in which the method was detailed first. Figures 1.5 and 1.6 provide a schematic outline of the thesis with the spatiotemporal scales of the chapters highlighted.

The study area and research design are introduced in Chapter 2. The physicochemical habitat characteristics of glacial streams in the French Pyrénées are explored in Chapter 3 and the concurrence of methods for monitoring and quantifying glacial influence assessed. A rigorous, inter-basin assessment of benthic habitat and community composition along a gradient of meltwater contribution is presented in Chapter 4. Here, the water source habitat template (harsh-benign) is used to assess mechanisms driving reach scale community diversity patterns, and findings are interpreted in the context of ecological stress/disturbance. Benthic trait composition and functional diversity patterns along a gradient of meltwater contribution are investigated in Chapter 5. Potential climate change ‘indicator’ trait profiles are identified and an insight into community assembly processes in alpine river systems is provided. The implications of climate induced range expansion are investigated experimentally in Chapter 6. Chapter 7 explores inter-annual and sub-seasonal, point scale thermal dynamics and heat exchange processes and employs a simple energy balance model to improve process understanding. Alpine river ecosystem change is the focus of Chapter 8 and (using a modified version of the predictive framework outlined in Figure 1.2) hydrological and ecological patterns are modelled in response to a future climate scenario. Finally, a synthesis of the major findings and suggestions for further research are presented in Chapter 9.

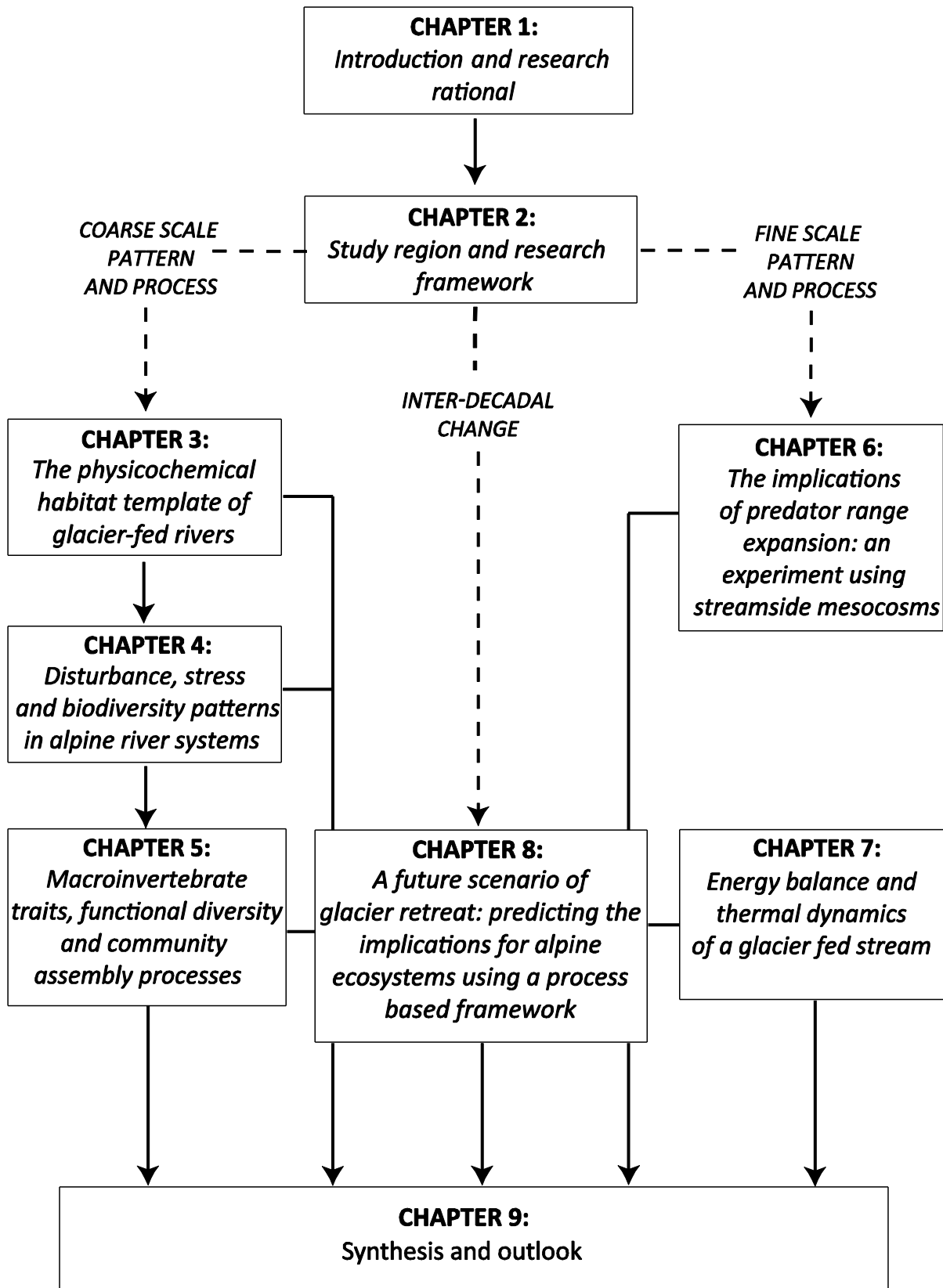


Figure 1.6. Thesis structure solid lines represent links between chapters, dotted lines represent the three study scales. Chapter 3-5 large(r)/coarse(r) spatial scale; Chapter 6-7 small(er)/fine(r) spatial scale and Chapter 8 inter-decadal temporal scale.

1.5. Chapter summary

A background and rationale for the research presented in this thesis has been provided in this chapter. The specific research gaps and objectives to be addressed have been presented and the structure of the thesis outlined. It should be noted that some of the research outlined in this thesis has been submitted to peer-reviewed journals. A Modified version of Chapter 6 has been submitted to *Freshwater Science*. The results from Chapters 3-8 have, in varying forms, been presented at conferences and workshops. Finally, data collected during the 2010/2011 field campaigns, has also led to a further publications in *Environmental Science and Policy* (Appendix A).

CHAPTER 2

Study region

2.1. Study region

2.1.1. Geography and topography

The Pyrénées mountain range is located in Southern Europe (42°-43° N) and spans the isthmus between the Iberian Peninsula and the rest of the European continent (Figure 2.1). The chain runs east–west (1° W-2° E), extending roughly 430km from the Atlantic ocean to the Mediterranean sea. The highest point in the range is Pico de Aneto (3404 m a.s.l), and there are a further 128 peaks above 3000m (Buyse 1993). Currently, roughly 1760km² of the range is considered in the alpine zone (4.5%).

2.1.2. Climate of the Pyrénées

The climate of the Pyrénées displays an eastward transition from Atlantic conditions in the West, to a Mediterranean climate in the east. Hence, the western Pyrénées are characterised by cyclonic precipitation and relatively small summer to winter temperature variations (Del Barrio *et al.* 1990); however, the maritime influence decreases further eastward, where typical Mediterranean conditions (warm and dry) prevail (Gomez *et al.* 2003). In addition to this west–east climatic gradient, a north south gradient is also apparent. The northern (French) slopes of the range are steep and exposed to north-western Atlantic influence, while the southern (Spanish) slopes are generally more gentle and have a warmer exposure. Three critical isotherms have been identified (Del Barrio *et al.* 1990). The lowest is the 0°C mean winter isotherm at 1694m a.s.l. This represents the limit of the ‘high mountain belt’ as above this point there is stable snow cover between December and March. The 10°C mean annual air temperature, located at 2438m a.s.l., represents the potential upper limit of the timber line. Finally, the 0°C mean annual air temperature isotherm is found at 2726m a.s.l. representing the theoretical limit of soil permafrost (Del Barrio *et al.* 1990).



Figure 2.1. Map of the Pyrénées with the major peaks highlighted.

2.1.3. *Geology of the Pyrénées*

In the western Pyrénées the lithology is predominately limestone and shifts through calcareous/siliceous to predominately siliceous rocks in the east. Palaeozoic granites, sandstones and schists were formed during the Variscan orogeny by an underlying axis uplift (Zwart 1986). Some of the highest calcareous peaks in Europe (e.g. Pic Aneto, 3404m) were formed during the early Tertiary when major alpine folding of Mesozoic limestones occurred. Rocks of volcanic origin are patchy across the range and, due to extensive glacial activity above 800m, till deposit, gravel beds and alluvial terraces can be found (Gomez *et al.* 2003).

2.1.4. *Vegetation of the Pyrénées*

The lower limit of the alpine zone is ~2300m; however, fire, grazing and logging has lowered this across much of the mountain chain (Dupias 1985). The vegetation on northern slopes of the central and western Pyrénées is similar to that of the Alps, while southern slopes and eastern sectors are more similar to the Iberian mountains (i.e. sub Mediterranean) (Gomez *et al.* 2003).

The alpine flora of the Pyrénées consists of more than 800 species of which about 10% are endemic (Dupias 1985). A number of distinct habitat zones exist; from the treeline ecotone (*Pinus* spp. and *Juniperus* spp.) through shrub heath (e.g. *Vaccinium* spp. and *Rhododendron* spp.), grassland (e.g. *Festuca* spp. and *Campanula* spp.), scree and rock communities (e.g. *Saxifraga* spp. *Veronica* spp. and *Androscae* spp.) to the snowbed communities (e.g. *Salix* spp. and *Carex* spp.) (Sese *et al.* 1999; Gomez *et al.* 2003).

2.2. Glaciers of the Pyrénées



Figure 2.2. Location of all remaining glaciers in the Pyrénées. Numbers correspond to individual glaciers or glaciated massifs with multiple glaciers (see Table 2.1). The grey dashed line represents the French-Spanish border and black circles settlements. The elevation colour ramp is as Figure 2.1.

There are currently 21 glaciers in the Pyrenees (González Trueba *et al.* 2008) representing the southern limit of contemporary European glaciation (Hannah *et al.* 2007). All glacierized peaks are higher than 3000m and are located in western half of the range (Figure 2.2), occupying a region between Balaïtous and Maladeta (Calvet 2004). The current ice coverage consists of 10 glaciers on the Spanish side (2.6 km²) and 11 in French territory (2.35 km²). The climatic snowline rises from about 2900m in the west to over 3100m in the east (Grunewald & Scheithauer 2010). All glacier termini are at altitudes greater than 2500m (Association Moraine Pyrénéenne de Glaciologie 2009) and are predominately located on

northern and eastern slope (Serrat & Ventura 1993). Unlike the Alps, valley glaciers are absent and most glaciers are small cirques, relics of the Little Ice Age (LIA) maximum when tongues extended up to 2km (González Trueba *et al.* 2008).

During the Holocene the glaciers of the Pyrenees reached their maximum area towards the end of the LIA a period of climatic cooling between 1550 and 1850. During the LIA 20 massifs were glaciated constituting a network of around 115 high mountain cirque glaciers (González Trueba *et al.* 2008). The total ice covered area at the end of the LIA was thought to be 20-40 km². Today some 21 glaciers remain covering an area of roughly 5 km². This retreat has primarily been driven by an increase in air temperature, with changes in precipitation patterns exacerbating or dampening the retreat (Serrat & Ventura 1993). Bücher & Dessens (1991), analysing climate records for an 89 year period (1882-1970), identified a 0.83°C increase in mean temperature. This was due to a large increase in the minimum temperature (+2.11°C). Further analysis of cloud data revealed a 15% increase in annual mean cloudiness during the 89 year period, suggesting increased potential for longwave heating.

Table 2.1. Location, aspect and dimensions of all remaining glaciers in the Pyrénées.

Number	Massif	Glacier	Area (km²)	Aspect	Measurement date
1	Balaïtous (3144m)	Las Néous	0.04	E	2009
2	Enfer (3082)	Enfer Central	0.06	N	2007
3	Vignemale (3298 m)	Oulettes de Gaube	0.13	N	2009
		Petit Vignemale	0.03	N	2009
4	Vignemale (3298m)	Ossoue	0.46	E	2009
5	Gavarnie – Mont Perdu (3355m)	Gabiétous	0.08	N	2009
6	Gavarnie – Mont Perdu (3355m)	Taillon	0.09	N-E	2009
7	Gavarnie – Mont Perdu (3355m)	Pailla Ouest	0.04	N	2000
		Pailla Est	0.05	N	2000
		Astazou	0.06	N-N-E	2000
		Cylindre	0.06	N-E	2007
		Mont Perdu	0.32	N-E	2007
8	Munia (3133m)	Munia	0.04	N-N-W	2007
		Barroude	0.05	N-N-E	2001
9	Posets (3375m)	Llardana	0.09	N-O	2007
		Paoules	0.06	N-N-E	2007
		Posets	0.02	E	2007
10	Perdiguère (3222m)	Gourgs Blancs	0.03	N-N-O	2006
		Seil de la Baque Ouest	0.02	N-N-O	2007
		Seil de la Baque Est	0.11	N-E	2009
		Portillon d'Oô	0.04	N	2009
		Boum	0.06	N-N-E	2009
11	Aneto (3404m)	Maladeta	0.33	N	2007
		Aneto	0.64	N-N-E	2007
		Barrancs	0.08	N-E	2007
		Tempêtes	0.10	N-E	2007

Serrat & Ventura (1993) identified four periods of fluctuation between the end of the LIA and 1980:

1. 1850 – 1905 rapid retreat due to increased air temperature;
2. 1905-1912 slight advance;
3. 1912 – 1950 retreat due to warmer and drier conditions (numerous glaciers disappear);
4. 1950 -1979 stabilisation due to increased precipitation.

A fifth period of rapid retreat can be added running from 1980 to the present day, during which time a number of smaller glaciers disappeared and those remaining lost roughly half their pre-1980 surface area (Serrat & Ventura 1993; Association Moraine Pyrénéenne de Glaciologie 2009).

2.3. Study catchments

2.3.1. Study region and river basin selection

To enable the over arching aim of this research to be addressed it was necessary to select a region with a number of glacier fed river catchments located in relatively close proximity to one another. The Hautes-Pyrénées region, France, in the north-western sector of the mountain chain (Figure 2.3), represented an ideal location as more than 50% of the French Pyrenean glaciers are located within a 30km radius (Figure 2.2). Furthermore, the glacierized catchments are accessible by road or on foot and are all within the Parc National des Pyrénées (i.e. minimal anthropogenic disturbance).



Figure 2.3. Study region; Hautes-Pyrénées, France.

Five glacierized river basins were selected for study in this thesis (Figure 2.4; Table 2.2).

These were chosen to represent;

1. a gradient of glacier size from the Ossoue (glacier cover 0.46 km^2) to the Néous (glacier cover 0.04 km^2);
2. the variable geology of the Pyrénées (i.e. crystalline and sedimentary);
3. a range of basin sizes (Table 2.2);
4. a range of basin hypsometric distributions (Figure 2.5).

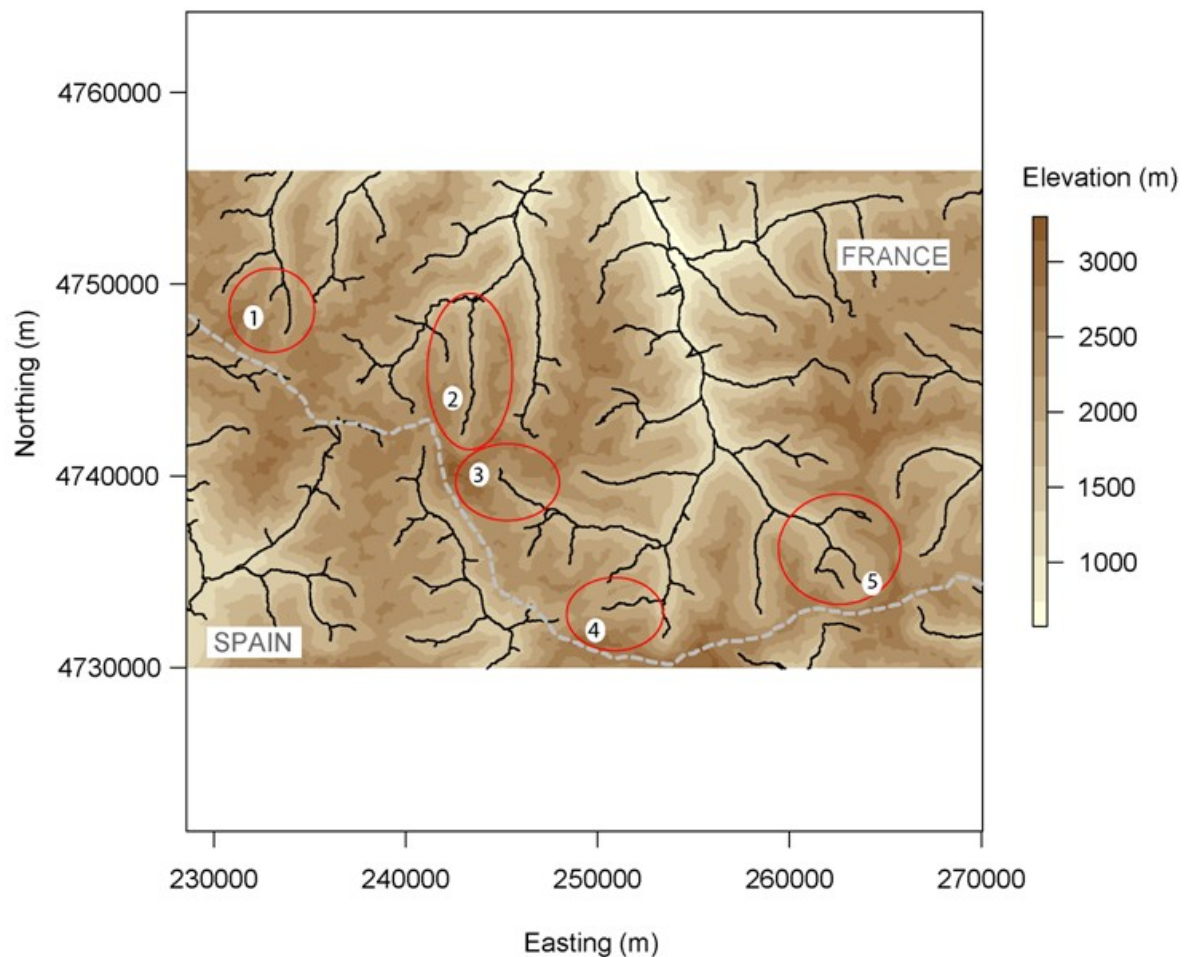


Figure 2.4. Location of the five study basins in the Parc National des Pyrénées. Grey dashed line represents the French-Spanish border, solid black lines the river network and red the basin location. The numbers correspond to the basin name see Table 2.2 for names and basin characteristics.

Table 2.2. Study basin area, glacier cover and mean elevation (basin number corresponds to Figure 2.4). Thesis chapter in which data collected from the corresponding river basin is presented is also highlighted.

Basin	Thesis chapters	Glacier area (km²)	Watershed area (km²)	Geology	Mean (max) elevation
1: Néous	Chapters 4&5	Las Néous (0.04)	10.3	Crystalline	2340 m (3144 m)
2: Vignemale	Chapters 3-5	Oulettes (0.13); Petit Vignemale (0.03)	11.6	Crystalline	2281 m (3298 m)
3: Ossoue	Chapters 3-5	Ossoue (0.46)	8.0	Mixed	2574 m (3298 m)
4: Taillon-Gabiétous	Chapters 3-8	Gabiétous (0.08); Taillon (0.09)	6.7	Sedimentary	2288 m (3144 m)
5: Tromouse	Chapters 4 &5	Munia (0.04)	6.6	Sedimentary	2360 m (3133 m)

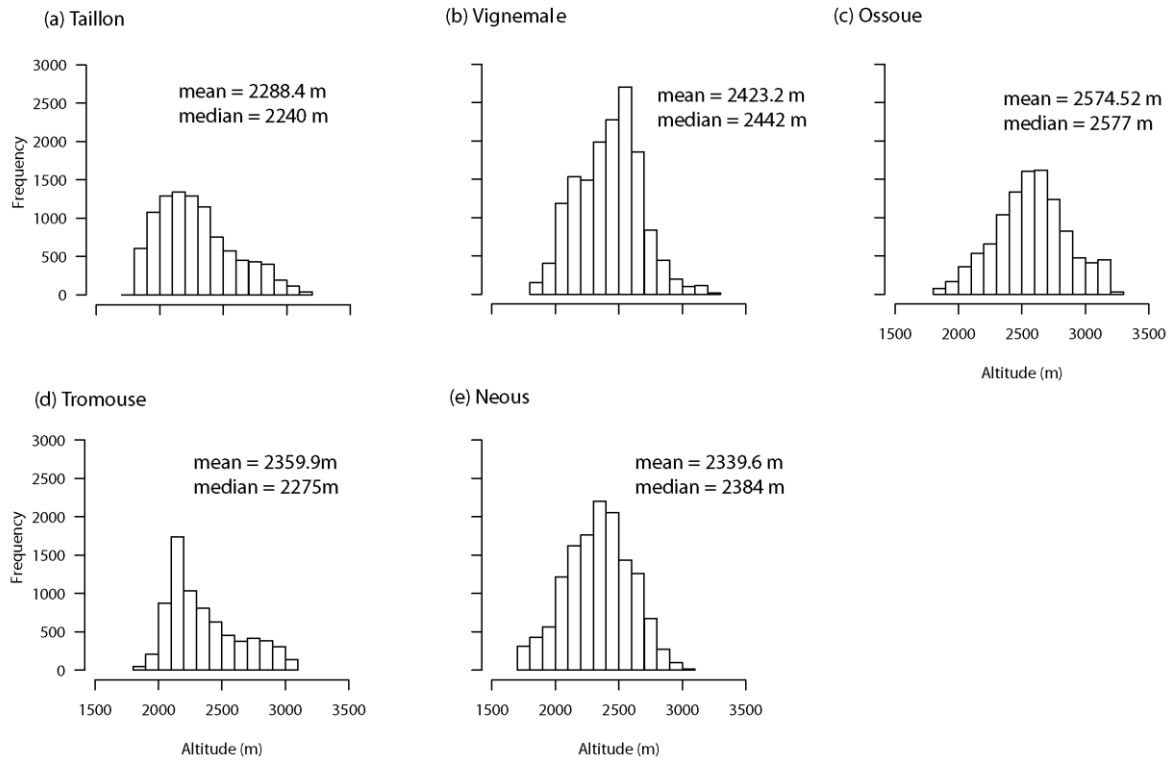


Figure 2.5. Hypsometric curves, basin altitude-basin area, for: (a) Taillon-Gabiétous; (b) Vignemale; (c) Ossoue; (d) Tromouse; and (e) Néous. All frequency distributions were constructed from DEMs of 30m resolution

2.3.2. Taillon-Gabiétous basin

The Taillon-Gabiétous basin, Cirque de Gavarnie (42°42'N, 0°01'W), was chosen as the 'core' research catchment. It has been studied by numerous research teams from the University of Birmingham over the last 20 years, see Hannah *et al.* 2007) for a detailed review, and is accessible by both road (Col de Tentes) and on foot from the nearby village of Gavarnie.

Briefly, the catchment spans an altitudinal range from 1790m to 3144m covering an area of 6.7 km² (Figure 2.6; Figure 2.7). The underlying geology is sedimentary and composed of predominantly sandstone (Marbore sandstone) and limestones (Santonien and Coniacien

series). Vegetation was sparse above 2200m and isolated patches of *Saxifraga* spp. and *Veronica* spp. interspersed a scree matrix. There was significant soil development in the lower basin (<2100m) and on south facing slopes, where grazed alpine meadow and scattered shrubs were present. Ice covered ~3% of the catchment, with two small cirque glaciers (see Plates 2.1 & 2.2), the Glacier du Taillon (0.09 km²) and the Glacier des Gabiétous (0.08 km²), both north facing, feeding the Taillon and Tourettes streams respectively (Figure 2.6). An extensive network of karst springs in the lower basin was primarily sourced from snowmelt on the higher north facing slopes (Parc National des Pyrénées 1991). A further network of hillslope springs, fed by shallow groundwater aquifers, was located on the south facing slopes. A more detailed description of the catchment can be found in Smith *et al.* (2001).

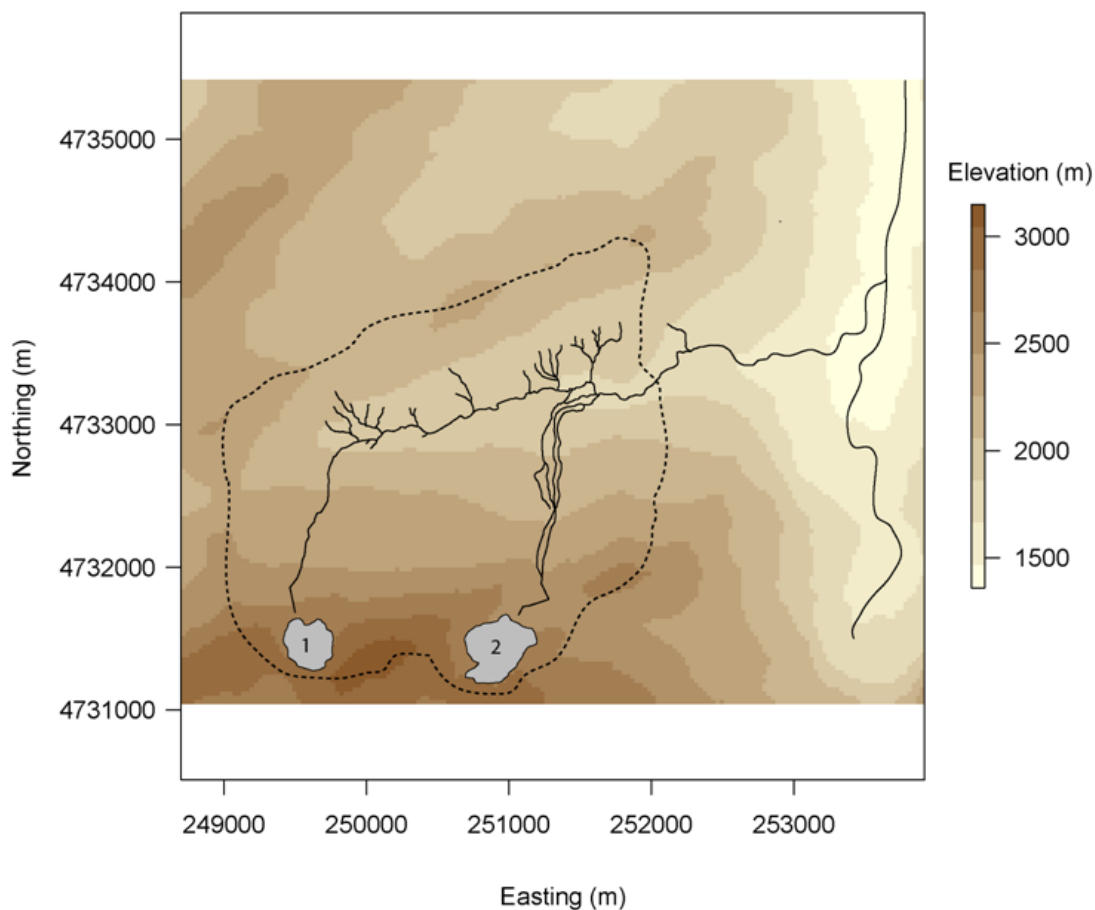


Figure 2.6. Map of the Taillon–Gabiétous basin displaying the major topographic features, glaciers (grey shading), river network (solid black lines) and watershed (dashed line). The numbers correspond to the glacier name (1) Glacier des Gabiétous and (2) Glacier du Taillon.

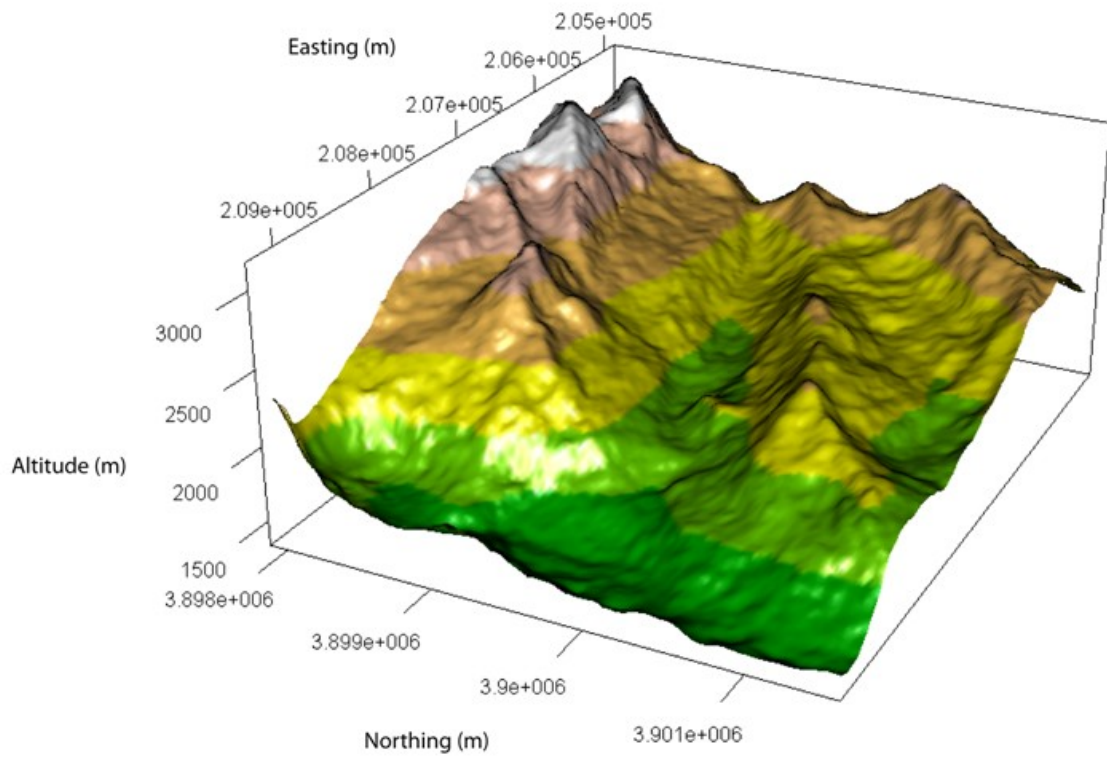


Figure 2.7. Digital elevation model of the Taillon-Gabiétous catchment.



Plate 2.1. Glacier du Taillon, August, 2011.

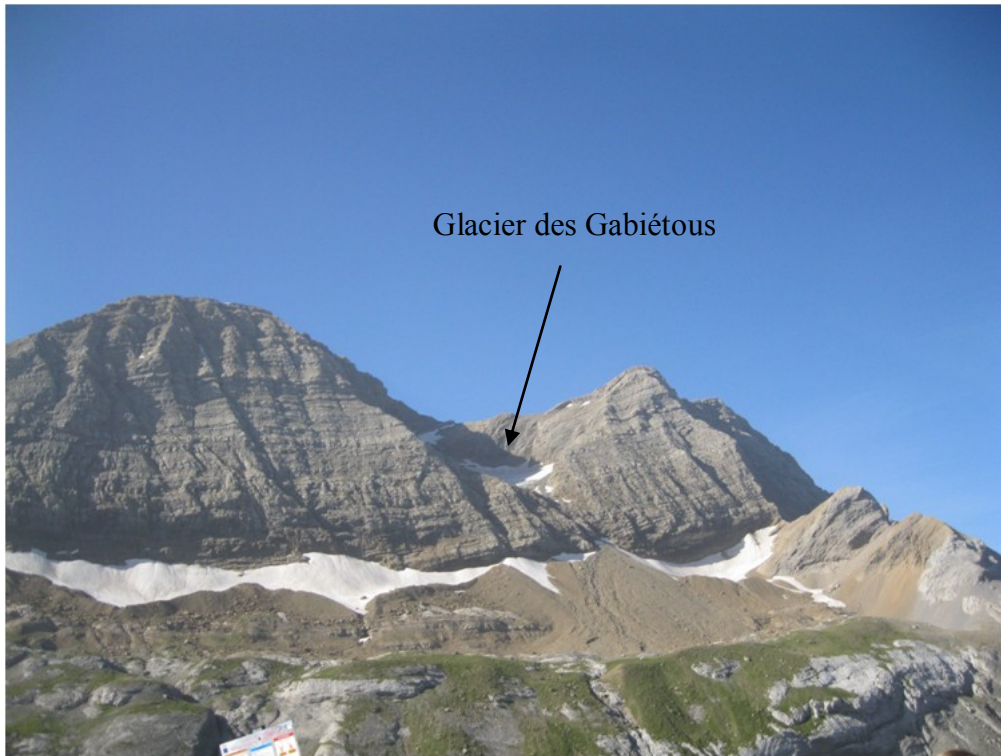


Plate 2.2. Glacier des Gabiétous, August, 2010.



Plate 2.3. Confluence of the Tourettes and Taillon streams.



Plate 2.4. Taillon stream (1850m a.s.l.) roughly 100m above the confluence with the Tourettes stream, July 2011. The automatic weather station (left) and river flow gauging station (right) are in the foreground.

2.3.3. *Ossoue basin*

The Ossoue river basin, 42°45'N, 0°06'W, spans an altitudinal range from 1850m to 3298m and has a catchment area of 8.0km² above the lowest sample point (Figure 2.8; Figure 2.9). Roughly 6% of the catchment is covered by glacier ice with the Glacier d'Ossoue (0.46 km²; Plate 2.5), located on the east facing slope of the Vignemale massif, which provides a major water source for the Oulettes d'Ossoue stream (Plate 2.6). The underlying geology is composed of a mixture of metamorphic (marble limestones) in the upper catchment (Del Río *et al.* 2012) and sedimentary rocks in the lower catchment (Debelmas 1974). Vegetation cover (*Festuca* spp.) and soil development was apparent up to 2400m in the north east of the catchment, where a number of groundwater springs were sourced (Figure 2.8). On the east

facing slopes (Vignemale massif) vegetation and was sparse with skeletal soils interspersing loose scree and exposed bedrock plains.

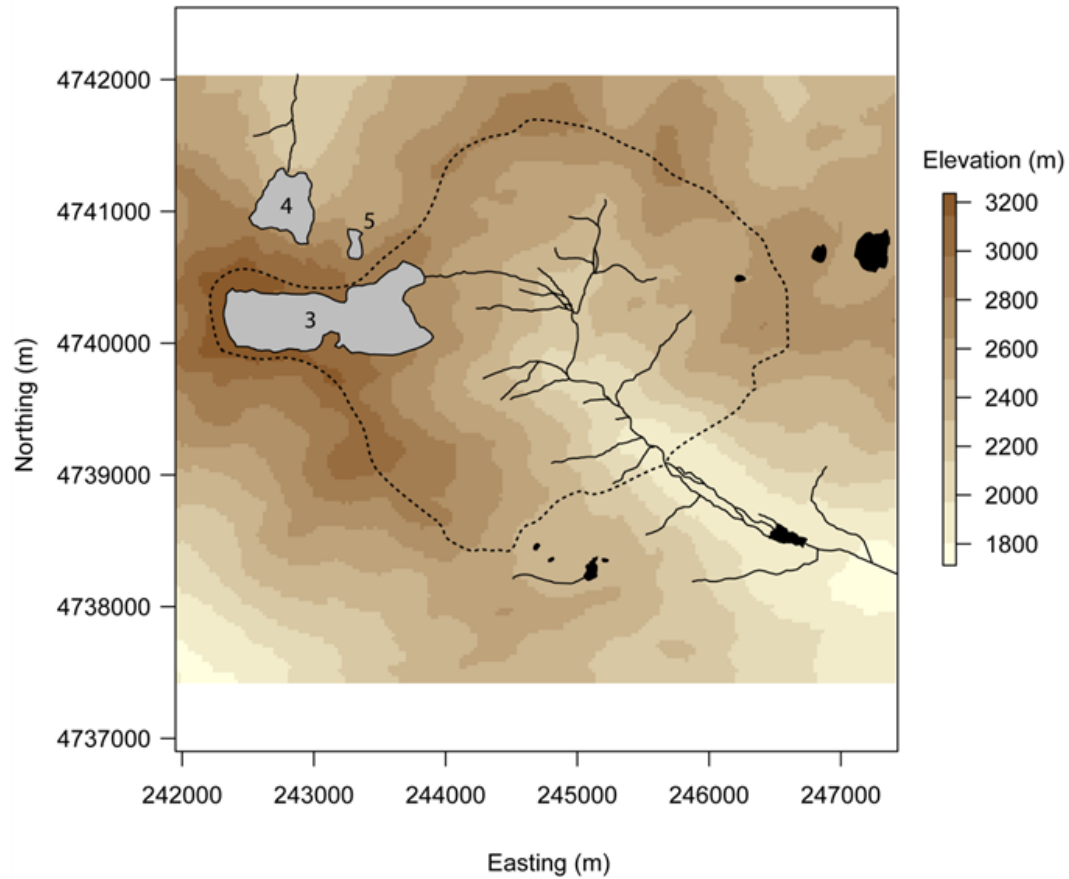


Figure 2.8. Map displaying the major topographic features, glaciers (grey shading), river network (solid black lines), lakes (black shading) and watershed (dashed line) for the Ossoue basin. The numbers correspond to glacier names: (3) Glacier d'Ossoue, (4) Glacier du Oulettes and (5) Glacier Petit Vignemale.

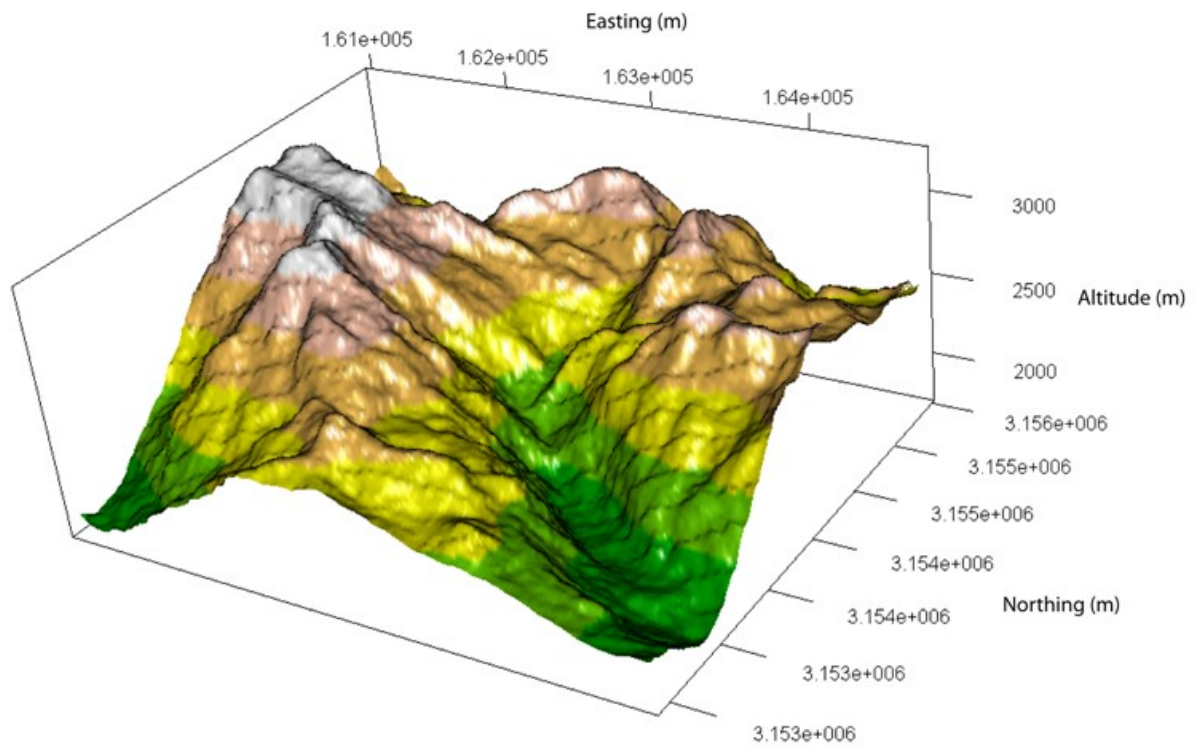


Figure 2.9. Digital elevation model of the Ossoue catchment.

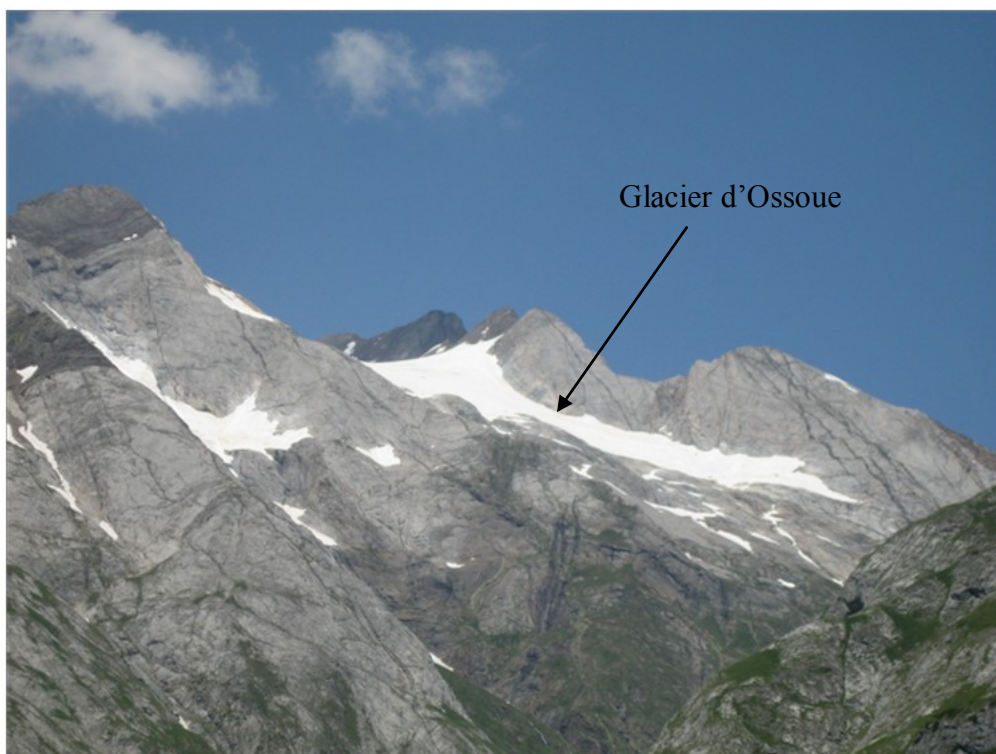


Plate 2.5. The Glacier d'Ossoue looking approximately south-east, July 2011.



Plate 2.6. Gauging station at the study catchment outlet, Oulettes d'Ossoue stream, June 2011.



Plate 2.7. Bedrock cliff roughly 1km downstream from the snout of Glacier d'Ossoue.

2.3.4. *Vignemale basin*

The Vignemale catchment, 42°48'N, 0°08'W, spans at altitudinal range of 1820m to 3298m and covers an area of 11.2km² above the lowest sample point (Figure 2.10; Figure 2.11). Ice covers approximately 1% of the catchment (Plate 2.8), with discharge from the Glacier des Oulettes (0.13 km²) and Glacier du Petit Vignemale (0.03 km²) feeding the Gave des Oulettes (Plate 2.9). The catchment is predominately underlain by igneous rocks (primarily granodiorite) (Debelmas 1974). The gradient of the main river channel was significantly shallower than in the other study basins and livestock grazing was also less intensive. Two vegetated floodplains were apparent above 2000m, one of which was a relatively stable glacial floodplain at the head of the catchment where *Eriphorum* spp. and *Festuca* spp. were abundant (Plate 2.10). However, closer to the Glacier de Oulettes, the north west of the floodplain network, riparian vegetation was minimal and scree and exposed bedrock were apparent (Plate 2.10). Trees (*Pinus* spp.) and scattered shrubs were apparent on the steeper valley sides up to 2000m however the floodplain was free from tree cover.

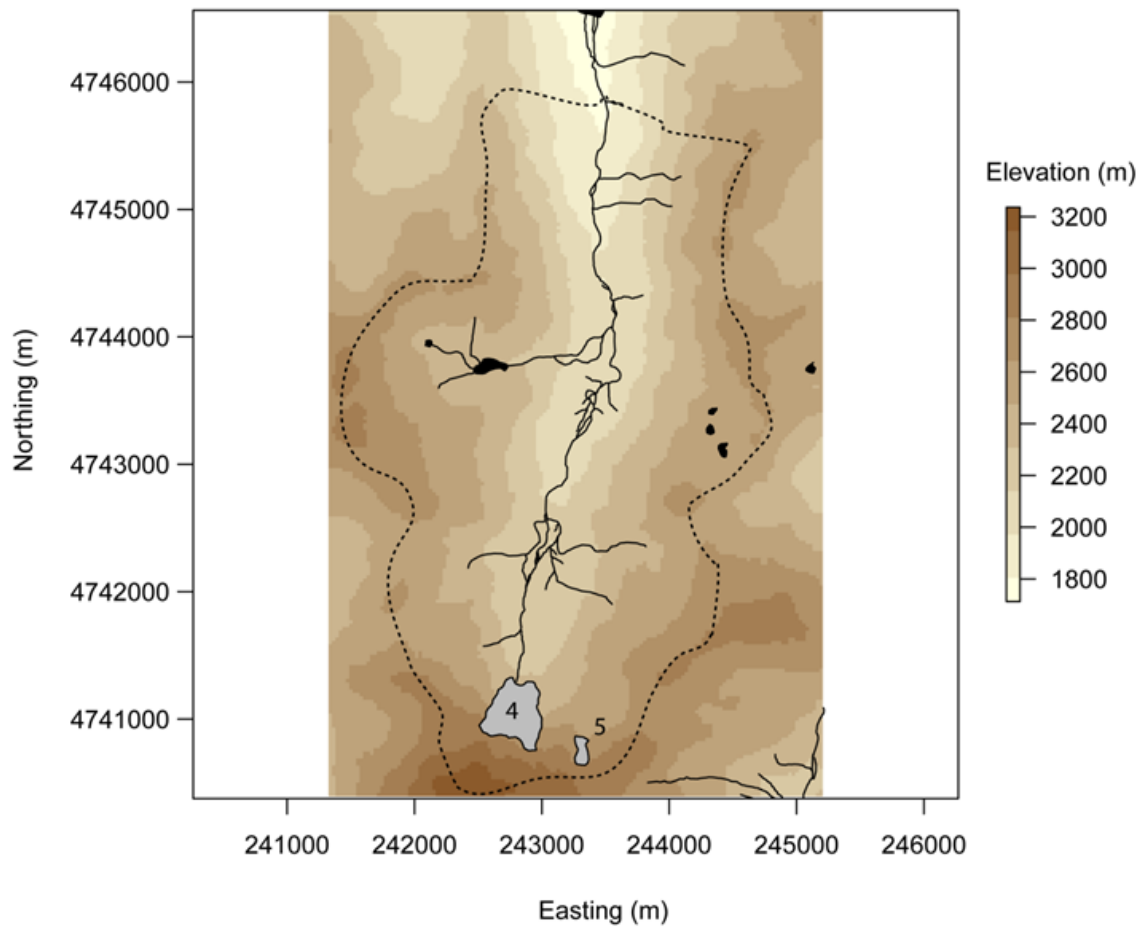


Figure 2.10. Map displaying the major topographic features, glaciers (grey shading), river network (solid black lines), lakes (black shading) and watershed (dashed line) for the Vignemale basin. The numbers correspond to glacier names: (4) Glacier du Oulettes and (5) Glacier Petit Vignemale.

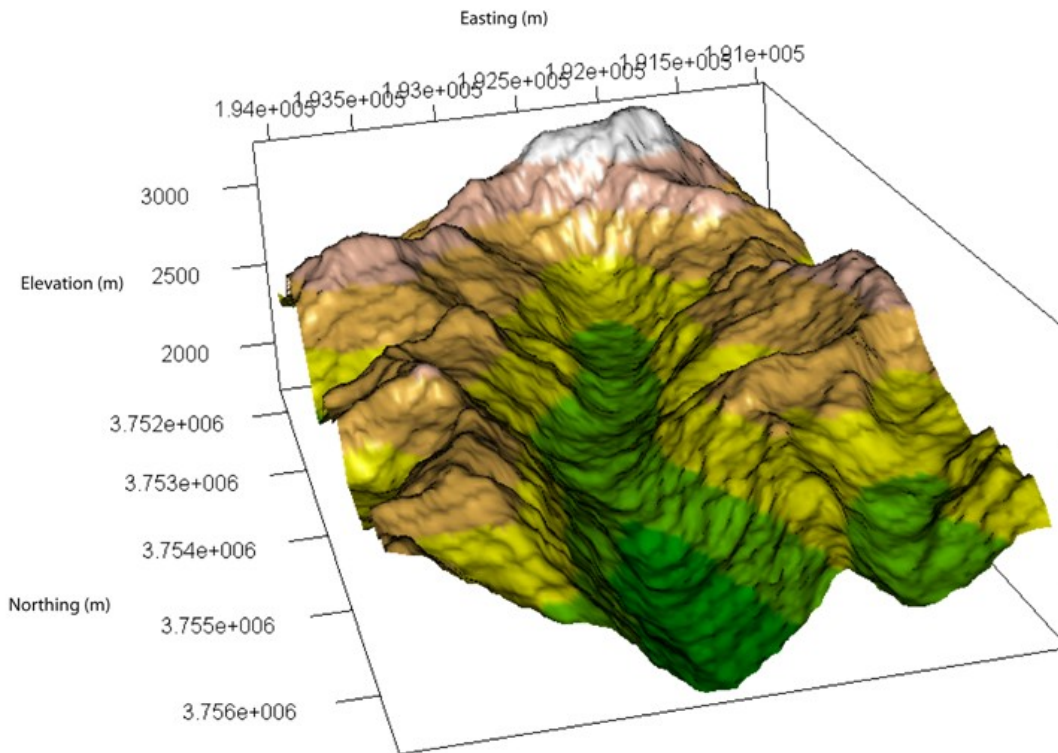


Figure 2.11. Digital elevation model of the Vignemale catchment.

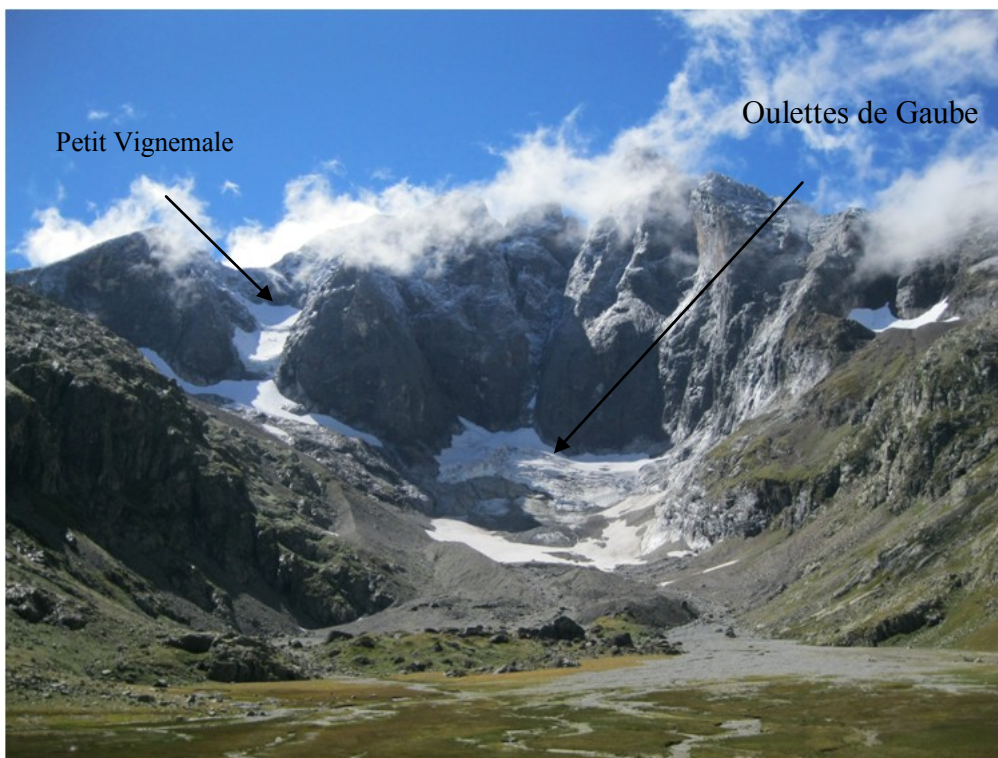


Plate 2.8. Vignemale massif facing south, September 2010. The Glaciers are highlighted.



Plate 2.9. Gave des Oulettes approximately 2.5km from the glacier looking south, June 2010.



Plate 2.10. Flood plain below Oulettes de Gaube looking north, August 2011.

2.3.5. *Tromouse basin*

The Cirque de Tromouse catchment, 42°43'N, 0°06'E, spans at altitudinal range of 1740m to 3133m and covers an area of 6.6 km² above the lowest sample point (Figure 2.12; Figure 2.12). Ice covers currently covers <1% of the catchment, with discharge from the Glacier de la Munia (0.04 km²; Plate 2.11) feeding the Gave des Touyeres (Plate 2.12). A number of springs which drain the eastern slopes of the catchment represent an important water source for the Gave des Touyeres and are rely on recharge from semi-permanent snow field. The catchment is underlain by sedimentary rocks, primarily limestones and shales ; however, scattered crystalline outcrops are apparent (Gellatly & Parkinson 1994). Soils on the cirque floor are generally well developed (Parkinson & Gellatly 1991) and the vegetation is dominated by coarse grasses (*Deschampsia* spp. and *Nardus* spp.). The cirque headwalls are steep and frequently rockfalls has lead to the development of extensive boulder fields and talus slopes (Gellatly & Parkinson 1994).

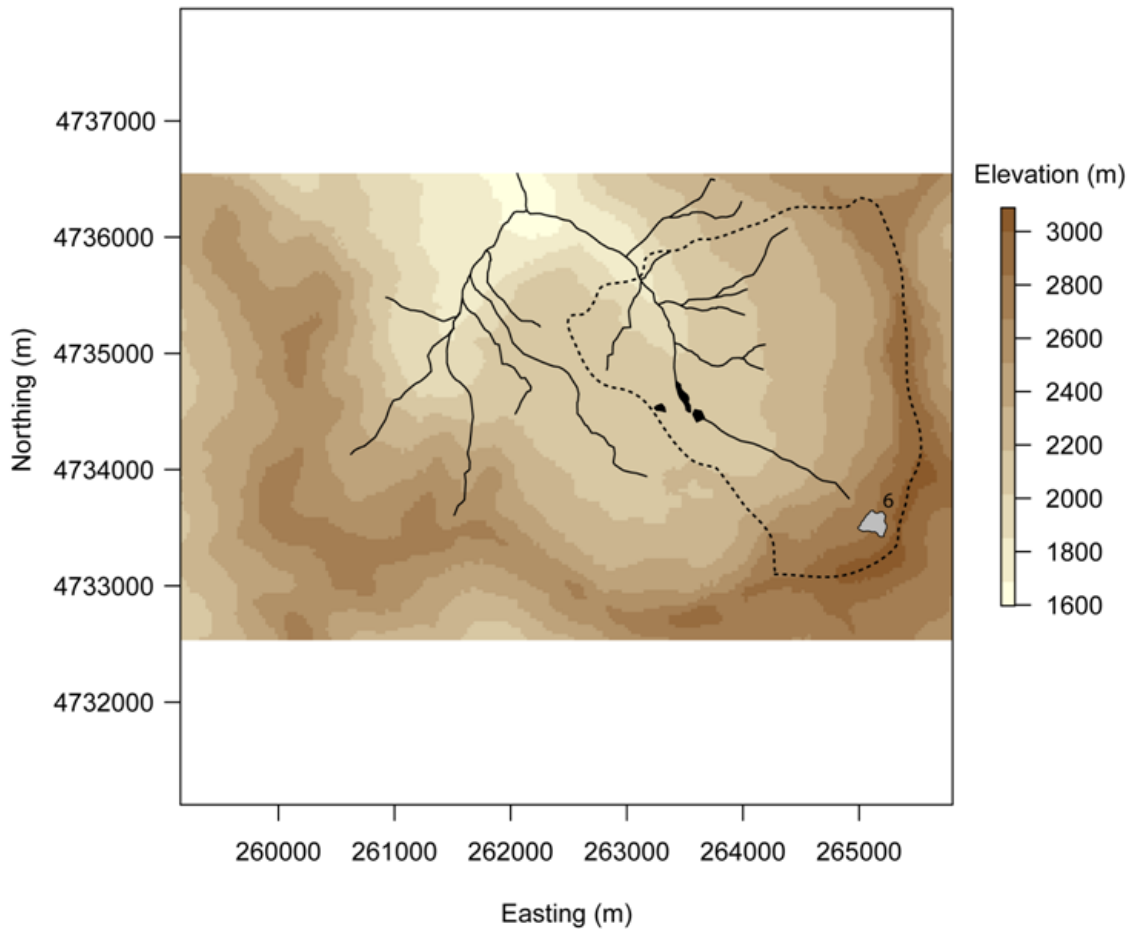


Figure 2.12. Map displaying the major topographic features, glaciers (grey shading), river network (solid black lines), lakes (black shading) and watershed (dashed line) for the Tromouse basin. The number (6) corresponds to glacier names Glacier Munia.

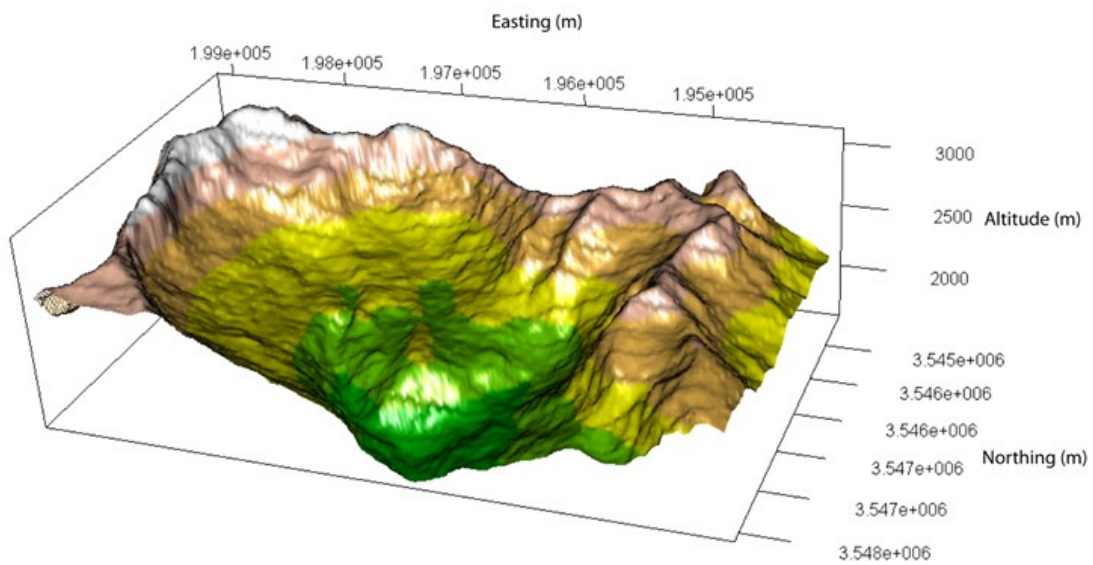


Figure 2.13. Digital elevation model of the Cirque de Tromouse catchment.



Plate 2.11. Glacier Munia looking south, July 2011.



Plate 2.12. Gave des Touyeres looking north from the lip of the cirque floor, July 2011.

2.3.6. Néous basin

The Néous catchment, 42°51'N, 0°16'W, spans at altitudinal range of 1740m to 3144m (Pic Balaïtous and covers an area of 10.3km² above the lowest sample point (Figure 2.13; Figure 2.14). The Balaïtous massif represents the western extent of current glacier cover in the Pyrénées. Ice covers <1% of the catchment, with discharge from the Glacier las Néous (0.04 km²; Plate 2.13) feeding the Gave d'Arrens (Plate2.14). The catchment is underlain by crystalline rocks, composed of a mixture of granite and schist (Debelmas 1974). Vegetation (alpine meadow) and soils are well developed in the lower valley (<1900m). The upper catchment (south-west) largely consists of scree and talus slopes (Plate 2.15), with sparse, skeletal soil and patchy vegetation cover.

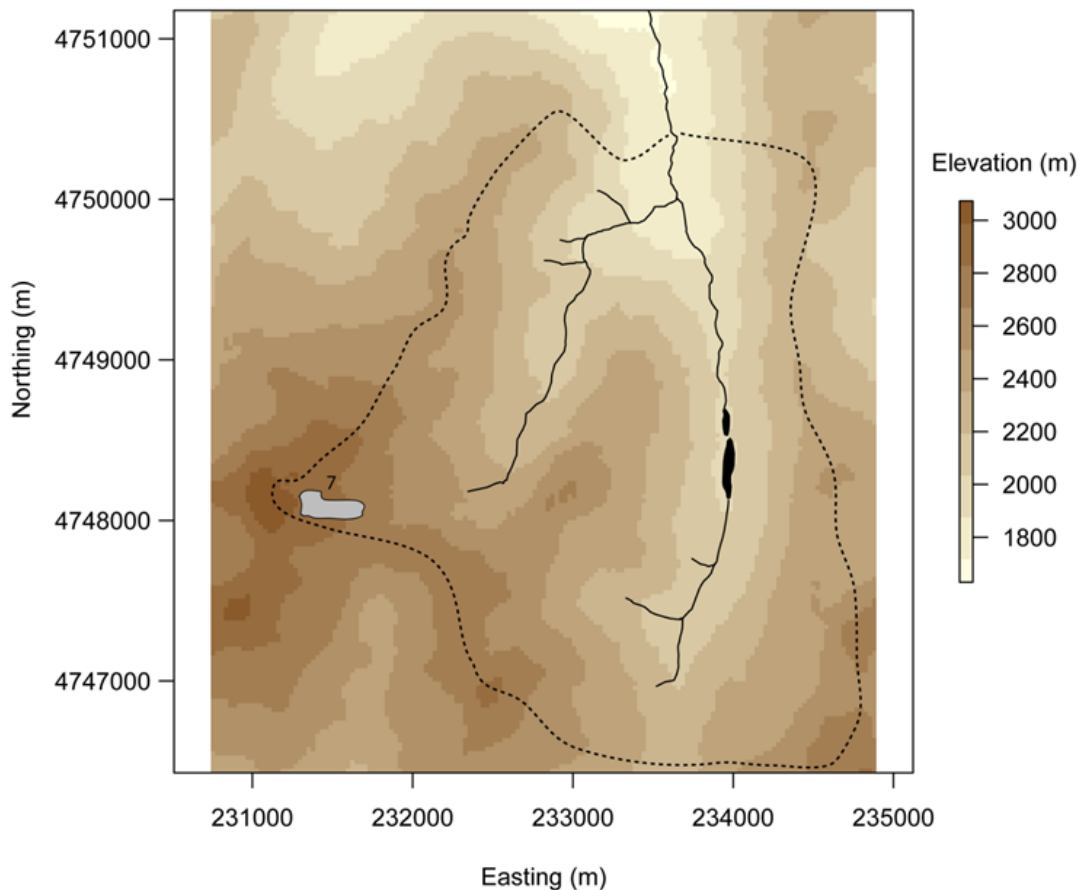


Figure 2.14. Map displaying the major topographic features, glaciers (grey shading), river network (solid black lines), lakes (black shading) and watershed (dashed line) for the Néous basin. The number (7) corresponds to Glacier las Néous.

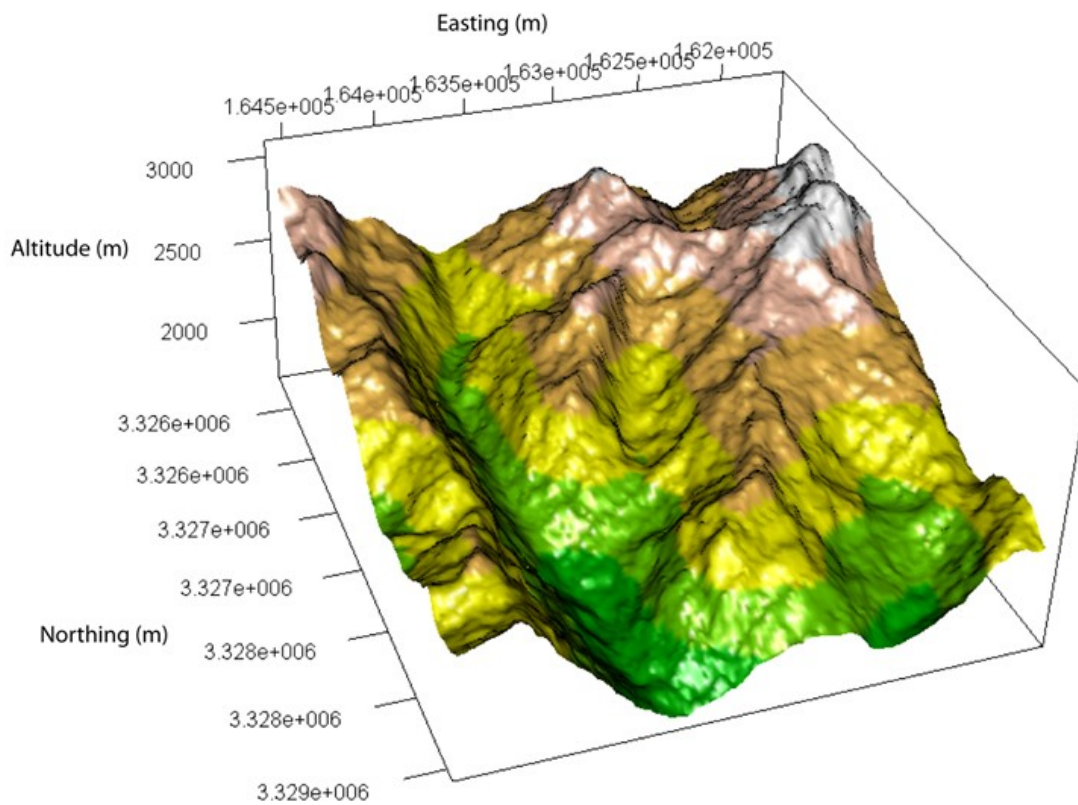


Figure 2.15. Digital elevation model of the Néous catchment.



Plate 2.13. The Glacier Las Néous taken from Association Moraine Pyrénéenne de Glaciologie (2009).



Plate 2.14. The Gave d'Arrens at the Néous catchment outlet, September 2010.



Plate 2.15. The upper Néous catchment looking roughly east towards Pic Balaïtous, July 2011.

2.4. Chapter Summary

A brief background to the climate, geography and glaciers of the Pyrénées has been presented. The study catchment selection process and physical properties of the selected catchments have also been highlighted in this chapter. Methods, data processing and statistical techniques specific to the relatively broad objectives of this thesis are presented in the methods section of subsequent chapters.

CHAPTER 3

*The physicochemical habitat template of
alpine glacier-fed river systems:
methods for monitoring environmental
change*

3.1. Introduction

The impact of climate change on the hydrological cycle is expected to be most pronounced at mid-high latitudes, particularly in regions where seasonal snow and ice melt represents an important water source during summer months (Barnett *et al.* 2005). Here the cryosphere is predominately located in mountainous regions, where rates of warming over the last century have been considerably greater than observed in lowland areas (Stewart 2009; Beniston 2012). During the same period snow cover extent and glacier volumes have decreased, particularly across European mountain ranges (Dyrgerov & Meier 2000; Scherrer *et al.* 2004; Zemp *et al.* 2006; Grunewald & Scheithauer 2010). This pattern of cryospheric recession is predicted to continue in line with projected increases in air temperature (Barnett *et al.* 2005; Zemp *et al.* 2006). Hence, it is likely alpine river basin hydrology will be severely altered (Brown *et al.* 2007a; Stahl *et al.* 2008; Stewart 2009). The most probable manifestations are: (i) an earlier snowmelt peak, primarily due to changes in precipitation patterns (amount and state); (ii) a reduction in glacier melt during summer due to a loss of ice mass (Adam *et al.* 2009; Milner *et al.* 2009; Huss 2011); and (iii) proportionally greater groundwater contributions to flow during summer months (Brown *et al.* 2006d). These hydrological changes will have implications for alpine river ecosystems, altering the instream physicochemical habitat template, biodiversity patterns and ecological functioning of alpine river systems (Milner *et al.* 2010; Füreder 2012; Déry *et al.* 2012) and will likely drive a number of specialist taxa to extinction, to the detriment of regional diversity (Brown *et al.* 2007a). However, the identification, monitoring and prediction of hydroecological change still remains a key challenge for river basin management in alpine systems (Hannah *et al.* 2007; Brown *et al.* 2009b).

The strong interconnection between abiotic processes, which are predominately climate driven, and biological patterns (Moore *et al.* 2009) make alpine river networks ideal indicator sites for monitoring climate change (Grabherr *et al.* 2000; Williams *et al.* 2002). Here, anthropogenic disturbance is often negligible (national parks and protected areas), environmental gradients are steep, and ecological complexity is comparatively low (Füreder *et al.* 1998). However, current methods and biotic metrics for quantifying hydroecological responses to environmental change still need development and refinement. The conceptual framework underpinning established bio-assessment tools (e.g. RIVPACS/LIFE), which involves the creation of baseline conditions from a reference data set (Feio & Poquet 2011), may not be the most useful approach for alpine systems. Here, river habitat heterogeneity is primarily governed by hydrological source (Ward 1994) and river discharge can be traced back to two key stores: snow/ice (meltwater) and groundwater (Brown *et al.* 2006d). Glacier meltwater tends to be more turbid, due to higher suspended sediment concentrations (SSC), flow regimes are variable at a range of scales (resulting in unstable river beds and channels) and water temperature is low. Groundwater flow is less turbid (lower SSC), water temperature is generally warmer, and flow less variable leading to stable river channels and beds (Smith *et al.* 2001; Brown *et al.* 2003). The mixing of these water sources in different proportions leads to variability in benthic habitat and associated benthic assemblages across a range of scales (Malard *et al.* 2006; Milner *et al.* 2009). Hence, the accurate and reliable quantification of glacier (meltwater) influence at a certain point in space and time becomes an important requirement when monitoring for climate induced change (Hannah *et al.* 2007).

A number of approaches for quantifying glacier influence at a given river reach have been proposed to facilitate both monitoring and future prediction (Milner *et al.* 2009). First, a simple, intuitive method involves the calculation of the proportion of glacier cover in the

catchment upstream of a sampling reach (GCC). This technique has been employed to successfully predict macroinvertebrate species richness (Milner *et al.* 2009; Jacobsen *et al.* 2012), algal richness (Rott *et al.* 2006) and the occurrence of resistant and resilient traits (Füreder 2007). GCC can be calculated using satellite imagery and GIS, which is both accurate and able to pick up broad scale temporal variations. This metric is appealing due to the simplicity of calculation; however, it is not directly transferable across space and shorter time scales (evolution of melt season hydrology). A particular concern with this approach is that it is unable to account for inter-basin variability in the attenuation of the glacier melt signal by groundwater tributaries or lakes (Milner & Petts 1994). A similar metric, the index of glacier influence proposed by Jacobsen & Dangles (2011), is a dimensionless measure of environmental harshness calculated using glacier size and distance from the glacier terminus. While this index is very similar to GCC it may be easier to calculate if access to aerial imagery or GIS software is unavailable but has similar drawbacks to GCC regarding transferability.

Ilg and Castella (2006), proposed an alternative Glaciality Index which is calculated using a suite of measured physicochemical variables sensitive to changes in glacier runoff. Site data for suspended sediment concentration (SSC), electrical conductivity (EC), water temperature (T_w) and bed stability are ordinated, and sites ranked along a glaciality component based on their loadings (Ilg & Castella 2006). This approach has been used to predict the occurrence of macroinvertebrate traits across a number of glacier fed streams in the Swiss Alps and taxa abundances in glacier fed streams in the French Pyrénées (Ilg & Castella 2006; Brown *et al.* 2010b). However, the main drawback to this method is that the scale is only relative to the sites and date(s) used in the ordination procedure (Brown *et al.* 2010b).

Hannah *et al.* (2007) proposed a top-down process chain linking climate – hydrology – ecology as a framework on which to develop alpine river conservation strategies (Hannah *et al.* 2007). Climatic forcing drives meltwater production and timing through the exchange of mass and energy, and thus the water source dynamics (i.e. the proportions of flow sourced from snow/ice/groundwater at a given reach and point in time) (Smith *et al.* 2001; Hannah *et al.* 2007). Each water source has a unique physicochemical signal, which when mixed in different proportions, creates distinct habitat types (Brown *et al.* 2003) and ultimately dictates the benthic community which can establish, by filtering (selecting for) species possessing traits matched to the physicochemical habitat template (Hieber *et al.* 2005). Based upon this conceptual process cascade, Brown *et al.* (2007, 2010) used quantitative measurement of water source contribution, to develop ARISE (Alpine River and Stream Ecosystems) and successfully predict macroinvertebrate community metrics and identify potential indicator species (e.g. those sensitive to climate change). To date this approach has only been validated for single river basins and needs to be expanded to test its utility across multiple river basins. However, this approach is particularly labour intensive as sufficient characterization of potential water sources requires numerous samples (Christophersen & Hooper 1992). Hence, in certain situations this approach may be impractical.

The predictable habitat characteristics of glacier fed rivers have been widely reported (Malard *et al.* 2006; Moore *et al.* 2009; Srivastava *et al.* 2012; Fellman *et al.* 2013; Blaen *et al.* 2013b). However, while the potential of catchment scale properties to modify longitudinal patterns has been recognised (Milner & Petts 1994), no studies have explicitly quantified the effect on glacier-habitat relationships. For example, stream water temperature in alpine and Arctic river systems has recently received attention in the academic literature but the focus has been on catchment/reach scale drivers, e.g. topographic shading, river aspect, river

morphology, tributary inputs and lakes/reservoirs and climatic drivers (Brown & Hannah 2008; Richards *et al.* 2012; Dickson *et al.* 2012), but have not rigorously tested links between temperature and glacier influence (yet see Fellman *et al.* 2013). Bedrock geology is an important regional/catchment scale variable which controls a range of water quality variables such as pH, turbidity and EC (Sponseller *et al.* 2001; Young *et al.* 2005; Nelson *et al.* 2011). Dissolution of bedrock can directly influence the proportion of nutrients available for instream plant growth (periphyton), while weathering rate controls soil development and vegetation cover which can indirectly influence instream primary productivity (Biggs & Gerbeaux 1993; Stevenson 1997). However, to date few studies have directly considered the role of bedrock hardness in an alpine stream habitat context (Weekes *et al.* 2012), despite the high probability that glacier melt pulses interact with the underlying geology causing varying rates of erosion and dissolution, which in turn leads to differing basin/river morphology and chemical properties of the water.

The aim of this study was to identify the relationship between multiple methods for measuring glacial influence, and their relationship with physicochemical habitat variables across multiple alpine river basins in an attempt to provide an initial roadmap for future environmental monitoring in glacierized river basins.

The specific objectives were as follows:

1. To assess the spatial and temporal variability in methods for quantifying glacier influence across four glacier fed streams in the Pyrénées and link to physicochemical habitat variables of biological importance;
2. To assess the effect of basin geology on the relationship between glacial influence and physicochemical habitat; and

3. To identify the level of concordance between methods for quantifying glacier influence at the reach scale.

3.2. Methods

3.2.1. Study region

The Pyrénées represent an ideal location to test and compare the sensitivity of methods for quantifying glacier influence, as the glaciers are small and the characteristic physicochemical signal associated with meltwater is quickly attenuated downstream by groundwater inputs (Brown *et al.* 2006d; Finn *et al.* 2013). Hence, a gradient from high to low glacier influence can be studied across a spatial scale which is logistically practical given the difficulty associated with remote field work in high altitude regions. Of the 11 remaining French Pyrenean glaciers (See Chapter 2), all are located within the Parc National des Pyrénées. This enabled a gradient of glacial influence to be sampled across a relatively homogenous habitat (i.e. alpine, above the treeline) with limited anthropogenic disturbance. Furthermore, due to the variable geology in the region it was possible to select glacier-fed catchments on both sedimentary and crystalline geology.

This study was carried out within the Parc National des Pyrénées (PNP) across two consecutive summer melt seasons (2010 and 2011). Four glacier-fed streams were selected spanning three river basins (Figure 3.1). The Taillon–Gabiétous river basin (Figure 3.1a), which has two small cirque glaciers, the Glacier du Taillon (0.09 km²) and the Glacier des Gabiétous (0.08 km²) with an underlying geology of predominately sandstone (Marbore sandstone) and limestones (Santonien and Coniacien series). The Ossoue river basin (Figure

3.1b) with the Glacier d'Ossoue (0.46 km²) with a mixed geology of metamorphic (marble limestones) in the upper catchment (Del Río *et al.* 2012) and sedimentary rocks in the lower catchment (Debelmas 1974). The Vignemale river basin (Figure 3.1c) with the Glacier des Oulettes (0.13 km²) and Glacier du Petit Vignemale (0.03 km²) and an igneous geology (primarily granodiorite) (Debelmas 1974). More information on the study basins can be found in Chapter 2.

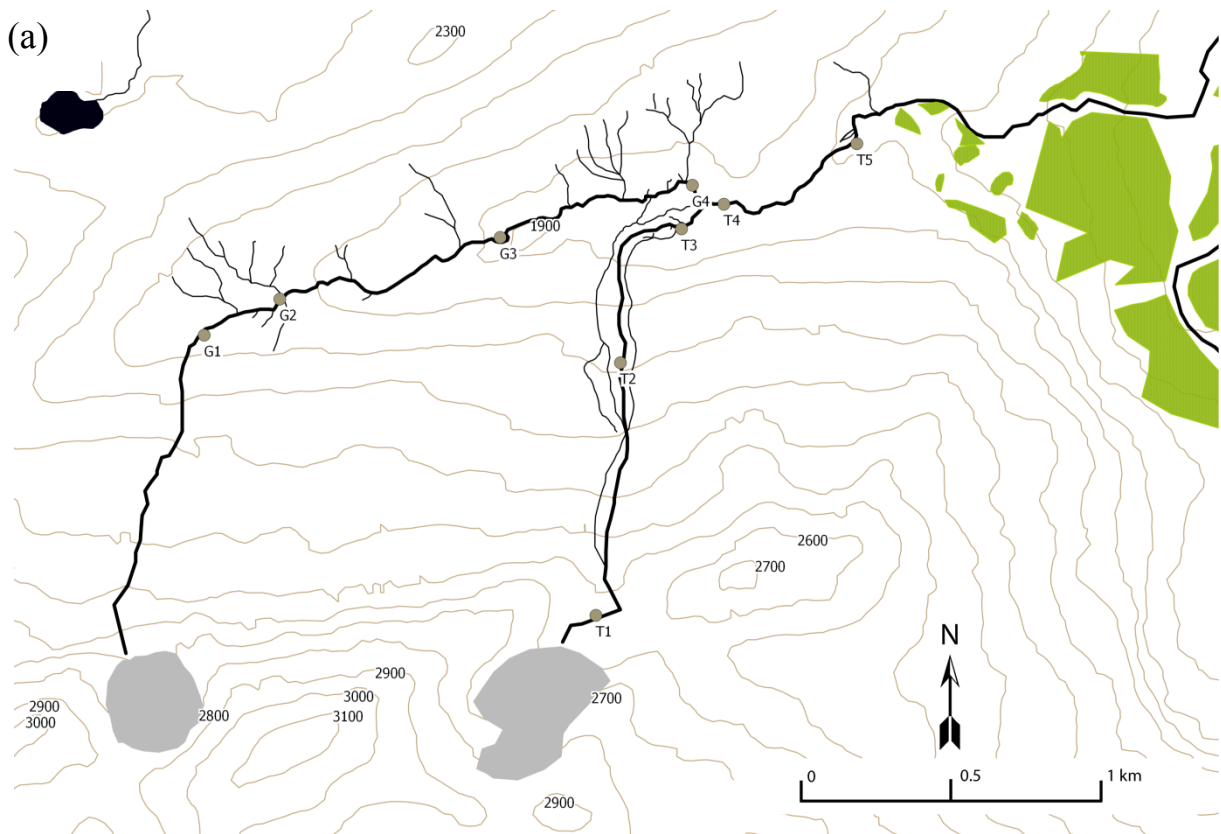


Figure 3.1. Maps of the study basins with sampling sites marked: (a) Taillon – Gabiétous catchment; (b) Ossoue catchment; and (c) Vignemale catchment. River channels (black lines), glacier ice (grey shading), forest (green shading) and lakes (black shading) are also highlighted.

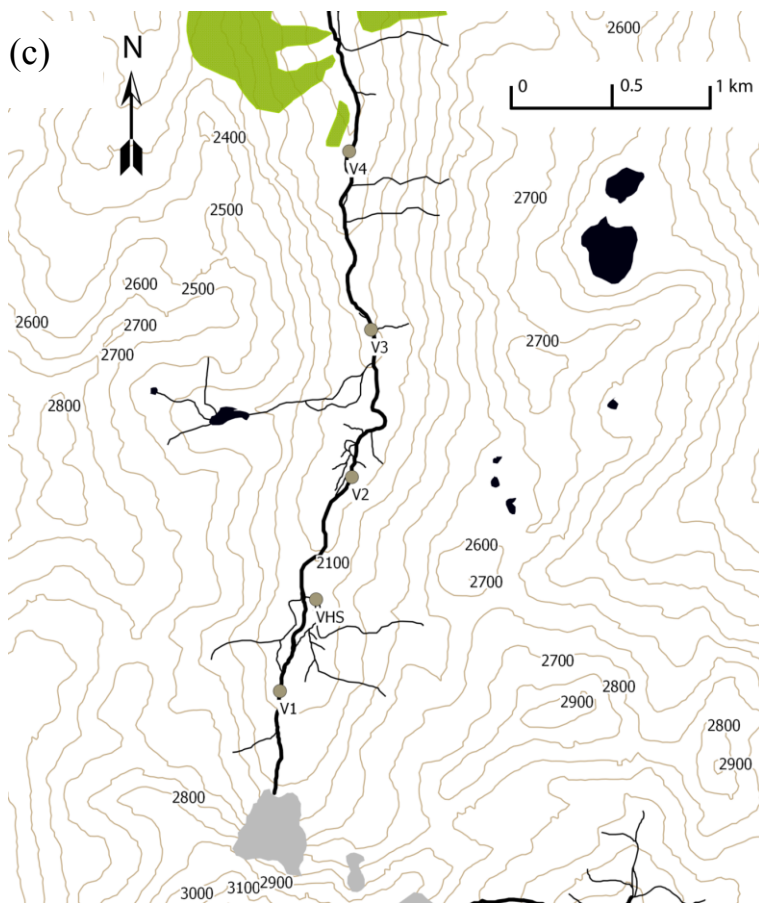
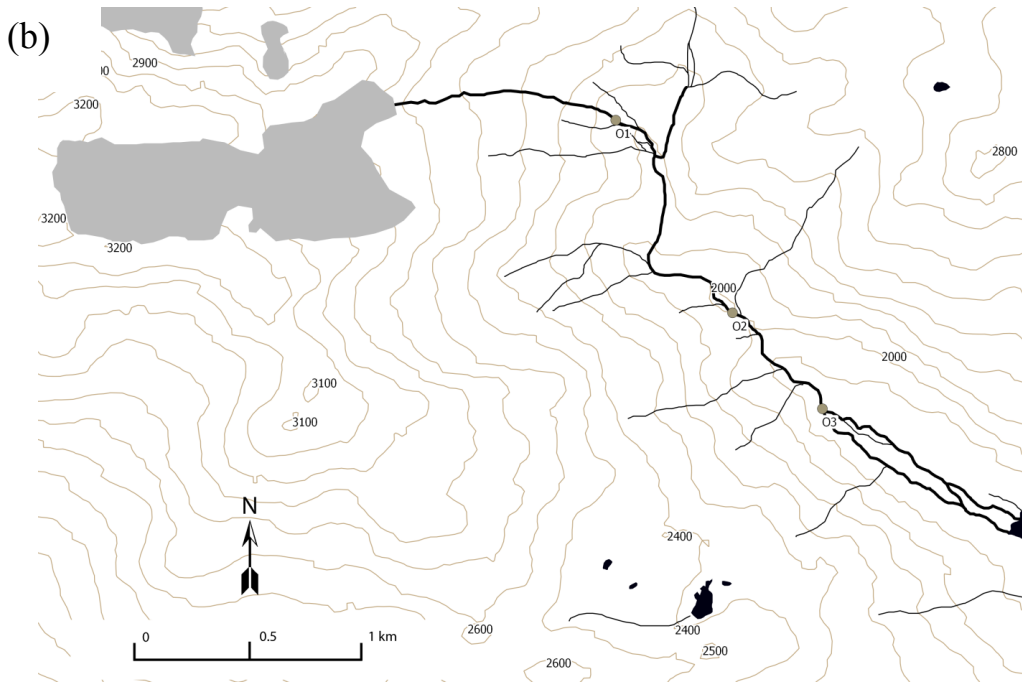


Figure 3.1 cont, Maps of the study basin with sampling sites marked: (a) Taillon – Gabiétous catchment; (b) Ossoue catchment; and (c) Vignemale catchment. River channels (black lines), glacier ice (grey shading), forest (green shading) and lakes (black shading) are also highlighted.

3.2.2. *Physicochemical habitat sampling*

Seventeen study reaches were selected (a minimum of three located along each stream) to represent a gradient of glacier influence (see Table 3.2 for site characteristics). Discharge (Q) was continuously recorded at sites T3, T4 and G4 during the 2010 melt season. During 2011 three additional sites were monitored; O3, V4 and V2. At all sites, except V2 and V4, Druck PDCR pressure transducers were placed in stilling wells to provide accurate depth measurements. Data were recorded at 15 min intervals and stored on CR 1000 dataloggers (Campbell Scientific). At sites V2 and V4 Trutrack WT-VO pressure transducers were installed and data was stored internally at 15 min intervals. Stage – discharge relationships (see Appendix 3.1) were created for all gauging stations using both salt dilution (Moore 2003) and velocity-area methods (Herschy 1985).

Field measurements were carried out at each study site on three occasions, during both field seasons (see Table 3.1 dates). At each reach, spot measurements of pH and electrical conductivity (EC) were taken in the thalweg using a Hannah HI 98129 handheld probe. Water temperature was recorded continuously during both field seasons using a combination of miniature digital temperature dataloggers (Gemini Tinytag aquatic/Plus 2, instrument error $\pm 0.2^{\circ}\text{C}$) and CS547A temperature probes (Campbell Scientific, instrument error $\pm 0.2^{\circ}\text{C}$).

Water samples (500ml) were collected at each reach to determine suspended sediment concentration (SSC). Samples were filtered through pre-weighed glass fibre filter papers (Whatman GF/C), dried at 95°C for 2 hours then re-weighed to the nearest mg (ATSM D3977 – 97). At each reach the bottom component of the Pfankuch index (PFAN) was also calculated to estimate substrate stability. This involves a qualitative assessment of five

variables (rock angularity, substrate brightness, particle packing, percentage of stable materials, scouring and aquatic vegetation) with higher scores representing unstable channels (Pfankuch 1975). At five random locations in the thalweg of each study reach, water velocity (measured using a Sensa RC2 electromagnetic current meter) and water depth was recorded. Wetted width was also recorded at three randomly selected points along each 30m reach.

Reach slope, site altitude and catchment area were calculated for each site in ARC map 10 using an ASTER DEM (30m resolution). Reach slope and average water depth were then used to calculate shear stress (Castella *et al.* 2001):

$$SS = g s d \rho \quad (3.1)$$

Where g is the acceleration due to gravity, s the reach slope, d the mean depth and ρ the water density.

Table 3.1. Sampling periods and corresponding dates.

Sample period	Dates
<i>2010</i>	
a	14/06 - 07/07
b	26/07 - 08/08
c	28/08 - 10/09
<i>2011</i>	
a	14/06 - 26/06
b	16/07 - 29/07
c	16/08 - 28/08

Table 3.2. Stream/sampling reach physical habitat characteristics.

Basin	Stream	Site	Catchment area (km²)	Glacier cover (%)	Distance from glacier (km)	Altitude (m)	Slope
<i>Taillon-Gabiétous (Calcareous)</i>	<i>Tourettes</i>	G1	1.10	7.27	1.0	2150	0.10
		G2	1.60	5.00	1.4	2030	0.10
		G3	3.60	2.22	2.1	1900	0.04
		G4	4.65	1.72	2.8	1850	0.04
	<i>Taillon</i>	T1	0.28	32.14	0.2	2560	0.10
		T2	0.61	14.75	1.0	2150	0.15
		T3	1.72	5.23	1.4	1870	0.06
		T4	6.27	2.71	1.7	1850	0.05
<i>Ossoue (Metamorphic)</i>	<i>Oulettes d'Ossoue</i>	T5	6.70	2.54	2.2	1800	0.05
		O1	1.70	24.71	1.0	2250	0.20
		O2	5.01	8.38	1.9	2005	0.08
<i>Vignemale (Igneous)</i>	<i>Gave des Oulettes</i>	O3	8.00	5.80	2.5	1870	0.03
		V1	1.20	10.83	0.5	2250	0.11
		VHS	1.30	2.31	1.3	2150	0.06
		V2	5.77	2.25	2.1	2050	0.04
		V3	9.40	1.38	3.2	1980	0.04
		V4	11.60	1.12	4.5	1820	0.04

3.2.3. Glacier cover and Glaciality Index (Jacobsen and Dangles)

Glacier size (km²) and the distance each sampling site was from the glacier margin were calculated from geo-referenced, high resolution aerial images in ARC Map 10. For each site the proportion of catchment covered by glacier ice was calculated as follows:

$$\text{Glacier cover (\%)} = \frac{\text{Size}_i}{\text{CA}_i} 100 \quad (3.2)$$

where Size is the glacier cover (km²) upstream of the *i*th site and CA the catchment area (km²) upstream of the *i*th site. From here in glacier cover in the catchment will be referred to by the acronym GCC. The index of glacier influence outlined by Jacobsen and Dangles (2011) was calculated by combining glacier size with distance from the glacier margin as follows:

$$\text{GI}_{\text{J\&D}} = \frac{\sqrt{\text{Size}}}{\text{Dist} + \sqrt{\text{Size}}} \quad (3.3)$$

where GI_{J&D} is the glacial index and Dist is the distance (km) of the study site from the glacier's terminus. The index can be viewed as a dimensionless measure of environmental harshness associated with flow derived from glacier melt. A value of 1 represent maximum glacial influence, scores then decrease exponentially with increasing distance downstream (Jacobsen & Dangles 2012).

3.2.4. *Glaciation Index (Ilg & Castella)*

Four physicochemical variables: (i) minimum water temperature (T_{\min}); (ii) electrical conductivity (EC); (iii) suspended sediment (SSC); and (iv) bed stability (PFAN), were used to calculate the Glaciation Index ($GI_{I\&C}$). Due to the differing bedrock geology of the sites used in this study, EC was scaled between 1 and 0 for each basin individually. This ensured the predictable downstream increase of EC, associated with decreased glacier melt to groundwater proportions, was maintained. For all site-dates raw values of T_{\min} , EC (standardised by basin due to varying geology), $1/SSC$ and $1/PFAN$ were scaled between 1 and 0, hence, lower values were associated with increased glacier influence. The data were then processed using a non-centred principal component analysis and ordination scores along the first axis (PC_1) were used as the $GI_{I\&C}$ (Ilg & Castella 2006). To aid interpretation, $1/GI$ was calculated and then scaled between 1 and 0. This brought the GI in line with the other methods for which a higher value indicates greater glacier influence.

3.2.5. *Water sources and mixing model*

In each river basin, water samples were collected from a range of potential hydrological sources or 'end members' (snow, ice and groundwater) and a further sample was collected at each study reach. All samples were collected between 09.00 & 14.00 GMT to minimise the influence of diurnal melt dynamics on spatial patterns. These were filtered through cellulose nitrate filters (Whatman 0.45 μ m) in the field, retained in HDPE bottles (60ml) and frozen for storage. To identify and account for sub-seasonal dynamics in water sourcing the sampling sweep was repeated on six occasions across the two melt seasons (see Table 2 for dates). In the laboratory samples were defrosted and silica [Si] concentrations calculated following the molybdosilicic method (ASTM D859 – 10) using a Helios Gamma spectrophotometer

(Thermo Fisher Scientific). Analytical precision of this procedure was high, with errors during both years <5%. Si was chosen as a tracer due to its slow reaction rates and ability to identify groundwater contributions to bulk streamflow (Anderson *et al.* 2000; Brown *et al.* 2006d).

Basin specific, two end member mixing models were then constructed for individual sample dates and all dates combined (Table 3.3). A hydrograph separation approach, based on the end member Si concentrations, was then adopted to calculate meltwater/groundwater proportions for each reach using steady state mass balance equations (Sueker *et al.* 2000):

$$Q_s = Q_m + Q_g \quad (3.4)$$

$$C_s Q_s = C_m Q_m + C_g Q_m \quad (3.5)$$

Where Q is the discharge, C the Si concentration and the subscripts s , m and g relate to the total discharge, the meltwater contribution and the groundwater contribution respectively. For this calculation Q_s was always unity, hence the relative contribution rather than volume of each end member was calculated.

Uncertainty (95% confidence) was calculated for each flow component following the method outlined by Genereux (1998):

$$W_{fm} = \sqrt{\left[\frac{C_g - C_s}{(C_g - C_m)^2} W_{C_m} \right]^2 + \left[\frac{C_s - C_m}{(C_g - C_m)^2} W_{C_g} \right]^2 + \left[\frac{-1}{C_g - C_m} W_{C_s} \right]^2} \quad (3.6)$$

Here, W is the uncertainty and f is the mixing fraction. To gain uncertainty estimates for each end-member the SD of the mean Si concentrations were multiplied by the appropriate t

value (related to sample size). Following Blaen *et al.* (2013a) calculations were conducted for each river sample individually and uncertainty was taken as the analytical precision.

3.2.6. *Statistical analysis*

Ordination was used to identify habitat gradients within the network of sampling sites. A normalised principal component analysis (PCA) was carried out using twelve habitat variables sensitive to glacier runoff and of biological importance. Principal components which explained a large proportion of the variance (i.e. eigen values > 1) were retained for analysis (Snook & Milner 2001). Contour plots in PC₁ and PC₂ space were created for each method of quantifying glacier influence, to identify relationships to the underlying environmental gradients.

Linear Mixed Models (LMMs) were used to investigate relationships between methods for quantifying glacier influence (excluding GI_{I&C}) and key habitat variables. The mean (T_{mean}), maximum (T_{max}) and minimum (T_{min}) water temperature metrics were calculated for each site and sample. LMMs were successively fitted with quadratic and cubic terms and the optimum model identified using Akaike's information criterion (AIC). Analysis of Covariance (ANCOVA) was then used to investigate the influence of stream (covariate) on glacial influence – T_w associations; however, due to a limited number of independent observations for GI_{J&D} and GCC (both static over the study period) models were unrealistic so only models for meltwater contribution, with predictor observations covering the full range of potential values, are presented.

For other habitat variables a set of candidate models were tested:

- (i) predictor + random effect,
- (ii) predictor + geology (sedimentary/crystalline) + random effect,
- (iii) predictor * geology (sedimentary/crystalline) + random effect.

From the candidate set, the model which displayed the highest AIC score was retained. For the variables which displayed a significant interaction with geology (EC, SSC, PFAN, pH,) all regression coefficients are reported. For variables without a significant interaction (e.g. shear stress, slope and channel width), t-values and significance of the regression coefficients are reported and used to identify the strength and direction of the relationship between response and predictor (method of measuring glacial influence). Temporal autocorrelation was accounted for in the regression and ANCOVA models by including site as a random effect nested within sampling year. This induced a compound correlation structure on the residuals (i.e. samples from the same site are equally correlated), which, due to uneven time periods between sample dates, was preferred to an autoregressive structure (Zuur *et al.* 2009).

To assess relationships between: (i) each method for quantifying glacier influence and distance from the glacier margin; (ii) each method and river flow metrics (mean Q and standardised flow range); and (iii) each quantification method, Spearman's rank correlation coefficient was used. For each method sites were ranked where 1 = highest glacial influence and 17 = lowest glacier influence. Euclidean distance was then used to calculate the distance between each method based on site ranks for: (i) all sites; and (ii) just sites <1.5 km from the glacier margin.

3.3. Results

3.3.1. Glaciality Index

The first axis of the PCA for the $GI_{I \& C}$ calculation (PC_1) explained 79% of the variation observed in the physicochemical habitat data (Table 3.3). All physicochemical variables made significant contributions to PC_1 ; SSC and PFAN had the highest correlations (-0.54) and EC the lowest (-0.41). Scores along the PC_1 ranged from 3.28 (lowest glacier influence) at O3 to 0.69 (highest glacier influence) at site T1.

Table 3.3. Eigen values and physicochemical variable loadings for PC_1 - PC_3 of the non-centred PCA analysis for the calculation of $GI_{I \& C}$

	PC₁	PC₂
Eigen value	1.78	0.76
Variance	0.79	0.14
<hr/>		
T_{min}	-0.51	-0.08
EC	-0.41	0.32
1/PFAN	-0.54	-0.30
1/SSC	-0.54	-0.30

3.3.2. End-members and hydrograph separation (water sources)

Differences in Si concentration between snow/ice samples and the more enriched groundwater samples were pronounced (Table 3.4). Water samples collected from study sites, (stream samples), were bounded by the two end members (Figure 3.2). While there was negligible variability between basins regarding the Si concentration of the ‘meltwater’ end member, the Si concentration for the groundwater end member did vary between basins (Table 4). The highest value was recorded for the Taillon-Gabitéous catchment (1.26 ± 0.4) and lowest value for the Ossoue catchment (0.77 ± 0.29). The Si concentrations of the

groundwater end member also varied between sample dates (Table 3.3), with lower concentrations recorded for sample date a in both 2010 & 2011, suggesting groundwater runoff was diluted by hillslope snowmelt.

Table 3.4. Mean Si concentrations, SD and number of samples for meltwater and groundwater end members.

Basin	Period / end member	Si concentration (mg/L)								
		2011			2010			Lumped		
		Mean	SD	N	Mean	SD	n	mean	SD	
Vignemale										
	GW Period a	0.91	0.18	3	0.89	0.06	4			
	GW Period b	1.28	0.16	7	0.76	0.19	4			
	GW Period c	1.16	0.25	7	0.99	0.12	6			
	GW season mean	1.16	0.24	17	0.89	0.16	12	1.03	0.20	
	Meltwater	0.04	0.05	10	0.05	0.04	10	0.05	0.05	
Ossoue										
	GW Period a	0.54	0.17	3	0.76	0.14	4			
	GW Period b	0.61	0.23	6	1.24	0.36	4			
	GW Period c	0.81	0.21	8	0.81	0.26	5			
	GW season mean	0.70	0.24	17	0.84	0.34	13	0.77	0.29	
	Meltwater	0.01	0.03	12	0.03	0.04	12	0.02	0.04	
Taillon-Gabiétous										
	GW Period a	1.41	0.27	5	0.95	0.26	5			
	GW Period b	1.44	0.29	5	1.29	0.37	6			
	GW Period c	1.39	0.69	10	1.09	0.13	6			
	GW season mean	1.41	0.50	19	1.12	0.30	17	1.26	0.40	
	Meltwater	0.06	0.09	16	0.02	0.02	26	0.04	0.05	

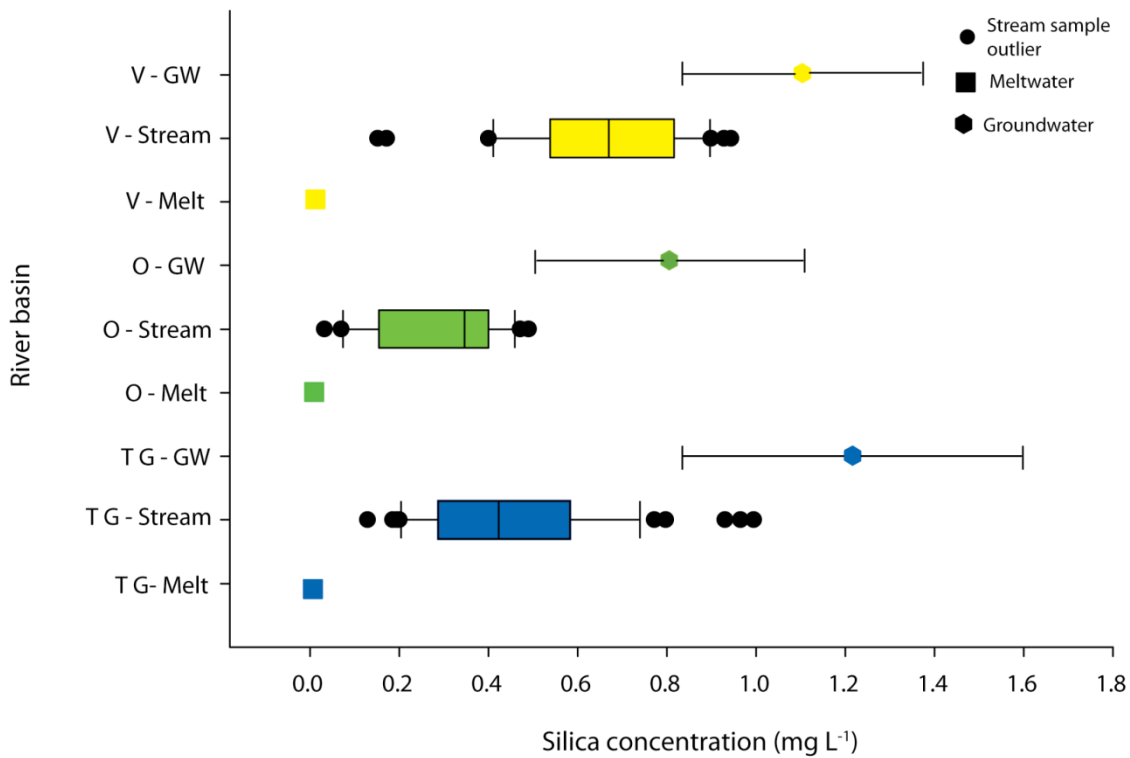


Figure 3.2. Mixing plot for all basins, all dates combined. Boxplots represent stream water samples squares and hexagons represent end members (\pm SD). T G (blue) is Taillon-Gabiétous, O (green) is Ossoue and V (yellow) is Vignemale.

A seasonal lumped mixing model (Figure 3.2) was preferred to account for the dilution of the groundwater end-member by snowmelt. No significant differences in mean meltwater contribution by site ($n = 6$), calculated using the date specific model and the lumped model were identified (ANOVA, $P > 0.05$). For all further analysis in this chapter results from the lumped model are used. Mean uncertainty estimates (95% confidence level) for the hydrograph separation ranged from 5% at O1 during 2011, to 40% for O2 during 2010. Uncertainty was generally highest at sites with lower meltwater contribution (Appendix 3.2) as the groundwater component generally contributed $>70\%$ of the total uncertainty, with the

highest at O3 during 2011(98.9%) and lowest at T1 during 2011 (45.5%). The uncertainty attributed to analytical error (i.e. for river samples) was low for all sites:dates (<5%).

3.3.3. *Spatial and temporal patterns in glacier influence*

Spatiotemporal patterns were only investigated for meltwater contribution to bulk discharge and $GI_{I\&C}$, as the other methods were considered temporally static due to the relatively short time span of this study. Hence, only spatial patterns were investigated for GCC and $GI_{J\&D}$.

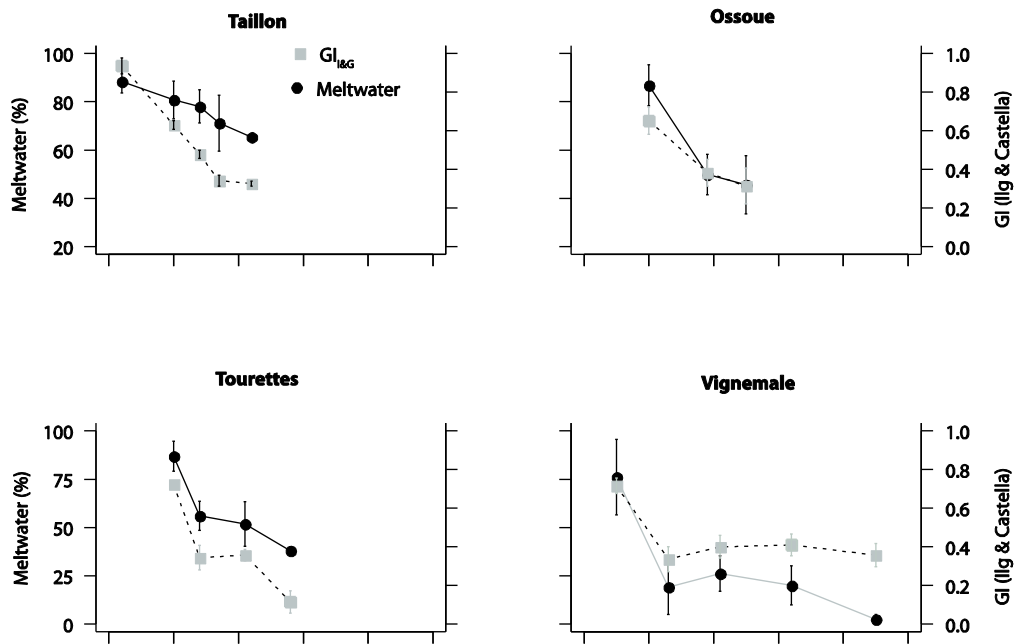
The highest mean meltwater contribution was recorded for the Taillon stream (78.0 ± 10.3), where all sites had a mean meltwater contribution of greater than 60% (Figure 3.3a). The lowest meltwater contributions were recorded for the Vignemale river basin (38.7 ± 18.5) where all sites except V1 had a mean meltwater contribution of less than 40% (Figure 3.3). A general trend of decreasing meltwater contribution with increasing distance from the glacier terminus ($\rho = -0.78$, $P < 0.001$) was stronger when streams were considered individually (all $\rho > 0.8$) except for the Vignemale ($\rho = -0.68$, $P < 0.001$). Differences in the rate at which meltwater proportions were reduced downstream due to groundwater inputs, varied between streams (Figure 3.3:Table 3.5). The Taillon displayed the shallowest response with the mean meltwater contribution at site T5 (>2km from the glacier) ~60 % (Figure 3.3). For the other three study streams meltwater proportions decreased rapidly between 1km and 2km from the glacier margin to ~50%.

Table 3.5. Values of the four methods for measuring glacier influence. SD is displayed in parentheses for $GI_{I\&C}$ and Meltwater (%).

Site	Glacier cover (%)	$GI_{J\&D}$	$GI_{I\&C}$		Meltwater (%)	
			2010	2011	2010	2011
G1	7	0.22	0.73 (0.02)	0.72 (0.01)	80.4 (3.8)	93.5 (2.8)
G2	5	0.17	0.34 (0.09)	0.35 (0.04)	52.7 (8.3)	59.4 (6.4)
G3	2	0.12	0.37 (0.03)	0.35 (0.03)	45.9 (11.8)	57.9 (10.5)
G4	2	0.09	0.14 (0.07)	0.09 (0.03)	37.1 (1.7)	39.1 (2.2)
O1	25	0.4	0.60 (0.07)	0.70 (0.02)	80.5 (4.9)	93.2 (5.9)
O2	8	0.26	0.34 (0.08)	0.42 (0.02)	48.4 (4.5)	51.3 (12.3)
O3	7	0.21	0.27 (0.05)	0.36 (0.11)	50.2 (7.4)	41.1 (15.8)
T1	32	0.6	0.90 (0.01)	0.97 (0.03)	85.9 (6.0)	90.9 (1.5)
T2	15	0.23	0.63 (0.01)	0.63 (0.03)	75.6 (7.9)	85.9 (3.0)
T3	5	0.18	0.48 (0.02)	0.48 (0.02)	73.1 (6.1)	83.0 (2.7)
T4	3	0.15	0.33 (0.04)	0.35 (0.01)	64.1 (13.3)	78.3 (2.6)
T5	3	0.12	0.33 (0.01)	-	65.5 (0.9)	-
V1	11	0.44	-	0.72 (0.04)	-	80.9 (15.7)
V2	2	0.16	0.42 (0.07)	0.39 (0.06)	40.7 (8.2)	41.1 (8.2)
V3	1	0.11	0.40 (0.08)	0.42 (0.04)	37.9 (7.3)	33.2 (10.0)
V4	1	0.08	0.37 (0.07)	0.33 (0.06)	22.2 (1.8)	21.7 (2.6)
VHS	2	0.12	0.34 (0.04)	0.34 (0.10)	41.3 (12.6)	29.4 (7.8)

Mean standardised $GI_{I\&C}$ scores (1-0) were highest for the Taillon stream (0.56 ± 0.23) and lowest for the Tourettes stream (0.39 ± 0.23). A strong negative correlation was apparent between GI and distance from the glacier terminus ($\rho = 0.66$, $P < 0.001$). The relationship between distance from the glacier terminus and $GI_{I\&C}$ was stronger when streams were considered individually (all $\rho > 0.8$); except for the Vignemale stream ($\rho = 0.8$, $P < 0.05$) (Figure 3.4). $GI_{I\&C}$ patterns mirrored those displayed by meltwater the highest mean value recorded at T1 (Table 3.5); however, for the Taillon stream, the downstream gradient was steeper than that displayed by meltwater contribution (Figure 3.3a).

(a)



(b)

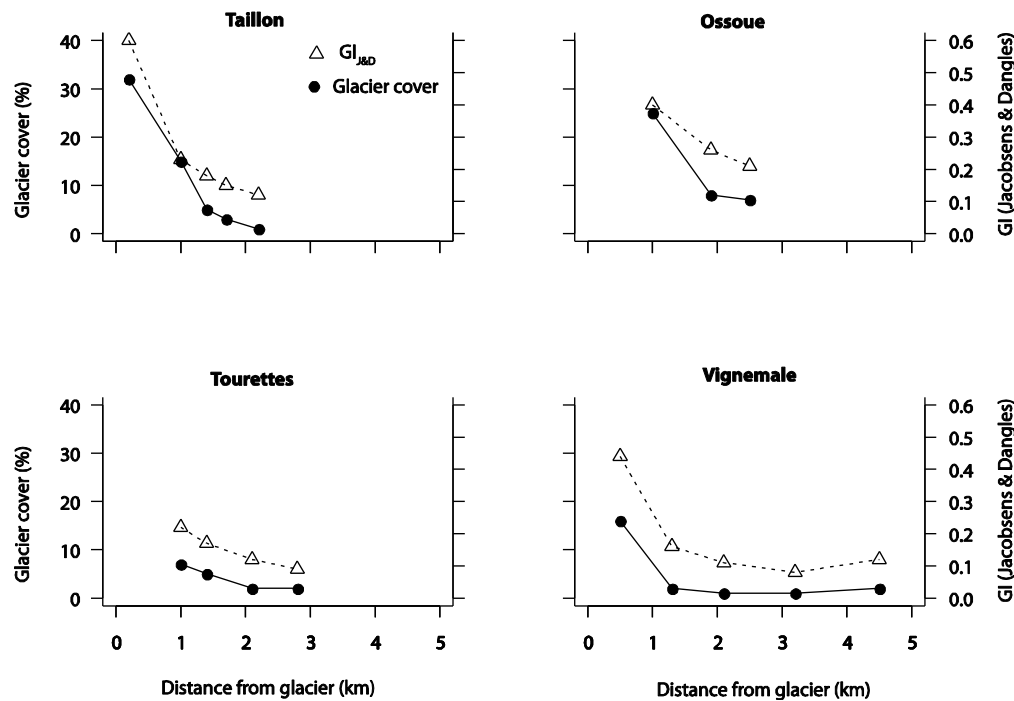


Figure 3.3. The relationship between distance from the glacier margin and; (a) the proportion of discharge sourced from meltwater (mean \pm SD) and the $GI_{I\&C}$ (mean \pm SD), and (b) the proportion of glacier cover in the catchment and $GI_{J\&D}$.

GCC and the $GI_{J \&D}$ displayed almost identical patterns along the downstream gradient (Figure 3.3b). However, the Ossoue had the highest mean value for glacier cover (13.33 ± 10.1) and $GI_{J\&D}$ (0.29 ± 0.19) in contrast to the $GI_{I \&C}$ and meltwater. Downstream patterns were broadly similar to those displayed by the other methods, and the highest values for both GCC and $GI_{J\&D}$ were recorded at T1 and lowest at V4 (Table 3.5). Unlike patterns for meltwater contribution, the Taillon stream displayed the steepest gradient for GCC and $GI_{J\&D}$ (Figure 3.3b).

Mean meltwater contribution recorded across both years were comparable at all sites (Table 3.5) with the exception of O1 and G1, where higher meltwater proportions were recorded in 2011. No clear temporal patterns were apparent across the individual melt seasons. However, particularly low meltwater contributions were recorded in 2010, sample date a, for the Taillon basin and Vignemale basin (Figure 3.4; Table 3.5). This corresponded to the coldest period recorded across the sampling period, with limited surface energy receipt available for snowpack melt (see Chapter 7; Appendix 3.3). Meltwater contribution was lower during 2010 for sites > 1 km from the glaciers and was linked to reduced valley snowpack size (lower winter precipitation during 2010/2011) and earlier melt onset (i.e. warmer spring conditions during 2011). This was particularly pronounced in the Vignemale basin (Figure 3.4). Interestingly, at the sites closest to the glaciers (T1, G1 and O1), meltwater contribution were higher during 2011 unlike $GI_{I\&C}$ scores which were comparable between years (Figure 3.4; Table 3.5). Temporal variability for $GI_{I\&C}$ was limited, with the differences between sample dates smallest for sites closer to the glacier margin (Figure 3.5; Table 3.5).

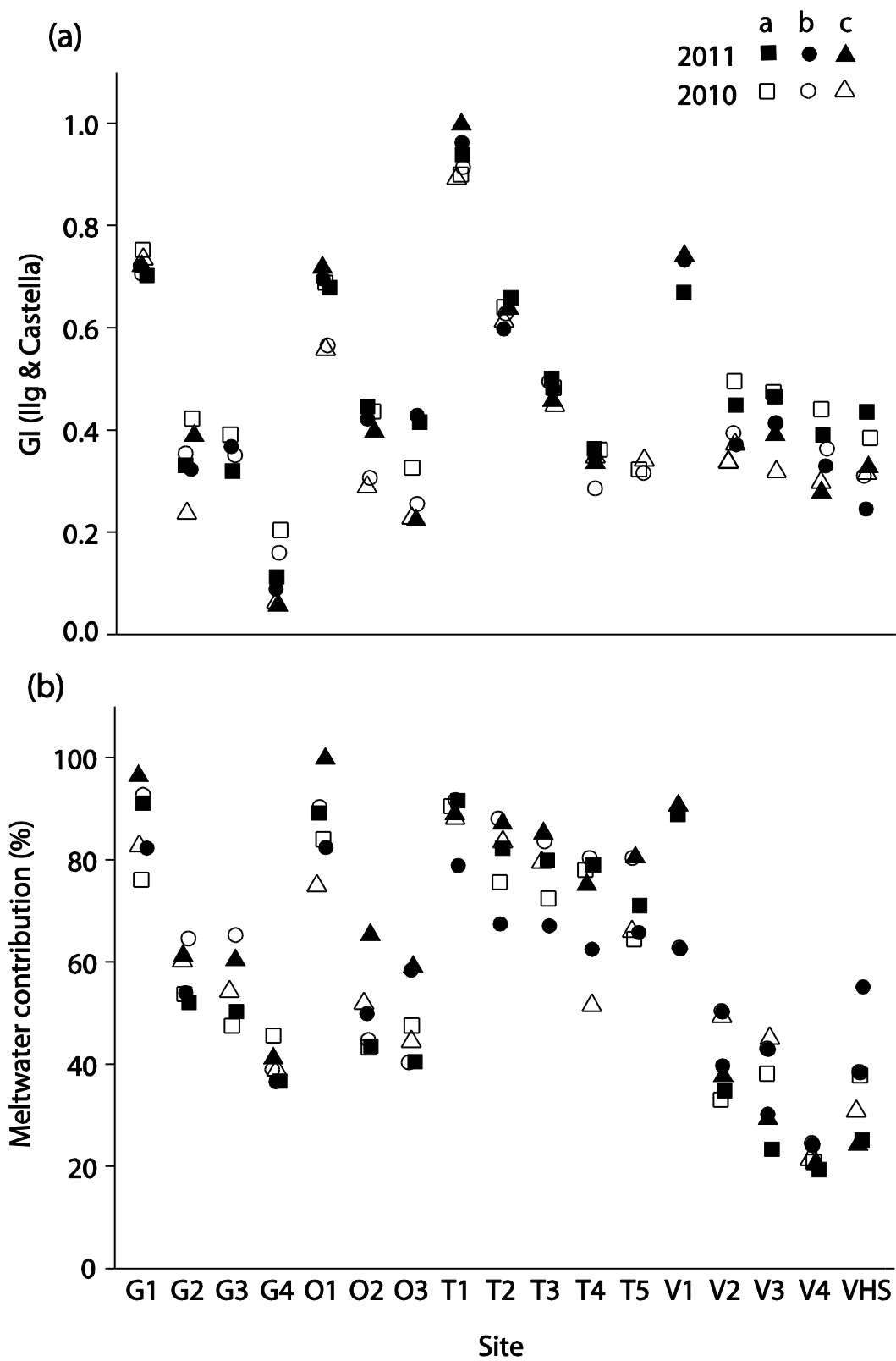


Figure 3.4. (a) GI (Ilg & Castella) and (b) meltwater contribution to bulk discharge recorded for all sampling sites and dates.

3.3.4. *Physicochemical habitat patterns along the glacier influence gradient*

PCA ordination of the twelve selected habitat variables, identified distinct gradients across the network of study sites (Figure 3.5). PC₁ explained 35% of the variance and represents a gradient of glacial (or meltwater) influence, with strong negative loadings for T_{min} and T_{mean} and strong positive loadings for PFAN, SSC, PH and shear stress (Table 3.6). PC₂ explained 17% of the variance and represents a geological and stream size gradient with negative loadings for EC and positive loadings for stream width and water depth. PC₃ explained 13% of the variances and is associated with a substrate size gradient (strong positive loading for D50). Sites were stretched along PC₁ (Figure 3.5) and those with positive scores for this axis were associated with higher meltwater contribution, GI scores and GCC (see Figure 3.6 for contour plots). Sites with positive scores for PC₁ displayed limited spread along PC₂. However, sites with negative scores (i.e. lower meltwater contribution/GI scores) were stretched along PC₂; this separated the sites with predominately crystalline geology (Vignemale and Ossoue) from the sites on sedimentary rock (Taillon and Tourettes). Three distinct groups could be identified: (i) the sites with high glacial influence; (ii) sites with lower glacial influence and sedimentary geology; and (iii) sites with lower glacier influence contribution and crystalline geology.

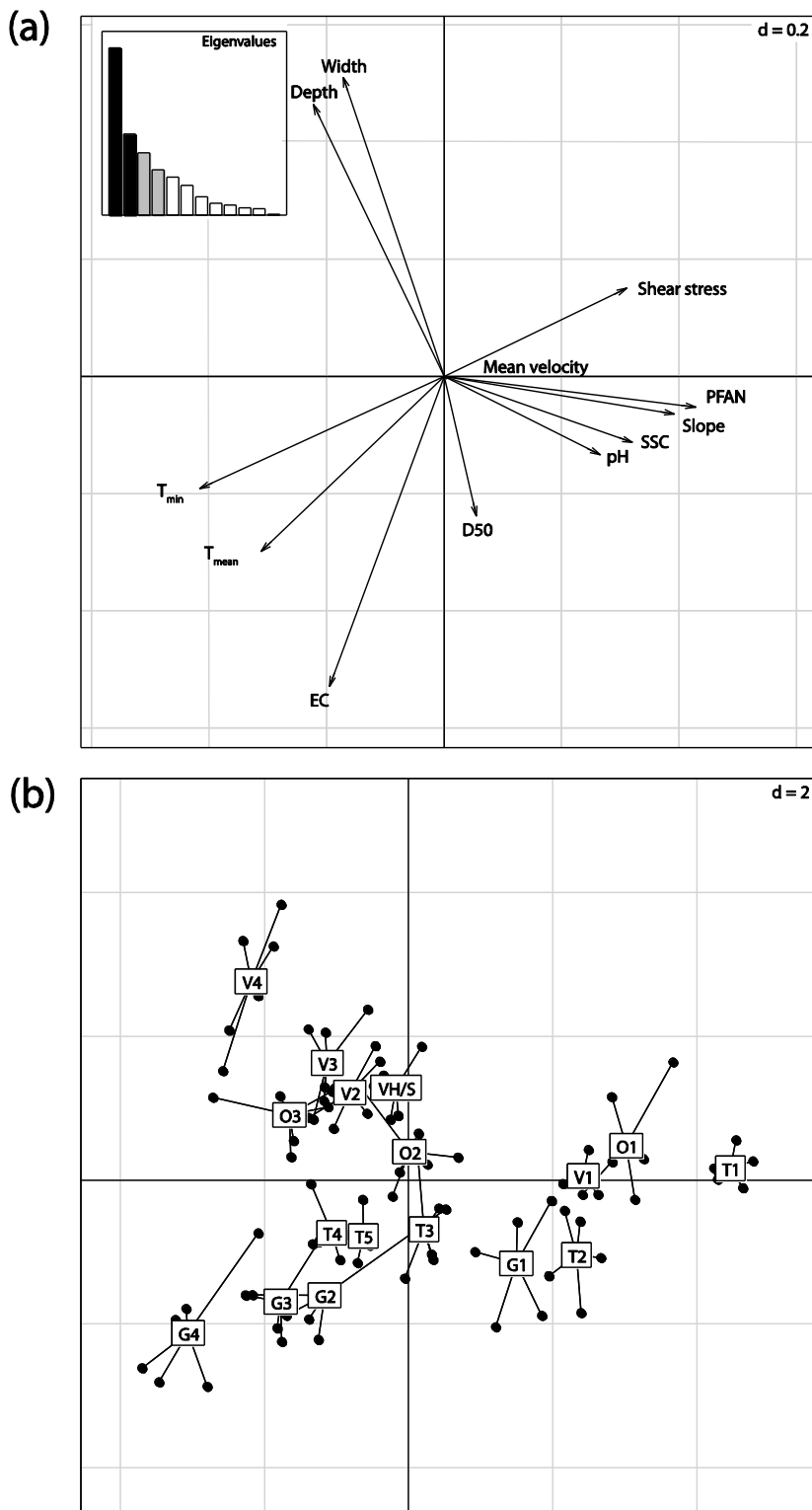


Figure 3.5. PCA ordination of 12 habitat variables for all sample dates. (a) Vector plot displaying the relationship between all habitat variables within the PC1 and PC2 axes. (b) location of all site-sample dates in ordination space defined by the PC1 and PC2. Site labels represent the centroid for all sample dates. Lines link individual sample dates to the site centroid. D denotes the ordination plot scale (i.e. the sub-grid dimension).

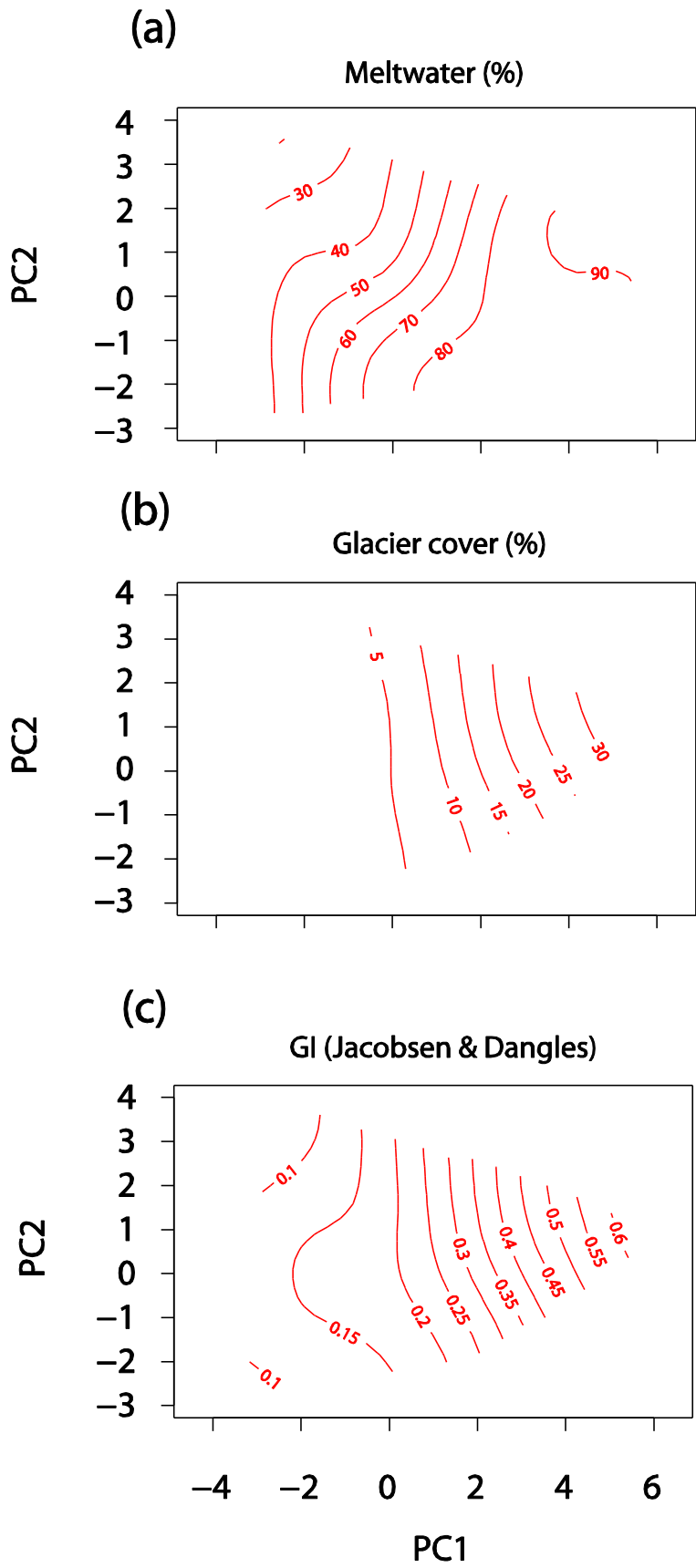


Figure 3.6. Surface plot of (a) meltwater porportion (b) glacier cover and (c) $GI_{J\&D}$ in relation to PC_1 and PC_2 .

Table 3.6. Eigen values and loadings of 12 measured habitat variables for the retained principal components.

	PC ₁	PC ₂	PC ₃	PC ₄
Eigen value	4.95	2.05	1.89	1.02
Variance	0.41	0.17	0.16	0.09
Stream width	0.37	0.77	-0.10	-0.27
Water depth	0.62	0.56	0.22	0.14
T _{mean}	0.65	-0.42	-0.39	0.30
T _{min}	0.89	-0.28	-0.06	0.13
pH	-0.68	-0.23	0.51	-0.24
EC	0.42	-0.83	0.11	-0.09
D50	-0.23	-0.23	-0.65	-0.26
PFAN	-0.90	-0.03	0.16	-0.11
SSC (log ₁₀)	-0.67	-0.22	0.45	0.12
Mean velocity	-0.32	-0.01	-0.66	-0.49
Shear stress	-0.68	0.21	-0.35	0.56
Slope	-0.83	0.00	-0.43	0.32

3.3.5. Physicochemical habitat – glacier influence relationships

Discharge. At all gauging stations an early season peak in flow was followed by a decline in discharge as the melt season progressed (Figure 3.7). However, this pattern was punctuated by precipitation events which corresponded to the highest observed flows. The highest mean discharge, $1.36 \pm 0.54 \text{ m}^3\text{s}^{-1}$ and lowest mean discharge $0.06 \pm 0.04 \text{ m}^3\text{s}^{-1}$ were recorded for site V4 and site G4 respectively while discharge was positively related to catchment area, ($\rho = 0.88, P < 0.05$). The standardised daily flow range (range/ mean discharge) was lowest at site V4 (0.17) and highest at site T3 (0.43) and was correlated to meltwater contribution ($\rho = 0.89, P < 0.05$) and, to a lesser extent, GCC ($\rho = 0.66, P < 0.1$) (Figure 3.8). No significant correlations were found between standardised flow range and GI_{J&D} or GI_{I&C} (Figure 3.8).

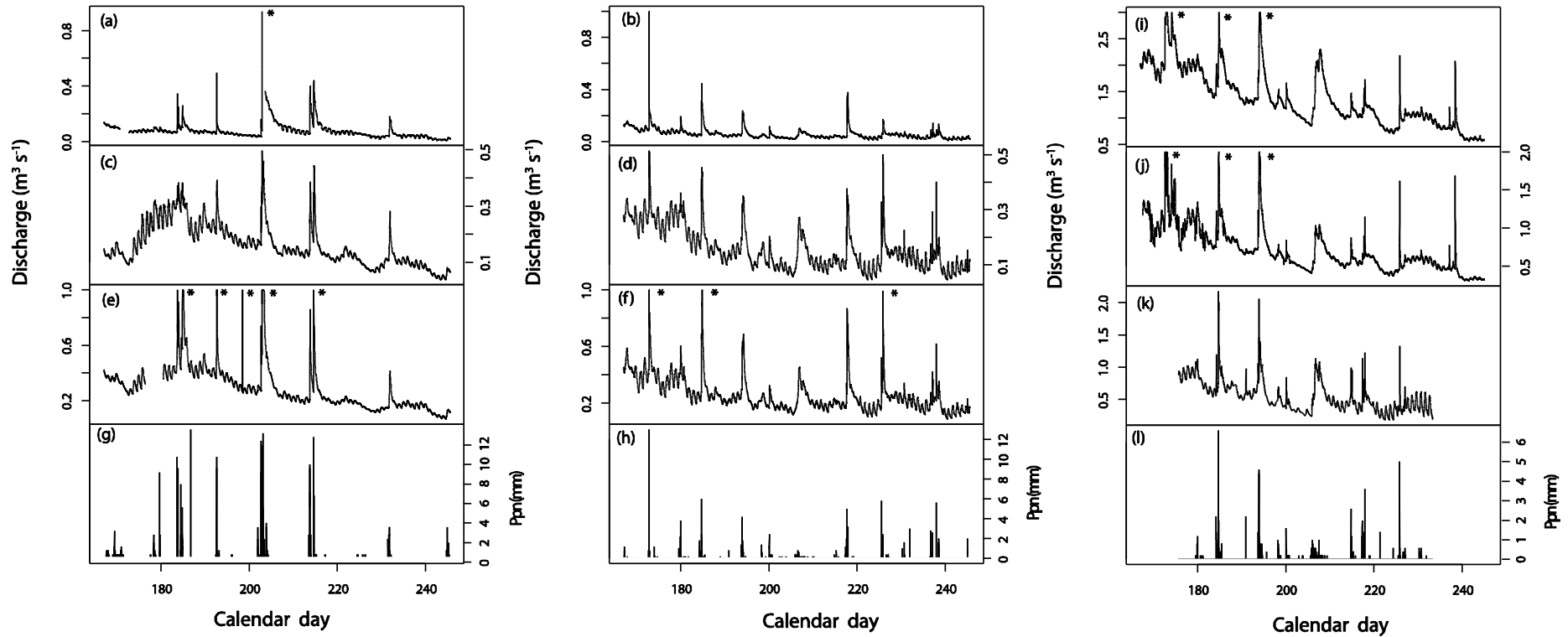


Figure 3.7. Discharge time series (15 min average) for: Tourettes gauge G4 during (a) 2010 and (b) 2011; Taillon gauge T3 during (c) 2010 and (d) 2011 and Taillon gauge T4 during (e) 2010 and (f) 2011. Precipitation time series (15 min totals) for the Taillon basin during (g) 2010 and (h) 2011. Discharge time series (15 min average) for: (i) Vignemale gauge V4 during 2011, (j) Vignemale gauge V2 during 2011 and (k) Ossoue gauge O3 during 2011. (l) Precipitation time series (15 min totals) for the Ossoue basin. *High flow events significantly greater than displayed axis range.

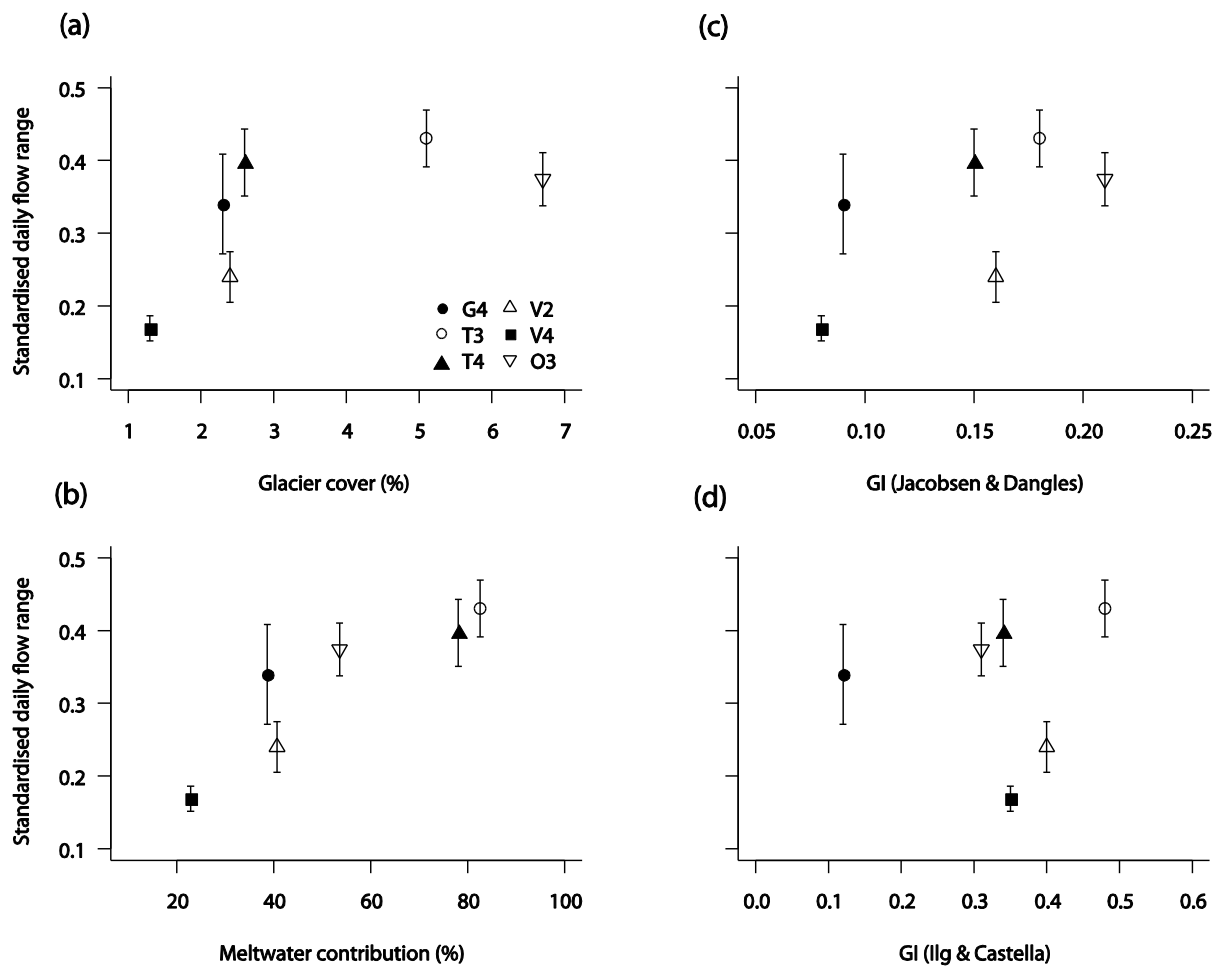


Figure 3.8. The relationship between mean standardized daily discharge range and (a) glacier cover in the catchment, (b) mean meltwater contribution at gauging site, (c) GI (Jacobsen and Dangles), and (d) GI (Ilg and Castella).

Table 3.7. Gauging site characteristics and flow metrics for the 2011 melt season. Ppn corrected range is the average diurnal discharge range for days when total precipitation was less than 3mm. SD is displayed in parentheses.

	Taillon-Gabiétous			Vignemale		Ossoue
	G4	T3	T4	V2	V4	O3
Gauge characteristics:						
Catchment area (km ²)	4.65	1.72	6.47	5.77	11.60	6.46
Glaciated area (%)	2.0	5.2	2.7	2.3	1.1	6.5
Mean meltwater proportion (%)	38.7(2.0)	82.6(6.9)	78.1(11.5)	40.7(7.3)	22.9(2.0)	53.6(12.1)
Daily flow metrics:						
Mean discharge (m ³ s ⁻¹)	0.06 (0.04)	0.16 (0.08)	0.26 (0.12)	0.71 (0.31)	1.36 (0.54)	0.54 (0.23)
Range (m ³ s ⁻¹)	0.03 (0.12)	0.09 (0.20)	0.16 (0.07)	0.29 (0.40)	0.36 (0.42)	0.31 (0.32)
Range, Ppn corr. (m ³ s ⁻¹)	0.02 (0.03)	0.07 (0.04)	0.10 (0.08)	0.17 (0.19)	0.23 (0.18)	0.20 (0.13)
Standardized flow metrics:						
Mean discharge (m ³ s ⁻¹ km ²)	0.01 (0.01)	0.09 (0.05)	0.04 (0.02)	0.12 (0.04)	0.12 (0.04)	0.08 (0.03)
Range (range/mean)	0.34 (0.07)	0.43 (0.04)	0.40 (0.05)	0.24 (0.03)	0.17 (0.02)	0.37 (0.04)

Water temperature. T_{\min} , T_{\max} and T_{mean} displayed strong negative relationships with GCC and $GI_{J \& D}$ (Table 3.8; Figure3.9) and the AIC scores suggested that difference in predictive power were negligible (all $AIC\Delta < 10$). Meltwater – water temperature relationships were generally weak with no significant relationship for T_{\max} or T_{mean} however a quadratic relationship was observed with T_{\min} (AIC = 338.8), yet the AIC score was significantly lower for GCC ($AIC\Delta = 30.6$) and $GI_{J \& D}$. ($AIC\Delta = 30.0$) (Table 3.8; Figure3.9). Further investigation of meltwater- T_w relationships (mixed effect ANCOVA) revealed a significant interaction between meltwater and stream for T_{\max} and T_{mean} , while for T_{\min} significant differences in intercepts between streams were apparent (Figure 3.10). For all sites and temperature metrics the slopes were negative and notably steeper for the Taillon. However the Ossoue was the exception as the slope for T_{mean} was close to 0 and for was positive for T_{\max} (Figure3.10).

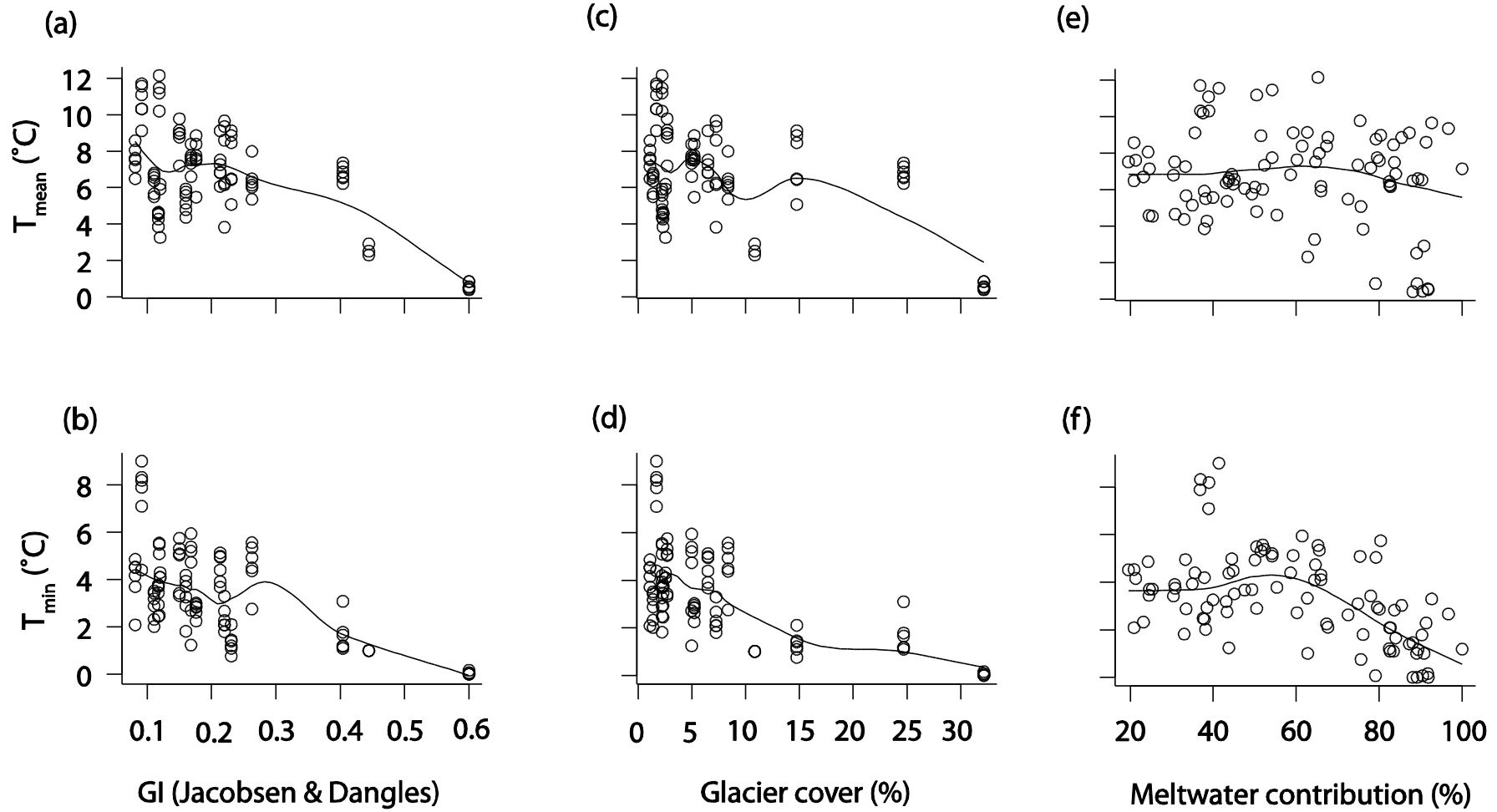


Figure 3.9. Scatterplots for the relationship between: (a) GI and T_{mean} ; (b) GI and T_{min} ; (c) glacier cover and T_{mean} ; (d) glacier cover and T_{min} ; (e) meltwater proportion and T_{mean} ; (f) meltwater proportion and T_{min} . Fitted line for each plot is a LOESS smoother (span = 0.5).

Table 3.8. Linear Mixed Model results for the relationship between water temperature metrics (response) and methods for quantifying glacier influence (predictor). Both significant and non-significant coefficients are displayed with standard errors. ***P < 0.001, **P < 0.01, ns = not significant.

Predictor variable	Response variable	T _{mean}			T _{min}			T _{max}		
		Value ± SE	t-value	P	Value ± SE	t-value	P	Value ±SE	t-value	P
Meltwater (%)	Intercept	6.37±0.84	7.51	***	1.35±1.23	1.09	ns	8.73±2.56	3.41	**
	Predictor	0.007±0.01	0.61	ns	0.11±0.04	2.68	**	0.11±0.09	1.21	ns
	Predictor ²	-	-	-	-0.001±0.00	-3.27	**	-0.001±0.001	-1.06	ns
			<i>AIC</i>	364.8		<i>AIC</i>	338.8		<i>AIC</i>	465.5
GI _{J&D}	Intercept	9.44±0.64	14.61	***	5.33±0.47	11.31	***	15.43±1.19	12.88	***
	Predictor	-12.46±2.57	-4.84	***	-9.14±1.74	-5.25	***	-17.38±4.94	-3.51	**
			<i>AIC</i>	336.5		<i>AIC</i>	303.8		<i>AIC</i>	431.3
Glacier cover (%)	Intercept	8.04±0.53	15.4	***	4.48±0.31	14.07	***	13.54±0.91	14.91	***
	Predictor	-15.97±4.47	-3.57	**	-14.09±2.73	-5.15	***	-21.57±7.77	-2.77	**
			<i>AIC</i>	342.4		<i>AIC</i>	303.2		<i>AIC</i>	434.1

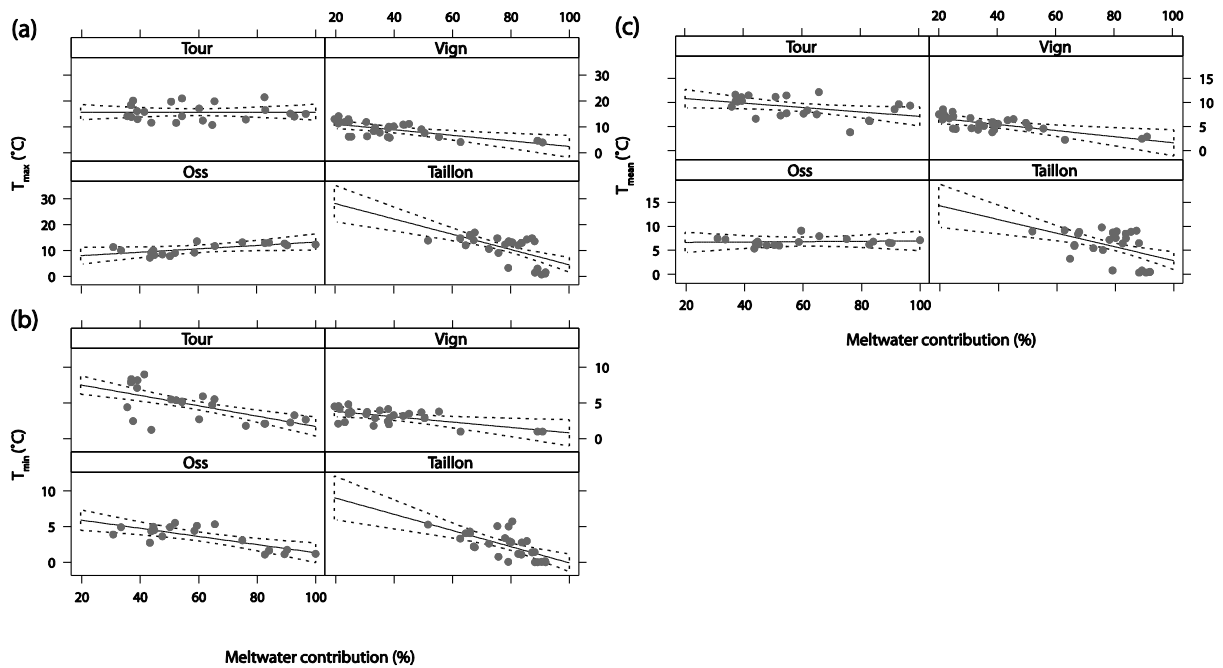


Figure 3.10. Panels represent fitted models for meltwater contribution by stream for: (a) T_{\max} (ANCOVA; Meltwater*Stream, $F = 2.91$, $P = 0.04$); (b) T_{\min} (ANCOVA; Meltwater*Stream, $F = 4.1$, $P = 0.02$); and (c) T_{mean} (ANCOVA: Meltwater*Stream, $F = 5.2$, $P = 0.003$). Tour = Tourettes, Vign = Vignemale and Oss = Ossoue). Dashed lines represent 95% confidence bands.

Other variables. All glacier influence metrics were negatively related to width and depth of the river channel and positively correlated related to Shear stress and slope (Table 3.9). Only meltwater contribution was positively related to D50, while mean/max velocity and % cobbles (clasts >100mm) were not correlated to any of the methods (Table 3.9).

Table 3.9. The t-values of the regression parameter (beta coefficient) from liner mixed models investigating the relationship between method of measuring glacier influence and physicochemical variables. The significance of the term is displayed ($\hat{P} < 0.1$, $*P < 0.05$, $**P < 0.001$ and $***P < 0.001$, ns = not significant).

Variable	Melt-water (%)	Glacier cover (%)	GI (J & D)	GI (I & C)
Width	-1.68 [^]	-1.74 [^]	-1.82 [^]	ns
Depth	-2.88 ^{**}	-3.22 ^{**}	-3.11 ^{**}	ns
D50	2.34 [*]	ns	ns	ns
Shear stress	3.32 ^{**}	4.45 ^{***}	3.14 ^{**}	3.94 ^{**}
Slope	2.95 ^{**}	6.36 ^{***}	4.68 ^{***}	3.39 ^{**}
% cobbles	ns	ns	ns	ns
Mean velocity	ns	ns	ns	ns
Max velocity	ns	ns	ns	ns

Glacier influence-geology interaction. Significant differences in EC, pH and SSC were recorded between sites of differing geology (Table 3.10). For crystalline sites EC, SSC and pH were all lower than for sedimentary sites (Figure 3.11). However, no significant difference in bed stability (PFAN) was recorded but significant interactions were recorded between meltwater contribution and geology for all tested habitat variables except pH (Table 3.11; Figure 3.12). For PFAN and SSC the slope was steeper for sedimentary sites, while for EC the slope was shallower and the intercept greater (Table 3.11; Figure 3.12). Both GCC and GI_{J&D} displayed significant interactions with geology for EC, SSC and pH but not for bed stability (PFAN). The slopes for SSC and pH were steeper and for EC shallower when considering the relationships for sedimentary sites (Table 3.11; Figure 3.12). AIC scores and R² values suggest meltwater is the better predictor of EC (AICΔ = 16.3), while GI_{J&D} is the best predictor of PFAN (AICΔ = 7.9) and GCC and GI_{J&D} are comparable (AICΔ < 3) predictors for, SSC and pH.

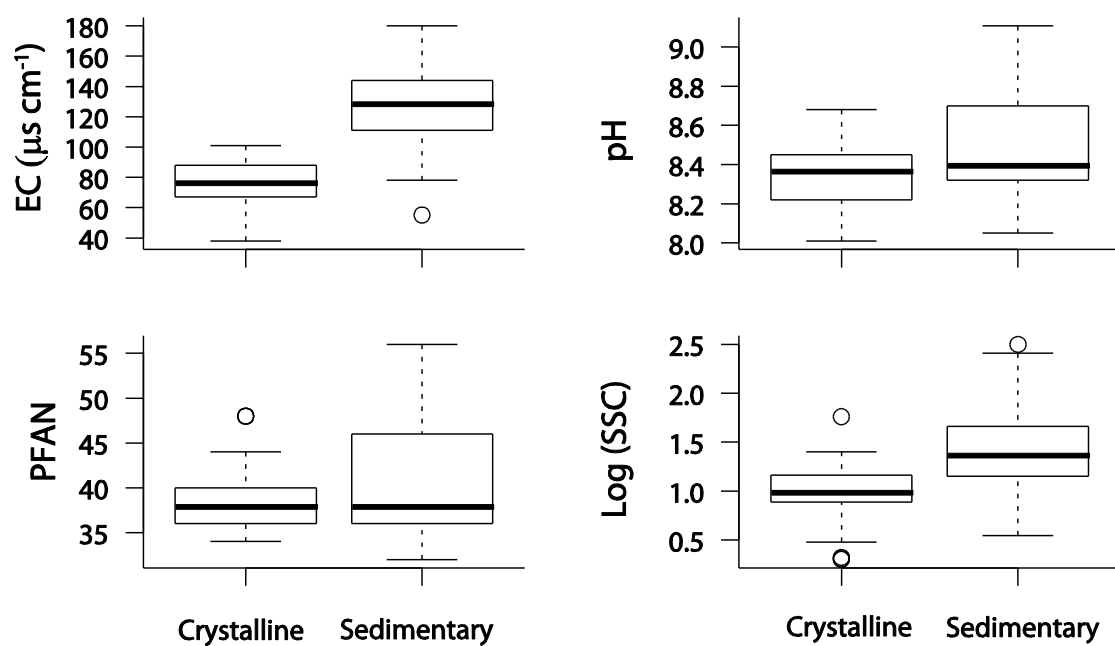


Figure 3.11. Boxplots of habitat variables grouped by geology.

Table 3.10. One way-mixed effect ANOVA testing the difference in physicochemical variables (EC, pH, SSC and PFAN) between sites of different geology. The random effects were multi-levelled with site nested within year to account for repeated measures at each site. (* $P < 0.05$, ** $P < 0.001$ and *** $P < 0.001$, ns = not significant).

Variable	Df	F	P
EC	29	57.2	***
pH	29	4.8	*
Log ₁₀ (SSC)	29	8.6	**
PFAN	29	1.8	ns

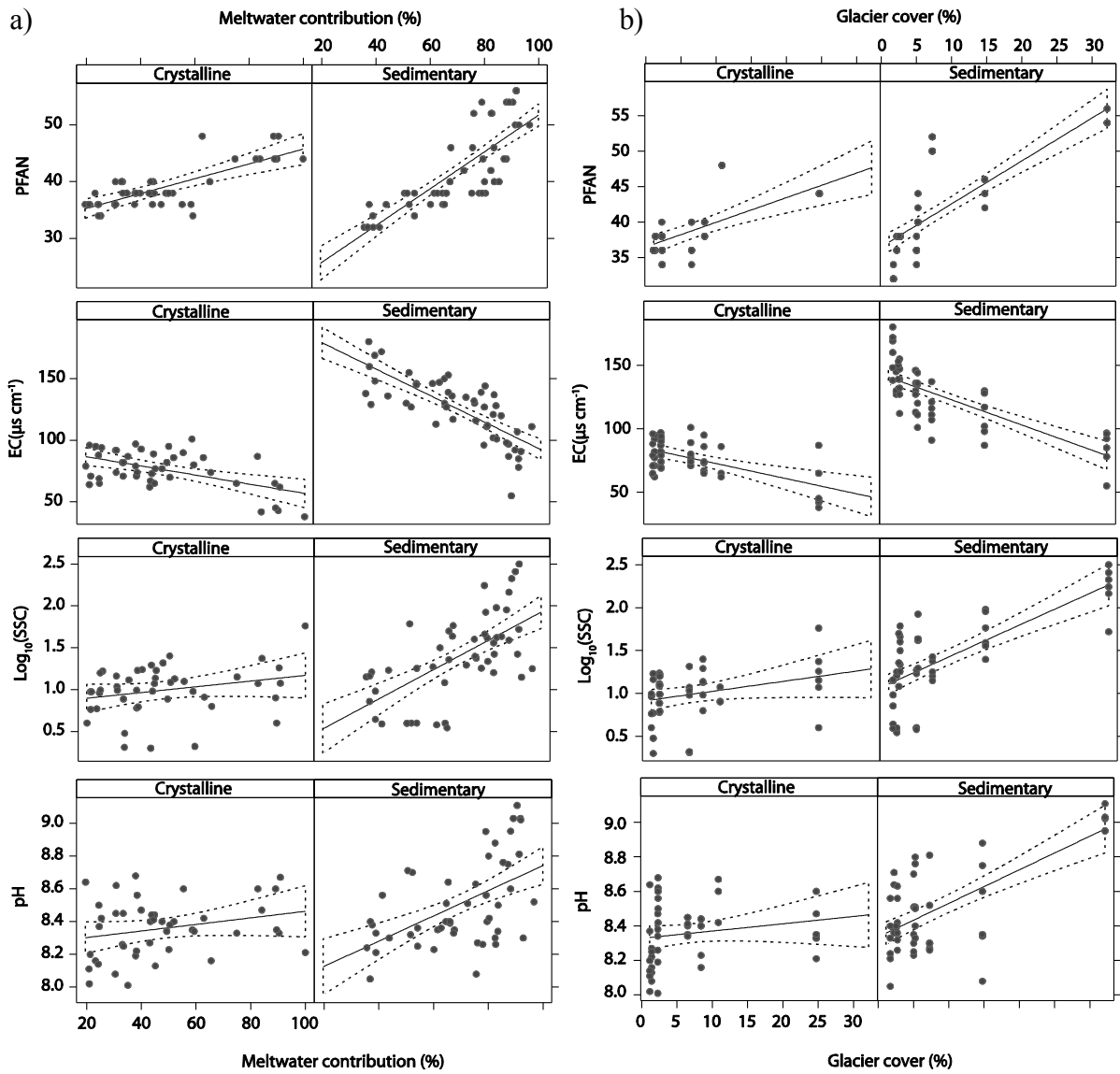


Figure 3.12. Panels represent fitted models for (a) meltwater contribution and response variables (PFAN, EC, SSC and pH) by geology and (b) glacier cover in the catchment by geology. Dashed lines represent 95% confidence bands.

Table 3.11. Mixed-effect model (site nested in year) results for the interaction between geology and methods for estimating glacier influence (CP = continuous predictor). * $P < 0.05$, ** $P < 0.001$ and *** $P < 0.001$, ns = not significant.

Response	Predictor	CP: Meltwater				CP: Glacier cover				CP: GI _{J&D}			
		Value	SE	<i>P</i>	AIC	Value	SE	<i>P</i>	AIC	Value	SE	<i>P</i>	AIC
PFAN													
	Intercept	39.50	1.65	***	422.2	36.48	1.24	***	398.3	33.16	1.65	***	390.4
	CP	-0.01	0.02	ns		34.74	12.05	**		27.32	6.84	***	
	Geology (Sed)	-3.18	2.83	ns		-0.04	1.70	ns		-0.08	2.13	ns	
	CP x Geology (Sed)	0.09	0.03	**		26.02	15.11	ns		12.62	8.57	ns	
EC													
	Intercept	93.19	7.75	***	749.5	84.86	5.75	***	765.8	88.51	7.09	***	771.1
	CP	-0.35	0.12	**		-116.66	32.99	**		-56.18	23.25	*	
	Geology (Sed)	94.35	11.90	***		57.26	4.69	***		63.75	7.23	***	
	CP x Geology (Sed)	-0.55	0.18	**		-79.19	41.42	*		-69.26	29.10	*	
Log(SSC)													
	Intercept	0.89	0.19	***	60.6	0.91	0.11	***	48.6	0.85	0.15	***	49.9
	CP	0.00	0.00	ns		1.20	0.83	ns		0.71	0.54	ns	
	Geology (Sed)	-0.62	0.28	ns		0.14	0.12	ns		0.01	0.17	ns	
	CP x Geology (Sed)	0.01	0.00	**		2.60	1.04	*		1.69	0.68	*	
pH													
	Intercept	8.28	0.10	***	-52.7	8.33	0.06	***	-68.5	8.28	0.08	***	-71.3
	CP	0.00	0.00	ns		0.40	0.48	ns		0.37	0.30	ns	
	Geology (Sed)	-0.05	0.18	ns		0.02	0.07	ns		-0.04	0.09	ns	
	CP x Geology (Sed)	0.00	0.00	ns		1.50	0.61	*		0.88	0.37	*	

3.3.6. Relationship between methods

All methods showed reasonably good agreement and significant positive correlations were evident for all pairwise comparisons (Figure 3.13). As expected, $GI_{J\&D}$ and GCC in the catchment were highly correlated ($\rho = 0.94$) and displayed a linear relationship. For meltwater contribution the strongest correlation was with $GI_{I\&C}$ ($\rho = 0.71$). Spread was greater at the lower values and was related to the differing meltwater-temperature relationships between streams, particularly the Tourettes and Vignemale (Figure 3.14).

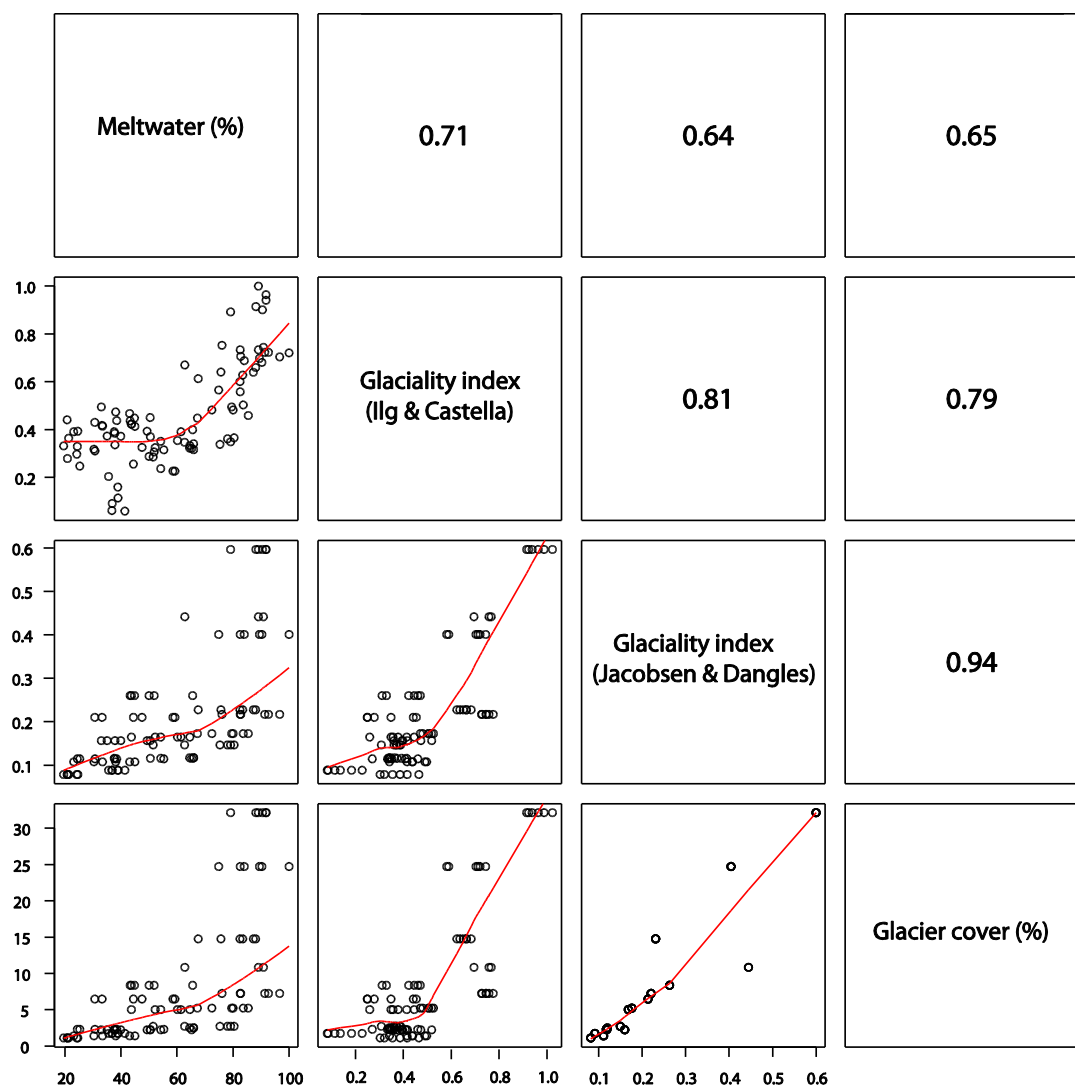


Figure 3.13. Scatter plot matrix for all methods for estimating glacier influence. Fitted line for each panel is a LOESS smoother (span = 0.5). Values in upper panel are Pearson's product moment correlations (all correlations are significant at $P < 0.01$).

While relationships between meltwater- $GI_{J\&D}$ and GCC were weaker ($p < 0.7$), the relationship was non-linear and appears to be exponential (Figure 3. 13). When sites ranked according to each method (i.e. 1= highest glacier influence, 17 = lowest glacier influence), GGC and $GI_{J\&D}$ were closest ($d = 6.6$) and glacier cover and $GI_{I\&C}$ furthest ($d = 18.8$). Meltwater contribution was closest to GGC ($d = 10.6$) and furthest from $GI_{I\&C}$ ($d = 16.5$). However, when only sites $< 1.5\text{km}$ from the glacier margin were considered $GI_{I\&C}$ rankings were closet to meltwater contribution ($d = 1.4$) and furthest from glacier cover.

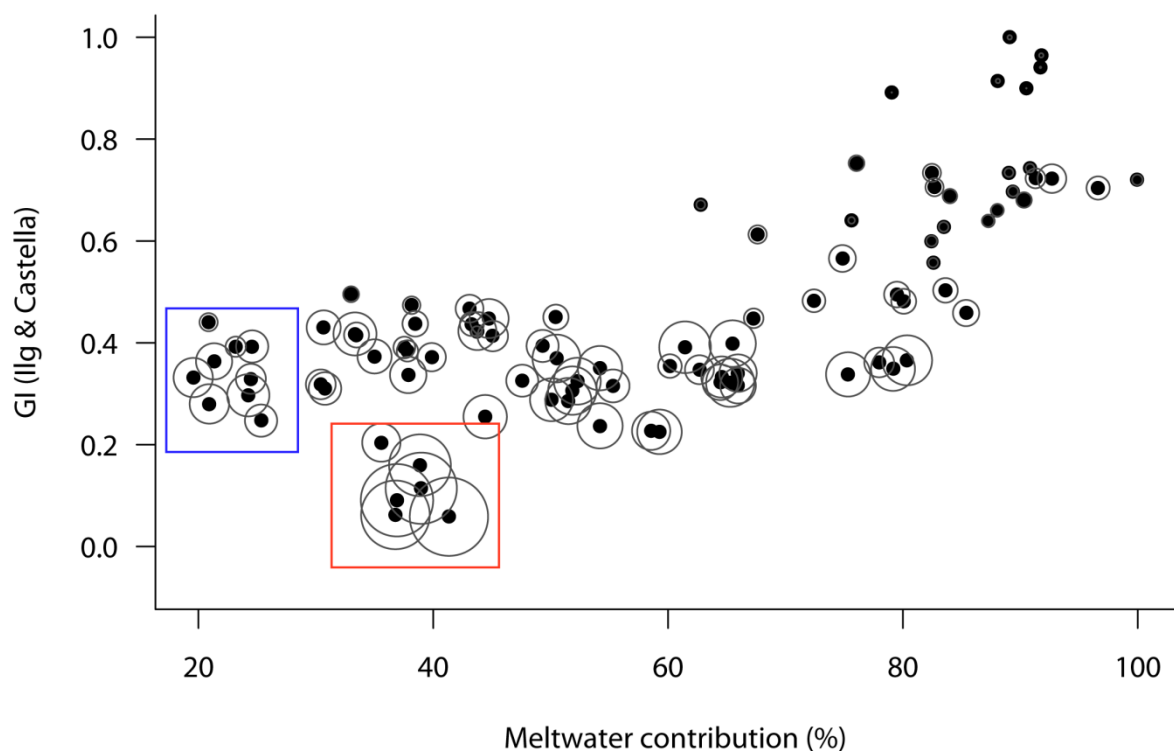


Figure 3.14. Relationship between meltwater proportion and $GI_{I\&C}$. The circles represent water temperature (T_{\min} °C) with the radius proportional to the scaled (0-1) water temperature. The red and blue boxes highlight samples from Tourettes (G4) and Vignemale (V4) respectively.

3.4. Discussion

The aim of this chapter was to identify the relationship between multiple methods for measuring glacial influence, and their relationship with physicochemical habitat variables across multiple alpine river basins. Herein the detailed analysis presented in section 3.3 is synthesised to give fresh insight into (i) the physicochemical habitat template of alpine rivers and how the various metrics of glacier influence represent/reproduce this, (ii) the role of geology as a macro scale filter on the relationship between habitat and glacier influence, and (iii) the relationship between these metrics.

3.4.1. *Spatial and temporal patterns in methods for measuring glacial influence*

In this study all sites were specifically selected to represent a gradient of glacier influence to enable direct comparison between methods for quantifying glacier influence. As expected each method identified a distinct downstream gradient of decreasing glaciality with increasing distance from the glacier snout. However, the downstream rate of change varied between streams and methods. This was particularly the case for the Taillon and Tourettes streams (Figure 3.3), with the downstream attenuation of the glacier signal in the Taillon stream less rapid when considering meltwater contribution compared to other methods. This was probably due to the limited tributary inputs (alluvial groundwater/karstic springs) along the section of the stream upstream of the confluence with the Tourettes stream (Smith *et al.* 2001). Hence, while GCC and $GI_{J\&D}$ decreased due to the static linear relationship with glacier size and distance from the snout, the lack of tributary inputs meant very little change in the meltwater:groundwater ratio occurred. While for the Tourettes stream both meltwater contribution and $GI_{I\&C}$ identified distinct downstream decreases which the other methods did not (Figure 3.3). Again, this appears to be related to groundwater tributary inflow, as there

are numerous hillslope tributaries between site G1 and G4, which reduced the meltwater:groundwater ratio (Brown *et al.* 2006d, 2007c).

The greater temporal variability for meltwater contribution than $GI_{I\&C}$, was interesting given that Brown *et al.* (2010b) identified a strong linear relationship between the two methods. In addition no distinct temporal trend regarding meltwater contribution could be identified unlike that of Brown *et al.* (2006d) which could be due to the lower resolution of either the sampling regime employed in this study or the mixing model used. Brown *et al.* (2006d) and Mellor (2012) both used a three component mixing model approach and split the meltwater contribution into two end members; quickmelt (englacial melt and snowmelt) and distributed melt (slower routed meltwater which has passed through the sub-glacial drainage system) and identified shifts from quickmelt to distributed flow as the melt season progressed. In this study, due to the broader spatial scale it was not possible to collect sufficient samples to enable a three component separation for all streams due to logistical constraints. Therefore, in this study the shift from quickmelt dominated flow to distributed flow identified by Brown *et al.* (2006d) and Mellor (2012) could not be identified, while as in this study, shifts in groundwater contribution were generally more subtle. Water sourcing is also particularly sensitive to prevailing meteorological conditions (Hannah *et al.* 2000; Blaen *et al.* 2013a); however, it should be noted that this did not appear to change the general trends identified in this study. For example, in early 2010 (sample date a), air temperature and surface shortwave radiation receipt were particularly low (Appendix 3.4), likely leading to reduced meltwater production (Hannah *et al.* 2000), yet a clear downstream reduction in meltwater contribution was still apparent for the Taillon stream (See Figure 3.4b).

3.4.2. *Relationship between glacial influence and important biological variables*

Numerous biological studies have examined benthic habitat characteristics of alpine glacier fed streams in relation to faunal patterns (e.g. Snook and Milner 2001, Knispel and Castella 2003, Lencioni, and Rossaro 2005, Cadbury *et al.* 2011). However, many of these have been related to spot measurements on single sample dates or to single streams/basins. In this study multiple sample dates across two years (i.e. 6 sample dates) were used and multiple streams/basins were investigated. A distinct harsh-benign gradient was identified running from high to low glacial influence (see PCA ordination Figures 3.5 and 3.6) as in other studies from alpine river systems (Milner *et al.* 2001; Brown *et al.* 2007b; Füreder 2007). However, some important differences were identified regarding the precise nature of the physicochemical habitat template described by each method of measuring glacial influence.

Diurnal discharge variability; the daily glacial melt pulse, is an important control on benthic diversity patterns (Cauvy-Fraunié *et al.* 2013a) and in this study was strongly associated with meltwater contribution. This is likely due to the quantification of meltwater contribution being hydrologically meaningful which can account for both groundwater attenuation and also snow melt contribution, which other methods did not account for (Brown *et al.* 2009b, 2010b). For example, the weaker relationships between discharge variability and GGC may be due to variability in the attenuation of the glacier meltwater signal between streams, such as that outlined above for the Taillon and Tourettes streams.

Water temperature metrics (T_{mean} , T_{max} and T_{min}) were related to glacier cover and $GI_{J\&D}$ but only T_{min} was related to meltwater contribution (Table 3.8). For all temperature metrics an increase was associated with a decrease in glacial influence which is similar to other studies which have shown the presence of glaciers has a strong moderating effect on stream temperature in many studies (Cadbury *et al.* 2008; Fellman *et al.* 2013; Blaen *et al.* 2013b). Primarily, glaciers provide a constant cold water input, dampening the relationship with air temperature which is particularly apparent in systems fed by larger glaciers (Cadbury *et al.* 2008; Chikita *et al.* 2010), where stream discharge and meltwater volumes are high and thus increase the thermal capacity of the water column (Poole & Berman 2001). In this study, while glacier cover and $GI_{J\&D}$ were the best predictors of stream water temperature the residuals displayed heteroscedasticity, with greater spread for lower predictor values (see Appendix 3.5). This was probably due to: (i) at sites with lower glacier cover, other controls on stream temperature become more important (Fellman *et al.* 2013) hence, variability between streams is more pronounced; and (ii) the low number of sites with >10% glacier cover, hence a better coverage of the range of predictor values spread is required to make confidence predictions based on glacier cover.

The residuals for the meltwater LMMs did not suggest violation of homogeneity (Appendix 3.5) and good coverage across the range of possible values for the predictor (meltwater) was apparent. Further investigation using ANCOVA analysis identified a significant interaction with stream (Figure 3.10). This was probably due to a number of factors such as differing stream morphology (i.e. depth:width ratios), groundwater tributary water temperatures aspect and topographic shading (Isaak & Hubert 2001; Poole & Berman 2001; Brown & Hannah 2008). For example the Taillon stream displayed rapid downstream warming due to a high width to depth ratio (Brown *et al.* 2006a) despite only a small decrease in the meltwater

contribution. While for the Ossoue no warming was apparent, probably due to the steep valley sides and incised river channel between O1 and O2 which result in increased topographic shading, reducing solar warming of the water column (Isaak & Hubert 2001). Finally, the temperature of groundwater tributaries recorded in this (see Appendix 4.1) and other studies (Brown & Hannah 2008) was highly variable and punctuated the thermal patterns associated with decreases in glacial influence (Milner & Petts 1994).

Shear stress which can limit both the biota able to colonise a specific river reach (Snook & Milner 2001; Milner *et al.* 2001) and primary productivity (Uehlinger *et al.* 2010) was associated with all methods for measuring glacier influence (Table 3.9). Mérioux and Dolédec (2004) showed hydraulic stress was related to benthic taxa distributions and found the functional groups clinger and filterer were associated with higher shear stress conditions. As in this study, Snook & Milner (2001) observed reductions in shear stress or 'hydraulic stress' at sites of lower glacial influence which limited the benthic community to taxa with resistant and resilient traits (Snook & Milner 2002). Interestingly only meltwater contribution was associated with D50 (median particle size), which is surprising as reach scale particle sorting is generally related to distance downstream and shear stress (Knighton 1980). This could again be a function of the hydrological process basis of the meltwater contribution approach, as sites with increased meltwater contribution would likely have greater annual variability in shear stress and tractive force. SSC, bed stability, EC and pH were also associated with all methods of quantifying glacial influence but geology interacted with these variables and is discussed below.

3.4.3. *Interaction between glacier influence and habitat characteristics*

Bedrock geology was an important control on a number of reach scale habitat variables; particularly EC, pH and SSC/turbidity as in other studies (Richards *et al.* 1996; Young *et al.* 2005). The higher solubility of sedimentary rocks, such as those underlying the Taillon and Tourettes drainages, lead to the increased EC and pH at these sites (Young *et al.* 2005). Furthermore, the higher SSC recorded at sedimentary sites compared to crystalline sites is similar to findings by Sadle and Wohl (2006), who recorded high sediment volume and smaller grain size of fine sediments at sites draining sandstone catchments. Kelson and Wells (1989) also recorded a smaller bedload grain size at sedimentary sites and attributed it to the higher stream power and discharge per unit area for crystalline sites. While this appears to be the case for the sites studied here (i.e. highest discharge per km² for crystalline sites V2 and V4), the presence of glaciers is an important factor which needs to be considered. Particularly as the stream with the highest SSC is fed by a glacier which has undergone significant retreat and downwasting since the late 19th century (Hannah *et al.* 2000). The development of a significant glacial outwash plain at the terminus of the Taillon now serves as a sediment source where deposited sediments can be mobilised both during both high flow events and the diurnal glacier melt cycle.

The interaction of bedrock geology and glacier influence, altered the physicochemical habitat trajectory for a number variables (Table 3.11, Figure 3.12). The general amelioration of habitat condition as glacial influence reduces has been widely reported (Füreder *et al.* 2001; Snook & Milner 2001; Knispel & Castella 2003; Milner *et al.* 2010); however, other than the influence of lakes on habitat characteristics macro-scale basin properties have been largely ignored (Milner & Petts 1994; Hieber *et al.* 2005). In sedimentary streams SSC was greater

but decreased rapidly as glacier influence decreased probably driven by differences in erosion and sediment production between rocks of differing resistance which can be orders of magnitude greater for glaciers on sedimentary geology (Hallet *et al.* 1996). For EC increases in are associated with decrease in glacier influence, this was particularly pronounced for sedimentary streams, where EC of groundwater tributaries was significantly greater than the main channel due to the more rapid dissolution of bedrock in groundwater aquifers (Brown *et al.* 2006d). In crystalline streams residence time of groundwater is often shorter and dissolution/weathering of bedrock material slower (Soulsby *et al.* 1998); hence, tributary inputs can punctuate the increase in EC associated with decreasing glacier influence. For pH the interaction with geology was not as pronounced and higher pH was associated with sites closest to the glacier margin. This is primarily due to CO₂ being excluded from weathering sites (closed systems) and a large supply of comminuted rock and a dilute water supply (Brown 2002). Interestingly, bed instability, measured as PFAN, was higher under increased glacier influence for sedimentary streams (Figure 3.12), possibly due to the higher sediment transport and deposition rates leading to a prevalence of wandering channels.

3.4.4. *Concordance between methods for glacier influence*

The distinct linear relationship between meltwater contribution and GI_{I&G} identified in other studies (i.e. Brown *et al.* 2010) was not apparent here (Figure 3.13). While it did appear to be linear at higher meltwater contribution, at lower meltwater contributions and GI_{I&G} values this breaks down. This is likely related to differences in water temperature between river basins (highlighted in Figure 3.14); with lower water temperature in the Vignemale and Ossoue leading to higher GI values despite comparable, or in the case of the Vignemale lower meltwater contribution. As expected glacier cover and GI_{J&D} strongly related and can be

considered interchangeable measures of glacier influence. The distinct non-linear relationship between these two measures and meltwater contribution was not surprising as a certain threshold is reached regarding glacier cover/GI_{J&D} whereby increases will cause negligible increases in meltwater contribution as this has reached an asymptote and sampling closer to the glacier while increasing the glacier cover in the upstream catchment will not change the relative proportions of meltwater and groundwater. When considering how these methods ranked the sites in terms of glacier influence, it is not surprising that GGC and GI_{J&D} showed the highest concordance (lowest distance). However, perhaps of most interest for conservation and monitoring in the context of climate change, for sites closest to the glacier margin GI_{I&C} and meltwater contribution were closest. Particularly as it is the instream physicochemical habitat template, directly used in the calculation of GI_{I&C} which dictates benthic diversity patterns (Hannah *et al.* 2007; Brown *et al.* 2010b).

3.5. Conclusions

Data collected across two consecutive summer melt seasons from a network of stream monitoring sites enabled a robust assessment of relationship between methods for defining glacial influence and physicochemical habitat. While the four methods were all associated with a similar suite of habitat variables some important differences and similarities have been identified. First, a spatial mismatch in the quantification of glacial influence, particularly when comparing static (i.e. glacier cover) and dynamic (i.e. meltwater contribution) measures, which appeared to be associated with varying rates of downstream attenuation of the glacial signal by tributary inflows (Objective 1). Second, the relationships with hydrological variables (flow and water temperature) were particularly variable between methods (Objective 3). As the quantification of meltwater contribution was the only method

underpinned by hydrological processes it is not surprising that it was related to ecologically important flow metrics, such as diurnal discharge variability (Cauvy-Fraunié *et al.* 2013). However, water temperature was not strongly related to any of the monitoring methods and, particularly at lower glacial influence, basin and reach scale controls appear to become increasingly important (Fellman *et al.* 2013; Blaen *et al.* 2013b). Hence, the need for a monitoring approach which incorporates a suite of biologically important variables (Brown *et al.* 2003). Third, basin geology interacted with habitat-glacial influence relationship and needs to be considered when monitoring for change (Objective 2). These points need to be carefully considered when either using these methods as tools for identifying hydroecological change or to define a habitat gradient for elucidating pattern and process of alpine benthic communities. Furthermore, it is clear that the predicted rise in surface air temperature for southern European alpine regions (Beniston 2012) will lead to a significant reduction in cryospheric land cover (Zemp *et al.* 2006; Grunewald & Scheithauer 2010). This in turn will likely have significant implication for alpine river habitats, as the steep environmental gradients identified in this chapter will become less pronounced, potentially altering the structure and composition of associated benthic communities. Large scale monitoring networks are required which cover the range of macro-scale abiotic diversity as, while only bedrock geology was investigated in this chapter, it is likely other features, such as basin morphology or exposure (leeward/windward), modify the relationship between glacier influence and habitat (Weekes *et al.* 2012). Isolation of the climate (glacier retreat) signal from the noise (i.e. macro-scale heterogeneity) is particularly important if we are to develop adaptable conservation strategies for this highly dynamic ecosystem.

3.6. Chapter summary

In this chapter methods for quantifying glacial influence have been assessed and interpreted in the context of the physicochemical habitat template. All methods of quantifying glacier influence described a similar habitat template; from harsh (high glacial influence) to benign (low glacial influence), and the relationship with some habitat variables was modified by basin geology. The meltwater contribution approach, due to its physical process underpinning, was related to a suite of physical, chemical and hydrological variables of ecological importance (Milner *et al.* 2010). Hence, in subsequent chapters this method of water source quantification will be explored as a tool for predicting benthic community patterns (Chapter 4) and functional diversity/community assembly processes (Chapter 5) across multiple river basins.

CHAPTER 4

*Disturbance concepts predict aquatic
biodiversity response to alpine glacier
retreat*

4.1. Introduction

Ecologists have long strived to identify the processes generating and maintaining biotic patterns (Chesson & Huntly 1997; Cardinale *et al.* 2006). Disturbance or stress, referred to as an event or 'state' which removes biomass and opens niche space (Menge & Sutherland 1987), is thought to play a key role in structuring biodiversity at a range of scales and levels of ecological organization (Pickett *et al.* 1989; Lake 2000; Evanno *et al.* 2009; Mayor *et al.* 2012). A number of well-tested models and hypotheses link diversity patterns to both natural and anthropogenic environmental stress (Death 2010). For example, both the Intermediate Disturbance Hypothesis (IDH; Connell 1978) and Harsh-Benign Concept (HBC; Menge & Sutherland 1976; Peckarsky 1983) predict that diversity will peak at intermediate levels of stress. However, the specific mechanisms driving this relationship are often misinterpreted (Fox 2013). Recent theoretical studies suggest interactions between disturbance and productivity determine the response shape (Kondoh 2001; Cardinale *et al.* 2006), with unimodal responses occurring when stress and productivity balance to create a trade off between competition and colonization (Kondoh 2001). Yet, knowledge of how climate change (e.g. temperature extremes and altered flows) will alter natural disturbance regimes remains limited (Shea *et al.* 2004). Understanding the potential interactions and feedbacks (i.e. abiotic-biotic interactions) and effects on biodiversity are vital for guiding mitigation and conservation efforts (Kulakowski *et al.* 2011), particularly as it is often difficult to determine ecosystem resilience to persistent press and ramp disturbance (Lake 2013).

Mountain environments have distinct environmental gradients (e.g. temperature, land cover and seasonality), which have been utilized extensively to test ecological theory (Körner 2007). For example, alpine flora have been used widely to develop and test ideas around

environmental stress and facilitation along temperature and moisture gradients (Kikvidze *et al.* 2011). Alpine river systems also represent an ideal ‘natural laboratory’ for testing disturbance and environmental stress concepts due to the relatively simple, yet multi-trophic, structure of benthic communities and a spatiotemporal natural stress gradient (Milner *et al.* 2009). Here, water source dynamics represent a major control on biotic patterns at a range of scales across the river network (Malard *et al.* 2006; Brown *et al.* 2007a; Füreder 2007). Runoff tends to be sourced from two major hydrological stores: (i) meltwater (glaciers and snowpacks); and (ii) groundwater aquifers (Brown *et al.* 2006b), which represent two poles of an environmental stress gradient. Glacier meltwater typically carries more suspended sediment (SSC), and associated flow regimes are highly variable at a range of temporal scales (Hock *et al.* 2005). Discharge variability leads to unstable river beds, and rapid sediment deposition creates braided, wandering channels (Malard *et al.* 2000; Moore *et al.* 2009). Groundwater dominated flow represents the ‘benign’ end of the gradient, with typically clear water (low SSC) and less variable flows leading to more stable river channels and beds (Smith *et al.* 2001; Brown *et al.* 2003). The subsequent mixing of these water sources in different proportions creates variability in the characteristics of physicochemical habitat and associated benthic assemblages across a range of spatial and temporal scales (Malard *et al.* 2006). Despite this recognised natural stress gradient, alpine river systems have to date not been used to empirically test disturbance related ecological hypotheses.

Studies of European glacierized catchments have identified predictable patterns of macroinvertebrate diversity and species assemblages driven by changes in environmental conditions (Snook & Milner 2001; Finn *et al.* 2013). Species poor communities, dominated by *Diamesa* (Diptera:Chironomidae), typically prevail close to glaciers (Lods-Crozet *et al.* 2001). Here, meltwater contribution to bulk discharge is high and environmental stress is at a

maximum (Füreder 2007). As groundwater contributions increase, habitat conditions become more favourable and disturbance intensity is reduced (Brown *et al.* 2006). The relatively benign conditions enables a more diverse benthic community to establish, including Ephemeroptera, Plecoptera and Trichoptera (EPT) and other chironomid taxa (Milner *et al.* 2001). Hence, rapid changes in physicochemical habitat and environmental stress regimes can create high beta diversity across relatively small river networks (Finn *et al.* 2013). As sites of higher meltwater contribution (stress), although species poor, are particularly important for both basin scale and regional diversity due to the presence of unique, specialist taxa (Brown *et al.* 2007a; Jacobsen *et al.* 2012).

Milner *et al.* (2001) invoked an analogy between the HBC and temporal changes in environmental conditions and macroinvertebrate community structure in glacier fed streams. Here, the more favourable environmental conditions of spring and autumn (e.g. low turbidity, low discharge variability and increased algal growth), promote increased macroinvertebrate diversity and abundance. This idea was further developed by Brown *et al.* (2007b), and a spatial, watersource (meltwater-groundwater) related, harsh-benign gradient was added, which predicted richness peaks in groundwater dominated channels. Füreder (2007), drawing parallels between the continuum of habitat types in alpine river ecosystems and ecological disturbance theory, suggested alpine benthic diversity patterns may be unimodal rather than linear (c.f. Brown *et al.* 2007b) depending on the specific glacier influence or ‘environmental harshness’ gradient. Recently, an intercontinental study of alpine river ecosystems identified taxonomic richness peaks at sites with intermediate glacier influence (5-30% glacier cover in the catchment) (Jacobsen *et al.* 2012). However, this study was based on a static measure of glacier influence, which is insensitive to the temporal and spatial variability of hydrological sources (e.g. snowpacks and ephemeral springs), pathways (e.g. tributary structure) and

associated benthic habitat (Brown *et al.* 2010). A quantitative measure of meltwater:groundwater contributions that incorporates these features has been developed but tested to date in just a single river basin across a limited meltwater contribution spectrum (Brown *et al.* 2007a).

In this present study benthic habitat and community composition were characterised along a gradient of meltwater contribution, across five alpine river basins in the French Pyrénées (all of which have active glaciers). The water source habitat template (harsh-benign) was used to assess mechanisms driving reach scale community diversity patterns, and relate observed patterns to ecological stress/disturbance concepts. Four complementary hypotheses were tested: (H₁) where meltwater contribution to streamflow is greatest environmental conditions are harshest, and vice versa; (Brown *et al.* 2007b); (H₂) meltwater contribution gradients create predictable macroinvertebrate assemblages patterns which are comparable between river basins of differing bedrock geology; (H₃) a unimodal relationship exists between macroinvertebrate community structure and meltwater contribution (the stress gradient), representing a shift from abiotic to biotic controls; and (H₄) invertebrate taxa display mixed responses across the meltwater spectrum, with specialists at extremes of the gradient and generalists more evenly distributed.

4.2. Methods

4.2.1. Field location

The study was conducted across five alpine river basins in the Gave de Pau catchment, French Pyrénées (Figure 4.1). All sites were located above the tree line (1670m – 2560m a.s.l) and within the Parc National des Pyrénées (PNP). Anthropogenic disturbance was minimal, although light grazing by sheep and cattle occurs. Riparian vegetation was sparse above 2200m, with thin soils interspersed with bare rock and scree. Riparian zones were more developed at sites <2200m, consisting of alpine grasses and scattered herbaceous plants. More detailed basin descriptions are provided in Chapter 2.

Twenty-six, 15m reaches were identified across the five study basins (Appendix 4.1). In three of the river basins, seven sites were selected from hillslope springs sourced exclusively from groundwater aquifer flowpaths (ridge top and hillslope snow was absent). The other 19 sites were located on five glacier-fed rivers (Appendix 4.1). The meltwater component was considered a mixture of ‘quick flow’ sourced from ice and permanent snowpacks with minimal rock contact time, and slower routed meltwater ‘distributed flow’ which had travelled through sub-glacial drainage systems (Brown *et al.* 2006d).

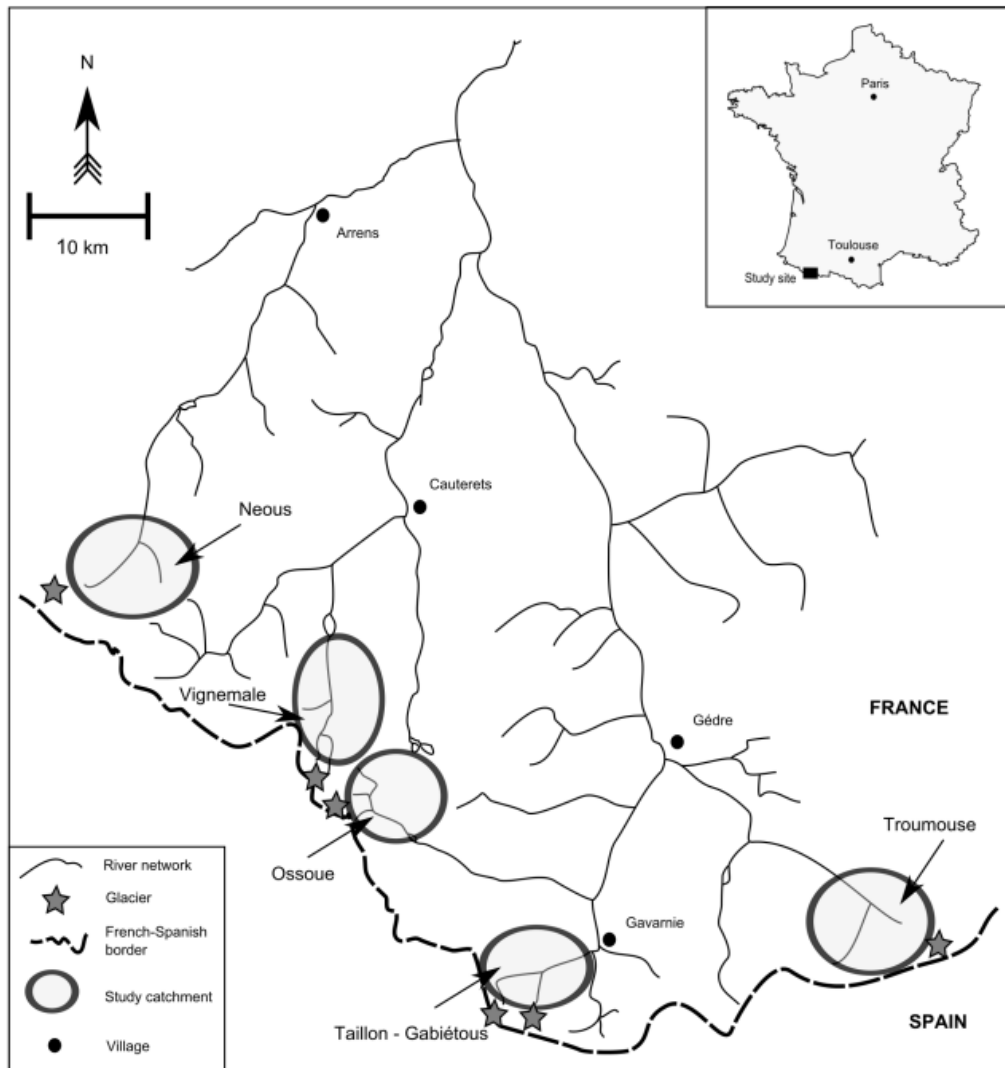


Figure 4.1. Location of the study basins within the Gave de Pau drainage. Grey ellipse outlines represent the drainage areas for each basin and stars represent glaciers (not to scale). The broken dashed line is the French – Spanish border.

4.2.2. River water source contribution and physicochemical data

In each basin, water samples were collected from a range of potential hydrological sources or 'end members' (i.e. snow, ice and groundwater springs), and a further sample was collected at each of the 26 study reaches. Water was filtered through cellulose nitrate filters (0.45µm pore size) in the field, retained in pre-rinsed HDPE bottles (60ml) and frozen for storage. In the laboratory, samples were defrosted and silica [Si] concentrations determined using the molybdosilicic method (ASTM D859 – 10). Si was chosen as a tracer due to its slow reaction rates and ability to identify groundwater contributions to bulk streamflow (Brown *et al.* 2006d). Basin specific, two end member mixing models (meltwater:groundwater) were then constructed and meltwater/groundwater proportions calculated for each reach using mass balance equations (Suecker *et al.* 2000). A more detailed outline of this method can be found in Chapter 3.

At each site, spot measurements of pH and electrical conductivity (EC) were taken in the thalweg, using a Hannah HI 98129 handheld probe. The mean and range of water temperature were calculated from records collected continuously for two weeks prior to sampling using digital temperature dataloggers (Gemini Tinytag Plus, instrument error $\pm 0.2^{\circ}\text{C}$). Water samples (500ml) were collected at each reach to determine suspended sediment concentration (SSC). Samples were filtered through pre-weighed glass fibre filter papers (Whatman GF/C), dried at 95°C for 2 h then re-weighed to the nearest mg (ATSM D3977 – 97). At each reach the bottom component of the Pfankuch Index (Pfankuch 1975) was used to estimate substrate stability. River stage (m) was continuously recorded (15 min intervals) at sites T3, T4, G4, O3, V4 and V2 during the 2011 melt season (June-Sept). Stage discharge relationships were created for each site (Chapter 3).

4.2.3. Biological sampling and processing

Macroinvertebrates were collected in August 2011 (18th–28th) using a Surber sampler (0.09m²; 250 µm mesh). At each reach, five replicate samples (three replicates for groundwater streams/springs due to their smaller area (Smith *et al.* 2003)) were collected randomly in riffle habitat. Organisms were preserved in 70% ethanol prior to sorting in the laboratory. Ephemeroptera, Plecoptera, Trichoptera (EPT) and Chironomidae, were identified to the lowest practical taxonomic level (species where possible) using a selection of identification keys (Müller-Liebenau 1969; Tachet *et al.* 2000; Zwick & Vinçon 2009). Chironomids were first identified and counted at the sub-family level using a binocular microscope (Ziess stemi 2000-C, 6.5x – 75x) fitted with a supplementary lens (2x). For samples with high chironomid abundances, subsamples of 50 individual Chironomidae were taken. Chironomid head capsules were cleared in 10% KOH at 90°C (Snook & Milner 2001), mounted in dimethyl hydantoin formaldehyde and identified using a stage microscope (Nikon Optiphot-2 microscope, magnification 100-1000x). Other taxa were typically identified to genus, but to family for some Diptera or order/subclass for Oligochaeta, Collembola, Hydracarina and Nematoda. A dissecting microscope (Ziess stemi 2000-C, 6.5–75x) was used for enumeration of all non-chironomid taxa. Three randomly selected cobbles were also retained from each reach and the epilithon retained for chlorophyll *a* (chl *a*) analysis (see Ledger *et al.* (2006) for methods).

4.2.4. Data analysis

Standardised daily flow variability (daily discharge range/mean discharge) was calculated for each site with discharge records. Linear regression (OLS) was adopted to test relationships between meltwater contribution and reach scale physicochemical-habitat variables (including standardised flow range). To account for differences in sampling effort between glacial and groundwater streams, three randomly selected Surber samples were retained for each site. Reach scale macroinvertebrate community metrics were calculated as follows: (i) total taxonomic richness (γ); (ii) total density (ind m²); (iii) number of EPT taxa; (iv) evenness measured as the numbers equivalent of the shannon index divided by total richness (e^h / γ); (v) proportion of the community that were predators; (vi) beta diversity (γ/α); (vii) proportion of the community that were Ephemeroptera/Trichoptera/Plecoptera/Diptera (EPTD); and (viii) abundance of a characteristic taxon from each order (E: *Baetis alpinus* (Pictet); T: *Rhyacophila evoluta* (McLachlan); P: *Protonemura* sp.; D: *Diamesa latitarsis* gr.). Where necessary count data were $\log_{10}(x+1)$ transformed to stabilise variances.

Generalized Additive Models (GAMs) and Generalized Linear Models (GLMs) were used to investigate the relationship between meltwater contribution and the response variables outlined above. Models were run with and without geology (i.e. crystalline/sedimentary) included as an interaction term. Analysis of deviance was then conducted to identify whether the interaction term improved the model (Zuur *et al.* 2009). Due to the detection of overdispersion, negative binomial (count data) or quasibinomial (proportion data) distributions were used. However, as the value for the overdispersion parameter is rarely known *a priori*, it was estimated following the recursive approach outlined by (Barry & Welsh (2002). For GAM's the optimum smoothing was selected using a cross-validation

approach outlined by Wood (2008). Explained deviance was used to evaluate model performance, a measure analogous to R^2 in OLS regression (Zuur *et al.* 2009). Model residuals were tested for spatial autocorrelation using a Mantel test (all $P > 0.05$) following methods outlined by Zuur *et al.* (2009) (see Appendix 4.2).

Sites were then grouped ($n = 4$) using *a priori* knowledge of habitat conditions. Analysis of similarity (ANOSIM) was conducted on the physicochemical habitat data and the R value retained as a benchmark ($R = 0.61$, $P < 0.001$). Multiple permutations, with differing group numbers (2-5) and differing meltwater thresholds for group membership (varied in 5% increments), were undertaken and ANOSIM calculated. The highest R value ($R = 0.67$, $P < 0.001$) was obtained for a three group classification: (i) high meltwater contribution $> 75\%$ (HMC); (ii) mid-meltwater contribution 10-75% (MMC); and (iii) low meltwater contribution, $<10\%$ (LMC).

Prior to multivariate analysis, taxon abundances were $\log_{10}(x+1)$ transformed and site assemblages tested for spatial autocorrelation with a Mantel test ($R = 0.02$, $P > 0.05$) with 999 permutations (Lloyd *et al.* 2005). Non-metric multidimensional scaling (NMDS) with Bray-Curtis dissimilarity was used to examine patterns in community composition across the meltwater gradient. Reach-scale variables were related to the NMDS ordination using a vector fitting algorithm outlined by Faith & Norris (1989). The relationship between taxon abundance and the NMDS scores from both axes were examined using Spearman's rank correlation. A Multi-Response Permutation Procedure (MRPP) was adopted to test for significant differences between meltwater groups and assess overlap in community composition (Mayor *et al.* 2012).

Taxonomic turnover (Bray-Curtis distance) was employed as a multivariate measure of beta diversity (Anderson *et al.* 2011) and the mean distance between all sites within the three meltwater groups calculated. A two-way nested ANOVA was used to test differences between meltwater group (fixed factor) and river basin nested in meltwater group (random factor) for the response variables; total abundance ($\log_{10}(x+1)$), taxonomic richness, EPT richness and mean pair-wise Bray-Curtis dissimilarity. This was followed by Tukey's post hoc test with Bonferroni correction. To assess the possible effect of climate change induced glacier loss on biodiversity patterns, community diversity and structure were determined for all sites and then for the MMC and LMC groups only.

All analysis was carried out in R 2.14.1. using the *vegan* package (Oksanen *et al.* 2012) for NMDS, ANOSIM and MRPP, and the *mgcv* package (Wood 2006) for regression analysis.

4.3. Results

4.3.1. Physicochemical habitat

All habitat variables, with the exception of T_w (mean and range), displayed linear relationships across the meltwater gradient (Figure 4.2). SSC ($F_{1,24} = 23.2$, $R^2 = 0.50$, $P < 0.001$) and PFAN ($F_{1,24} = 56.1$, $R^2 = 0.69$, $P < 0.001$) were positively related, and Chl *a* ($F_{1,24} = 28.1$, $R^2 = 0.52$, $P < 0.001$) negatively related, to meltwater contribution (Figure 4.2). Weaker relationships were also recorded for pH ($F_{1,24} = 10.2$, $R^2 = 0.30$, $P < 0.01$) and EC ($F_{1,24} = 4.5$, $R^2 = 0.16$, $P < 0.05$). Standardised daily flow range was also positively related to meltwater contribution ($F_{1,4} = 10.2$, $R^2 = 0.78$, $P < 0.05$).

4.3.2. Taxonomic patterns and diversity

Macroinvertebrate abundance, taxonomic richness and EPT richness displayed unimodal responses across the meltwater spectrum (Figure 4.3). Macroinvertebrate abundance, taxonomic richness and EPT richness all peaked between 40 and 60% meltwater contribution (Figure 4.3a,b,c; Table 4.1), with the lowest values recorded at sites with >90% meltwater contribution. Predator proportion (Figure 4.3e) and within reach beta diversity (Figure 4.3f) were negatively related to meltwater contribution. Community evenness displayed a more complex relationship with meltwater, the lowest values were between 40 and 60% meltwater contribution, and the highest at high and low meltwater contributions (Figure 4.3d). Plecoptera and Trichoptera proportions decreased along the meltwater spectrum (Figure 4.4b,c). Diptera proportion increased with meltwater contribution (Figure 4.4d), while Ephemeroptera proportion peaked at moderate meltwater contribution (Figure 4.4a). For community level metrics a significant interaction with geology was only identified for the

response variables total macroinvertebrate density and beta diversity (Appendix 4.3). The response curves were, however, broadly similar for both models (Figure 4.5).

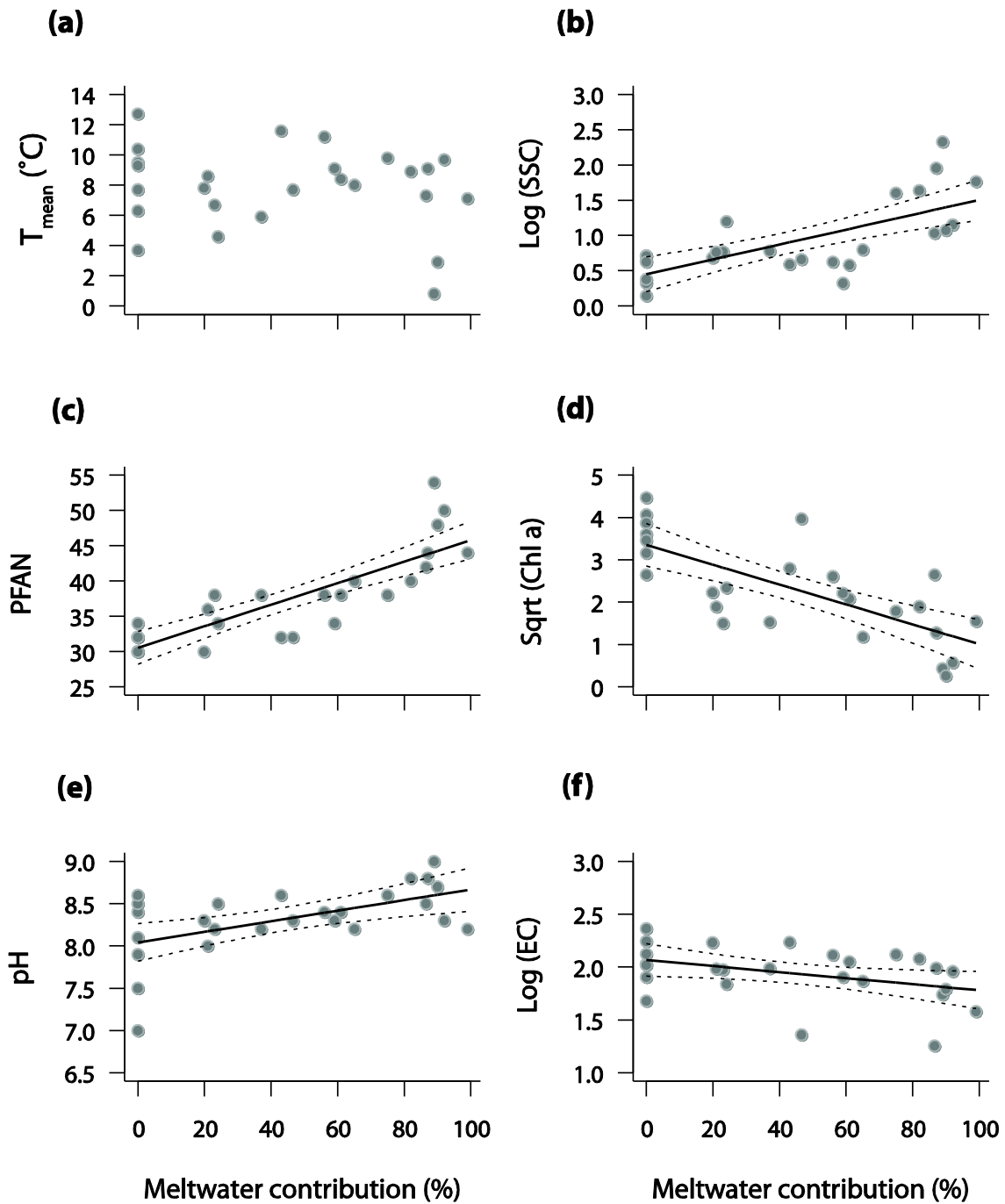


Figure 4.2. Meltwater-habitat relationships for: (a) mean water temperature; (b) suspended sediment concentration (SSC); (c) bed stability (PFAN); (d) chlorophyll *a*; (e) pH; and (f) EC. The solid lines are OLS regression fits and dashed lines represent 95% confidence intervals.

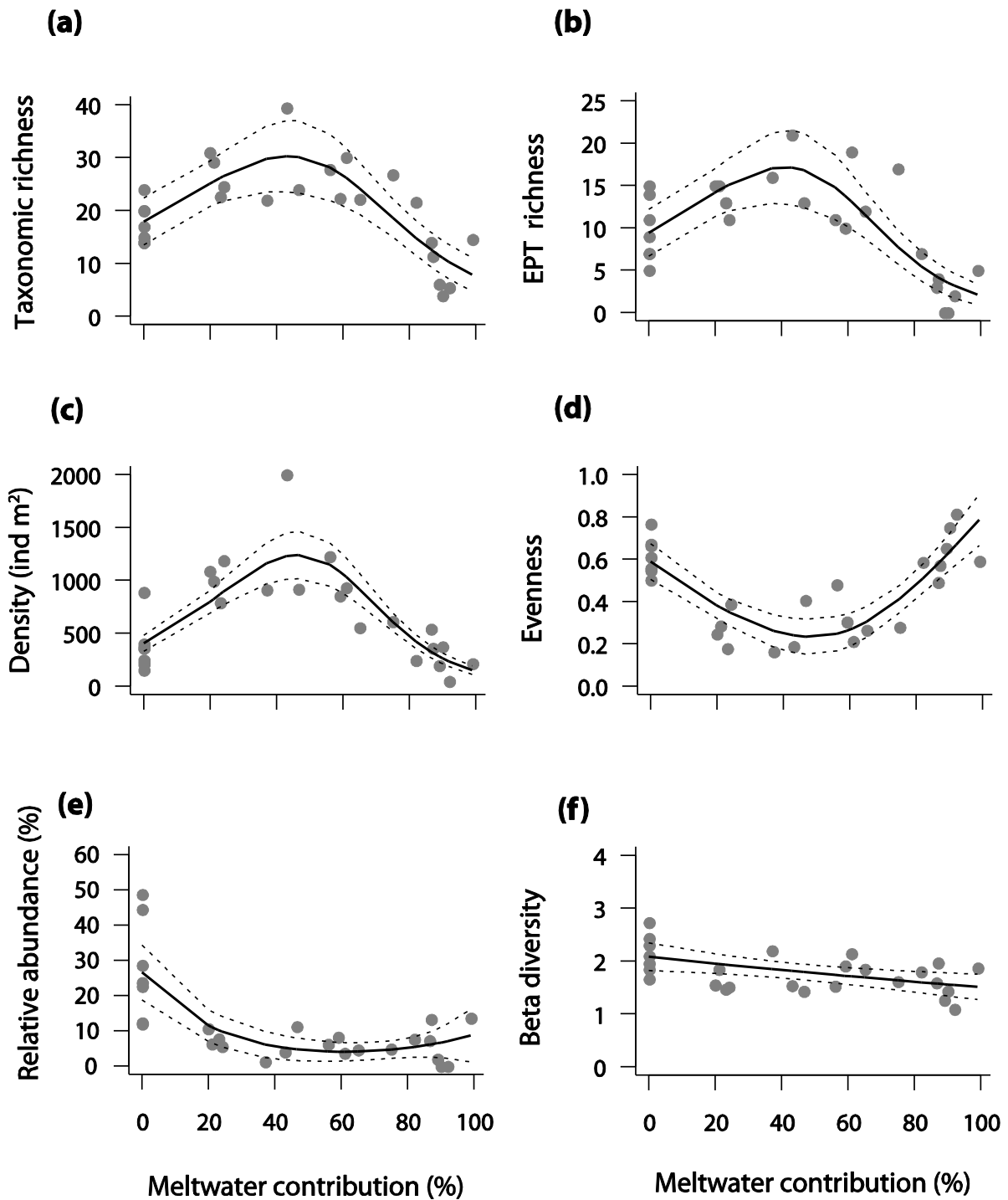


Figure 4.3. Generalized additive models (GAM's) for the relationship between meltwater contribution to stream flow and: (a) taxonomic richness; (b) total density (ind m²); (c) EPT richness; (d) evenness; and (e) predator relative abundance (%). (f) Generalized linear model (GLM) of reach scale beta diversity in response to meltwater contribution. Dashed lines represent 95% confidence intervals.

Table 4.1. Summary of the GAM and GLM models for the relationship between meltwater (dependant variable) and community/population level responses. ^{ns} denotes no significant relationship between meltwater and the response variable after controlling the False Discovery Rate (FDR) associated with multiple tests (Benjamini & Hochberg 1995).

Response variable	Method (distribution)	Significance of meltwater term		Deviance explained (%)
		χ^2 (<i>F</i>)	<i>P</i>	
Total density	GAM (negative binomial)	130.2	<0.001	61.5
Taxonomic richness	GAM (negative binomial)	26.3	<0.001	58.7
EPT richness	GAM (negative binomial)	33.9	<0.001	55.4
Predator proportion	GAM (negative binomial)	24.8	<0.001	75.3
Evenness	GAM (poisson)	24.2	<0.001	65.3
Beta diversity	GLM (gaussian)	7.1*	<0.05 ^{ns}	22.9
Trichoptera proportion	GAM (quasibinomial)	12.0*	<0.001	55.7
Ephemeroptera proportion	GAM (quasibinomial)	16.6*	<0.001	66.7
Plecoptera proportion	GAM (quasibinomial)	5.6*	<0.01	34.6
Diptera proportion	GAM (quasibinomial)	7.7*	<0.01	44.4
<i>R. evoluta</i> density	GLM (gaussian)	5.4*	<0.05 ^{ns}	15.4
<i>B. alpinus</i> density	GAM (negative binomial)	9.8	<0.001	47.9
<i>Protonemura</i> density	GAM (negative binomial)	11.1	<0.001	65.6
<i>D. latitarsis</i> density	GAM (negative binomial)	10	<0.001	44.2

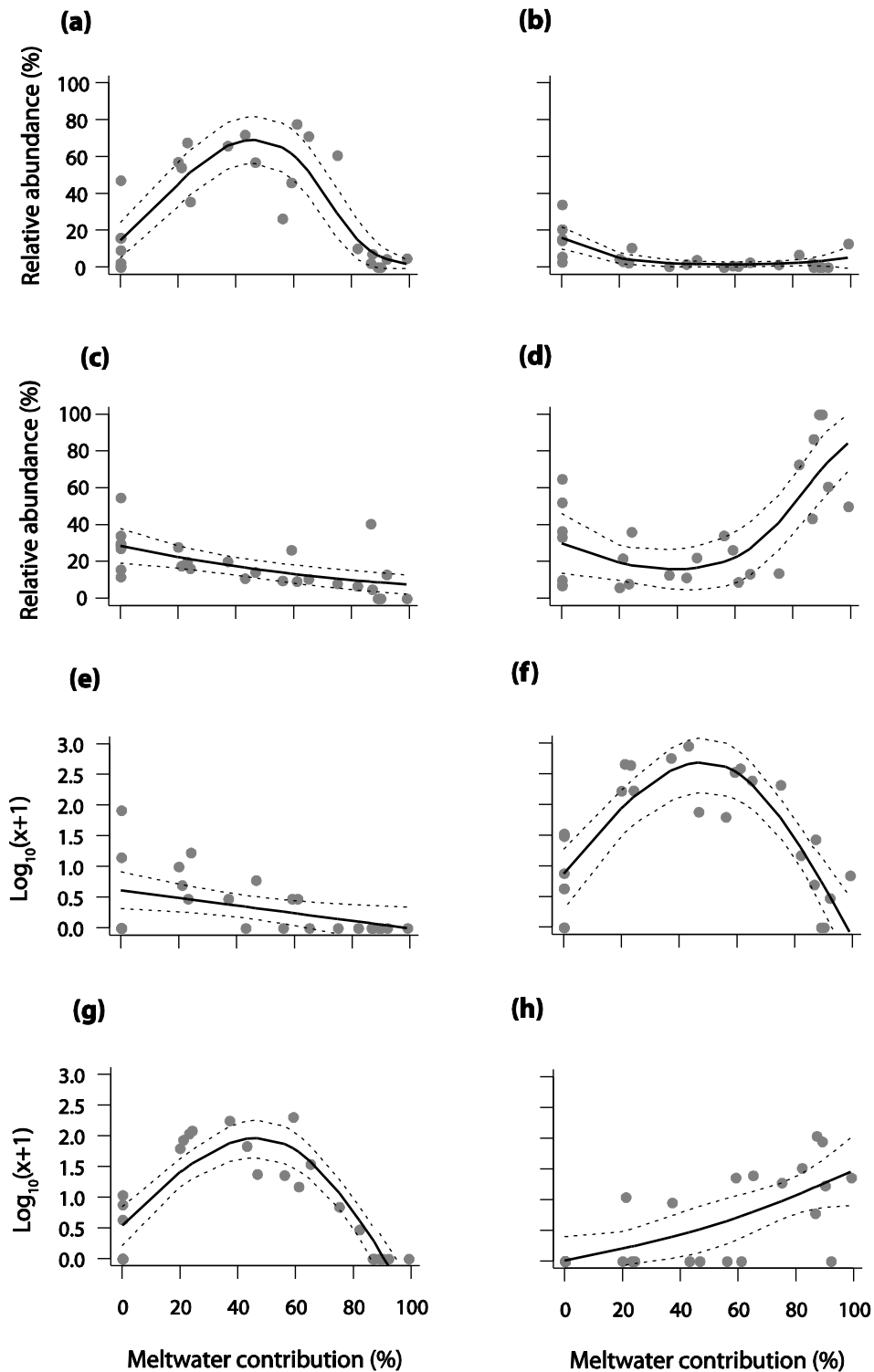


Figure 4.4. Relationship between meltwater contribution to streamflow and: (a) Ephemeroptera relative abundance; (b) Trichoptera relative abundance; (c) Plecoptera relative abundance; (d) Diptera relative abundance; (e) *Rhyacophila evoluta* density ($\log_{10}(x+1)$); (f) *Baetis alpinus* density ($\log_{10}(x+1)$); (g) *Protonemura* spp. density ($\log_{10}(x+1)$); and (h) *Diamesa latitarsis* gr. density ($\log_{10}(x+1)$). All lines of best fit represent GAM's, except c and e which are GLM's. Dashed lines represent 95% confidence intervals.

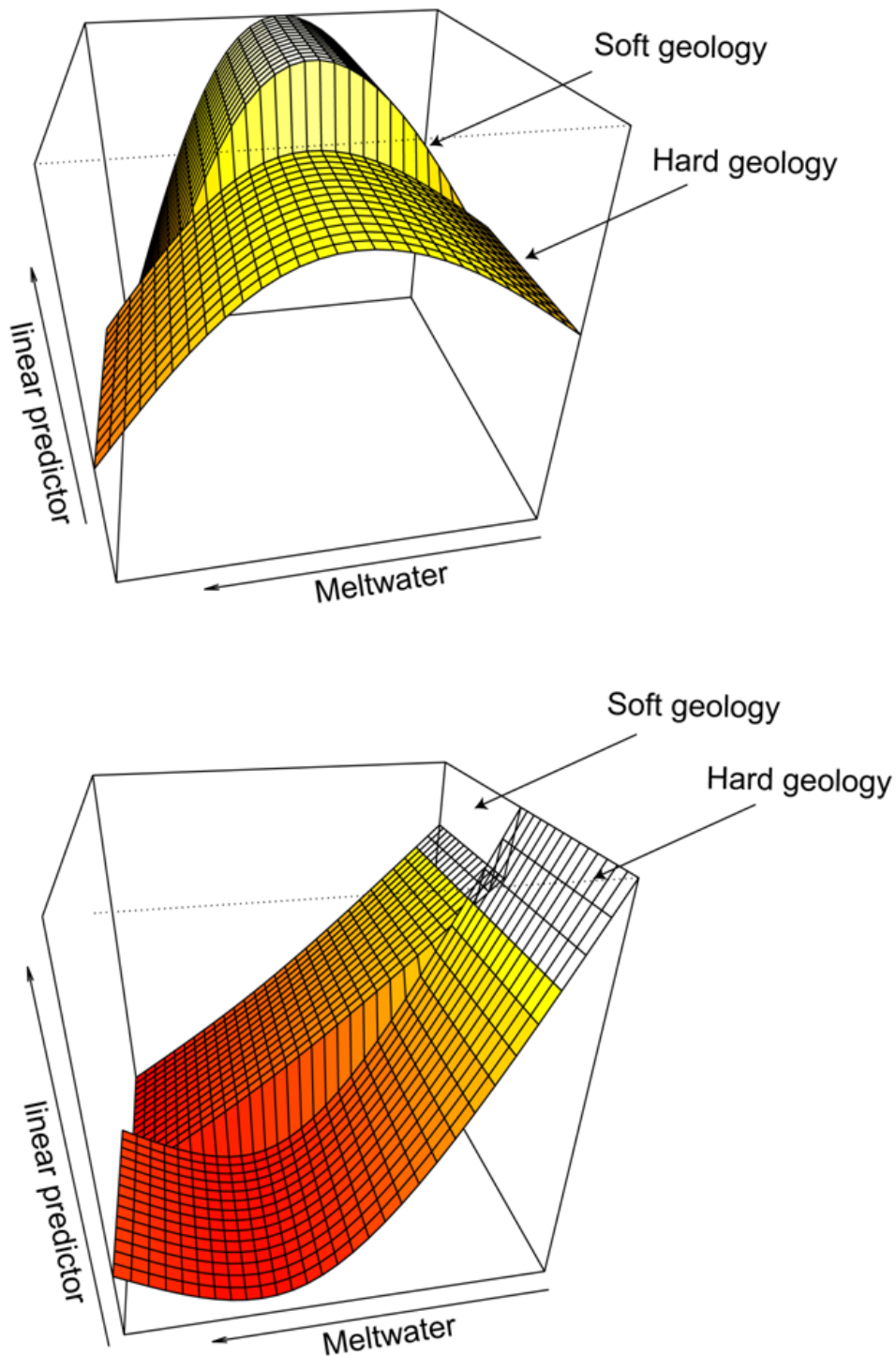


Figure 4.5. Three-dimensional graphs displaying the effect of geology on the meltwater-total abundance linear predictor (upper panel) and the meltwater–beta diversity linear predictor (lower panel). Soft rock corresponds to sites underlain by sedimentary lithology and hard rock those underlain by crystalline lithology.

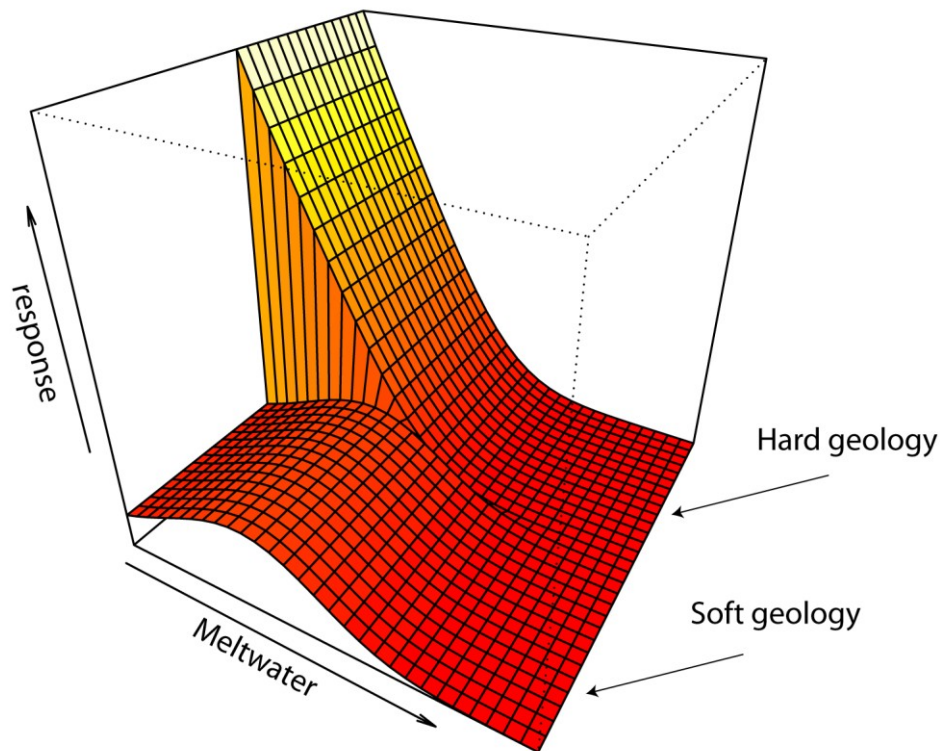


Figure 4.6. Three-dimensional graph displaying the effect of geology on the meltwater – *R. evoluta* density linear predictor. Soft rock corresponds to sites underlain by sedimentary lithology and hard rock those underlain by crystalline lithology.

Taxon specific responses varied with *R. evoluta* and *D. latitarsis* gr. displaying negative and positive relationships respectively, while *B. alpinus* and *Protonemura* spp. density peaked at moderate meltwater contribution (Figure 4.5e-h; Table 4.1). Unlike the community level responses, significant interactions between geology and meltwater contribution were recorded for taxon specific responses (Appendix 4.3; Figure 4.6). These were apparent for the taxa found at the extremes of the meltwater spectrum (i.e. *D. Latatarsis* gr. and *R. evoluta*) but not for the more common, generalist taxa (Appendix 4.3).

The NMDS ordination (2-dimensional solution, stress = 0.14), stress plot indicated a negligible amount of the variation in the original data set was lost ($R^2 = 0.98$). Axis 1 divided the HMC sites from the LMC, whereas axis 2 separated MMC sites from the other groups (Figure 4.7). Of the reach scale variables correlated with the NMDS ordination, PFAN (bed stability) displayed a highly significant relationship ($R^2 = 0.72$, $P < 0.001$) associated with negative scores for both axes 1 and 2. Weaker relationships were also apparent for SSC ($R^2 = 0.44$, $P < 0.01$) and pH ($R^2 = 0.34$, $P < 0.01$), which were both inversely related to the two axes, while T_w ($R^2 = 0.45$, $P < 0.001$) and EC ($R^2 = 0.25$, $P < 0.05$) were positively related to axis 1 scores (Figure 4.7). *Diamesa* spp. and Empididae displayed the strongest negative correlation to axis 1 whilst *Agapetus fuscipies* (Curtis), *Leuctra fusca* gr., *Polycelis* spp. and *Isoperla* sp. displayed the strongest positive correlation. *Perla grandis* (Rambur), *Microspectra* sp. Simuliidae, *B. alpinus* and *Rithrogena* spp. were correlated negatively to axis 2 whilst *Arcynopteryx compacta* (McLachlan) and *Crenobia alpina* (Dana) were correlated positively (Table 4.2). MRPP identified significant differences in community composition between meltwater groups ($P < 0.001$). Overlap between communities was lowest for the HMC and MMC groups ($A = 0.15$) and highest for the MMC and LMC groups ($A = 0.10$).

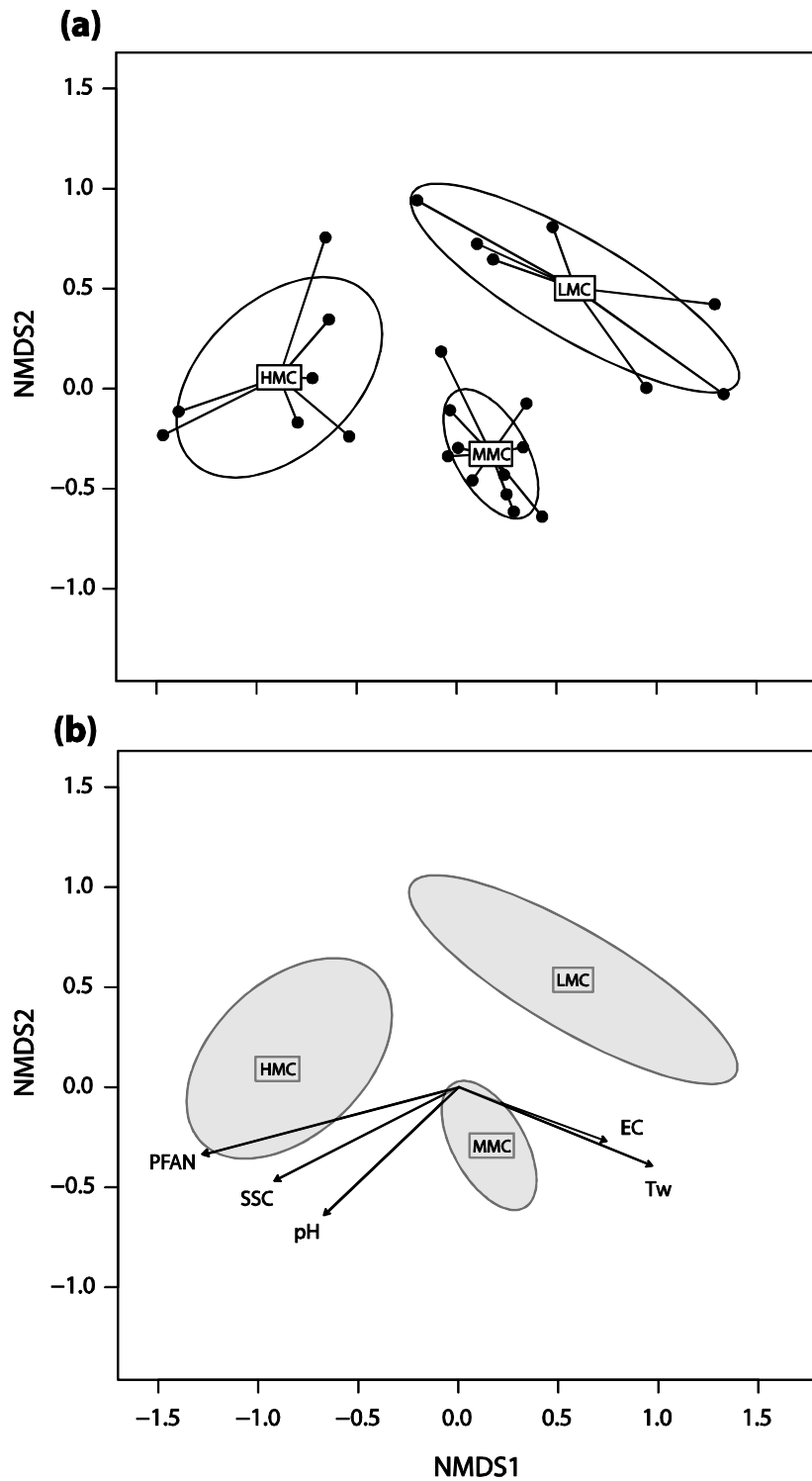


Figure 4.7. NMDS ordination of $\log_{10}(x+1)$ transformed community data. Rectangles represent meltwater group centroids and ellipses the 95% confidence limits of the group mean. Arrows represent post-hoc vector fit of reach scale physicochemical habitat variables. All vectors are scaled relative to their correlation coefficient; PFAN ($R^2 = 0.72$, $P < 0.001$), SSC ($R^2 = 0.44$, $P < 0.01$), pH ($R^2 = 0.34$, $P < 0.01$), Tw ($R^2 = 0.45$, $P < 0.001$) and EC ($R^2 = 0.25$, $P < 0.05$).

Table 4.2. Spearman rank correlations between taxa abundances and NMDS axis scores. All correlations are significant at $P < 0.05$ after holm's correction for multiple tests.

Axis 1		Axis 2	
Taxa	<i>r</i>	Taxa	<i>r</i>
<i>Diamesa cinerella/zernyi</i>	-0.73	<i>Micropsectra</i> sp.	-0.82
<i>Diamesa bertrami</i> (Edwards)	-0.71	<i>Perla grandis</i> (Rambur)	-0.78
<i>Diamesa latitarsis</i> gr.	-0.67	<i>Prosimulium</i> spp.	-0.75
<i>Diamesa aberatta</i> (Lundb.)	-0.52	<i>Simulium</i> sp.	-0.69
Empididae	-0.51	<i>Baetis alpinus</i> (Pictet)	-0.68
<i>Agapetus fuscipes</i> (Curtis)	0.65	<i>Rhithrogena semicolorata</i> (Curtis)	-0.68
<i>Leuctra fusca</i> gr.	0.64	<i>Rhithrogena loyolaea</i> (Navàs)	-0.65
<i>Polycelis</i> sp.	0.58	<i>Hydraena</i> sp.	-0.63
<i>Isoperla</i> spp.	0.58	Athericidae	-0.60
<i>Ecdyonurus</i> sp.	0.56	<i>Protonemura</i> spp.	-0.59
<i>Pentaneuriini</i> spp.	0.53	<i>Esolus</i> spp.	-0.59
<i>Baetis gemellus</i> (Eaton)	0.49	<i>Parametriocnemus stylatus</i> (Kieffer)	-0.51
<i>Simulium</i> spp.	0.49	<i>Tvetenia bavarica</i> (Goetghebuer)	-0.50
<i>Siphonoperla torrentium</i> (Pictet)	0.43	<i>Crenobia alpina</i> (Dana)	0.53
<i>Plectrocnemia</i> sp.	0.42	<i>Arcynopteryx compacta</i> (McLachlan)	0.56

Significantly higher mean density (ANOVA; $F_{2,23} = 16.9$, $P < 0.001$), taxonomic richness (ANOVA; $F_{2,23} = 21.7$, $P < 0.001$) and EPT richness (ANOVA; $F_{2,23} = 26.3$, $P < 0.001$) were identified for the MMC group when compared to the other two groups. However, Bray-Curtis dissimilarity (beta diversity) was lowest within the MMC group (0.65), and both the HMC group (0.79) and LMC group (0.83) had significantly greater species turnover (ANOVA: $F_{2,23} = 5.6$, $P < 0.01$) (Table 4.3). Differences in the community metrics were not apparent within each meltwater group between river basins (ANOVA; $P > 0.05$). When HMC sites were omitted from calculations mean taxonomic richness increased, while Bray-Curtis dissimilarity (beta diversity) decreased (Table 4.3).

Table 4.3. Macroinvertebrate community abundance and diversity (mean \pm 1 SE) for all sites combined, mid-meltwater contribution (MMC) and low-meltwater contribution (LMC) groups combined and each groups considered independently.

Group	Total density (ind m²)	Taxonomic richness (α - diversity)	EPT richness	Bray – Curtis distance (β - diversity)
HMC	282 (59)	12.2 (0.4)	3.0 (1.0)	0.79 (0.04)
MMC	1006 (108)	31.5 (0.5)	14.4 (1.3)	0.65 (0.02)
LMC	375 (92)	15.4 (0.4)	9.7 (1.4)	0.83 (0.01)
MMC+ LMC	773 (101)	25.2 (0.4)	12.7 (2.5)	0.76 (0.01)
All sites	641 (88)	22.8 (0.3)	10.1 (1.3)	0.82 (0.01)

4.4. Discussion

4.4.1. Physicochemical characteristics of the meltwater stress gradient

Sampling across the meltwater spectrum, with glacier melt dominated streams (harsh) and groundwater streams (benign) at the two poles, identified a steep environmental stress gradient thus supporting H_1 (Brown *et al.* 2007b; Füreder 2007). Here, SSC and channel stability (PFAN) were positively related to meltwater as predicted by the ARISE habitat template (Brown *et al.* 2009). Chl *a* biomass was greatest in groundwater streams due to a combination of high bed stability and low turbidity (Uehlinger *et al.* 2010). At higher meltwater contribution reduced periphyton cover was potentially due to: (i) more frequent hydrological disturbance and bed movement; and (ii) higher SSC which increased abrasion and turbidity (Uehlinger *et al.* 2010).

Mean water temperature showed no clear relationship with meltwater contribution, likely due to variability in geomorphic and stream habitat characteristics between and within basins (i.e. aquifer depth, stream azimuth and depth:width ratios), which can interact with meltwater to influence stream water temperature (Isaak & Hubert 2001; Brown & Hannah 2008). Using meltwater contribution as a predictor of community structure does, however, capture numerous facets of environmental stress in alpine river systems (e.g. SSC and chl *a*). Furthermore, diurnal flow variability, which can act as major control on biodiversity, was also strongly related to meltwater contribution (Cauvy-Fraunié *et al.* 2013a). From an organismal perspective both physiological stress (conditions outside the tolerance range) and physical stress (mechanical forces) are represented when examining the meltwater contribution stress gradient (Menge & Sutherland 1987).

4.4.2. *Assemblage composition and beta diversity*

The three distinct benthic assemblages associated with differing water source contributions supported H₂, that distinct community assemblages would be driven by water source gradient rather than spatial gradients. A high meltwater assemblage dominated by *Diamesa* spp., with low mean abundance and alpha diversity represented the ‘harsh’ end of the abiotic stress gradient. Here a combination of low water temperature, limited food resources, unstable river beds and high SSC prevented the majority of taxa from successfully colonising (Milner *et al.* 2009 Lencioni *et al.* 2006). Only those taxa that are well adapted to the habitat conditions are able to sustain populations. At mid-meltwater contributions an assemblage characterized by Ephemeroptera (*Baetis* spp. and *Rhithrogena* spp.) and Plecoptera (*Protonemura* spp.) with higher mean abundance and alpha diversity was recorded as can be predicted from studies showing deterministic trajectories of community succession in glacier fed streams (Milner *et al.* 2001; Brown & Milner 2012). The shift from a *Diamesa* to EPT dominated community was linked to the more ‘benign’ environmental conditions (warmer water temperature and lower turbidity) associated with reduced glacier influence, manifested as lower meltwater contribution (Brown *et al.* 2007b). Groundwater spring/stream assemblages with moderate alpha diversity and abundance were dominated by Perlodidae (*Arcynopteryx compacta* and *Perlodes* sp.), the net spinning trichopterans, *Hydropsyche* sp. and *Plectrocnemia* sp., and the flat worm *Crenobia alpina*. These taxa tend to have more specialized habitat requirements, such as specific flow velocities for net spinning caddis (Edington & Hildrew 1995) and constant (cool) water temperature for *C. alpina* (Wright 1974), thus limiting the distribution to stable conditions of groundwater fed channels (Bottazzi *et al.* 2011).

The significant differences in community composition between meltwater groups (Figure 4.7) is supported by both the HBC and IDH, which predict that assemblage composition should differ among communities depending on the level of disturbance (Connell 1978; Mayor *et al.* 2012). This has important implications for future biodiversity patterns as small alpine glaciers are expected to disappear in the coming century (Zemp *et al.* 2006), altering the current stress gradient/disturbance regime and reducing beta diversity (Jacobsen *et al.* 2012). When the HMC group sites were omitted from diversity calculations (Table 4.3), beta diversity (measured as Bray-Curtis) decreased, while alpha diversity (taxonomic richness) increased. This finding was likely due to a number of factors, including: (i) the absence of *Diamesa aberrata* and *Diamesa dampfyi*, cold adapted glacier stream specialists, at sites with lower meltwater contribution (Rossaro *et al.* 2006; Muhlfeld *et al.* 2011); (ii) the loss of heterogeneous distributions of certain taxa (e.g. *R. angelieri* and *Pseudokiefferiella* spp.) as meltwater proportions decreased, which led to greater similarity between sites (Jacobsen *et al.* 2012); and (iii) the dominance of the ephemeropteran taxa (e.g. *B. alpinus* and *R. Loyolaea*) at MMC sites, which represented a shift from a specialist to generalist community and increased the similarity between reaches (Finn *et al.* 2013). These findings emphasise concerns regarding the potential for substantial changes in aquatic biodiversity as glaciers retreat and meltwater contributions decrease (Brown *et al.* 2007a).

4.4.3. Diversity and abundance patterns along the meltwater stress gradient

In support of H₃ unimodal responses of community level metrics (e.g. taxonomic richness and total density) were observed across the meltwater gradient. There has been much debate in the literature regarding the generalities of the IDH and HBC (Shea *et al.* 2004; Hughes *et al.* 2007; Death 2010; Fox 2013); however, this study appears to demonstrate agreement with

disturbance/stress related concepts. While it has been suggested that diversity-disturbance relationships are generally not consistent (e.g. non-significant, unimodal or monotonic; Hughes *et al.* 2007), the hump shaped response appears to be more frequently associated with natural disturbance regimes (Mackey & Currie 2001). This would agree with the findings in this study as a unimodal diversity-disturbance relationship was apparent across the meltwater disturbance/stress regime. Furthermore, the lack of significant modification to community level observed patterns, i.e. no geology interaction, suggests that the quantification of meltwater contribution, interpreted in the context of disturbance, could provide a useful framework for predicting community level change (Ligeiro *et al.* 2013). It is, however, important to carefully consider the mechanisms driving the unimodal response as these are often misinterpreted (Fox 2013).

To date most empirical evidence for the IDH and HBC has come from marine and terrestrial habitats (see Shea *et al.* (2004) for a review). For freshwater river systems, findings have been far from conclusive, both supporting (Townsend *et al.* 1997; Miyake & Nakano 2002) and refuting (McCabe & Gotelli 2000; Parker & Huryh 2011) disturbance-diversity hypotheses. This inconsistent response may be because riverine communities predominately consist of highly mobile juvenile taxa, hence, immigration/emigration rather than reproduction controls can dominate population dynamics (Death 2010). A recent analysis, which examined species richness along a continuum of glacier influence, identified diversity peaks at intermediate glacial influence (Jacobsen *et al.* 2012), comparable to the peaks observed in this study between 40 and 60% meltwater contribution. This is likely due to the highly adapted regional species pool in alpine environments with all taxa displaying, to varying degrees, resilience or resistance to environmental stress (Füreder 2007).

Townsend *et al.* (1997) suggested that both disturbance intensity and frequency play a role in determining community structure. Glacier fed streams have a unique stress regime as a diurnal flow disturbance pulse, interspersed by extreme flood events, occurs within the context of an underlying harsh physicochemical habitat (Malard *et al.* 2006). This represents a combination of pulse and press disturbance and exerts a strong control on community structure and colonisation patterns (Collier & Quinn 2003). Hence, the low number of species able to colonise HMC sites is due to stressors, such as low water temperatures and limited food availability, that are exacerbated further by frequent flow and SSC related disturbance pulses (Milner & Petts 1994). This suggests deterministic, niche controlled community assembly processes at higher meltwater sites (Brown & Milner 2012). Additionally, minimal refugia, upstream/tributary re-colonisation potential and short ecological ‘windows of opportunity’ (Milner *et al.* 2001; Füreder *et al.* 2005) could also limit abundance and richness close to the glacier. However, it should be noted that taxa associated with this habitat (e.g. *Diamesa*) often represent species complexes, such as *Diamesa latitarsis* gr. (Snook & Milner 2001; Rossaro *et al.* 2006). The development of species complexes is often a feature of disturbed environments (Gray 1989) and, as the taxonomy of alpine *Diamesa* is incomplete (Rossaro 1980), the presence of cryptic diversity at these high meltwater sites is highly likely. While higher resolved taxonomy is unlikely to alter the strong unimodal patterns observed, it may contribute significantly to beta diversity patterns (Finn *et al.* 2013).

The richness and density peak at intermediate environmental stress (i.e. MMC sites) is likely due to two key factors. First, as groundwater contribution increases the potential for drift and colonisation from more stable groundwater tributaries increases, which is thought to be an important driver of community structure (Brown *et al.* 2007c). Investigating an alpine glacial floodplain, Robinson *et al.* (2002) found that drift was generally highest and most consistent

from a groundwater channel and increased with distance from the glacier terminus in the main channel. Refugia connected to the main channel increases with distance from the glacier terminus, and thereby the potential pool of aquatic colonists (MacArthur & Wilson 1967). Second, due to the reduced intensity of disturbance pulses and increased stream size (width), a patchwork of refugia and disturbance can develop, which enables both *r* and *k* selected species to coexist at the reach scale (Wilson 1994).

Both the IDH and HBC postulate that richness is lower at stable sites due to negative biotic interactions (e.g. predation and competition) which reduce abundance and exclude inferior competitors (Connell 1978). In this study groundwater streams supported low diversity and abundance, despite having the highest Chl *a*, contrary to the findings of Tonkin *et al.* (2012) which suggested productivity and disturbance are additive. A higher abundance of predatory Plecoptera, and Trichoptera (Figure 4.3) along with predatory amphibians (*Calotriton asper* and *Rana* spp.: K. Khamis Pers. Obs.) in groundwater dominated environments, suggests negative biotic interactions (i.e. predation) may have limited community development in this study (Peckarsky *et al.* 1990). Furthermore, my experiment has demonstrated that prey taxa densities are reduced in the presence of predatory Plecoptera through a combination of drift and direct consumption (Chapter 6).

Responses to meltwater stress varied among individual taxa and therefore H₄ (the most abundant invertebrate taxa would display mixed responses across the meltwater spectrum) could not be rejected. At MMC sites a higher density of smaller bodied Ephemeroptera (*B. alpinus*) and Plecoptera (*Protonemura* spp.) was evident (see Figures 4.3 & 4.4). Many alpine Ephemeroptera and Plecoptera display flexible and resistant life history traits, making them successful in reaches with temporally dynamic environmental conditions (Knispel *et al.* 2006;

Brittain 2007). Strong dispersal capabilities enable rapid (re)colonisation of disturbed patches (Matthaei *et al.* 1997). However, other *Baetis/Protonemura* traits, such as swimming/crawling and gill respiration, may limit colonisation of HMC sites. Here, high flows would inhibit the locomotive strategy (swimming) and high SSC would reduce gill efficiency (Larsen *et al.* 2011). Furthermore, due to conspicuous swimming and feeding behaviour, *Baetis* are particularly susceptible to invertebrate predation at LMC sites (Peckarsky & Penton 1989). Interestingly, community evenness was lowest at MMC sites (Figure 3.3) which is probably due to the dominance of *Baetis/Protonemura* (Figure 4.4).

Two abundant taxa *D. latitarsis* gr. and *R. evoluta* displayed positive and negative responses along the gradient respectively (Figure 4.4). *R. evoluta* is a large bodied predator, which are affected more by environmental harshness due to longer generation times and lower fecundity (Menge & Sutherland 1987; Trexler *et al.* 2005). *D. latitarsis* gr. is a glacial stream specialist which is adapted to low water temperature, high variability in flows and limited food availability (Clitherow *et al.* 2013), and thus reaches higher density at HMC sites but is probably competitively inferior under more benign conditions, when interspecific biotic interactions are more likely (Flory & Milner 1999). It should be noted that catchment geology was an important variable modifying the distribution of these two taxa along the meltwater gradient (Appendix 4.3). This suggests that indicator taxa approaches to monitor change may need to be interpreted in the context of macro-basin properties.

4.5. Conclusion

This study identified a strong environmental stress gradient, related to SSC, bed instability and diurnal flow variability, and basal resources (chl *a*), running from ‘harsh’ meltwater habitats to benign groundwater habitats. Community composition overlapped little between

HMC and LMC sites, and although supporting low alpha diversity, HMC sites were important for beta diversity due to a highly specialist and sometimes endemic fauna. Despite a linear stress gradient taxonomic richness, EPT richness and density (community/population) responses were unimodal along the meltwater stress gradient with peaks at sites of intermediate meltwater contribution (stress) due to a shift from strong niche filtering (high stress and disturbance) to competitive interactions at low meltwater contributions.

The findings of this study partially support the conceptual models for alpine river ecosystems of Brown *et al.* (2007b), but biotic interactions (predation and competition) at lower meltwater contributions may play an important role in structuring benthic communities. Hence, the linear harsh – benign response suggested by Brown *et al.* (2007b) is only apparent when hillslope groundwater springs are not considered. The Füreder (2007) model, which placed emphasis on the deterministic nature of alpine stream communities, may be applicable in higher altitude alpine environments and during the early melt season particularly when melting hillslope snowpacks may dilute the groundwater signal. A refined environmental stress model for ‘late melt season’ hydroecological conditions (i.e. minimal snowmelt influencing hillslope springs) is presented in an attempt to unify previous understanding (Figure 4.8). A shift from predominately abiotic to biotic controls along the meltwater gradient is hypothesised as the key control on community structure (Figure 4.8a). However, biotic interactions do still occur at highly stressed, meltwater dominated sites as demonstrated by a recent study which highlighted intra-guild predation and omnivory (Clitherow *et al.* 2013). The unimodal patterns of richness and abundance are due to a combination of abiotic niche filtering under higher meltwater conditions, strong top-down biotic controls at lower meltwater contributions and a smaller upstream colonisation pool at both ends of the stress

gradient. The evenness response represents the dominance of generalist taxa with good dispersal/colonization abilities at sites of moderate stress/disturbance (Figure 4.8b).

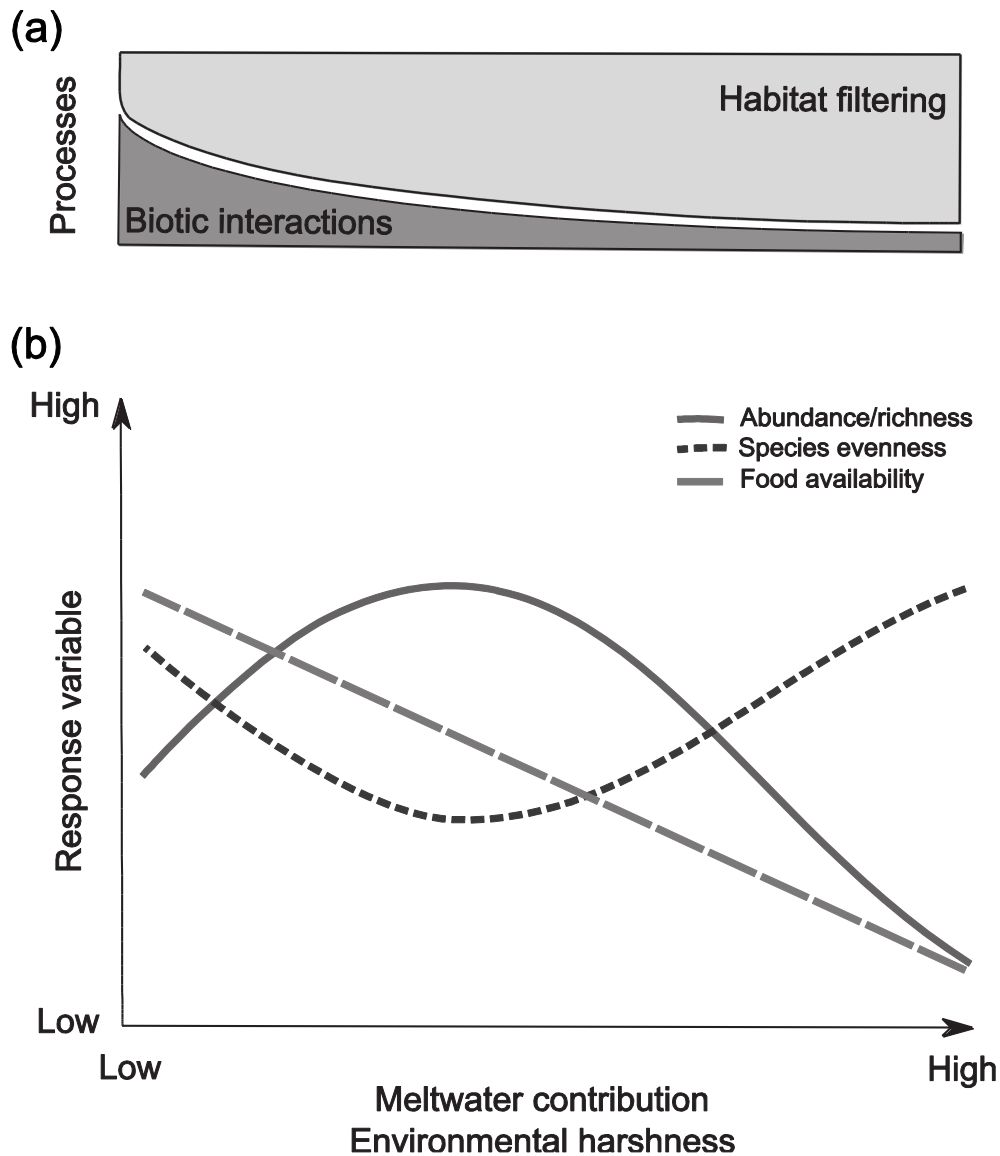


Figure 4.8. Theoretical alpine macroinvertebrate community structure responses during the late melt season: (a) the dominant process controlling community characteristics at the reach scale; and (b) hypothetical community responses along the meltwater (environmental harshness) gradient.

Future glacier and snowpack retreat will likely lead to more homogeneous alpine river ecosystems, with less distinct stress/disturbance gradients. An increase in mean diversity at the reach scale is predicted as habitats become more benign (Brown *et al.* 2007a; Jacobsen *et*

al. 2012). However, a reduction in beta diversity and potential loss of specialist taxa highlight the importance of higher meltwater influenced habitats for regional diversity (Jacobsen *et al.* 2012; Finn *et al.* 2013). Yet not all impacts will be negative as an increase in macroinvertebrate secondary production is likely, which will increase food availability for insectivorous terrestrial species such as the European dipper (*Cinclus cinclus*) and the Pyrenean Desman (*Galemys pyrenaicus*) (Stone 1987; Ormerod & Tyler 1991). However, range expansions by aquatic vertebrates (e.g. brown trout (*Salmo trutta*) and introduced brook trout (*Salvelinus fontinalis*)) are likely, as previously inhospitable habitats become more benign (Comte & Grenouillet 2013). This could potentially have important implications for within stream biotic interactions and cross boundary resource fluxes (Benjamin *et al.* 2011). As the current trend in glacier retreat is predicted to continue, conservation efforts should focus on maintaining alpine stream network connectivity, by limiting further flow regulation and tourist infrastructure, to ensure meta-population dynamics and genetic diversity are maintained.

4.6. Chapter summary

In this chapter the role of disturbance and environmental stress in maintaining biodiversity patterns was investigated across a meltwater gradient in the French Pyrénées. From the findings of this research it is possible to make inferences about future community trajectories in the context of climate change and glacial retreat. Interestingly, despite findings in Chapter 3, geology did not seem to be important for determining community level patterns. Interpreting and conceptualizing these findings in the context of community assembly processes (see Figure 4.8) would appear to explain observed diversity and distribution

patterns. In Chapter 5 these ideas are investigated further and functional diversity patterns and community assembly processes are quantified across the meltwater spectrum.

CHAPTER 5

*Biological traits, functional diversity
and community assembly processes in
alpine river systems*

5.1. Introduction

Climate change will have significant implications for aquatic biodiversity and ecosystem functioning (Woodward *et al.* 2010c). High altitude and latitude ecosystems are particularly sensitive as rates of warming are already greater than that at lower latitude/altitude (Beniston 2012) and many taxa are range restricted specialists at their climatic limits (Heino *et al.* 2009). High altitude glaciers and snowpacks are predicted to recede significantly over the coming century (Barnett *et al.* 2005; López-Moreno *et al.* 2009), with significant implications for alpine river ecosystems due to the strong coupling between cryospheric processes (snow and ice melt), river flow and benthic physicochemical habitat (Hannah *et al.* 2007). Changes in the timing and magnitude of meltwater production are expected to modify habitat conditions, with implications for ecosystem functioning and biological diversity at a range of scales and levels of organisation (Brown *et al.* 2007a; Jacobsen *et al.* 2012; Finn *et al.* 2013; Friberg *et al.* 2013). However, to date the focus has predominately been on taxonomic patterns and responses (Milner *et al.* 2009), with only a few studies assessing common features (traits) shared by taxa sensitive to climate change (Snook & Milner 2002, Ilg & Castella 2006, Brown & Milner 2012).

For an organism from the regional species pool to occur at a given location, conceptually it first must pass through a series of habitat ‘filters’, of which the broadest spatially is climate (Poff 1997; Naeem & Wright 2003). A further suite of filters then operate at nested scales to dictate the community composition at a given reach (Statzner *et al.* 2001). These range from broad scale watershed properties (e.g. lithology and hydrological regime), to meso and micro scale filters, (e.g. substratum size or hydraulic stress) (Poff 1997). Glacier meltwater fed rivers represent ‘extreme’ freshwater habitats; low water temperature, highly variable flows

and unstable channel beds limit colonists to cold stenothermic taxa with flexible life cycles, freeze tolerance and adaption to high flow velocity (Lencioni 2004; Füreder 2007). Such harsh environmental conditions are analogous to a fine mesh, allowing only a small subset of the regional pool to successfully colonise a habitat patch, resulting in species poor assemblages that display similar traits (Statzner *et al.* 2001). Habitat-trait approaches can therefore be applied across multiple bio-geographical regions where taxonomic comparisons may not be viable (Buisson & Grenouillet 2009; Menezes *et al.* 2010). For example, taxonomic comparison between the glacier fed rivers of Europe and New Zealand is made difficult by differences in the faunal composition (Cadbury *et al.* 2011): in Europe *Diamesa* (Chironomidae: Diptera) dominate but they are absent in New Zealand, their place taken by *Deleatidium* (Leptophlebiidae: Ephemeroptera). However, despite the utility of biological traits for assessing benthic community response to climate change (Bonada *et al.* 2007; Poff *et al.* 2010; Brown & Milner 2012) our understanding of habitat–trait–biodiversity relationships in alpine river systems, remains limited (Ilg & Castella 2006; Füreder 2007).

The comparatively few studies which have focused on functional traits in glacierized river catchments have identified distinct patterns in trait diversity and composition across space (Snook & Milner 2002, Ilg & Castella 2006, Füreder 2007) and time (Brown & Milner 2012). Low trait diversity has been recorded in glacier-dominated river habitats due to the strong environmental filtering, limiting colonists to fauna exhibiting resistant and resilient traits (Füreder 2007). Small body size, body shape (streamlined or cylindrical), clinger habit and short generation times have been identified as traits which offer resistance and resilience to the predominately harsh environmental conditions (Snook & Milner 2002). A number of other resistant and resilient traits were identified by Füreder (2007), such as cold water adaption, dispersal capabilities and number of life stages in the aquatic environment.

Interestingly, a study by Brown & Milner (2012) in an Alaskan glacierized river basin did not identify body size or clinger habit as traits associated with glacial influence. It is postulated that as this study system was at lower altitude and in close proximity to the Pacific Ocean the large Salmon population it supports may suppress colonisation by both larger bodied and clinging taxa (Monaghan & Milner 2009).

Recently, the measurement of Functional Diversity (FD) has become increasingly popular in biodiversity studies as it offers, to some degree, a measure of ecosystem function, and can be used to infer stability or resilience to environmental disturbance (Gerisch *et al.* 2012; Paillex *et al.* 2013). Furthermore, FD can give insights into habitat filtering, community assembly (niche based vs stochastic) and how species interact and coexist (McGill *et al.* 2006; Cadotte *et al.* 2011), which in turn can be used to inform conservation and restoration strategies (Paillex *et al.* 2013). However for glacierized river systems FD patterns and contemporary community assembly processes are not well understood (Ilg & Castella 2006; Brown & Milner 2012). To aid predictions of biodiversity response to future scenarios of environmental change a better understanding of these patterns and processes is required (Götzenberger *et al.* 2012; Brown & Milner 2012).

A mechanistic understanding of multi-taxa communities in relation to physicochemical habitat can be obtained through functional-traits-on-gradient approaches (McGill *et al.* 2006) which in alpine river environments, given the steep environmental gradients, has been the dominant approach. However, these have been based on either: (i) static habitat measures (i.e. % glacier cover in the catchment); or (ii) synthetic habitat measures of glacier influence (e.g. habitat variables sensitive to changes in glacier melt contribution). Static habitat measures do

not account for between catchment variability in rates of tributary inflow (attenuation of glacier melt signal) or the temporal variation in water source contribution (Malard *et al.* 2006); hence, the spatial-temporal habitat template to which organisms respond is not accounted for (Southwood 1977). Synthetic habitat measures are only relative to the study system or data set used, thus comparisons across space and time are difficult (Brown *et al.* 2010b). Brown *et al.* (2007) used a quantitative measurement of water source contributions (meltwater: groundwater proportions) to detect subtle spatial and temporal changes in river habitat characteristics and benthic biodiversity patterns. The hydrological, process basis of this approach (water source-river habitat-biota cascade), defines a habitat template which is sensitive to subtle spatial and temporal variability (Hannah *et al.* 2007) and therefore represents an ideal, climate sensitive, gradient for trait based studies in alpine river systems. This is particularly important when trying to identify trait profiles sensitive to changes in climate and glacier influence which could be used as indicators of change (Füreder 2007). However, the ‘watersource’ approach has, to date, only been used to explore taxonomic patterns in alpine river systems (Brown *et al.* 2009b, 2010b).

The objectives of this study were: (i) to identify the traits possessed by the ‘regional’ species pool across five glaciated river basins in the French Pyrénées; (ii) to characterise benthic macroinvertebrate trait-environment relationships along a gradient of meltwater contribution, and thus identify potential climate change ‘indicator’ trait profiles; and (iii) using the water source template, assess the potential implications of glacier retreat for functional (trait) diversity and community assembly in alpine river systems.

5.2. Methods

5.2.1. Field location

This study was conducted across five alpine, headwater basins in the French Pyrénées (see Chapter 2 for a detailed description of the study basin) within the Gave de Pau catchment (Figure. 5.1). Twenty-six, 15m reaches were identified across the five study basins (Appendix 4.1). In three of the river basins, seven sites were selected from hillslope springs and streams which were assumed to be sourced exclusively from groundwater aquifers flowpaths, as ridge top and hillslope snow was absent in August 2011. The other 19 sites were located on five glacier fed streams (Appendix 4.1). The meltwater component was considered a mixture of ‘quickflow’ sourced from ice and permanent snowpacks with minimal rock contact time and slower routed meltwater (‘distributed flow’) which had travelled through glacier sub-drainage systems (Brown *et al.* 2006d).

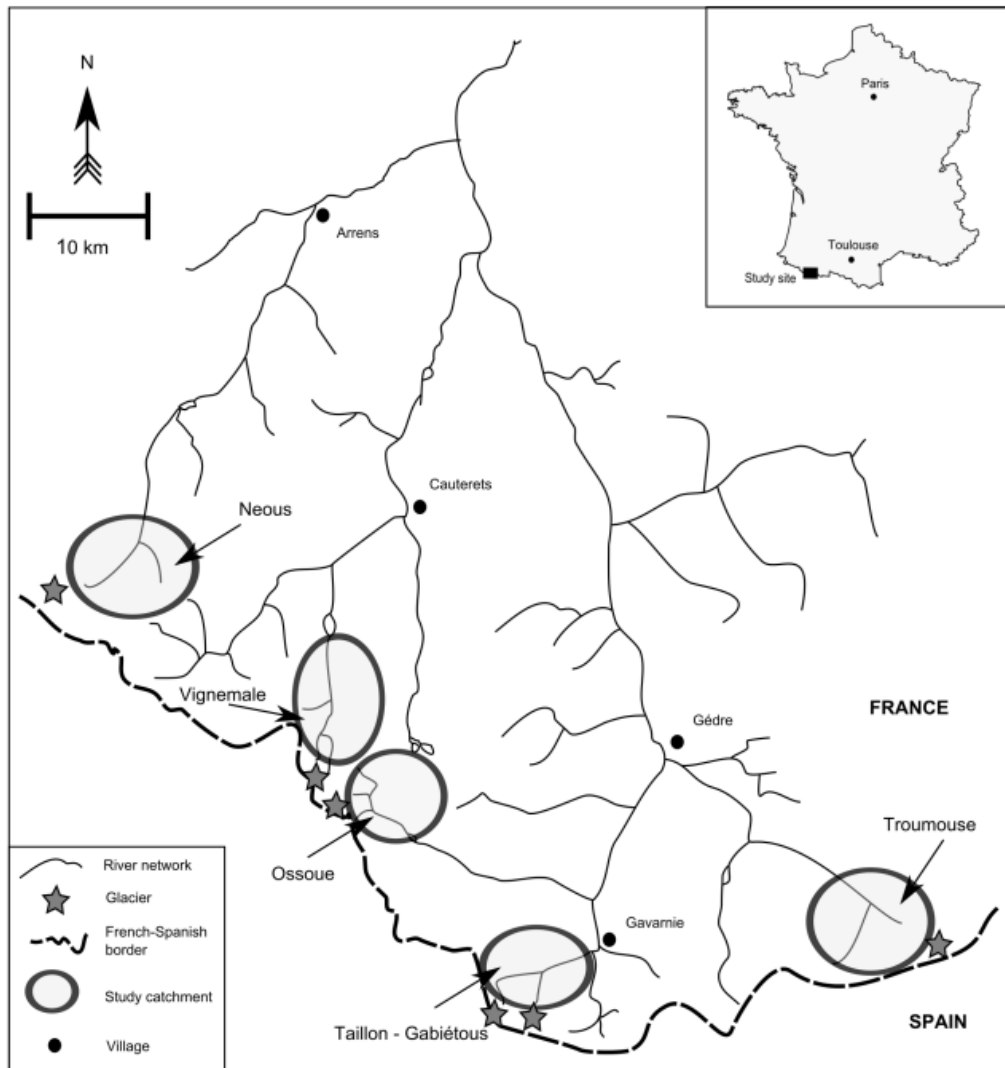


Figure 5.1. Location of study basins within the Gave de Pau drainage. Grey ellipses represent the drainage areas for each basin and stars represent glaciers. The broken dashed line is the French–Spanish border.

5.2.2. *Physicochemical data and watersource contribution*

Water source contributions (Meltwater:groundwater) were calculated for each site using end member mixing analysis. Detailed methods for this procedure are outlined in Chapters 3 and 4. At each reach, pH, electrical conductivity (EC), suspended sediment concentration (SSC), water temperature (T_w), Pfanckuch Index (PFAN) were determined as in Chapters 3 and 4.

5.2.3. *Biological sampling and processing*

Replicate benthic samples were collected between 18 August and 28 August, 2011 (Chapter 4). In the laboratory samples were processed and macroinvertebrates identified as outlined in Chapter 4. Three randomly selected cobbles were also collected from each reach and the epilithon retained for chlorophyll *a* (chl *a*) analysis (see Ledger *et al.* (2006) for methods).

5.2.4. *Biological traits*

Trait information was collated from a number of existing databases (Tachet *et al.* 2000; Snook & Milner 2002; Ilg & Castella 2006), selected published works and expert opinion. Twelve biological traits, with a total of 54 modalities (trait categories), were identified and recorded for each taxa (Table 5.1). The fuzzy coding approach outlined by Tachet (2000) was adopted where the affinity a taxa has to a given trait category is scored between either 0 or 5 (for a trait with >4 modalities) or 0 and 3 (for a trait with <5 modalities). This enables ontogenetic diet shifts, omnivory and trait plasticity to be incorporated into the analysis (Dolédéc *et al.* 2006). Data were compiled for the 51 most abundant taxa (Appendix 5.1) and where possible genera trait information was used. However, taxa within the genus *Drusus* were coded at the species level as feeding specialization has led to species within this genera occupying distinct trophic niches (Graf *et al.* 2009; Waringer *et al.* 2010). For taxa identified

to a higher taxonomic level (i.e. Family or Order), an average of the genera within that order was calculated (Beche *et al.* 2006). This information was then transformed into a frequency distribution and rescaled so that the modalities in each trait summed to 1 (Bady *et al.* 2005).

5.2.5. Data analysis

Classification of sites into meltwater groups. Following methods outlined in Chapter 4 sites were classified into groups based on physicochemical habitat variables (water source not included). A three group classification was identified: (1) high meltwater contribution > 75% (HMC); (2) mid-meltwater contribution 10-75% (MMC); and (3) low meltwater contribution, <10% (LMC).

RLQ analysis. To relate macroinvertebrate traits to the recorded environmental variables a combination of RLQ analysis (Dolédec *et al.* 1996) and fourth-corner tests (Dray & Legendre 2008) were used. RLQ is a three table ordination method which enables simultaneous analysis of abundance-site data (L table), site–environmental habitat data (R table) and species-trait data (Q table). First, Correspondence Analysis (CA) was conducted on the L table and row and column weights retained to couple the R and Q tables. Second, Principle Component Analysis (PCA) was carried out on the R table. Third, Fuzzy Correspondence Analysis (FCA) (Chevenet *et al.* 1994) was used to ordinate the taxa based on their trait profiles (Q table). Analysis of trait–FCA axes correlations and inter-trait correlations (RV coefficients: c.f. Ilg & Castella 2006) also enabled the identification of trait patterns within the regional taxa pool. Finally, RLQ analysis then combined the three ordinations, through an eigenvalue analysis of the matrix $R^T L Q$, to maximise the covariance between environmental

variables and species traits (Dziocik *et al.* 2011). A permutation test with 999 repeats was used to test the significance of the R–Q relationship.

Table 5.1. List of the biological traits and modalities (categories) used for analysis in this study. Those modalities marked (*Resil*) represent resilient traits and those marked (*Resis*) resistant traits in the context of glacier fed streams.

Trait	Modality	Trait	Modality	
Maximal body size	<2.5 mm (<i>Resil</i>)	Substrate relationship	Swimmer	
	2.5–5 mm (<i>Resil</i>)		Crawler	
	5–10 mm (<i>Resil</i>)		Burrower	
	10–20 mm		Interstitial (<i>Resis</i>)	
	20–40 mm		Clinger (<i>Resis</i>)	
Voltinism	Semivoltine	Diet	Micro-organisms	
	Univoltine		FPOM	
	Multivoltine (<i>Resil</i>)		CPOM	
Aquatic stages	Egg		Periphyton	
	Larvae		Macrophytes	
	Pupae		Dead animals	
	Adult		Invertebrates	
Reproduction	Ovoviviparity	Functional feeding group	Scraper	
	Isolated eggs free		Shredder	
	Isolated eggs cemented		Collector	
	Clutches cemented or fixed		Filter	
	Clutches free		Predator - piercer	
	Clutches in vegetation		Predator - engulfer	
	Clutches terrestrial (<i>Resil</i>)		Streamlined (<i>Resis</i>)	
Dispersal	Asexual reproduction	Body form	Cylindrical (<i>Resis</i>)	
	Aquatic passive		Other	
	Aquatic active		Case construction	No case
	Aerial passive			Case
Resistance	Aerial active (<i>Resil</i>)			
	Eggs (<i>Resis</i>)			
	Diapause (<i>Resis</i>)			
Respiration	None			
	Tegument			
	Gills			
	Plastron			
	Spirical			

Fourth-corner analysis. Fourth-Corner Analysis was used to test the link between species' traits and habitat characteristics. For this analysis the R data table consisted of sites and meltwater contribution group (HMC, MMC, and LMC) membership. To test the null hypothesis that species traits are unrelated to meltwater contribution, a combination of permutation tests were adopted. This reduces Type I errors and provides a robust measure of links between the R, L and Q tables (see Dray and Legendre (2008) for detailed methods). Briefly, both site vectors and species vectors were permuted independently (999 repeats), then when both tests were significant the null hypothesis that traits, taxa abundance and environmental conditions are not linked was rejected. *P*-values were Bonferroni corrected for multiple comparisons (Gallardo *et al.* 2009).

Meltwater–trait relationships. For traits identified as displaying strong relationships with meltwater (4th corner analysis), the proportion of individuals displaying an affinity to that trait modality was then calculated for each site. The relationship between the selected traits and meltwater contribution was modelled using logistic regression. Here, the response variable was treated as a binomial event, with a success being an individual displaying an affinity to the trait of interest. This approach was chosen over arcsin square root transformation of the data as binomial regression demonstrates increased power and interpretability when compared to linear models with transformed data (Warton & Hui 2011). Logistic regression follows the basic linear model form:

$$Y_i = \alpha + \beta X_i + \varepsilon_i \quad (5.1)$$

Where;

$$Y_i \sim B(n_i, p_i) \quad (5.2)$$

$$E(Y_i) = n_i p_i \quad (5.3)$$

$$\text{var}(Y_i) = n_i p_i (1 - p_i) \quad (5.4)$$

$$\text{logit}(p_i) = \alpha + \beta(\text{Meltwater}) \quad (5.5)$$

n_i = number of invertebrates (individuals) sampled at a given site and p_i = the probability that a randomly selected individual displays an affinity to that trait modality. Explained deviance was calculated to evaluate model performance, this is a measure analogous to R^2 in OLS regression (Zuur *et al.* 2009)

Functional diversity. We first estimated FD as FD_{ric} after Petchey & Gaston (2002). Following Mouchet *et al.* (2008), multiple trait based dendrograms were built from the first four FCA axes using a range of cluster methods and distance metrics. The combination of method and distance that minimised dissimilarity between the initial distance and the cophenetic distance matrices was retained. FD_{ric} (Gower distance and UPGMA clustering; $c = 0.86$) was then calculated as the total branch length linking all taxa at a given site, based on the trait dendrogram (Mouchet *et al.* 2010). FD was also calculated using Rao's quadratic entropy (QE: Rao 1982) which combines both functional richness and functional divergence,

the FD components best suited to detecting community assembly processes (Mason *et al.* 2012). Orloci's chord distance was used to calculate the distance between all taxa pairs (Pavoine *et al.* 2009). The resultant functional distance matrix was used to calculate FD_{QE} following Botta-Dukát (2005). These two measures of functional diversity are recommended for studies when the number of taxa is small compared to the number of traits (Mouchet *et al.* 2010).

OLS regression was used to model relationships between meltwater contribution and functional diversity measures (FD_{ric} and QE). An iterative procedure was adopted to test successively higher order polynomial models. The best model was identified using the Akaike Information Criterion (AIC) (Paillex *et al.* 2013). OLS regression was also used to test relationships between functional diversity and taxonomic richness and the optimum model assessed as above. If a linear relationship (order 1) was identified, a slope of <1 was considered to represent functional redundancy and >1 functional singularity of rare species (Micheli & Halpern 2005).

To compare observed functional diversity (I_{obs}) with the functional diversity of a random assemblage (I_{exp}) a null model approach was adopted. For FD_{ric} the number of taxa (n) were held constant for each sample site, n taxa were then randomly selected from the regional species pool (999 repeats) and FD_{exp} calculated for each iteration (Flynn *et al.* 2009). For QE a matrix swap randomisation method, which holds richness and abundance constant at site specific and global levels, was adopted and QE_{exp} calculated for each iteration (999 repeats) (Mason *et al.* 2013). The null mean (X_{exp}) and variance (σ_{exp}) were calculated for both

measures of functional diversity and for each meltwater group. The standardized effect size (SES) was then calculated (Gotelli & McCabe 2002):

$$SES = (I_{\text{obs}} - x_{\text{exp}}) / \sigma_{\text{exp}} \quad (5.6)$$

When SES is not different from zero a random assembly is inferred. While $SES > 0$ and $SES < 0$ suggest, limiting similarity (trait divergence) and niche filtering (trait convergence) respectively. It should be noted that SES_{QE} is considered a pure index of functional divergence (i.e. becomes independent of functional richness) (Mason *et al.* 2012). OLS regression was used to model the relationship between SES and meltwater contribution to flow as above. Further to this, for each meltwater group, one-tailed Wilcoxon tests were used to determine whether mean SES values were significantly different from zero.

All analysis was carried out in R 2.14.1. using the *ADE4* package (Chessel *et al.* 2004) and *Vegan* package (Oksanen *et al.* 2012).

5.3. Results

5.3.1. Biological traits

The FCA of the Q table, identified grouping of genera by taxonomic order (Figure 5.2a). Axis F1 explained 26.1% of the variance and was strongly correlated to reproduction (0.53), functional feeding group (0.51), life history (0.38), body shape (0.34), body size (0.28) and diet (0.26). Diptera, Oligochaeta and Trichoptera had positive scores for the F1 axis while other orders were negative (Figure 5.3a). Plecoptera, Diptera and Trichoptera were arrayed along the F2 axis, which explained 12.4% of the variance and was correlated to functional feeding group (0.69), diet (0.35) size (0.33) and reproduction (0.23). Axis F3 explained 9.9% of the variance and was strongly correlated to case construction (0.61).

Taxa with positive scores on the F1 axis complete full metamorphosis, reach a small maximal body size (< 5mm), lay eggs in clutches (vegetation, terrestrial or free), were passive aerial dispersers with > 1 generation per year. These were predominately Chironomidae, Simuliidae, Oligochaeta, Elmidae and a number of Trichoptera genera (Figure 5.2b). Taxa with negative scores on the F1 axis carry out gradual metamorphosis, lay cemented eggs, have a larger body size which is flattened dorsal ventrally, are semivoltine and either predators or shredders. Plecopteran taxa from both the suborders Systelognatha (e.g. Perlodidae and Perlidae) and Euholognatha (e.g. Leuctridae and Nemouridae), *Baetis*, *Rhithrogena*, *Rhyacophila* and predatory dipterans (*Atherix*, *Dicranota* and *Tipula*) displayed negative scores along the F1 axis (Figure 5.2b).

Positive scores on the F2 axis were associated with large body size (>10mm) and a diet consisting of live or dead invertebrates. Plecopteran taxa from the suborder Systellognatha, predatory dipterans and caseless trichopteran taxa displayed positive scores along this axis. Negative scores on the F2 axis were associated with shredders and collectors, feeding predominately on detritus, macrophytes and algae, with the ability to enter diapause during unfavourable conditions. Plecoptera from the sub order Euholognatha, *Baetis* and *Rhithrogena* clustered negatively along axis F2 (Figure 5.2b).

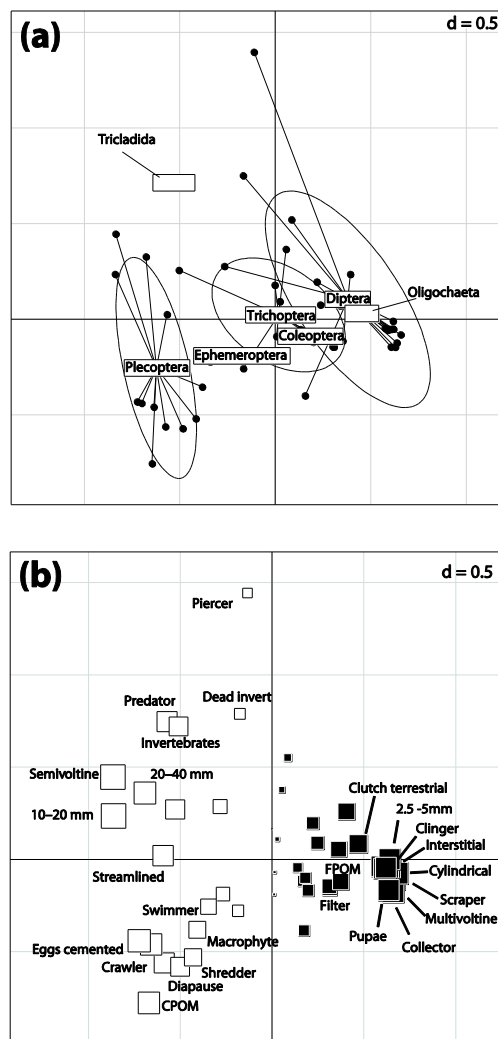


Figure 5.2. Fuzzy correspondence analysis results: (a) distribution of taxa on axes F1 and F2 in trait space. The taxa are grouped by order and labels represents the group centroid. (b) Bubble plot for all biological trait modalities in F1 and F2 trait space. The size of square represents trait score on the F1 axis, filled squares are positive scores and open squares negative scores. In both panels d denotes the distance associated with each grid sub-division.

5.3.2. Relationship between traits and habitat patterns

Axis one and axis two of the RLQ analysis explained 74.0% and 19.5% of the total variance respectively and a significant relationship between environmental variables and biological traits was identified (permutation test, $P < 0.001$, 999 repeats). The RLQ analysis also retained a large proportion of the inertia of the separate analyses (see Table 5.2).

Table 5.2. Summary of the results from the separate ordinations and RLQ analysis. Explained variance (%) is displayed in parentheses.

Analyses	Variable	Axis 1	Axis 2
R/PCA	λ (Variance)	2.9 (58.7)	1.7 (26.5)
Q/FCA	λ (Variance)	0.3 (26.1)	0.2 (12.4)
L/CA	λ (Variance)	0.4 (18.0)	0.3 (15.8)
RLQ			
	λ (Variance)	0.8 (74.0)	0.2 (19.5)
	Covariance	0.28	0.14
	Correlation	0.40	0.38
	R (Variance)	2.7 (84.6)	4.2 (86.1)
	Q (Variance)	0.2 (97.2)	0.3 (91.1)

Samples sites were split by meltwater contribution along the first RLQ axis, with HMC sites displaying positive scores and LMC sites negative scores (Figure 5.3b). SSC, bed instability (PFAN), EC and water temperature were most strongly correlated to the first axis (Figure 5.3a). Hence, from low to high values the first axis represented an environmental harshness gradient, strongly associated with meltwater contribution ($R^2 = 0.62$, $P < 0.001$, $y = 38.3 +$

21.8x). Axis two split the LMC sites from the other sites and correlated negatively with wetted width and river depth and positively with chl *a* (Figure 5.3a), representing a habitat size and resource gradient.

Trait modalities associated with positive site scores on RLQ axis 1 were clinger, multivoltine life history, FFG: scraper and collector/deposit feeder, small body size (<10mm), cylindrical body shape and egg laying in terrestrial clutches. Modalities associated with negative scores were crawler, univoltine life history, streamlined body shape, larger body size (10-20mm), instream oviposition (eggs/clutches) and desiccation resistant eggs (Figure 5.3c). Trait modalities associated with positive site scores on the RLQ axis 2 were predator feeding group, invertebrate diet, and large body size (>20mm). The trait modalities swimmer, shredder, CPOM, plastron and gill respiration, diapause and free egg laying were associated with negative scores (Figure 5.3c).

5.3.3. Relationships between traits and meltwater contribution

The fourth corner analysis identified 28 modalities which were significantly related to one of the meltwater contribution groups (Table 5.3). The HMC sites were positively associated with 9 trait modalities, primarily resistant and resilient life history traits and adaptations related to rheophily (Table 5.3). Negative associations between HMC and 6 modalities were identified, the strongest being crawler substrate relationship (-0.21) and desiccation resistant eggs (-0.18). The LMC sites were positively associated with 11 trait modalities, the strongest relationships were for predatory feeding, semivoltine life history and active aquatic dispersal, and negatively associated with 5 modalities collector deposit feeder (-0.2) and small body size (-0.15). The MMC sites were positively related to 4 modalities and negatively related to

5 modalities. The strongest relationships were recorded for gill respiration (0.17) and tegument respiration (-0.17) respectively (Table 5.3). Logistic regression identified strong relationships for a number of traits (Figure 5.4; Appendix 5.3), particularly those associated with life history, substrate relationship and feeding/diet (Figure 5.4).

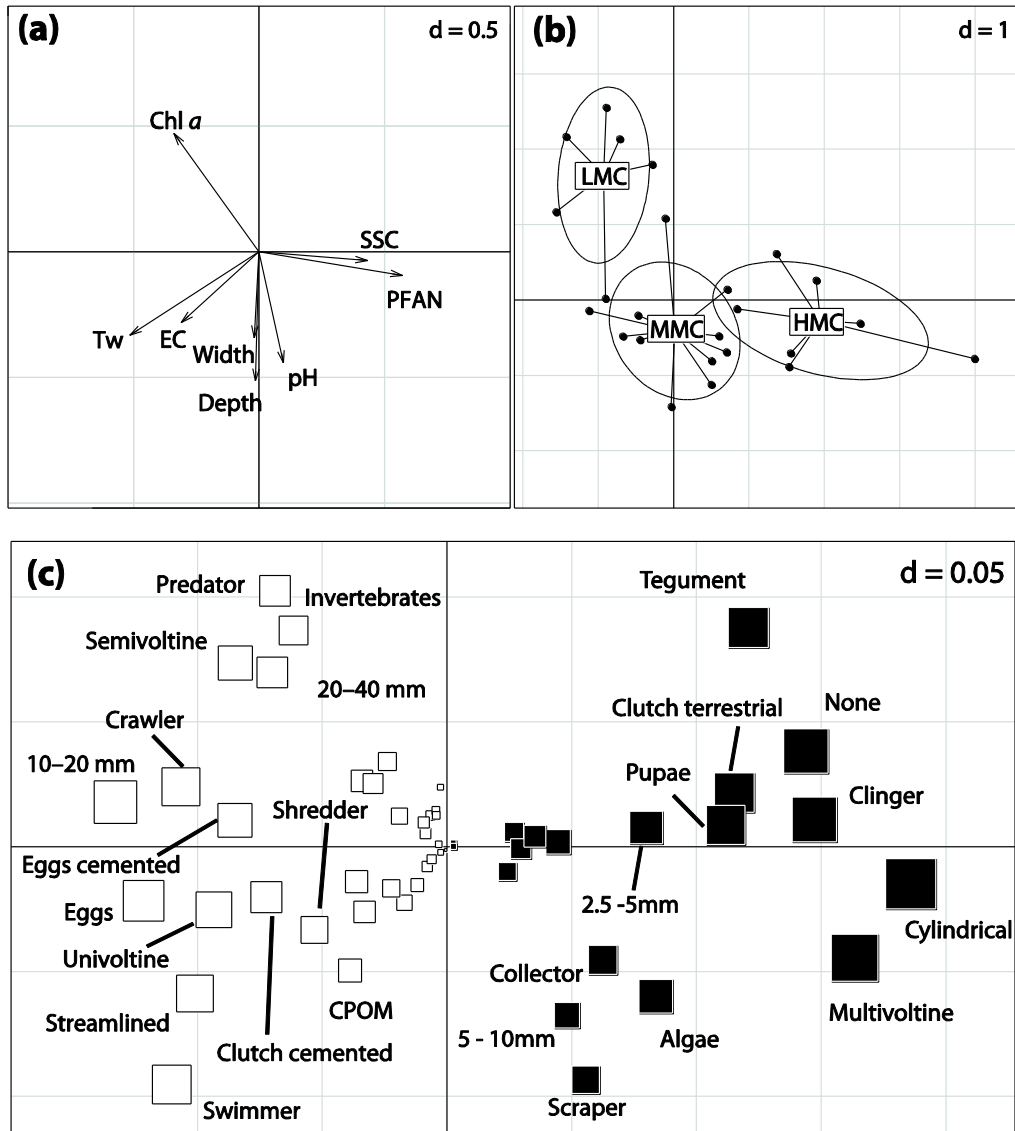


Figure 5.3. (a) Ordination of environmental variables along RLQ axes F1 and F2. (b) Location of sampling sites along RLQ axes F1 and F2 grouped by meltwater contribution; HMC = high meltwater, MMC = mid meltwater and LMC = low meltwater (label represents group centroid). (c) Bubble plot for all biological trait modalities in RLQ axes space, the size of square represents trait score on the F1 axis, filled squares are positive scores and open squares negative scores. In all panels d denotes the distance associated with each grid subdivision.

Table 5.3. Results of the “4th Corner Method” on the trait-habitat matrix, where HMC = high meltwater contribution group, MMG = mid meltwater group and LMG = low meltwater group. All r values were significant ($P < 0.05$) following a permutation procedure (999 runs) and Bonferroni correction for multiple comparisons.

Trait	Modality	Meltwater group			
		HMC r	MMC r	LMC r	
Maximal body size	2.5 -5 mm (<i>Resil</i>)	0.11	-	-0.15	
	20–30 mm	-0.14	-	0.14	
Voltinism	Semivoltine	-	-	0.16	
	Multivoltine (<i>Resil</i>)	0.16	-	-	
Aquatic stages	Adult	-0.11	-0.12	-	
	Pupae	0.11	-	-	
Reproduction	Clutch terr (<i>Resil</i>)	0.17	-	-	
	Asexual	-	-	0.1	
Dispersal	Aquatic passive	0.11	-	-	
	Aquatic active	-0.14	-	0.18	
	Aerial passive	-	0.12	-	
Resistance	Eggs	-0.18	-	0.11	
	Diapause	-	0.13	-	
	None	0.18	-	-	
Respiration	Tegument	-	-0.17	0.12	
	Gills	-0.12	0.17	-	
Substrate relationship	Crawler	-0.21	-	0.1	
	Burrower	0.12	-	-	
	Clinger (<i>Resis</i>)	0.15	-	-	
Diet	FPOM	-	-	-0.11	
	Algae/diatoms	-	-	-0.15	
	Dead invertebrates	-	-0.11	0.2	
	Invertebrates	-	-0.12	0.18	
Functional group	feeding	Scraper	-	-	-0.1
		Collector/Deposit feeder	-	0.14	-0.2
		Predator	-	-0.15	0.2
		Body form	Cylindrical (<i>Resis</i>)	0.16	-
		Other	-	-	0.15

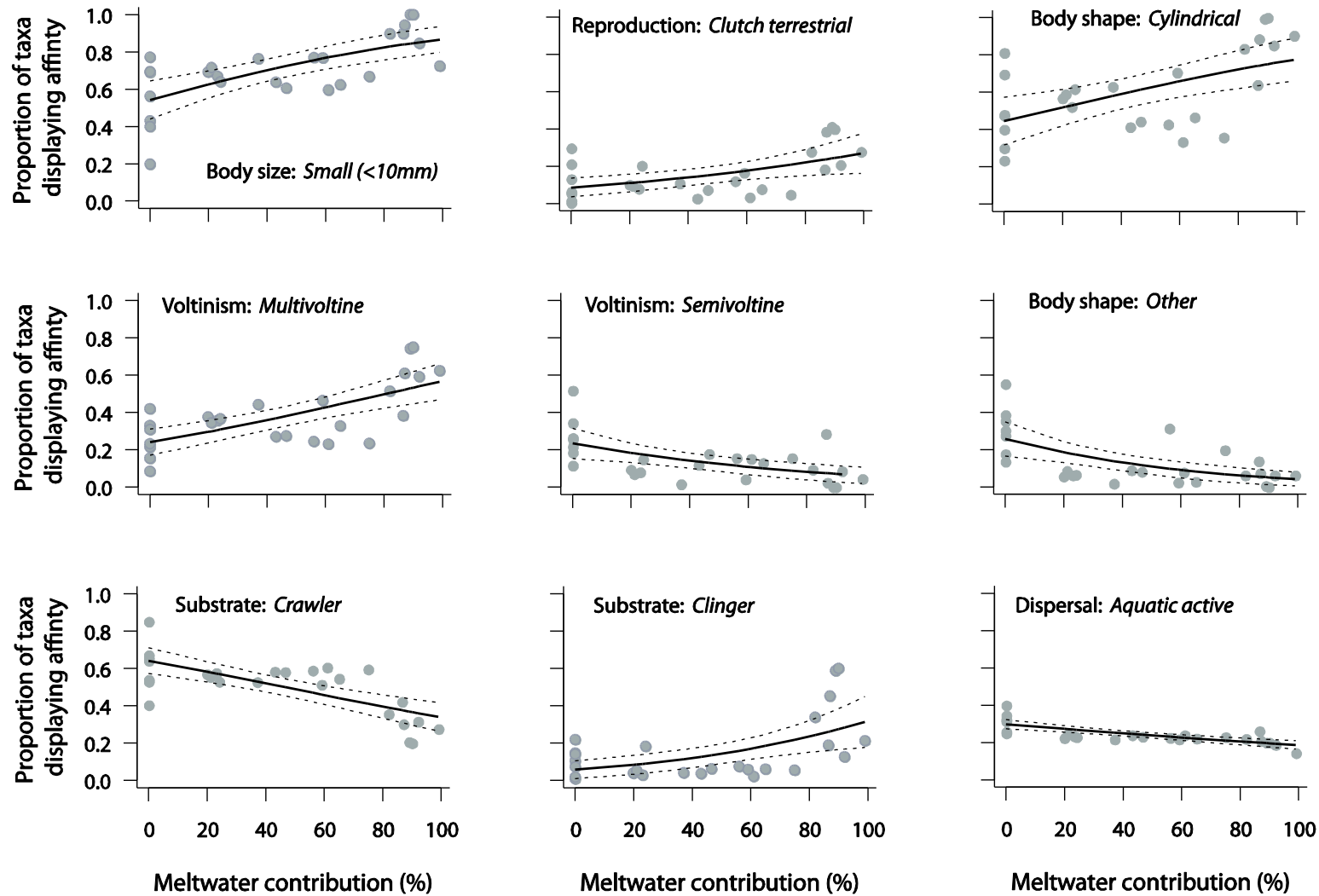


Figure 5.4. Logistic regression (GLM) models for meltwater contribution and the proportion of taxa with an affinity to traits identified as significant by fourth corner analysis. Dashed lines represent 95% confidence intervals

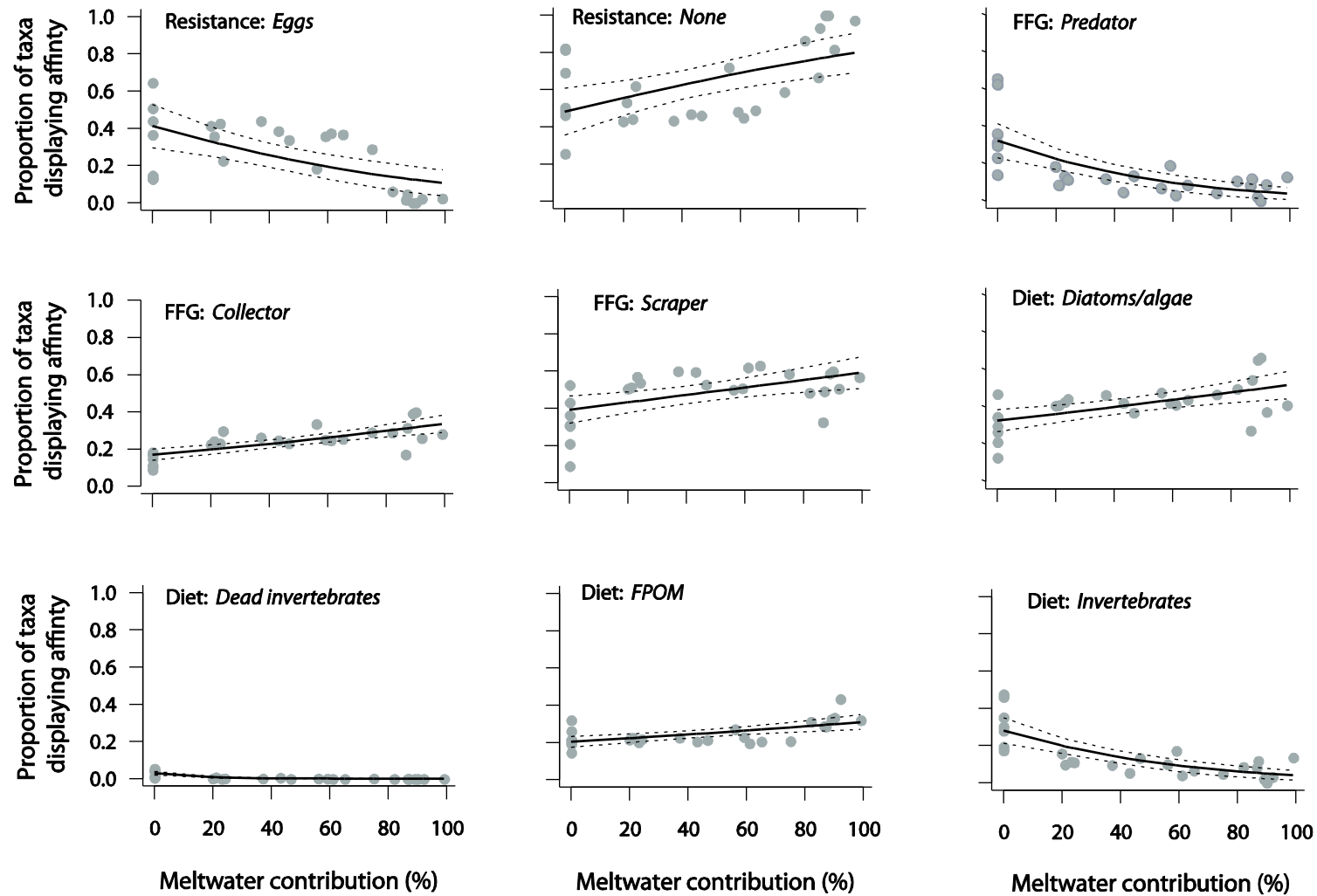


Figure 5.4 cont. Logistic regression (GLM) models for meltwater contribution and the proportion of taxa with an affinity to traits identified as significant by fourth corner analysis. Dashed lines represent 95% confidence intervals.

5.3.4. Functional diversity and meltwater contribution

The relationship between meltwater contribution and FD was unimodal ($R^2 = 0.68$, $P < 0.001$, $y = 0.35 + 0.02x - 0.0001x^2$, Figure 5.5a), with the highest FD between 40-60% meltwater contribution and lowest at HMC sites, >75%. QE displayed a negative relationship with meltwater ($R^2 = 0.42$, $P < 0.001$, $y = 0.29 - 0.002x$, Figure 5.5b). FD_{ric} was positively related to indexed taxonomic richness ($R^2 = 0.87$, $P < 0.0001$, Figure 5.5c), however the slope (1.07 ± 0.09) was not significantly different from 1, suggesting all taxa contributed to functional richness. QE and taxonomic richness were not linearly related (Figure 5.5d). $SES_{FD_{ric}}$ was negatively related to meltwater contribution ($R^2 = 0.31$, $P = 0.004$, $y = -1.66 - 0.012x$, Figure 5.6a). A quadratic relationship was apparent between SES_{QE} and meltwater contribution ($R^2 = 0.41$, $P = 0.001$, $y = 0.87 - 0.066x + 0.0006x^2$, Figure 5.6b) with the lowest values at intermediate meltwater contribution.

When considering differences between meltwater groups FD_{ric} was greatest at MMC sites ($H = 20.1$, $P < 0.0001$) but for QE was greatest at LMC sites ($H = 16.8$, $P < 0.0001$). For all meltwater groups the $SES_{FD_{ric}}$ values were significantly less than zero (Figure 5.6c; one-tailed Wilcoxon test, $P < 0.05$). For SES_{QE} values, LMC sites were significantly greater than zero, MMC sites significantly less than zero and HMC displayed no difference (Figure 5.6d).

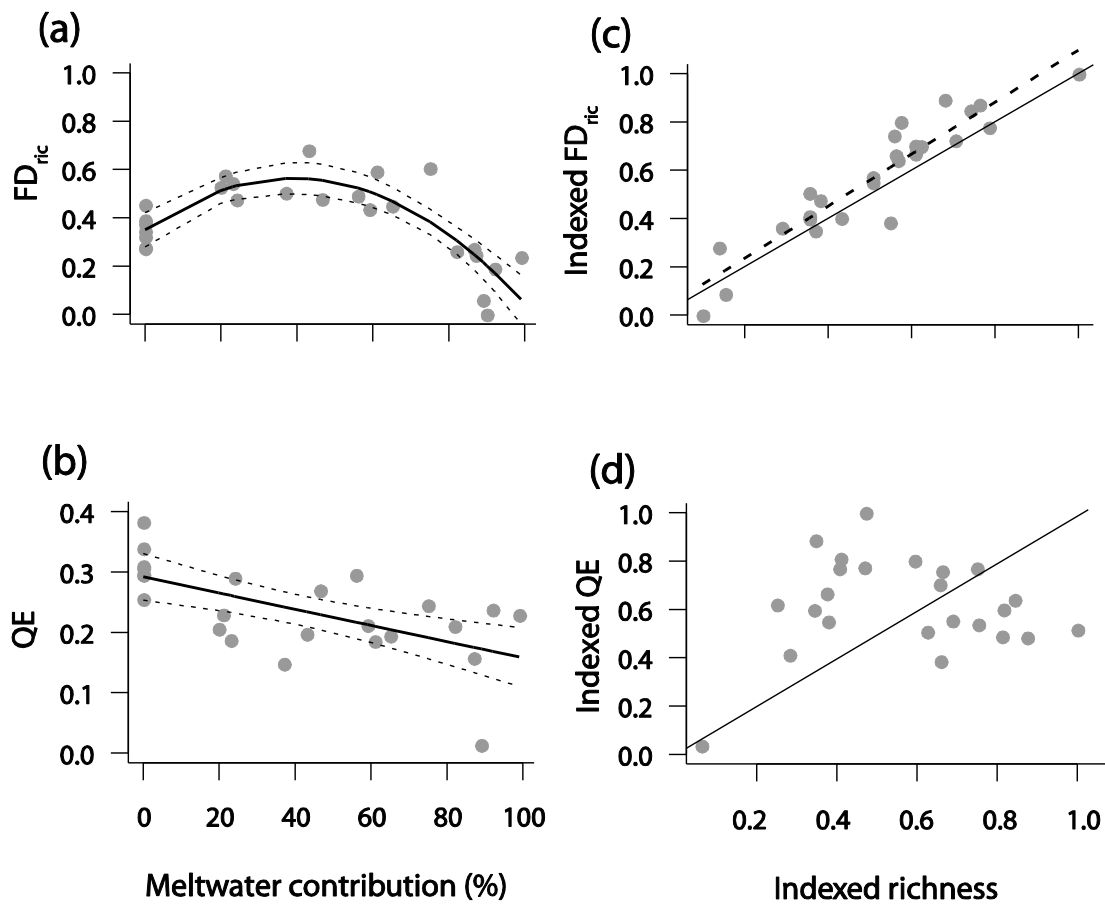


Figure 5.5. Linear and polynomial regression models of the relationship between: (a) FD_{ric} and meltwater contribution; (b) QE and meltwater contribution; (c) FD_{ric} and indexed taxonomic richness; and (d) QE and indexed taxonomic richness. For a & b dashed lines represent 95% confidence intervals. For c & d the solid lines represent a 1:1 relationship and dashed line represents a linear regression fit.

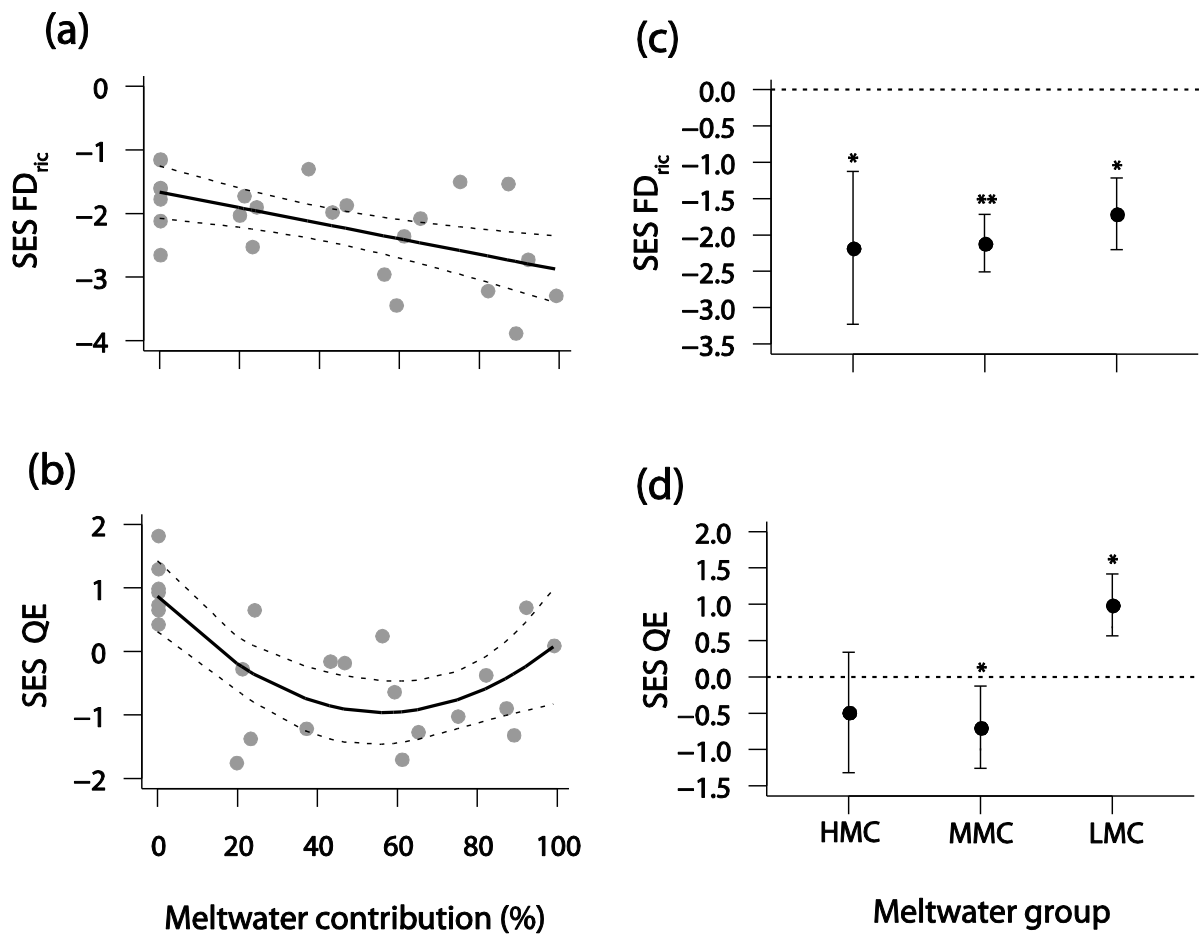


Figure 5.6. Relationship between meltwater contribution and: (a) the standardized effect size (SES) for FD_{ric} ($R^2 = 0.31$, $P < 0.01$); and (b) SES for QE ($R^2 = 0.41$, $P < 0.01$). The solid line represents the regression model's fit and dashed lines the 95% confidence intervals. Standardized effect size (SES) by meltwater contribution group for: (c) FD; and (d) Rao's QE. Filled circles denote mean SES value and whiskers 95% confidence intervals * $P < 0.05$, ** $P < 0.01$; one-tailed Wilcoxon test.

5.4. Discussion

While previous studies in alpine river systems have linked macroinvertebrate functional trait patterns to spatial changes in catchment glacier cover (Snook & Milner 2002; Füreder 2007), this study was the first to link them to quantitative measurement of glacier meltwater contribution. Thus, a mechanistic link between glacial influence and functional diversity was provided due to the spatially discrete habitat template meltwater contribution described. A number of resistant and resilient traits sensitive to changes in meltwater contribution (i.e. glacier influence) were identified and have the potential to act as indicators of climate induced, hydroecological change in alpine river systems (Brown & Milner 2012). Interestingly, although a steep physicochemical habitat gradient was sampled, trait convergence was apparent when all taxa were evenly weighted (FD_{ric}), however when taxa were weighted by abundance (FD_{QE}), trait patterns for HMC sites were random but for LMC sites trait divergence was apparent.

5.4.1. *Biological trait patterns and relationship to meltwater contribution*

Both the RLQ and PCA analysis identified an underlying environmental harshness gradient of SSC, bed instability and algal chl *a*. This distinct harsh-benign spectrum ran from high meltwater sites to groundwater sites (Brown *et al.* 2007b). This pattern was similar to that identified in a study across multiple glacierized river basins in the Alps, where distinct upstream-downstream harshness gradients (SSC, Tw and PFAN) were associated with glacier influence (Ilg & Castella 2006). However, at certain sites this pattern was modified by tributary inputs from variable water sources (e.g. glacier ice/groundwater). Thus, by quantifying meltwater contribution at each study reach, this study was able to directly link

glacier influence-habitat characteristics–traits, across multiple basins with varying stream network morphology and basin properties. We suggest that using meltwater contribution as a proxy for glacier influences determines a two dimensional habitat template related to both environmental stress and habitat consistency (see Brown *et al.* 2006a, 2007b) thus, both the spatial and temporal components identified by Southwood (1977) in his seminal work on evolution and the niche, are incorporated.

Despite all the studied sites being in low order streams and within 4km of their source, distinct functional trait niches (c.f. Poff *et al.* 2006; Verberk *et al.* 2013) were identified relating to life history, resource acquisition and substrate relationship/body shape. Both the RLQ and 4th corner analysis identified a similar suit of trait modalities associated with high meltwater contribution (Figure 5.4 and Table 5.4) which are ‘response traits’ rather than ‘effect traits’ (Díaz & Cabido 2001). A life history strategy continuum, running from r selected to k selected traits (Pianka 1970), was apparent and the extremes of which corresponded to high and low meltwater contributions, respectively. Diptera, predominately Chironomidae and Simuliidae, represented the r strategists with a small maximal body size, indicative of rapid growth (Townsend *et al.* 1997a), multiple generations per year, an affinity to aerial dispersal rather than aquatic and free egg/terrestrial egg laying. These resistant and resilient life history traits represent a ‘grab and hit’ strategy matched to unpredictable habitat conditions (Verberk *et al.* 2013).

In agreement with this study, Snook & Milner (2002) and Ilg & Castella (2006) found that taxa with a small maximal body size (<10mm) dominated at sites with high glacier influence. Small body size is related to shorter generation time and offers resilience in the face of

disturbance/environmental stress as populations can recover quickly due to sexual maturity being reached quickly (Townsend *et al.* 1997b). The prevalence of the bivoltine/multivoltine modality at high meltwater sites offers resilience and enables taxa to exploit short windows of opportunity (Füreder *et al.* 2005). However, there is some debate regarding the life cycle of *Diamesa* spp. in glacier fed streams, with some authors suggesting they take longer than one year to complete (i.e. are semivoltine), see Ilg & Castella (2006) for further details. In this study the coding was based on in-situ rearing experiments and malaise trapping carried out in the French Pyrénées. Two cohorts were identified during the summer melt season for both *Diamesa cinerella* and *D. Latitarsis* gr. (Snook 2000), which agrees with the findings from other systems (Nolte & Hoffmann 1992; Huryn & Wallace 2000). Furthermore, the assertion is that these taxa have an affinity to rapid growth and short generation times, whether or not the environmental conditions are suitable for multiple cohorts during an annual cycle is not necessarily important, the key is life history plasticity and the ability for rapid growth when the conditions permit (Nylin & Gotthard 1998).

At the other end of the meltwater spectrum (LMC sites) *k*-selected taxa, predominately predatory Plecoptera (Perlodidae and Perlidae) and Trichoptera (*Hydropsyche* and *Plectrocnemius*), displayed a different life history strategy (c.f. Pianka 1970). Large body size (indicative of slower growth), an affinity to semivoltinism, in stream dispersal and clustered in-stream egg laying were correlated with LMC sites. The combination of these trait modalities represents a strategy matched to the more stable conditions, where physicochemical habitat and resource supply are constant (Townsend & Hildrew 1994; Verberk *et al.* 2013). Similar life history strategies have been associated with reduced glacier cover in both the Alps and Pyrenees (Snook & Milner 2002; Füreder 2007) and also stable, mountain streams in SE Spain (Díaz *et al.* 2008). Hence, changes in the relative frequencies

of r to k selected taxa may provide a useful tool for monitoring hydroecological change in alpine river systems (Bongers & Ferris 1999).

Patterns related to resource acquisition were not so clearly linked to meltwater contribution. The strongest relationship was between LMC sites and predatory feeding behaviour. Here taxa belonging to the orders Plecoptera, Tricladida and Trichoptera predominated, as in studies by Snook & Milner (2002) and Ilg & Castella (2006) which also recorded an increase in predatory taxa at sites with reduced glacier influence. It is suggested that this pattern may be due to an interaction between habitat stability and primary productivity which can be important drivers of assembly processes maintaining increased food chain length (Post 2002; Townsend *et al.* 1998). Scrapers and shredders feeding on detritus and algae, primarily *Baetis* and *Rhithrogena* and *Protonemura* and *Leuctra*, were associated with MMC sites. This was likely due to resource limitations at HMC sites, where algal and detrital food sources are scarce due to high turbidity and abrasion limiting primary productivity (Uehlinger *et al.* 2010) coupled with low allochthonous input and retention capacity (Zah *et al.* 2001; Brookshire & Dwire 2003). While at LMC site the high abundance of invertebrate and vertebrate predators probably limited the abundance of conspicuous grazing and shredding taxa (Forrester *et al.* 1999). A less well defined omnivorous strategy was prevalent at HMC sites which has been validated by quantitative food web analysis from a glacier fed stream (Clitherow *et al.* 2013). Diptera, particularly Chironomidae and Empididae, were weakly associated with multiple feeding strategies (particularly scraping and deposit feeding; Appendix 5.2) and various food sources (FPOM, algae and invertebrates) and the fourth corner analysis did not identify any significant correlations for diet (Table 5.3). This feeding plasticity is thought to a key factor enabling persistence of taxa in reaches with high glacier influence and patchy food resources (Zah *et al.* 2001; Clitherow *et al.* 2013).

The modalities cylindrical body shape and clinger/semi-permanent attachment to the substrate were associated with HMC sites where the rheophilic *Diamesa* taxa were most abundant (Rossaro *et al.* 2006; Füreder 2007). This appears to represent a strategy for coping with the high flow velocities associated with glacier fed streams (Snook & Milner 2002; Füreder 2007). At LMC sites the modalities crawler and non-streamlined body shape were more common and was probably due to the hydraulically stable conditions (Snook & Milner 2002). However, it should be noted that while the non-streamlined body shape does not offer resistance to high flow stress, the crawler habit has been associated with higher flow stress in other studies (Puey 2010). In this study, as the regional species pool is small and the most abundant crawlers were plecopteran taxa, correlation with other non-resistant traits particularly longer generation time, may have caused the observed pattern (Appendix 5.2). Due to this it appears that trait profiles based on life history and feeding strategies may provide the best indicators for alpine hydroecological change (Figure 5.4). However, a larger scale study, spanning multiple bio-geographical regions is required to fully test the utility of these trait profiles.

5.4.2. *Functional diversity and meltwater contribution*

Current knowledge of the relationship between taxonomic richness (TR) and functional diversity is limited to a relatively small range of ecological systems and taxonomic groups (Naeem & Wright 2003). In this study we found a strong positive relationship between TR and FD_{ric} for alpine macroinvertebrates. No functional redundancy can be assumed as changes in TR were in proportion with changes in FD (i.e. slope equal to 1), similar to findings from other ecosystems and taxonomic groups (Micheli & Halpern 2005; Petchey *et al.* 2007). Interestingly, in an Alaskan watershed, functional redundancy was a prominent feature of macroinvertebrate community succession following glacial recession (Brown &

Milner 2012). This highlights an important difference between high altitude glacial river systems (i.e. this study) and lower elevation, costal, glacier fed river systems (i.e. Alaskan study) with regards to meta-community dynamics (Campbell Grant *et al.* 2007). It is highly likely that dispersal and colonisation, in costal systems, are primarily limited to between watersheds. Hence, highly mobile taxa (e.g. chironomids with similar trait profiles) will have the highest probability of establishing populations in watersheds undergoing rapid environmental change. In contrast dispersal and colonisation in alpine stream environments is predominately linear, via upstream-downstream pathways (Finn & Poff 2008). Thus, colonisation rates will be similar for taxa limited to river corridor movement (e.g. EPT) and highly mobile Diptera (e.g. chironomids and simuliids). Given this context it is likely that the communities of high altitude glacial systems (e.g. Pyrénées and Alps) will, in terms of functional traits, change at a faster rate than lower altitude glacial systems.

FD_{ric} mirrored TR patterns along the meltwater gradient, peaking at MMC sites, suggesting rare taxa with novel traits were recorded. However, it should be noted that FD_{ric} is particularly sensitive to changes in TR, as adding a species, unless it is perfectly redundant, increases the total branch length of the regional pool tree (Mouchet *et al.* 2010). SES values provide strong evidence for trait convergence, at all sites across the meltwater spectrum (Fig. 5a), suggesting environmental filtering was the dominant assembly process (Thompson *et al.* 2010). This was graded, with LMC sites closer to expected FD_{ric} (Figure 5.6) than HMC sites. This finding is similar to that of Brown & Milner (2012), from a glacier fed system in Alaska, where FD_{ric} values under low glacial influence suggested both deterministic and stochastic processes were operating. However, this finding may be a function of the null model used, which did not account for taxon rarity, potentially creating communities with artificially high FD_{ric} values (Thompson *et al.* 2010). Hence, the use of abundance weighted

functional diversity measures is often preferred when assessing community assembly processes (Mason *et al.* 2012; Paillex *et al.* 2013).

For QE, a measure which combines properties of functional divergence and richness and is abundance weighted (Mason *et al.* 2005; Mouchet *et al.* 2010), a negative relationship with meltwater contribution suggests greater niche differentiation and lower resource competition under the more benign conditions at LMC sites (Mason *et al.* 2005). QE was not linearly related to TR (Figure 5.5), which is an important requirement for FD measure particularly when trying to disentangle community assembly processes (Botta-Dukát 2005; Mason *et al.* 2013). The shift from negative to positive SESs as meltwater contribution decreased (Fig. 5 & 6) represents a shift in assembly processes from environmental filtering to limiting similarity (Mason *et al.* 2012). At HMC sites the harsh environmental conditions (e.g. low water temperature and high SSC) limited the taxa that could colonise to a small subset of the regional pool (Statzner *et al.* 2004). Hence, trait convergence was apparent with all abundant taxa exhibiting resistant and resilient functional traits such as morphological features associated with high flow adaptation and short life cycles (Füreder 2007). Interestingly, at HMC sites the SES was not significantly less than zero, suggesting stochastic processes may have also been operating. This is similar to the findings of Lepori & Malmqvist (2009) who found random assembly patterns in benthic communities in stream reaches with high levels of disturbance. In this study HMC beds and channels were constantly reworked and reconfigured; hence, catastrophic loss of taxa would likely be followed by idiosyncratic recolonisation.

As theory predicts inter-specific competition will be increased under more benign conditions (Menge & Sutherland 1987), it is likely that co-existing taxa will occupy distinct niches (trait divergence) at LMC sites, where habitat conditions are more favourable (Mason *et al.* 2008). Here a greater range of well defined trophic strategies (i.e. shredder, predator, scraper, filterer

and collector) were apparent, probably due to: (i) increased basal resource density and diversity (recorded in this study as chl *a* but increased retention of allochthonous matter is also likely (Brown *et al.* 2007a)), and (ii) more stable conditions (longer life cycles and larger body size) which enabled dedicated predators rather than omnivorous opportunists to colonize (Clitherow *et al.* 2013). The latter point probably also enabled a wider range of body forms and life history strategies to co-occur (Verberk *et al.* 2013). However, it remains to be tested if increased FD at lower meltwater represents a functioning response or whether increased FD is a function of the variability of ‘ecological opportunities’ (Heino 2005).

5.5. Conclusions

To summarise, this study identified key functional strategies within the Pyrenean macroinvertebrate regional taxa pool that have developed to enable colonization of high meltwater contribution habitats. These primarily consisted of: (i) a ‘grab and hit’ life history strategy with rapid growth (even at low temperatures), small maximal body size and potential for multiple generations; (ii) an omnivorous feeding strategy; and (iii) a body plan for coping with high flow velocity, namely cylindrical with elongated prolegs for clinging to the substrate. Trait profiles associated with these functional strategies could potentially be used as indicators of environmental change in alpine river systems. We do however stress the need for higher resolved trait coding, particularly for chironomids which are species rich in alpine environments (Rossaro *et al.* 2006). Also the use of traits more suited to cold environments such as freeze tolerance would be useful (Lencioni 2004), although further work at the molecular level would be required to identify heat shock proteins for a wider range of alpine taxa. Furthermore, as meltwater contributions decreased locally dominant taxa shifted from displaying trait convergence (i.e. the resistant/resilient functional strategy outlined above) to

displaying trait divergence. This suggests that community assembly processes are likely to change from niche filtering to stochastic/limiting similarity under future scenarios of glacier retreat. The use of FD indices provides a useful tool for gaining a more mechanistic understanding of how benthic communities assemble, for studying changes in alpine benthic communities and has potential to inform conservation strategies for maintaining biodiversity and monitoring responses to environmental change. However, stochastic factors such as dispersal and population dynamics may become increasingly important as water source contributions change for isolated high meltwater habitats. Further work at a larger spatial scale is required to: (i) gain insights into the importance of spatial scale for community assembly dynamics; and (ii) test the utility of the identified indicator trait profiles across multiple bio-geographical regions. This is particularly vital because a detailed understanding of how community interactions are likely to change under future scenarios of glacier retreat, and the identification of universal bio-indicators of this environmental change, are both needed to inform future conservation and monitoring strategies.

5.6. Chapter summary

In this chapter benthic macroinvertebrate trait patterns and community assembly processes in alpine river systems have been examined. Findings suggest that viewing the benthic community as functional units (i.e. based on biological traits) could be particularly useful for identifying river ecosystem change as glaciers recede. Furthermore, the conceptual model presented at the end of Chapter 4 has been largely validated as community assembly processes shifted from environmental determinism (high meltwater) towards stochastic/competition driven (low meltwater). Interestingly, trait convergence of abundant taxa was greatest at mid meltwater sites, further suggesting the shift towards a more

generalist community as meltwater contributions decline. In the next chapter the potential implications of climate driven predator range expansion for benthic stream communities are explored.

CHAPTER 6

*The potential implications of predator
range expansion in alpine river
ecosystems: an experimental approach
using streamside mesocosms*

6.1. Introduction

Future climate warming will alter ecosystem processes, biotic patterns and interactions across a range of spatial and temporal scales (Parmesan 2006; Bellard *et al.* 2012), which in turn will impact a wide variety of habitat types and taxonomic groups (Dirzo & Raven 2003; Thomas *et al.* 2004; Xenopoulos *et al.* 2005; Engler *et al.* 2011; Sauer *et al.* 2011). Mountain environments support a unique biota (Brown *et al.* 2009a; Engler *et al.* 2011), often at their range limits, and they are particularly sensitive to warming because current and predicted warming rates are typically higher than the global mean (Beniston 2012). Altitudinal range shifts or expansions, although less well documented than latitudinal expansions (Parmesan, 2006), have been observed for a variety of species (Pauli *et al.* 2007; Chen *et al.* 2011b). However, in freshwater ecosystems the spatial and temporal variability in trophic interactions make predictions about range shifts based on species-environment relationships potentially problematic (Woodward *et al.*, 2010).

The sensitivity of alpine benthic stream ecosystems to climate change and range expansions has been highlighted increasingly in recent years (Brown *et al.* 2007a; Muhlfeld *et al.* 2011; Sauer *et al.* 2011; Jacobsen *et al.* 2012; Finn *et al.* 2013). Many range restricted benthic organisms will represent the ‘losers’ of future climate change (Somero 2010) as they will be unable to respond spatially or physiologically to water temperature increase (Bellard *et al.* 2012). Synergistic impacts of climate/hydrological change and altered biotic interactions are likely to promote extinctions in these pristine river habitats (Tierno de Furoa *et al.* 2010). Warming will cause changes in meltwater dynamics, and thus stream discharge (magnitude and variability), water temperature and stream channel stability will be altered (Brown *et al.* 2007, Jacobsen *et al.* 2012). This will benefit some species: for example upstream

colonisation of more downstream or 'lowland' taxa is likely as these high altitude habitats become more hospitable (Brown *et al.* 2007a).

The type and strength of interactions between 'invaders' and 'native' taxa is size dependent (Woodward *et al.* 2005), with large size differences resulting in predator-prey relationships, but smaller differences leading to more competitive relationships (Yang & Rudolf 2010). A recent laboratory-based study investigating competitive interactions between two libellulid dragonflies (a Northern species and a range expanding Southern species), highlighted the potential for predator replacement through interference competition (Suhling & Suhling 2013). Other studies have highlighted the impact of predator invasions on both prey abundance and behaviour (reviewed by Sih *et al.* 2010). Woodward & Hildrew (2001) presented one of the few examples of (invertebrate) predator invasion impacts on a low order stream system, showing an increase in biotic interactions and food web trophic height following the invasion of a large bodied dragonfly (Woodward & Hildrew 2001). In the context of low order alpine streams, perturbations due to predator invasion are likely to have significant impacts because these food webs are characterized by high omnivory and dietary overlap (Zah *et al.* 2001), with relatively high connectance and short food chain lengths (Clitherow *et al.* 2013). Hence, factors affecting one node may propagate quickly through the network, with potential for cascading effects (Shurin *et al.* 2002). Therefore, in light of the rapid rate of environmental change predicted for alpine river ecosystems the potential impacts of predator range expansions on biotic interactions and community structure in these systems needs to be quantified (Milner *et al.* 2009).

Perla grandis (Plecoptera; Perlidae), a rheophilous mesothermal predatory stonefly, is widely distributed across the mountain ranges of Southern and Central Europe (Fenoglio *et al.* 2008)

and is common throughout mid-altitude Pyrenean streams where it represents the top invertebrate predator (Lavandier & Decamps 1984; Vincon 1987). In the alpine zone its distribution appears to be limited by stream water source contribution and altitude, as higher altitude streams, fed predominately by melting snow or ice in spring, have a habitat template that is unsuitable (i.e. low water temperature, unstable beds and high turbidity; Brown *et al.* 2007b). Sparse data exists regarding the feeding habits and ecology of *P. grandis* nymphs, with only a single study from a mid-elevation stream (800m a.s.l) in the Appenines, North West Italy (Fenoglio *et al.* 2007) reporting chironomids, *Baetis* spp. and other Ephemeroptera in the diet. Work on a similar species (*Dinocras cephalotes*: Perlidae) identified that other large bodied, predatory invertebrates were a dietary component (Bo *et al.* 2008). As glacier and snowpacks recede *P. grandis* is expected to expand its range upwards into lower order, higher altitude streams (Brown *et al.* 2007). However, brown trout (*Salmo trutta*), a potential competitor/predator of *P. grandis*, will be unable to track such range expansion due to migratory barriers such as waterfalls. Hence, the likely decoupling of this historical trophic interaction suggests *P. grandis*, will experience ‘enemy release’, with significant impacts on both prey and predators/competitors in the invaded community (Gilman *et al.* 2010; Sih *et al.* 2010).

To assess potential effects of climate driven range expansion (i.e. change in river water source dynamics) of the stonefly *P. grandis*, on stream benthic communities, this study adopted a field-based experimental approach using artificial through-flow channels fed by a first order stream, Four complementary hypotheses were tested:

(H_1) the abundance of key prey taxa will be reduced in *P. grandis* invaded systems through either direct consumption or non consumptive effects (e.g. increased drift);

(H_2) *P. grandis* invasion will alter community feeding guild structure through prey selection of active grazing taxa, and interference competition with other large bodied predators;

(H_3) *P. grandis* will increase the magnitude of the trophic cascade by decreasing prey abundance (H_1), particularly active grazing taxa (H_2);and

(H_4) through predation pressure and competition with resident predators, *P. grandis* will alter population and community body size distributions.

6.2. Methods

6.2.1. Study site and experimental channels

The study was conducted in the Taillon-Gabiétous catchment, Cirque de Gavarnie, French Pyrénées (43°6'N, 0°10'W) between July 4 and July 27, 2011. A detailed study basin description was provided by Hannah *et al.* (2007). Briefly, the catchment is above the tree line (i.e. alpine zone), with steep slopes (30-70°) and a sedimentary geology. On south facing slopes a number of groundwater fed streams are sourced from hillslope, alluvial aquifers. Here, allochthonous inputs are limited to grasses and sedges; hence, the basal resources in these systems consists of primarily diatoms and benthic algae. *P. grandis* is currently absent from these streams above 1900m. To emulate this habitat, experimental channels were located alongside a first order stream, approximately 2000m a.s.l. (Figure 6.1, Plate 6.1), where *P. grandis* was absent. Water was diverted from the stream using a feeder pipe (diameter = 10 cm) into two plastic header tanks (0.6 m x 0.4 m x 0.3 m). Each tank fed a block of four channels directly through equally spaced gate valves. Channels were made from rectangular plastic gutter (1m x 0.13 m x 0.17 m) with a 0.05 m diameter outflow pipe (Figure 6. 1) whereby water flowed into a drainage pipe which subsequently returned water to the main stream channel. Drift nets (250 µm mesh) attached to the outflow pipes captured emigrating *P. grandis* which were then returned to the channels. Gravel (5 – 25 mm) and pebbles (25 – 45 mm) were collected from the feeder stream, elutriated thoroughly to ensure attached organisms and eggs were removed, and then used to fill the channels to a depth of 5 cm. Five cobbles (intermediate axis >100 mm) were then placed in each channel, and the attached biofilm was inspected and macroinvertebrates removed with forceps.

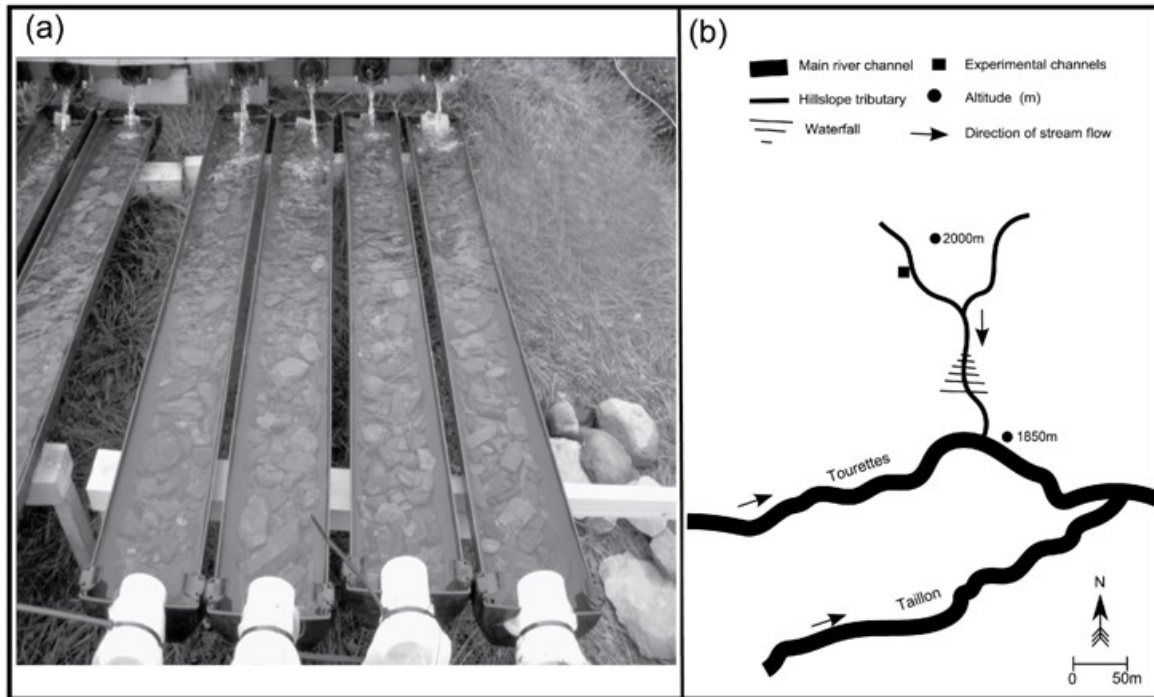


Figure 6.1. (a) Experimental channels (b) map showing field site and location of experimental channels



Plate 6.1. Mesocosm channels and feeder stream in the foreground.

Velocity was recorded on five occasions using a Sensa RC2 electro-magnetic flow meter. Mean velocity across all channels and dates was 0.13 ms^{-1} and was uniform between channels and over time (ANOVA; $F_{2,5} = 0.36$, $P = 0.71$). It should be noted that although flow velocity was low the channels did represent riffle habitat as, at the low water depth and water volume in channel, broken water was observed over the substrate.

Electrical conductivity (EC) and pH (measured using a Hanna HI 98129 handheld probe) were also near identical across all channels on each recording date, but EC increased from 174 to $189 \mu\text{Scm}^{-1}$ and pH from 8.57 to 8.69, between the start and end of the experiment. Water temperature was recorded continuously in one channel from each block using a Gemini Tinytag Plus (instrument error $\pm 0.2^\circ\text{C}$). The mean water temperature for both blocks was 10.2°C . Water depth was similar throughout all channels and ranged from 6cm above fine gravel to 2 cm above the cobbles. Before initiating the experiment, flow in the channels was established for three days with the inflow pipe covered by $100 \mu\text{m}$ mesh, to inhibit colonisation by drifting invertebrates whilst allowing algal colonisation (Ledger *et al.* 2006).

6.2.2. *Experimental design*

P. grandis ($n = 33$) were collected from the Tourettes stream (1800 m a.s.l; Figure 6.1) of which eight well developed nymphs of equal body length ($22.05 \pm 0.66 \text{ mm}$, mean \pm SE) were selected for the experiment. The remaining nymphs ($n = 25$) were retained for gut contents analysis and stored in 70% ethanol.

The experiment followed a systematic design of two treatments, replicated four times: (i) a predator free control; and (ii) a *P. grandis* treatment (two individuals per channel), corresponding to a density of 15 ind m⁻². The ambient density of *P. grandis* recorded in the Tourettes stream was between 10 and 30 ind m⁻². All *Perla* nymphs were placed in the treatment channels on 4 July 2011 and the mesh removed from the inlet pipe to enable colonisation from the local species pool of macroinvertebrates. Drift nets attached to the outflow pipes were inspected at least every 48h for *P. grandis*. Invertebrate emigration via drift was sampled on three occasions (10-11, 18-19 and 26-27 July) for 24h periods. Drift nets (250µm mesh) were emptied into Whirlpak bags and stored in 70% ethanol. The experiment was terminated after 23 days on July 27, 2011.

At the end of the experiment, three cobbles were selected from each channel for chlorophyll *a* (chl *a*) analysis and all attached invertebrates removed with forceps. Epilithon was removed from the surface of cobbles in the laboratory using a stiff toothbrush in 50ml of deionised water. The resultant slurry was then drawn through a Whatman GF/F filter paper (0.7 µm) and frozen immediately. Samples were analysed for chl *a* (using the trichromatic spectroscopy method outlined in ASTM D3731 (ASTM 2004). Pigment extractions were made using 90% acetone. Periphyton concentrations were converted to mass per unit area (mg m⁻²) using:

$$chl\ a = \frac{CaE}{A} \quad (6.1)$$

where *Ca* = concentration of chlorophyll *a* in the extract (mgL⁻¹), *E* = Extract volume (L) and *A* = substrate area sampled (m²).

All substrate from each experimental channel was transferred into a bucket, sieved, and the remaining organic material and invertebrates transported to the laboratory where macroinvertebrates were sorted from gravel under a bench lamp and stored in 70% Industrial Methylated Spirit (IMS). Individuals from both the drift and endpoint community were then identified to the lowest practical taxonomic level (i.e. 60% of all individuals were identified to genus level or below) using a selection of identification keys (Müller-Liebenau 1969; Tachet *et al.* 2000; Zwick 2004) and assigned to functional feeding groups following Moog (1995). For the most abundant taxa ($> 15 \text{ ind m}^{-2}$), body length (mm) was recorded using a dissecting microscope (Ziess stemi 2000-C, 6.5x – 75x) fitted with an eye piece graticule. Gut contents were assessed for the mesocosm *P. grandis* ($n = 8$) and the individuals collected from the Tourettes stream ($n = 25$). The entire gut was dissected and placed on a slide, the contents were then dispersed and identified using a dissecting microscope (Ziess stemi 2000-C, 6.5–75x) and stage microscope (Nikon Optiphot-2 microscope, magnification 100-1000x) as necessary. Partial specimens of consumed prey were only counted if the head was attached to the thorax.

6.2.3. Data analysis

Prior to statistical analysis all abundance data were first standardised to number of individuals per m^2 and the relative abundance (%) of functional feeding groups was determined. Taxonomic richness (i.e. number of taxa) and community dominance (Berger-Parker dominance index) were calculated for each channel using non-transformed abundance data. Drift propensity was calculated for the final sample date (24-25 July) by dividing the number of drifting individuals of a given taxa by the total number of individuals of that taxa recorded in the channel.

Chl *a*, macroinvertebrate abundance, drift, drift propensity and functional feeding group data were then tested for normality using a combination of QQ plots and the Shapiro-Wilk test, and variances were also tested for homogeneity using Levene's test (Zuur *et al.* 2010). Subsequently, Chl *a* and abundance data were square root ($x + 0.5$) transformed, relative abundance data were arcsin square root transformed and drift/drift propensity data were $\log_{10}(x + 1)$ transformed to meet assumptions of parametric analysis. One-way ANOVA was used to test for block effects (i.e. header tank effect) but no significant differences for total abundance, richness, drift or chl *a* were evident (all $P > 0.1$). Therefore, for all subsequent analyses, data were tested only for treatment effects.

One-way ANOVA was used to identify treatment effect on: (i) density of the most abundant potential prey taxa; (ii) functional feeding group density; (iii) functional feeding group relative abundance; and (iv) drift propensity. Two-way (treatment, time), repeated measures ANOVA was used to test for differences in drifting invertebrate abundance. Due to the large number of statistical tests, null hypothesis testing was complimented by the calculation of standardized effect size (SES; McCabe *et al.* 2012). Unlike the application of stringent bonferroni corrections, which both reduces power and increases type II errors to unacceptable levels (Nakagawa 2004), the calculation of SES enables the biological importance and significance to be assessed simultaneously and reduces publication bias of selective reporting of results (Garamszegi 2006). The SES (Cohen's *d*) for each test was calculated as:

$$d = \frac{\bar{X}_1 - \bar{X}_2}{S^2} \quad (6.2)$$

Where \bar{X}_1 is the mean of the control, \bar{X}_2 the mean of the treatment and S^2 the pooled standard deviation (SD) calculated as:

$$S^2 = \frac{(n_1 - 1)S_1^2 + (n_2 - 1)S_2^2}{n_1 + n_2} \quad (6.3)$$

Where S_i^2 is the SD of the of the i th group n_i the sample size. Confidence intervals (95%) were calculated for d in the R environment (R Development Core Team 2012) using script created by Smithson (2011) as part of a Statistical Package for the Social Sciences (available from: <http://psychology3.anu.edu.au/people/smithson/details/CIstuff/CI.html>).

Non-Metric Dimensional Scaling (NMDS), based on Bray-Curtis dissimilarity, was used to assess the effect of treatment on the prey community structure. Analysis of similarity (ANOSIM) was adopted to test whether the two treatments had different species composition (i.e. dissimilarities between treatments greater than within treatment).

Prey selection was determined using the raw abundance data from the treatment channels. The Log of the Odds Ratio (LOR) was calculated following Brodner (1998);

$$LOR = \ln \frac{(d_i(100 - d_i))}{(c_i(100 - c_i))} \quad (6.4)$$

where d_i is the relative abundance of taxon i found in the gut of *P. grandis* and c_i is the relative abundance of taxon i found in the treatment channels. This ratio varies from $-\infty$ to $+\infty$, and positive values represent preference.

Raw body size data were used for statistical analysis as they were normally distributed and displayed homogeneity of variance. Student t-tests were used to test for differences in mean body length between treatment and control. Violin plots (a combined box plot and kernel density plot) were used to assess body length differences between treatments as they display more information on data spread than boxplots alone. The probability density function of the data at different values is shown, much like a histogram; however, each block is centred at each data point rather than fixed in the form of class bins (Hintze & Nelson 1998). Predatory taxa which colonised the channels were split into two groups; individuals >10mm body length were classified as large bodied predators and those <10mm as small bodied (c.f. Ilg & Castella, 2006).

Body mass (ash free dry mass, mg) was calculated for the measured taxa using published length-mass regressions (Appendix 6.1). Data were pooled by treatment (taxonomy disregarded) and \log_{10} transformed to enable individual based assessment of treatment effect on body size (Brown *et al.* 2011). Transformed biomass data were sorted into five size classes (< -1.3, -1.3 to -0.7, -0.7 to -0.1, -0.1 to 0.5, > 0.5 mg). Treatment response was calculated as the percentage difference between treatment and control for each size class. Pair-wise comparisons were used to calculate the mean difference and standard error (SE) for each size class, here each treatment channel was compared to all control channels; hence, $n = 16$ for the mean and SE calculations. A Kruskal-Wallis test was used to test for treatment effect on the number of individuals within each body mass class.

All tests were considered significant at $P < 0.05$. All plots, t-tests and multivariate analyses were made using the *Base* and *Vegan* (Oksanen *et al.* 2012) packages within R, version 2.14.1 (R Development Core Team, 2012).

6.3. Results

6.3.1. Taxonomic composition of channels

P. grandis individuals acclimatised rapidly to the channels as only two individuals were returned from the drift nets to the channels. Thirty three invertebrate taxa in total colonised the experimental channels (Appendix 6.2), which were representative of the source stream community (K. Khamis unpublished), including several Diptera, Ephemeroptera and Coleoptera (larvae and adults). Trichoptera were more abundant in the control channels and Plecoptera taxa were rare in both treatment and control channels (Appendix 6.2). Oligochaeta and the triclad, *Polycelis* sp., were the only non-insect taxa to colonize the channels.

Baetis gemellus was the most abundant taxon in control channels, while Orthocladiinae dominated in treatment channels. Eight insect taxa (*B. gemellus*, *Baetis muticus*, *Baetis alpinus*, *Simulium* sp., *Elmis* sp., Orthocladiinae, Diamesinae, and Tanypodinae) were recorded at mean densities >15 ind m^{-2} (Appendix 6.2), other taxa were recorded in low densities (<15 ind m^{-2}). Large bodied species, other than *P. grandis*, were rare and consisted of five taxa: two Dipteran taxa (Tipulidae and Rhagionidae, <1 ind m^{-2}) and three predatory trichopterans, *Rhyacophila* spp., *Rhyacophila intermedia* and *Plectrocnemia* sp.. *Rhyacophila* spp. were exclusively found in the treatment channels (2 ± 2 ind m^{-2}), *R. intermedia* and *Plectrocnemia* sp. were recorded in higher densities (14 ± 5 ind m^{-2} and 8 ± 3 ind m^{-2} respectively) but exclusively in the control channels. The body size recorded for *R. intermedia* (12.87 ± 0.75 mm) and *Plectrocnemia* sp. (11.21 ± 0.67 mm) were markedly smaller than *P. grandis* (22.05 ± 0.66 mm).

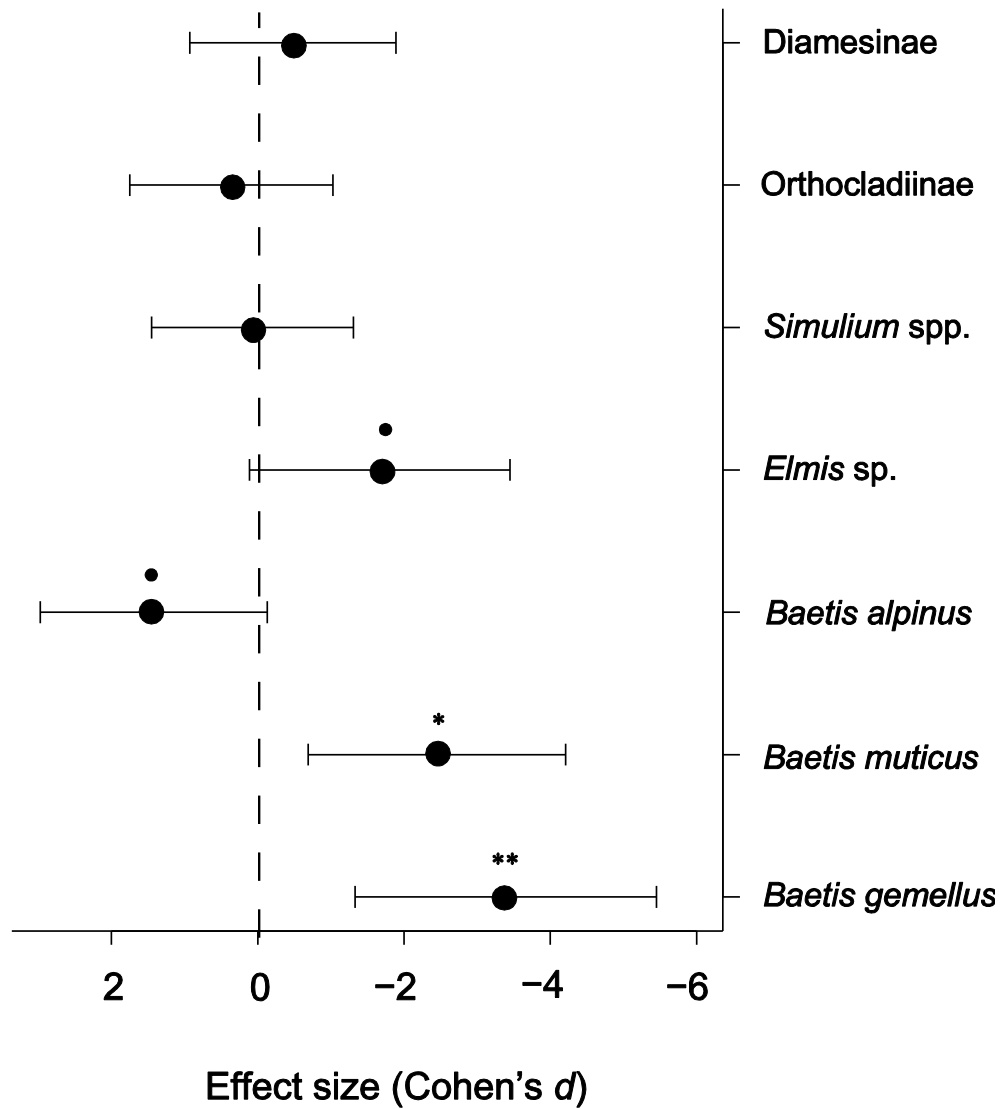


Figure 6.2. Standardized effect size (Cohen's *d*) for the difference between treatment and control channels for prey density (ind m²). Whiskers represent the 95% confidence intervals, with significant one-way ANOVA tests highlighted (** $P < 0.01$, * $P < 0.05$ and • $P < 0.1$).

6.3.2. Effects of *P. grandis* on invertebrate abundance and structure

Total macroinvertebrate density was on average greater in control channels ($1043 \pm 65 \text{ ind m}^{-2}$) than in treatment channels ($812 \pm 73 \text{ ind m}^{-2}$). The SES, though marginally nonsignificant (ANOVA; $P = 0.058$), was large ($d = -1.56$, CI = -3.18, -0.001). In the treatment channels the abundance of the mayflies, *B. gemellus* and *B. muticus*, was significantly lower ($d > 2$, $P < 0.05$), but for *B. alpinus* was greater ($d > 1.4$, $P < 0.1$) than in the control (Table 6.1; Figure 6.2). Other common prey taxa, i.e. Orthocladiinae and Diamesinae, showed no significant response to the treatment (Table 6.1; Figure 6.2). Mean species richness of the treatment and control channels were also comparable, 15.25 ± 0.75 and 14.75 ± 0.68 , respectively, while community dominance was significantly lower in treatment channels (ANOVA; $P = 0.0006$) and the effect size was large ($d = -4.7$, CI = -7.4, -2.0).

Ordination (NMDS) analysis of the most abundant insect taxa ($>15 \text{ ind m}^{-2}$) found the most stable solution (Stress = 0.04) consisted of two dimensions. The treatment and control channels were divided along axis 1 (Figure 6.3) and the stress plot indicated the loss of a negligible amount of the variation in the original data set ($R^2 = 0.99$). A significant effect of treatment on community structure was revealed (ANOSIM; $R = 0.468$, $P = 0.02$). Control channels were characterized by greater abundance of the mayfly species *B. gemellus* and *B. muticus*, and Orthocladiinae (Figure 6.3).

Table 6.1. One-way ANOVA examining the effect of *P. grandis* (treatment) on the abundance of potential prey taxa. The standardized effect size (Cohen's *d*) is presented with associated 95% confidence intervals.

Prey taxon	F _{1,6}	P	<i>d</i>	CI lower	CI upper
<i>Baetis gemellus</i>	22.64	0.003	-3.39	-5.45	-1.23
<i>Baetis muticus</i>	12.03	0.01	-2.45	-4.21	-0.62
<i>Baetis alpinus</i>	3.99	0.09	1.42	-0.13	2.96
<i>Elmis</i> sp.	5.59	0.06	-1.67	-3.28	0.06
<i>Simulium</i> spp.	0.01	0.92	0.07	-1.31	1.46
Orthocladiinae	0.27	0.62	-0.36	-1.03	1.79
Diamesinae	0.47	0.52	-0.48	-1.89	0.92

6.3.3. Effects of *P. grandis* on invertebrate feeding guild structure

Grazers were the most abundant feeding guild and shredders were the least abundant in both control and treatment channels (Table 2). Filter feeders (predominantly *Simulium* spp.) were numerically and relatively more abundant in treatment channels as were predators (predominately Tanypodinae). The density and relative abundance of grazers was significantly reduced in the treatment channels ($d \sim 2$, $P < 0.05$; Table 6.2; Figure 6.4). Shredder and collector abundances were similar between treatment and control channels (Table 6.2; Figure 6.4). When predators (excluding *P. grandis*) were divided into small (5 - 10mm) and large bodied (>10mm) a significant negative effect of treatment was observed for the large bodied predators (Table 6.2; Figure 6.4). The most common of these large bodied

predators, *R. intermediata*, were more abundant in control channels (13 ± 5 ind m^2) than treatment channels (2 ± 2 ind m^2).

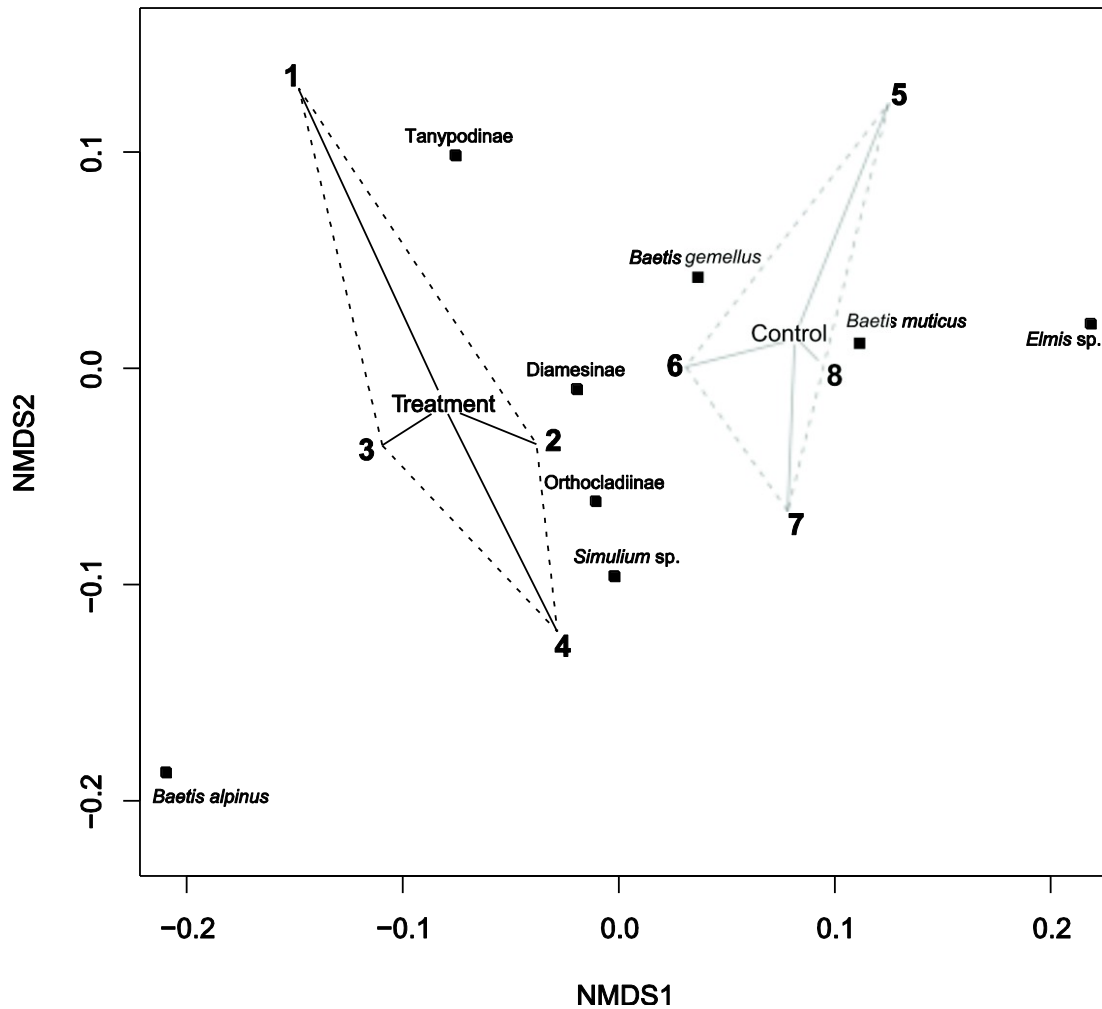


Figure 6.3. Non-metric dimensional scaling (NMDS) ordination of abundant taxa from experimental channels. Numbers denote channels (1-4 treatment and 5-8 control). Dashed line represents the convex hull for treatment (black) and control channels (grey).

Table 6.2. Mean abundance (ind m⁻²) and relative abundance (%) of functional feeding groups in control and treatment channels (SE is displayed in parentheses) and results of one-way ANOVA examining the effect of *P. grandis* (treatment) on the relative abundance (arcsin sqrt transformed) and actual abundance of functional feeding groups are also displayed.

Functional feeding group	Relative abundance		Abundance		Relative abundance		Abundance	
	<i>Control</i>	<i>Treatment</i>	<i>Control</i>	<i>Treatment</i>	<i>F</i> _{1,6}	<i>P</i>	<i>F</i> _{1,6}	<i>P</i>
Grazer	77.0 (7.1)	69.3 (5.9)	804 (40)	564 (40)	7.29	0.04	7.77	0.03
Shredder	2.1 (0.7)	2.6 (1.0)	21 (1)	21 (1)	0.30	0.60	0.00	0.97
Collector	3.6 (1.0)	3.5 (0.8)	37 (3)	27 (1)	0.01	0.93	0.83	0.40
Filter feeder	5.6 (1.5)	9.2 (3.6)	60 (5)	75 (6.1)	0.74	0.42	0.17	0.69
Predator	11.7 (2.5)	15.4 (3.3)	121 (7)	125 (9)	0.88	0.38	0.31	0.60
Large predator	0.02 (0.05)	0.01 (0.04)	25 (4)	6 (1)	10.0	0.01	4.66	0.07

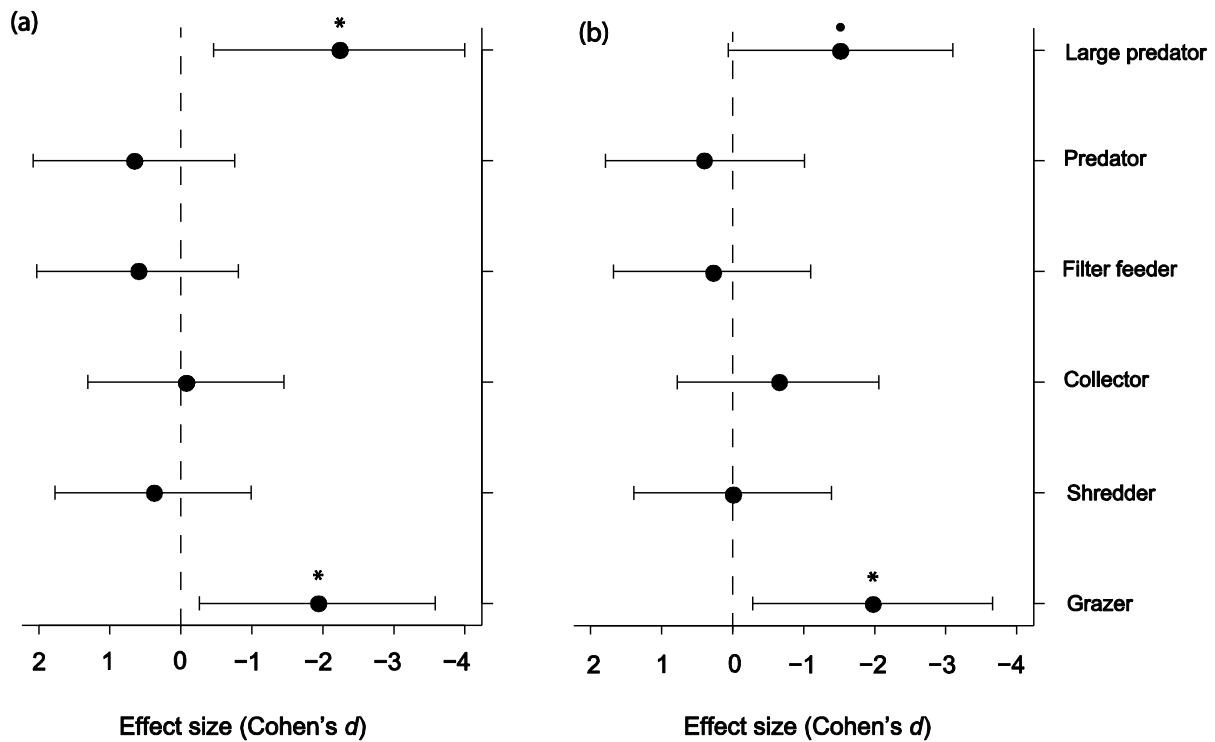


Figure 6.4. Standardized effect size (Cohen's d) for the difference between treatment and control channels for (a) functional feeding group density (ind m^{-2}) and (b) functional feeding group relative abundance. Whiskers represent the 95% confidence intervals and significant one-way ANOVA tests are highlighted (* $P < 0.05$ and • $P < 0.1$).

6.3.4. Consumptive and non consumptive effects of *P. grandis*

The average number of prey per *P. grandis* gut was similar in the Tourettes stream (3.4 ± 0.4) and the experimental channels (3.6 ± 0.5) and the diet was entirely carnivorous. All prey items were insects; with *Baetis* spp. and Orthocladiinae representing the most frequent prey items. However, *Baetis* spp. were proportionally more abundant in the guts of *P. grandis* in the experimental channels (Table 6.3). Large bodied prey items were also recorded, with *Rhyacophila* spp. and Limnephilidae found whole in the foreguts of *P. grandis* from the Tourettes stream. *P. grandis* showed a positive LOR and selectivity for *Protonemura* spp in both the channels (+2.85) and the Tourettes stream (+1.62), *Baetis* spp. (+0.26) in the

experimental channels and Orthoclaadiinae (+1.35) in the Tourettes stream (Table 6.3). High positive LOR values were also apparent for *Rhyacophila* spp (+1.37) and Limnephilidae (+1.13) in the Tourettes stream. *P. grandis* displayed no selectivity (negative LOR values) for Simuliidae in either the experimental channels or Tourettes stream (Table 6.3).

Although chlorophyll *a* content of the cobble biofilm in the control treatment (4.81 ± 0.86 mg m²) was lower than the *P. grandis* treatment (7.13 ± 2.16 mg m²), the difference was insignificant ($d = 0.63$, CI = 0.15,0.95, $P = 0.092$).

Table 6.3. Diet of *P. grandis* nymphs in the Tourettes stream (n = 25) and mesocosm channels (n = 8).

Location	Prey taxon	% found in gut	% found in substrate	LOR	Mean prey items per gut
Tourettes	<i>Baetis</i> spp.	37.6	57.1	-0.04	3.4
Stream	Orthoclaadiinae	34.1	6.2	1.35	
	<i>Protonemura</i> spp.	11.8	2.1	1.62	
	<i>Rhithrogena</i> sp.	4.7	21.2	-1.32	
	<i>Simulium</i> spp.	3.5	4.9	-0.31	
	Unidentified Arthropod	3.5	NA	NA	
	Limnephilidae	2.4	0.74	1.13	
	<i>Chloroperla</i> sp.	1.2	1.6	-0.32	
	<i>Rhyacophila</i> sp.	1.2	0.27	1.37	
	Experimental channels	<i>Baetis</i> spp.	48.3	37.4	0.26
Orthoclaadiinae		27.6	28.4	-0.01	
Unidentified Plecoptera		10.3	NA	NA	
Unidentified arthropod		6.9	NA	NA	
<i>Protonemura</i> spp.		3.4	0.2	2.85	
<i>Simulium</i> spp.		3.4	9.1	-0.96	

The mean number of individuals recorded in the drift was comparable across all three sampling dates and between *P. grandis* treatment channels and the control channels across all sample dates (Appendix 6.3). Of the *Baetis* species, which were the only prey taxa whose densities were reduced by the treatment, both *B. gemellus* and *B. muticus* were more abundant in the drift from the *P. grandis* treatment channels (Table 6.4). The predatory caddisfly, *Rhyacophila* spp., was also more frequent in the drift from treatment channels (n = 13) than control channels (n = 5) (Appendix 6. 3). *B. alpinus* and *Protonemura* spp. were the most abundant taxa in the drift compared to their channel densities (Figure 6.5). Drift propensity rates for all other key prey taxa (Orthoclaadiinae, *B. gemellus* and *B. muticus*) were low (< 1) (Figure 6.5). A positive treatment effect was recorded for the drift propensity rate of *B. gemellus*, in contrary to a negative treatment effect for *B. alpinus* (Table 6.5).

Table 6.4. Two-way repeated measure, ANOVA results for the effects of predator treatment, time and the interaction of time and treatment on the number *Baetis* spp. recorded in 24 hr drift samples. The standardized effect size (Cohen’s *d*) is presented with associated 95% confidence intervals.

Taxon	Factor						
	Treatment		Time		Interaction		<i>d</i> (95 % CI)
	<i>F</i> _{1,23}	<i>P</i>	<i>F</i> _{1,5}	<i>P</i>	<i>F</i> _{2,5}	<i>P</i>	
<i>Baetis muticus</i>	2	0.29	2.49	0.29	6.24	0.01	2.12 (1.38, 2.46)
<i>Baetis gemellus</i>	23.72	0.04	5.13	0.16	0.28	0.76	2.2 (0.54, 3.93)
<i>Baetis alpinus</i>	23.08	0.04	1.6	0.38	0.11	0.89	1.83 (1.6, 1.9)

Table 6.5. One-way ANOVA for the effects of predator treatment on the drift propensity (per capita 24 h drift rate) for date C (July 23-24). The standardized effect size (Cohen's d) is presented with associated 95% confidence intervals.

Taxon	$F_{1,23}$	P	d	CI lower	CI upper
<i>Baetis muticus</i>	2.82	0.23	0.94	0.42	1.48
<i>Baetis gemellus</i>	36.54	0.05	3.41	2.53	4.31
<i>Baetis alpinus</i>	28.07	0.05	-2.98	-3.81	-2.18

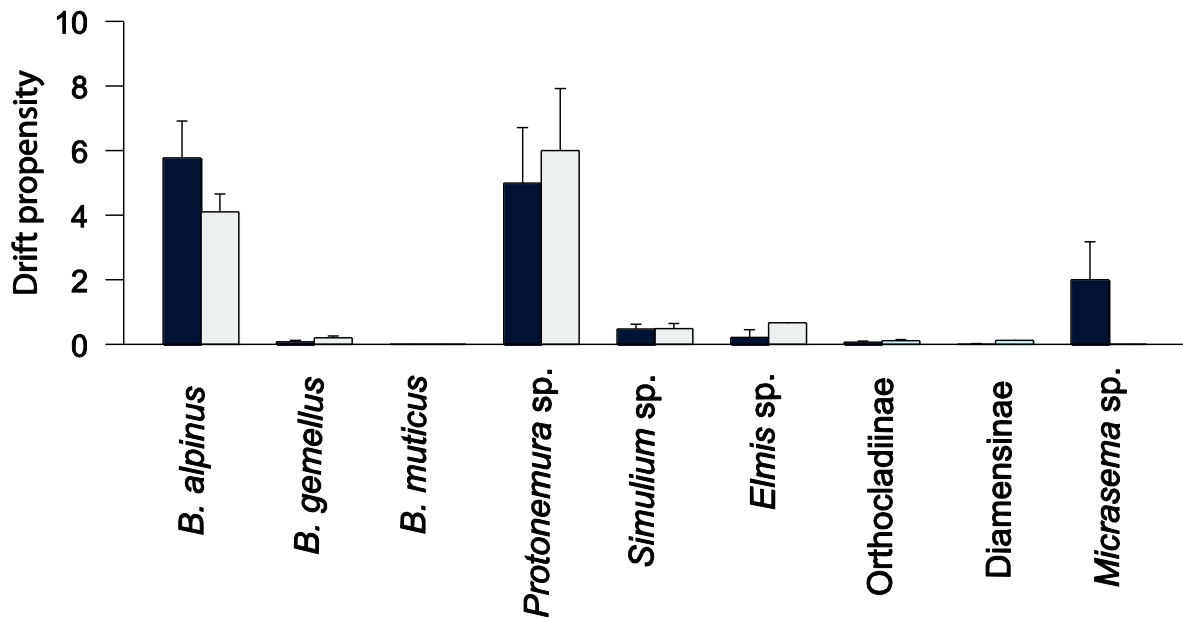


Figure 6.5. Drift propensity (emigration/benthic density) of the most abundant taxa recorded from the mesocosm channels during a 24 26-27 July.

6.3.5. Body size spectrum

The predator treatment had no significant effect on the body size of Orthocladiinae or *Simulium* spp. individuals (Table 6.6). Mean body lengths of *B. muticus* and *B. gemellus*, were 0.15mm and 0.25 mm smaller in the treatment channels, respectively (Table 6.6). However, effect sizes were smaller for both taxa ($d < 0.5$ $P < 0.1$; Table 6.6). Violin plots of *B. gemellus* body lengths revealed an asymmetric density distribution, with fewer 5-6 mm individuals and smaller median body size in the predator treatment channels (Figure 6.6).

Inspection of the body mass distributions for the control and treatment (including *P. grandis*) channels suggests broadly similar, unimodal distributions (Figure 6.7). There were, however, some important differences: (i) the treatment channels displayed strong right skew as *P. grandis* individuals were considerably larger than any other taxa; and (ii) there were fewer taxa between 1–10 mg in the treatment channels when compared to the control (Figure 6.7). When all taxa (excluding *P. grandis*) were pooled and allocated to body mass size classes, a significant negative treatment response was observed for the largest class, > 5 mg (Figure 6.8).

Table 6.6. Mean length (\pm SE in parentheses) of the four most abundant taxa recorded in the end point community. Results from student's t-test are complimented by SES (unbiased estimate of Cohen's d) \pm 95% CI.

Taxon	Body length (mm)		<i>n</i>	<i>t</i>	<i>P</i>	<i>d</i>	CI
	Treatment	Control					
<i>Baetis gemellus</i>	5.06 (0.09)	5.31 (0.09)	120	2.29	0.02	0.42	-0.78,- 0.05
<i>Baetis muticus</i>	5.99 (0.06)	6.14 (0.06)	80	1.79	0.09	0.36	-0.84, 0.04
Orthocladiinae	4.06 (0.16)	4.10 (0.15)	50	0.03	0.85	0.01	-0.13, 0.14
<i>Simulium</i> spp.	4.25 (0.13)	4.13 (0.15)	50	0.33	0.57	0.07	-0.07, 0.21

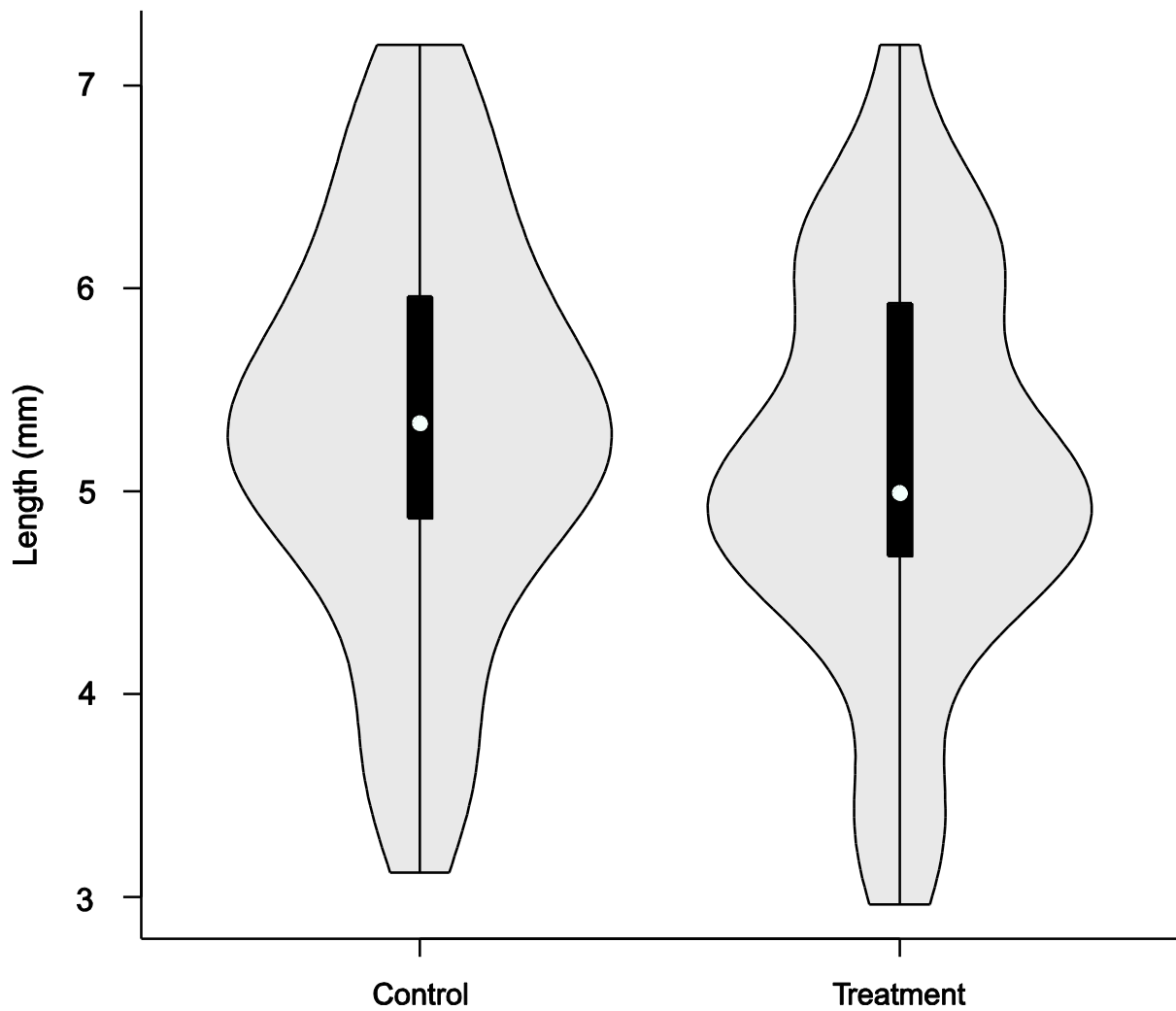


Figure 6.6. Violin plots for the length (mm) of *B. gemellus* recorded in the mesocosm channels. The light grey area represents a kernel density function. The black box and line represent a traditional boxplot and the white dot the median length.

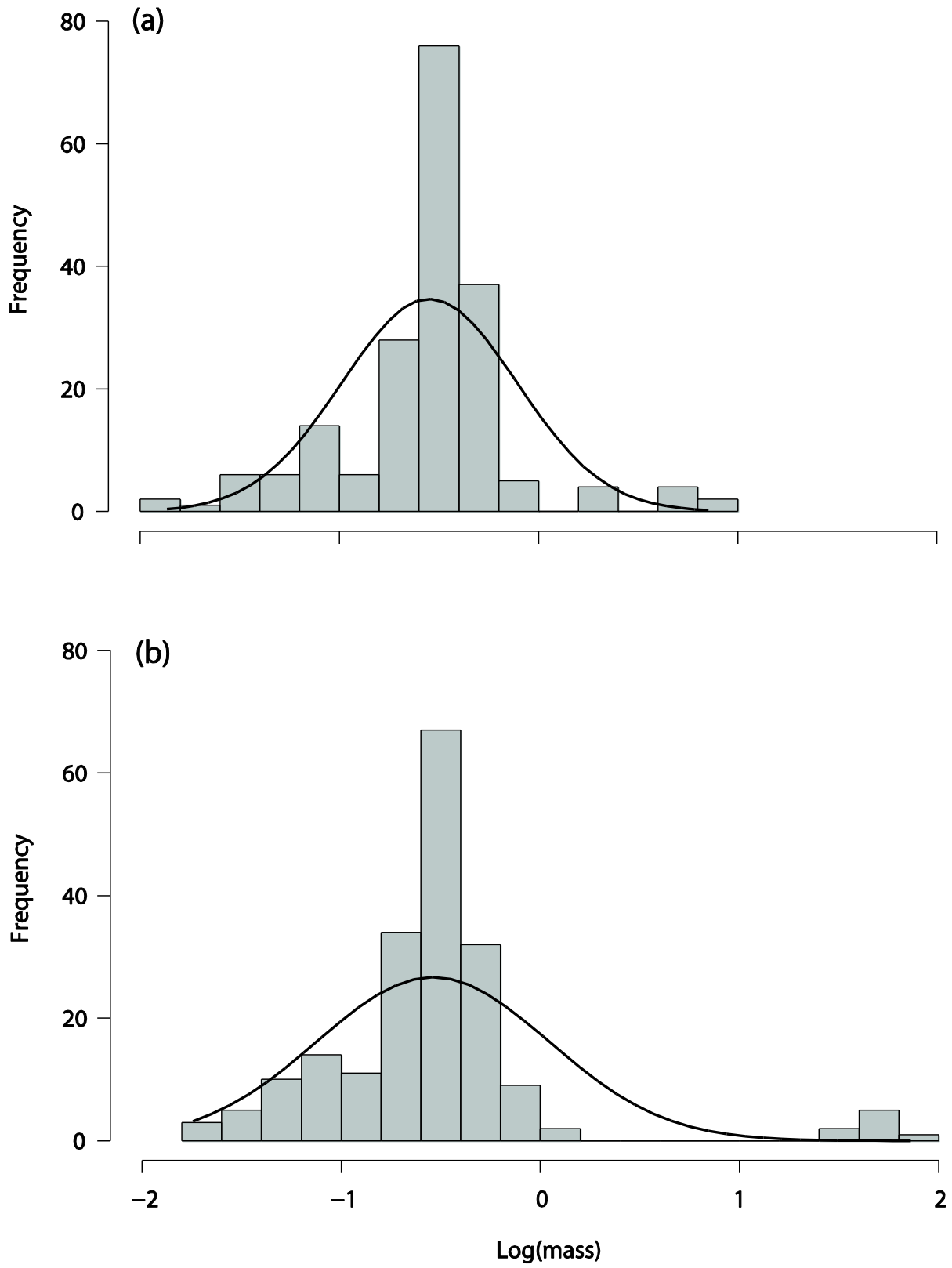


Figure 6.7. Body mass (log scale) distributions for (a) the control channels and (b) the treatment channels.

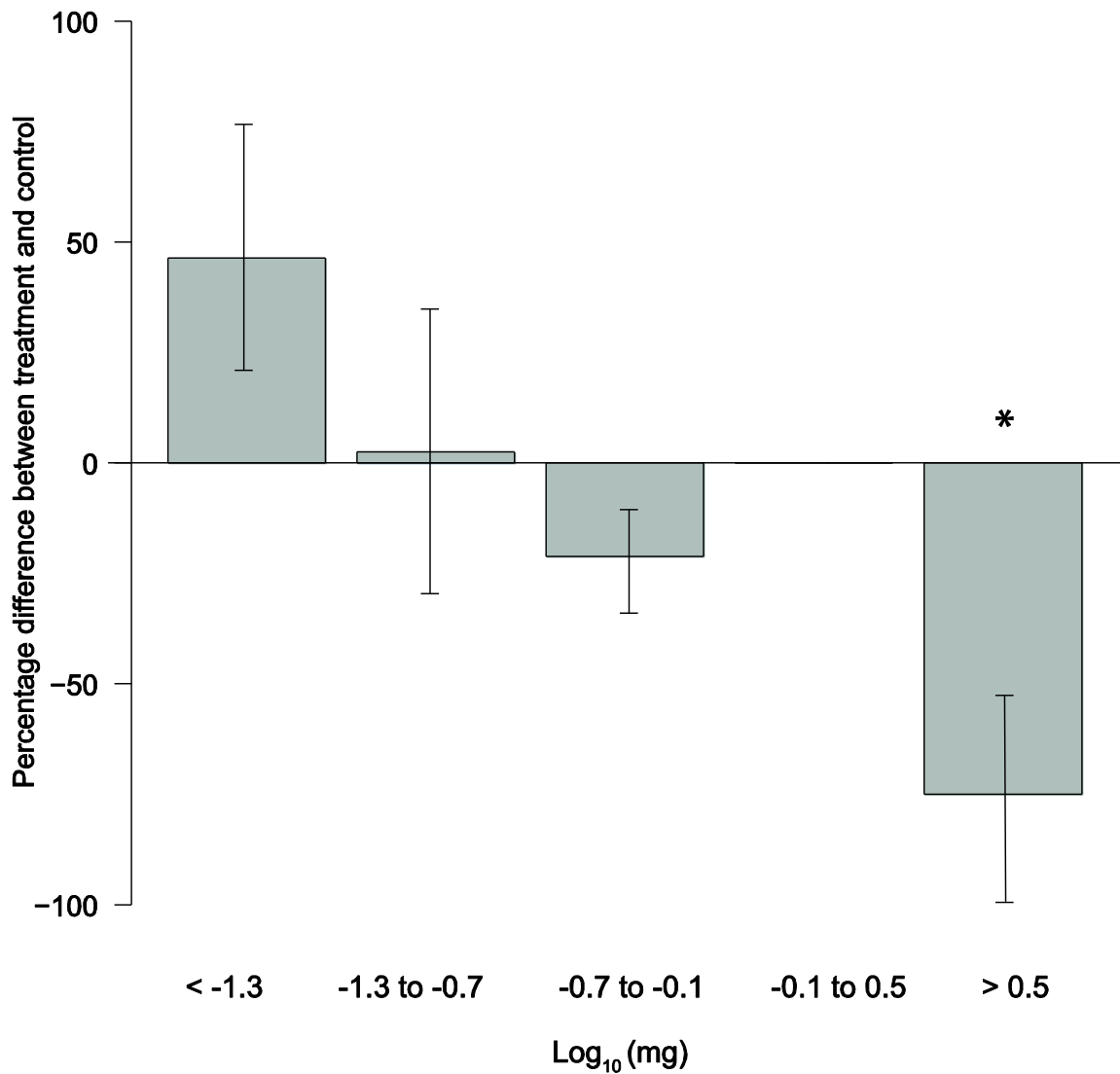


Figure 6.8. Mean percentage difference (\pm SE) between treatment (not including *P. grandis*) and control for the number of individuals in each of the five \log_{10} body mass size classes. Mean and SE calculated from all possible pair-wise comparisons between individual treatment and control channels (for each size class $n=16$). Asterisk denotes significance level: * $P < 0.05$ (Kruskal–Wallis test).

6.4. Discussion

Predation is a key biotic process in aquatic systems which can drive both physiological and behavioural responses of prey taxa (Peckarsky 1982), and alter community structure and functioning (Jefferies & Lawton 1984; Sih *et al.* 1998). This study identified a number of community and population level responses to the experimental simulation of *P. grandis* range expansion. The density of conspicuous grazing taxa (*Baetis* spp.) was depressed through both direct consumption and prey avoidance mechanisms (Lancaster 1990). However, no difference in the magnitude of the trophic cascade (basal resources estimated as chl-*a*) was observed, probably because predators were present in the control (i.e. *R. intermedia* and *Plectrocnemia* sp.). A negative shift in mean body size was observed in the presence of *P. grandis* at both the population level (*B.gemellus*) and community level (avoidance by potential competitors).

6.4.1. Impacts of *P. grandis* on macroinvertebrate abundance and structure

Despite a large effect size the reduction in total invertebrate abundance was not significant probably due to either: (i) high prey turnover rates, i.e. immigration replaced consumed or emigrated individuals (Lancaster 1990); or (ii) the small number of replicates (low statistical power). However, densities of two *Baetis* spp., which are typically important components of carnivorous stonefly diets (Peckarsky, 1985, Céréghino, 2006), were significantly reduced in our study. This finding supported H_1 (*P. grandis* would reduce prey abundance) and suggests that predatory stoneflies are more efficient at catching *Baetis* nymphs compared to other, more sedentary organisms such as chironomids (Peckarsky & Cowan 1995; Elliott 2003). This is primarily due to the conspicuous swimming behaviour of *Baetis* which acts as a predator stimuli (Peckarsky & Penton 1989).

Contrary to findings from this study, stonefly predation has been shown to reduce chironomid densities in other laboratory and field experiments (Peckarsky 1985; Lancaster 1990; Elliott 2003). These studies have either used ‘predation arenas’ (Allan *et al.* 1987; Elliott 2003), with the abundance and diversity of prey and predatory taxa strictly controlled, or field based mesocosms which have inhibited colonisation of other, non-target, large bodied invertebrates (e.g. Woodward and Hildrew 2002). In this experiment, predators other than *P. grandis* were free to colonise all the channels, the most abundant being *Rhyacophila* spp. (mainly *R. intermedia*) and Tanypodinae, both of which predominately feed on chironomids (Lavandier & Céréghino 1995; Woodward & Hildrew 2002b). As these predators were relatively abundant in the control channels, predation of orthoclad larvae likely occurred in both treatment and control channels but by different taxa (i.e. *P. grandis* consumed both *Baetis* and chironomids in the treatment channels while *R. intermedia* and tanypods consumed chironomids in the control channel).

6.4.2. *Effects of P. grandis on invertebrate feeding guild structure*

Distinct changes in functional feeding guild structure were identified in this study and appeared to support H_2 (*P. grandis* would alter community feeding guild structure through selective predation and competition). The density of grazing taxa was lower in the treatment channels, probably due to *Baetis* spp., the most abundant grazers recorded during the experiment, being more prone to stonefly predation (Peckarsky & Penton 1989; Elliott 2003). The significantly lower relative abundance of large bodied predators in the *P. grandis* channels was likely the result of intraguild predation/interference competition (Polis *et al.* 1989). It should, however, be noted that all *P. grandis* nymphs used in the experiment were fully developed and as the experiment ran for a relatively short time interval, ontogenetic

shifts in feeding habits of *P. grandis* and other predatory taxa were not incorporated (Lavandier & Céréghino 1995; Woodward & Hildrew 2001; Céréghino 2006). Yet, these findings suggest potential for future predator replacement as the physicochemical habitat template of low order alpine streams changes under a warmer climate (Khamis *et al.* 2013) facilitating *P. grandis* range expansion (Brown *et al.* 2007a).

Top down, predation driven, trophic cascades are more prevalent and often more pronounced in aquatic systems than terrestrial settings, primarily due to larger consumer to producer biomass ratios (Shurin *et al.* 2002). However, this study did not identify any significant change in the magnitude of the trophic cascade due to the presence of *P. grandis* (H_4 not supported). This may have been due to number of factors. First, the reduction in grazer densities observed in the treatment channels was relatively small (Table 6.2). Second, the high feeding plasticity of macroinvertebrate in alpine streams (Zah *et al.* 2001; Füreder *et al.* 2003; Clitherow *et al.* 2013) may increase ecological redundancy between feeding guilds (i.e. detritivores/predators also consuming algae), thus dampening the trophic cascade (Polis *et al.* 2000). Third, the presence of other large bodied predatory taxa (e.g. *Rhyacophila* spp.) would likely have had an impact on grazing taxa in the control channels, potentially reducing grazing efficiency (Wooster & Sih 1995).

6.4.3. *Consumptive and non consumptive effects of P. grandis*

The finding that *Baetis* spp. and Chironomidae larvae (Orthocladinae) were the most abundant prey items in the guts of *P. grandis* was similar to other studies on a range of predatory stoneflies from Europe and North America (Allan 1982; Peckarsky 1985; Elliott 2003). Recent diet studies from the French Pyrénées and the Iberian peninsula have also

found that *Baetis* spp. and chironomids are key prey items for carnivorous stonefly nymphs of the families Perlodidae and Perlidae (Céréghino 2006, Bo *et al.* 2008). In this study, *P. grandis* displayed a preference for *Baetis* spp. in the experimental channels (supporting H_1) but not in the Tourettes stream. Conversely, *P. grandis* displayed a preference for orthoclads in the Tourettes stream but not in the experimental channels. However, this represents the ‘last meal’ of *P. grandis* and their diet may have changed during the experimental run. The differences observed in this study between the Tourettes stream and experimental channels may be due to the different proportions of *Baetis* species present in the two environments. *B. alpinus* made up >90% of the Baetidae in the Tourettes stream, while *B. gemellus* >70% in the experimental channel. These two species appear to display different anti-predator behaviours; *B. alpinus* is a more mobile, stronger swimmer compared to *B. gemellus* (K. Khamis pers. obs.) and tended to drift more frequently, a common response to plecopteran predation pressure (Kratz 1996). *Calotriton asper*, the top predator in many alpine springs, typically selects for more mobile prey (Montori 1992). Hence, the more sedentary behaviour of *B. gemellus* when compared to *B. alpinus* reflects adaption to *C. asper* predation pressure, but a degree of prey ‘naivety’ in the presence of *P. grandis* (Cox & Lima 2006). Alternatively, it may have been an artefact of the small experimental channel size, which would have reduced the in channel predation refugia when compared to the Tourettes stream (Bechara *et al.* 1993).

The increased drift rate recorded for *B. gemellus* and *B. muticus* (from the *P. grandis* treatment) represents a behavioural response common among Baetidae (Wooster & Sih 1995; Peckarsky *et al.* 2008). It is thought to enable increased resource acquisition when mortality (predation) risk is high (Peckarsky 1996). However, *B. alpinus* exhibited a per capita drift rate far greater than the other *Baetis* spp., most likely due to its co-evolution with *P. grandis*

which has amplified this behavioural trait (McPeck 1990). These findings further support H_1 (*P. grandis* would reduce prey abundance) as the key prey found in the guts (*Baetis* spp.) were also more abundant in the drift from *P. grandis* channels. Interestingly, *B. alpinus* drift was significantly greater from the control channels and may be due to both apparent and exploitative competitive interactions between the *Baetis* spp. (Holt & Lawton 1994), with *B. gemellus* and *B. muticus* primarily predator (*P. grandis*) limited and *B. alpinus* primarily resource limited (Chase *et al.* 2002). Essentially the prey with superior resource acquisition capabilities, in this case *B. gemellus* and *B. muticus*, were also the most vulnerable to predation (Holt & Lawton 1994).

Intra-guild predation was recorded within the benthic community of the Tourettes stream, as large *Rhyacophila* spp. were recorded in the guts of *P. grandis*. However, further work is needed to ascertain the symmetry of this relationship, i.e. whether *P. grandis* is always the predator of *Rhyacophila* or do they switch depending on body size or life cycle stage (Polis *et al.* 1989). Both these taxa share chironomid prey (Lavandier & Céréghino 1995, K. Khamis unpublished), thus some degree of interference competition can be inferred. Bo *et al.* (2008) also found *Rhyacophila* and other caseless caddisfly larvae in the guts of stoneflies suggesting intraguild predation may be a common feature in low order streams. This is likely due to the low taxonomic diversity of foodweb constituents and omnivorous feeding behaviour displayed by consumers and predators in high alpine streams (Lavandier & Decamps 1984; Zah *et al.* 2001; Clitherow *et al.* 2013). Hence, the range expansion of *P. grandis* is likely to intensify biotic interactions by increasing the number of food web links with only a slight increase in the number of species (Woodward & Hildrew 2001). This will in turn reduce niche space, particularly amongst predators which, due to dietary overlap with *P. grandis*,

will increase competition for prey items (Wissinger & Mcgrady 1993; Woodward & Hildrew 2002a).

The increased drift exhibited by *B. gemellus* and *B. muticus* for the *P. grandis* treatment represents a behavioural response common among Baetidae (Wooster & Sih 1995; Peckarsky *et al.* 2008). It is thought to enable increased resource acquisition when mortality (predation) risk is high (Peckarsky 1996). However, *B. alpinus* exhibited a per capita drift rate far greater than the other *Baetis* spp., most likely due to its co-evolution with *P. grandis* which has amplified this behavioural trait (McPeck 1990). These findings further support H_1 (*P. grandis* would reduce prey abundance) as the key prey found in the guts (*Baetis* spp.) were also more abundant in the drift from *P. grandis* channels. Interestingly, *B. alpinus* drift was significantly greater from the control channels and may be due to both apparent and exploitative competitive interactions between the *Baetis* spp. (Holt & Lawton 1994), with *B. gemellus* and *B. muticus* primarily predator (*P. grandis*) limited and *B. alpinus* primarily resource limited (Chase *et al.* 2002). Essentially the prey with superior resource acquisition capabilities, in this case *B. gemellus* and *B. muticus*, were also the most vulnerable to predation (Holt & Lawton 1994).

6.4.4. Body size spectrum

The smaller individuals of *B. gemellus* in the treatment channels (as highlighted by the skewed violin plots) may be due to the size selective predation by *P. grandis* with a preference for larger individuals as prey. While few studies have investigated size selective predation in Plecoptera both Allan *et al.* (1987) and Peckarsky (1985) experimentally found developed stonefly nymphs (>25mg) exhibited a preference for medium sized prey (>0.2 mg). A second explanation of *B. gemellus* body size would concur with the findings of

Lancaster (1990) who found larger *Baetis* nymphs drifted more frequently from channels in the presence of a predatory stonefly.

When body size was considered at the community level (individual based rather than taxon based) individuals of the larger body size classes were less abundant in the predator treatment, supporting H₃. This was likely due to intraguild predation/interference competition, supported by the identification of *Rhyacophila* spp. in the diet of *P. grandis* and associated positive LOR scores. This suggests significant niche overlap between *Rhyacophila* spp. and *P. grandis* due to shared common prey (Lavandier and Céréghino 1995). Hence, the pattern of reduced body size in the treatment channels was due to other large bodied invertebrate predators being either eaten by, or actively avoiding *P. grandis* (Woodward & Hildrew 2002a; Vanak & Gompper 2010). This has important implications for food web stability and structure as changes in the body size spectrum (see Figure 6.7), particularly an increase in size of the apex predator, which can reduce refugia associated with gape limited predation (Woodward *et al.* 2005). It is, however, difficult to predict how such changes will propagate through the foodweb in alpine systems as changes in interaction strength and omnivory can destabilize and stabilize, respectively (Borrvall *et al.* 2000).

6.5. Conclusion

As alpine stream physicochemical habitat characteristics become more benign due to climate warming/river waters source changes, upstream migration of *P. grandis* is likely to increase trophic height of invaded communities as current invertebrate predators (e.g. *Rhyacophila* spp.) become prey. This study has highlighted interference competition and interguild predation as an important structuring mechanism, with the potential to alter the body size spectrum and food web interactions in *P. grandis* invaded systems (Woodward & Hildrew

2002b). Therefore, it is likely that the predicted range expansion will result in an intensification of biotic interactions (reducing niche breadth and increasing competition among predators). Furthermore, certain grazing taxa, primarily *B. gemellus* and *B. muticus*, are likely to be selectively predated, altering the community structure and potentially its ecological functioning.

This study has further emphasised the need to consider biotic interactions in species abundance models (Araújo & Luoto 2007), as both community structure and body size structure were altered under experimental predator range expansion. These findings have important implications for ecosystem stability as predator and prey body-size ratios control trophic interaction strengths (Emmerson & Raffaelli 2004; Woodward *et al.* 2005). Thus, ignoring or treating biotic interactions as ‘constant’ is likely to cause erroneous predictions regarding future distributions and extinction vulnerability. This is particularly relevant in alpine river networks as, despite having low alpha diversity, first order streams represent important sites for regional biodiversity (Finn *et al.* 2011). The movement upstream by predatory taxa will create synergistic feedbacks between biotic interactions and climate driven physicochemical habitat change. This is likely to increase the risk of species extinctions, which will be detrimental to both beta and gamma diversity (Brown *et al.* 2007a). Urgent work is therefore needed to ensure that additional anthropogenic pressures (e.g. water abstraction, hydro-power schemes, nutrient enrichment and cattle trampling) are limited to avoid further pressure to this unique and fragile habitat (Hannah *et al.* 2007; Khamis *et al.* 2013)

6.6. Chapter Summary

In this chapter an experimental approach was adopted to examine the potential effect of a climate induced, predator range expansion on the benthic community structure of a first order alpine stream. Results identified likely changes in community structure (taxonomic and FFG), body size distribution, trophic height and highlight the potential for predator replacement in invaded systems. These findings represent a significant improvement in our biotic process understanding of alpine river ecosystems and highlight the need to consider synergistic feedbacks when making predictions of ecosystem change due to cryosphere retreat. In the next chapter physical processes operating at the point scale are investigated to improve understanding of the fundamental controls on stream temperature.

CHAPTER 7

*Heat exchange processes and thermal
dynamics of a glacier fed, alpine stream*

7.1. Introduction

Water temperature is a key water quality variable that governs physical and biological processes in aquatic systems (Caissie 2006; Webb *et al.* 2008). Over the last century, stream and river temperature has been correlated with rising air temperature (Webb 1996; Lammers *et al.* 2007; Kaushal *et al.* 2010) as both respond to fluctuations in atmospheric energy fluxes (Johnson 2004). As climatic warming is predicted to continue during the 21st century (IPCC 2007), water temperature of lotic systems is also likely to rise (Mantua *et al.* 2010; Vliet *et al.* 2011). Hence, prediction of future thermal patterns is becoming increasingly important for directing mitigation and conservation strategies (Macdonald *et al.* 2013) but requires an understanding of the fundamental controls (heat fluxes) on river warming and cooling across a variety of river habitat types (Webb *et al.* 2008).

For rivers and streams, energy transfer occurs at two interfaces: (i) the atmosphere–water column; and (ii) channel bed–water column (Webb *et al.* 2008). At the air-water surface interface, energy gains occur through solar and longwave radiation, condensation and sensible heat transfer. Losses may occur through reflection of incident solar radiation, emission of longwave radiation, evaporation and sensible heat transfer (Hebert *et al.* 2011). At the water-stream bed interface, conduction and advection can act as both heat source or sink (Hannah *et al.* 2008) while fluid friction of the water column against the bed and banks represents a net gain of energy. Fluxes associated with precipitation and biological activity are deemed small and often omitted from energy balance calculations (Hannah *et al.* 2004; Hebert *et al.* 2011). Finally tributary inflows and groundwater-surface water interactions need to be taken into consideration (Webb & Zhang 1997; Hannah *et al.* 2004; Malcolm *et al.* 2004).

Alpine river systems are particularly sensitive to warming as climate-cryosphere interactions control diurnal to seasonal pulses of snow and glacier melt which both regulate river flows (Hannah *et al.* 1999) and stream water temperature (Hannah *et al.* 2007). Studies in these systems have focused predominately on climate-stream temperature relationships and spatial/temporal variability of thermal regimes (Malard *et al.* 2001; Uehlinger *et al.* 2003; Brown & Hannah 2008; Cadbury *et al.* 2008). Shifts in the timing, magnitude and duration of meltwater production are predicted in response to climatic change (Hock *et al.* 2005; Milner *et al.* 2009; Stahl *et al.* 2008), which will have implications for hydrological and ecological processes in alpine basins (Brown *et al.* 2007; Muhlfield *et al.* 2011; Jacobsen *et al.* 2012). Hence, an understanding of the energy and hydrological fluxes controlling stream temperatures in these systems is essential for further development of predictive models (Moore *et al.* 2009; Carrivick *et al.* 2012).

Our understanding of the deterministic controls of stream water temperature are rooted in research mainly focused on temperate zone lowland rivers (Wright & Elorral 1967; Brown 1969; Webb & Zhang 1997, 1999; Caissie *et al.* 2005) and regulated rivers (Webb & Walling 1997; Lowney 2000). To date, few detailed studies of the fundamental processes controlling energy transfer have been carried out in glacier fed rivers with the exception of Chikita *et al.* (2010) and Magnusson *et al.* (2012a). Despite being at different latitude both studies identified friction and net radiation as important heat sources. However, not all meteorological variables were recorded above or adjacent to the stream channel and both studies were conducted over single summer melt seasons. These shortcomings are not exceptional as many energy balance studies have either been conducted for short periods (e.g.

Evans and Petts, 1998; Webb and Zhang, 1997) or have used meteorological stations located many km from the stream environment (e.g. Caissie *et al.* 2007; Hebert *et al.* 2011). Garner *et al.* (2012) highlighted the need for longer term studies which enable characterization of year on year variability in heat flux components, yet to date no multi-year studies of heat exchange processes for alpine glacier-fed streams have been conducted.

Given the research gaps identified above, the aim of this study was to undertake the first detailed inter-annual study of the heat exchange processes and thermal dynamics for an alpine glacier-fed stream, recording all hydro-meteorological variables at the study location. The specific objectives were threefold: (i) to characterise in channel thermal dynamics and above stream microclimate and a glacier fed stream in the French Pyrénées; over two melt seasons; (ii) to quantify the heat exchange process driving thermal variability at seasonal and sub-seasonal scales; and (iii) model water temperature using calculated heat fluxes to understand further the key processes driving stream temperature dynamics.

7.2. Methods

7.2.1. Field site

This study was carried out in the alpine Taillon-Gabiétous catchment, Cirque de Gavarnie, French Pyrénées (43°6'N, 0°10'W), with an altitudinal range of 1800-3144m and area of 6.7km². The focus of this study was the Taillon stream, which drains a sub-catchment covering 1.72km², of which 5.2% was covered by glacier ice. The relief was dominated by steep (30-70°) slopes and the underlying geology is calcareous and composed of predominantly Marbore sandstone and limestones of the Santonien and Coniacien series. Vegetation was sparse above 2200m and the lower basin (<2100m) was grazed alpine meadow with no canopy cover. Mean daily minimum and maximum air temperatures recorded between 1990-2010 (at 1390m), were 2.6°C and 12.7°C respectively, and mean total annual precipitation 1466mm (Meteo France 2011). On north facing slopes the permanent snowline is located >2700m (Hannah *et al.* 2000). A small cirque glacier, the Glacier du Taillon (0.09 km²), feeds the Taillon stream. This glacier has downwasted and retreated rapidly over the last decade; the snout has receded by 67m since 2001 (Association Moraine Pyrénéenne de Glaciologie 2009).

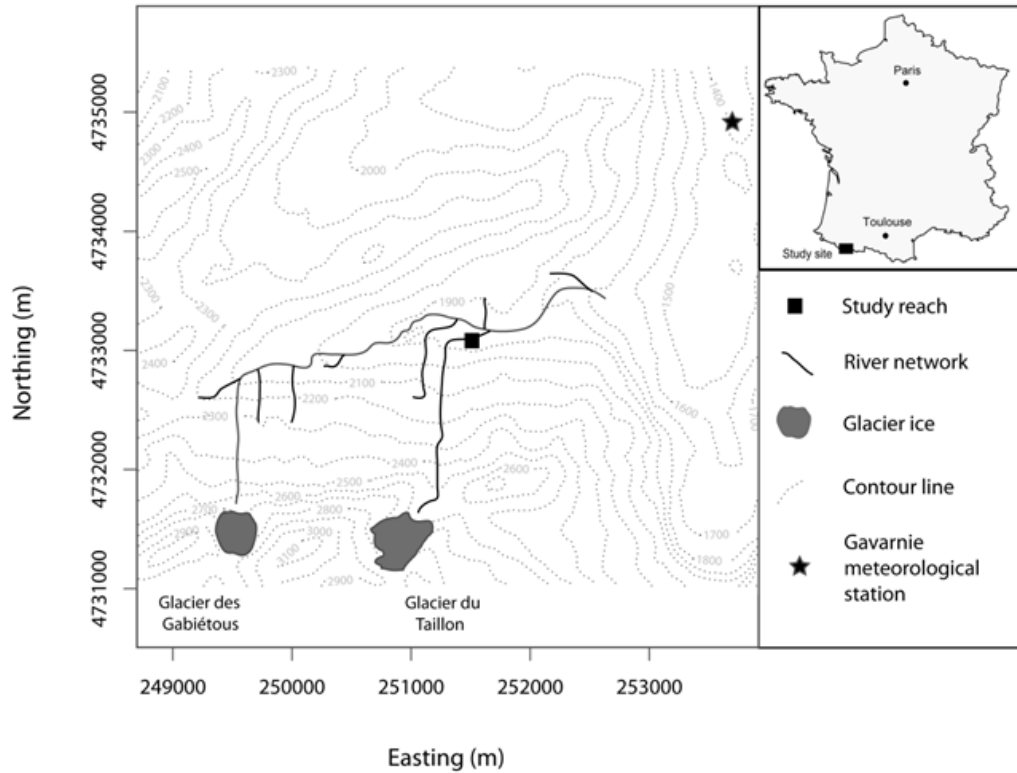


Figure 7.1. Study location with study reach and Gavarnie meteorological station highlighted. The map projection of the larger panel is UTM 31

7.2.2. Data collection

Microclimate data. Detailed hydro-climatological observations were made during two consecutive melt seasons: 2010 & 2011. Records between June 16 and September 2 (calendar days 166 – 245) are presented herein. An automatic weather station (AWS) was erected on the the main channel of the glacier-fed Taillon stream approximately 1.4 km from the glacier snout (Figure 7.1; Table 7.1). All sensors scanned at 10s intervals with 15 min average logged for air temperature (T_{air}), relative humidity (RH), barometric pressure (P), wind speed (ws), incoming solar radiation (K_{\downarrow}), reflected solar radiation (K_{\uparrow}), net radiation (Q^*) and bed heat flux (Q_{bhf}). Precipitation (P_{ppn}) data were stored as 15 min totals. A miniature datalogger, housed in a radiation shield, was placed at the Taillon Glacier (T_{glac}) to monitor air

temperature. The retreat of the transient snowline was recorded twice weekly). Fixed position digital images were taken, scaled and then compared to 1:25000 map (Institute Geographique National, 2003). Additional meteorological data were obtained for a Meteo France station located in Gavarnie (1390m), approximately 3km from the study site, and used to characterise winters conditions prior to both field campaigns.

Table 7.1. Meteorological and hydrological variables measured and instrumentation used.

Variable	Instrument	Location	Instrument error
Water temperature (at river gauges)	Campbell CS54A7 temperature probe	0.1m above the stream bed	0.2°C
Water temperature (at other sites)	Gemini Tinytag Plus and Aquatic	0.1m above the stream bed	0.2°C
Bed temperatures	Campbell 107 thermistor	Stream bed 0.05m, 0.2m 0.4m depth	0.2°C
Air temperature	Skye SKH 2013	1.75m above the stream surface	0.1°C
Incoming and outgoing short- wave radiation	Kipp and Zonen CM3	1.75m above the stream surface	<3%
Net radiation	Campbell NR-Lite	1.75m above the stream surface	5%
Relative humidity	Skye SKH 2013	1.75m above the stream surface	1-3%
Precipitation	Campbell tipping bucket rain gauge	On the river bank	0.05mm
Wind speed	Vector A100R 3 cup anemometer	1.75m above the stream surface	0.25ms ⁻¹
Atmospheric pressure	Skye SKPS 820 barometer	1.25m above the stream surface	0.1%
Bed heat flux	Hukseflux thermal sensor	Stream bed 0.05m	3%
River stage	Druck PDCR-830 pressure transducer	0.1m above the stream bed	0.1%

Water temperature data. Water column temperature (T_w) was recorded using a Campbell CS54A7's deployed 0.1m above the stream surface. Stream bed temperatures ($T_{b_{0.05m}}$, $T_{b_{0.20m}}$ and $T_{b_{0.40m}}$) were recorded using Campbell 107-T thermistors. All temperature loggers were synchronised (GMT) and recorded at 15 min intervals. Cross-calibration of all temperature sensors was conducted before and after the field season (Quilty & Moore 2007). Correction factors were then applied to each logger based on a regression, which related the individual logger reading to the mean reading of all loggers (Hannah *et al.* 2009).

River gauging. A stream flow gauging station was established next to the AWS. A pressure transducer (Table 7.1) was placed in a stilling well to provide depth measurements at 15 min resolution, and stage – discharge relationships were estimated using both salt dilution and velocity-area methods (Herschy 1985; Moore 2003), to provide a continuous record of river flow.

7.2.3. Calculation of energy budget

The total energy available to a watercourse (Q_n) without tributary inflow can be calculated as follows (Webb & Zhang 1997):

$$Q_n = Q^* \pm Q_h \pm Q_e \pm Q_{bhf} \pm Q_f \pm Q_a \quad (7.1)$$

Where Q^* = net radiation, Q_h = sensible heat, Q_e = latent heat, Q_{bhf} = bed heat flux, Q_f = fluid friction at the bed and banks, Q_a = advection.

The latent heat flux (Q_e) was calculated following Hannah *et al.* (2004). The Penman-type equation outlined by Webb and Zhang (1997) was adopted to calculate the rate of evaporation or condensation:

$$E_v = 0.165 (0.8 + U/100) (E_w - E_a) \quad (7.2)$$

where E_v = evaporation/condensation rate (mm d^{-1}), U = wind speed at a height of 1.75m above the water surface (km d^{-1}), E_w = saturated vapour pressure at the water surface temperature (mbar) and E_a = vapour pressure at air temperature (mbar). Vapour pressure was calculated from measurements of air temperature, water temperature and relative humidity. The energy flux (lost or gained) was expressed as:

$$Q_e = E_v L p \quad (7.3)$$

where Q_e = the latent heat flux (W m^{-2}), L = latent heat of vaporization ($^{\circ}\text{C J g}^{-1}$), and p = specific weight of water (g cm^{-3}). The latent heat of vaporization was calculated by:

$$L = 2454.9 - 2.366 T_a \quad (7.4)$$

where T_a = air temperature ($^{\circ}\text{C}$).

Sensible heat (Q_h), the heat exchange between the water column and air, was estimated using the product of the evaporative flux and the Bowen ratio. The Bowen ratio (β) was calculated according to Bowen (1926):

$$\beta = [0.61P \cdot (T_w - T_a) / (E_w - E_a)] / 1000 \quad (7.5)$$

where P = atmospheric pressure (mbar), and T_w = water temperature ($^{\circ}\text{C}$).

Net radiation (Q^*) was measured above the stream during the 2011 field season along with incoming and reflected shortwave radiation. The longwave radiation emitted by the water surface was calculated using the Stefan-Boltzman Law (Leach & Moore 2010):

$$L \uparrow = \epsilon_w \sigma (T_w + 273.2)^4 \quad (7.6)$$

where ϵ_w = emissivity of the stream set at 0.97, σ = Stefan-Boltzman constant and $L \uparrow$ emitted longwave radiation. $L \downarrow$ was estimated as:

$$L \downarrow = Q^* - K^* - L \uparrow \quad (7.7)$$

where K^* = net shortwave radiation ($K \downarrow - K \uparrow$). During the 2010 field season net radiation was not recorded directly due to sensor failure. $L \downarrow$ was determined following Meier *et al.* (2003):

$$L \downarrow = \epsilon_w \epsilon_a \sigma (T_a + 273.2)^4 \quad (7.8)$$

where the emissivity of the atmosphere (ϵ_a) was calculated following Brock and Arnold (2000). This model was first calibrated against the 2011 observations and at the daily time step the net longwave component of the radiation balance was determined accurately (RMSE = 0.02 MJ m⁻² d⁻¹).

Bed heat flux (Q_{bhf}) was directly measured to encapsulate both advective and conductive heat transfer after Hannah *et al.* (2004).

Fluid friction (Q_f , Wm⁻²) was estimated following Theurer *et al.* (1984):

$$Q_f = 9805 \cdot (F/W) \cdot S \quad (7.9)$$

where, F = flow volume at study reach (m³ s⁻¹), W = wetted width (m), and S = slope (m m⁻¹)

7.2.4. Water temperature model

The one-dimensional advection-dispersion equation has been employed widely to model stream water temperature (e.g. Benyahya *et al.* 2012; Caissie *et al.* 2007; Lowney, 2000; Moore *et al.* 2005; Younus *et al.* 2000). In reaches of spatially conservative water temperature, temporal changes in water column temperature at a point can be calculated as:

$$\frac{\partial Tw}{\partial t} = \frac{W}{\rho\theta A} Q_n \quad (7.10)$$

where t = time (day), ρ = the water density (1000 kg m⁻³), θ = the specific heat of water (4.19 x 10⁴ MJ kg⁻¹ °C⁻¹), A = the cross sectional area (m²). However in glacier-fed systems, the longitudinal rate of temperature change is often greater than the diurnal fluctuations. In such

situations equation (10) is unable to provide accurate predictions. Therefore, a simple modification of the heat dispersion equation was adopted (Caissie *et al.* 2007):

$$\frac{\partial T_w}{\partial t} = \frac{\partial Q_n}{\rho \theta d} \quad (7.11)$$

where ∂Q_n = the rate of change of total heat flux to the water column (Wm^{-2}) d = mean water column depth. The initial boundary condition was set as the mean water temperature on the day prior to the start of the simulation.

The root-mean-square error (RMSE) and mean absolute error (MAE) were adopted to evaluate goodness of fit for both modelled longwave radiation (2011) and stream temperature (Janssen & Heuberger 1995):

$$RMSE = \sqrt{\frac{\sum_{i=1}^n (O_i - P_i)^2}{N}} \quad (7.12)$$

$$MAE = \frac{\sum_{i=1}^n (O_i - P_i)^2}{N} \quad (7.13)$$

where N = the number of daily water temperature observations; O_i = the observed and P_i = the predicted daily mean or maximum water temperature.

7.2.5. Statistical analysis

Temperature duration curves were constructed for both water column and streambed temperature (c.f. Brown *et al.* 2010; Hannah *et al.* 2009), which provide a graphical depiction of the percentage of time a temperature is equalled or exceeded. Cross-correlation analysis was used to assess relationships between air, water column and streambed temperatures and calculate lag-lead times. This analysis used a maximum of 96 lags, to explore correlations within a window of ± 24 hrs (Malard *et al.* 2001). All data were tested for normality; discharge, Q_f and K^* were square root transformed to meet assumptions of parametric statistics. Relationships between hydro-meteorological variables, stream temperature and model errors were assessed using General Least Squares regression (GLS). For all regression models residuals were inspected using AFC plots, conditional box plots and QQ plots. If auto-correlation or heterogeneity was identified, auto-regressive moving average (ARMA) models and variance structures were fitted to successive models (Dickson *et al.* 2012). The optimum number of auto-regressive parameters (p) and moving average parameters (q), along with the appropriate variance structure, were selected through an iterative procedure which ranked successive models based on the Akaike information criterion (Zuur *et al.* 2009). R^2 values were then calculated following Buse (1973). All tests were considered significant when $P < 0.05$. All statistical tests were carried out using the *nmls* and *base* packages in R 2.14.1.

7.3. Results

7.3.1. Micro-climate, discharge and water temperature patterns

Antecedent winter conditions. The total amount of fresh snowfall prior to the 2010 season (1.16m) was greater than for the 2011 season (0.85m) and additional snowfall was recorded 2 months later into the 2010 season (0.10 m on 14/05/2010). Mean daily maximum air temperature was comparable in 2010 (9.1 °C) and 2011 (9.5 °C). However, mean daily maximum temperature between March and May was lower during 2010 (11.0°C) than 2011 (12.9°C).

Hydroclimatological context. Mean air temperature for both melt seasons was comparable (Table 7.2) with records from the valley AWS consistently warmer, and diurnal temperature fluctuations less than at the glacier snout (T_{glac}). No clear seasonal trend in air temperature was identified during either melt season (Figure 7.2); however, a notable cold period was apparent between days 166 and 172, 2010 ($T_{\text{AWS}} = -1.3^{\circ}\text{C}$ and $T_{\text{glac}} = -6.8^{\circ}\text{C}$). At the start of the 2010 study the seasonal snow pack extended to 2100m on north facing slopes, while patchy snow was present on South facing slopes. Air temperature was warmer during the early melt season of 2011 and the transient snow line extended to 2400m on north facing slopes with no snow present on south facing slopes. The snowline retreated rapidly between days 166 and 185 to 2600m and exposure of glacier ice occurred by day 185, 2011. During 2010 the snowline retreated rapidly to 2500m between days 172 and 190, however glacier ice was not exposed until day 211 (Figure 7.2). Total precipitation was lower during 2011 than 2010, with events of a higher frequency but lower intensity. For 2010 mean wind speed was lower and relative humidity was comparable to that recorded in 2011 (Table 7.2).

Table 7.2. Descriptive statistics for selected hydrometeorological variables over the 2010 (75 days) and 2011 (80 days) monitoring periods. All values are based on 15 minute averages except incoming shortwave radiation (daily totals) and precipitation (seasonal totals). The coefficient of variation is provided in parentheses.

Variable	Mean		Range		Max		Min	
	2010	2011	2010	2011	2010	2011	2010	2011
T _{air} (°C)								
Glacier	9.3 (0.53)	8.7 (0.40)	29.9	22.8	23.1	22.3	-6.8	-0.5
AWS	13.1 (0.40)	13.2 (0.36)	27.2	24.2	25.9	26.4	-1.3	2.2
Precipitation (mm)	308.8*	221.8*	-	-	11.2	13.0	0	0
Shortwave radiation (MJm ⁻² d ⁻¹)	21.04 (0.36)	17.48 (0.42)	29.21	23.65	31.11	29.55	2.90	5.90
Wind speed (m/s ⁻¹)	0.87 (0.66)	1.60 (0.59)	4.22	5.39	4.22	5.39	0	0
Atm pressure (mb)	822 (0.004)	818 (0.004)	21	19	832	826	811	807
Humidity (%)	72.1 (0.28)	71.8 (0.29)	80.0	79.6	100.0	99.8	20.0	20.4
Discharge (m ³ s ⁻¹)	0.15 (0.50)	0.16 (0.50)	0.45	0.46	0.50	0.51	0.01	0.04

*total for whole study period

Stream discharge declined across both study periods as the highest flows were associated with the retreat of the transient snowline and episodic precipitation events. However, a characteristic glacier-melt driven hydrograph was evident in the late 2011 melt season (Figure 7.2). The highest mean daily flows and variability (excluding days with $\text{ppn} > 20\text{mm}$) were recorded between days 172 and 190. The peak flows were comparable between seasons (2010 = $0.50\text{m}^3\text{s}^{-1}$ and 2011 = $0.51\text{ m}^3\text{s}^{-1}$) and were linked to prolonged, high intensity storms. The average diurnal flow variation during 2010 ($0.06\text{ m}^3\text{s}^{-1}$) was lower than 2011 ($0.09\text{ m}^3\text{s}^{-1}$). Strong inverse relationships between discharge and snowline altitude were apparent during both 2010 ($R^2 = 0.64, P < 0.001$) and 2011 ($R^2 = 0.67, P < 0.001$).

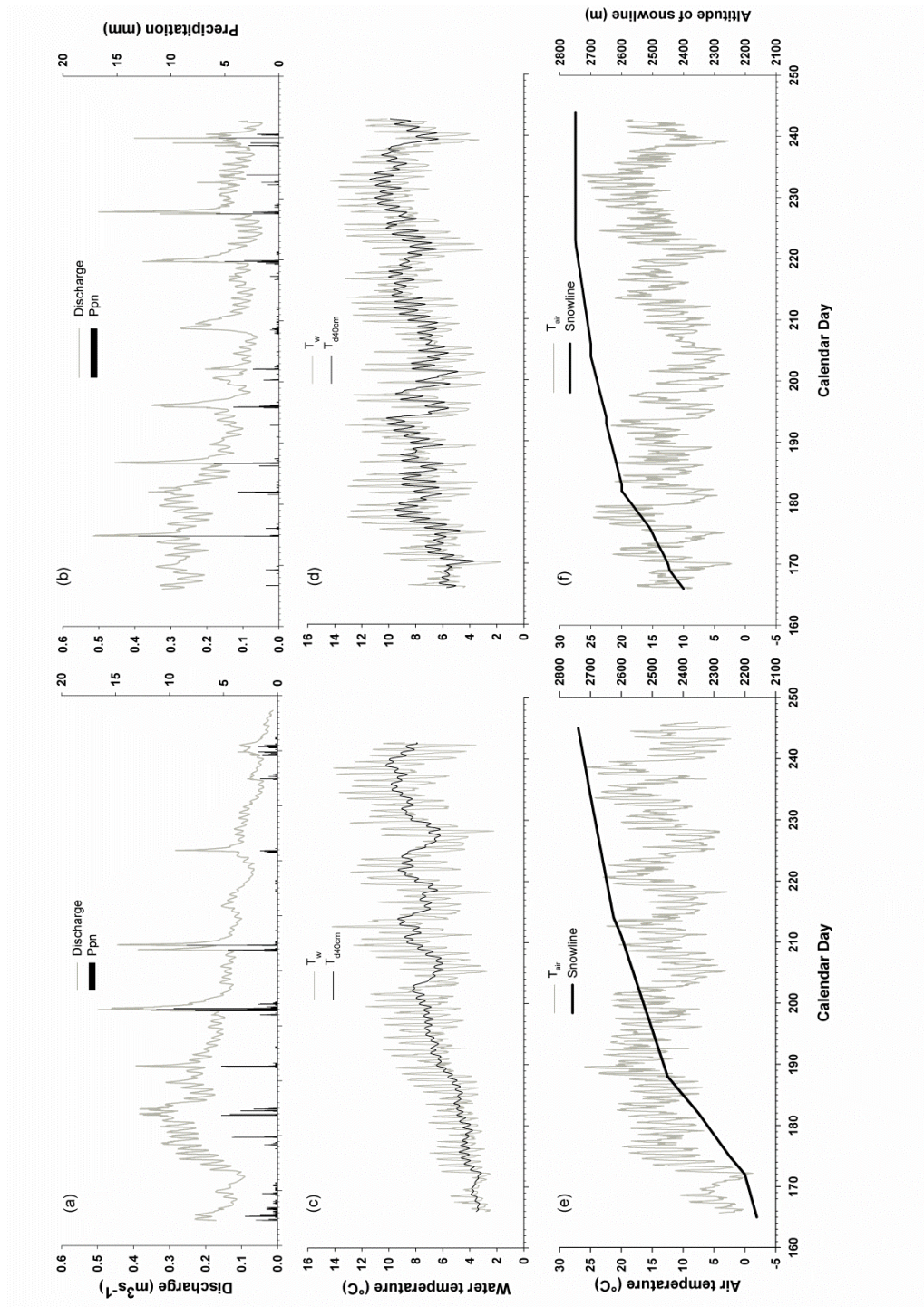


Figure 7.2. River discharge and precipitation time-series for: (a) 2010; and (b) 2011. Water column and stream bed temperature recorded for: (c) 2010; and (d) 2011. Air temperature and snowline altitude for: (e) 2010; and (f) 2011.

7.3.2. *Water column and streambed thermal patterns*

Stream water temperature increased over the 2010 melt season, the lowest (3.2°C) and highest (10.7°C) mean daily temperatures were recorded on calendar days 171 and 239. Water column temperature displayed significant positive relationships with distance from the transient snowline ($R^2 = 0.69$, $P < 0.001$), air temperature ($R^2 = 0.39$, $P < 0.001$) and negative relationships with stream flow ($R^2 = 0.12$, $P < 0.01$). A similar pattern was observed during the 2011 melt season with the lowest (4.9°C) and highest (10.5°C) daily mean stream temperatures recorded on days 169 and 232. As in 2010 water temperature displayed significant relationships with the transient snowline ($R^2 = 0.64$, $P < 0.001$), air temperature ($R^2 = 0.80$, $P < 0.001$) and stream flow ($R^2 = 0.22$, $P < 0.01$) in 2011. Both mean seasonal water column and bed temperatures were higher in 2011. During both summers, the water column displayed the greatest temperature range, while in the stream bed thermal stability increased with depth (Table 7.3). Steeper (flatter) temperature duration curves were apparent for the water column (stream bed) in both 2010 and 2011 (Figure 7.3). The thermal attenuation of the bed was greater in 2011 with an increased separation of curves at the temperature minima. Water column temperature and air temperature were cross-correlated with short lag times during 2010 (0.75 h) and 2011 (0.5 h). Streambed temperature was significantly cross-correlated with water column temperatures and lag times between water column and bed temperatures increased with depth at: 0.05m (2010 = 1.75h: 2011 = 2.5h), 0.20m (2010 = 3.5h: 2011 = 4.75h) and 0.40m (2010 = 9.25h: 2011 = 5.25h)

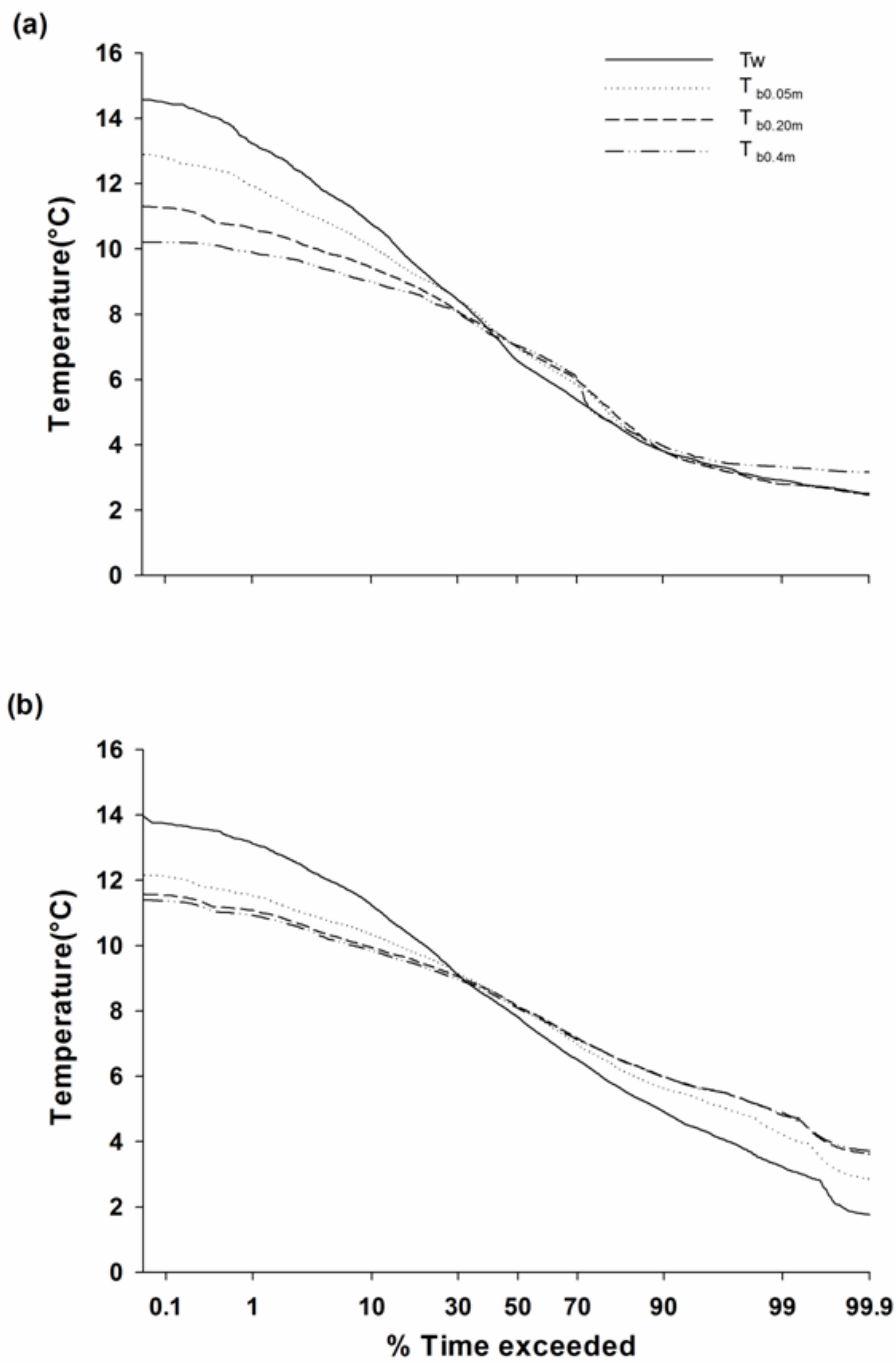


Figure 7.3. Temperature duration curves of the water column and stream bed temperatures for: (a) 2010; and (b) 2011.

Table 7.3. Summary statistics for water column and stream bed temperatures (°C) at AWS (lower site). Standard deviations are displayed in parentheses.

Variable	Mean		Range		Max		Min	
	2010	2011	2010	2011	2010	2011	2010	2011
T _w	7.0 (2.6)	7.8 (2.4)	12.4	12.6	14.6	14.3	2.3	1.7
T _{b0.05}	7.0 (2.3)	8.1 (1.8)	10.4	9.4	12.9	12.2	2.5	2.8
T _{b0.20}	6.9 (2.0)	8.1 (1.5)	8.8	8.0	11.3	11.6	2.5	3.6
T _{b0.40}	6.9 (1.9)	8.0 (1.5)	7.1	7.7	10.2	11.4	3.2	3.7

7.3.3. Heat budget

Seasonal heat budget. A large net gain in energy was recorded for the 2010 melt season (75 days = 1393 MJ m⁻²) and 2011 melt season (80 days = 1312 MJ m⁻²). The majority of this energy was exchanged at the air-water interface during both study periods and accounted for >96% of all heat gains. The channel bed was an energy sink during 2010 (-1.41 MJ m⁻²) and an energy source during 2011 (9.45 MJ m⁻²). Friction of the bed and banks by the water column created 30.77 MJ m⁻² and 54.77 MJ m⁻² in 2010 and 2011 respectively.

Table 7.4. Summary statistics for energy fluxes towards (heat gain) and away (heat loss) from the stream channel during summer 2010 and 2011 (SD = standard deviation).

Variable	Mean		SD		% of heat loss/gain	
	2010	2011	2010	2011	2010	2011
<i>Heat gain</i>						
Q^* (Net radiation)	14.78	12.90	7.67	7.21	78.4	77.8
K^* (Net SW)	17.42	17.35	8.41	7.16	-	-
Q_h (Sensible heat)	2.43	2.24	1.48	1.28	12.8	13.6
Q_e (Condensation)	1.16	0.49	1.14	0.66	6.1	2.9
Q_{bhf} (Bed heat flux)	0.06	0.15	0.12	0.31	0.3	1.6
Q_f (Friction)	0.44	0.68	0.21	0.31	2.3	4.1
<i>Heat loss</i>						
Q^* (Net radiation)	0.04	-	0.14	-	15.9	
L^* (Net LW)	3.89	4.42	1.79	1.84	-	-
Q_h (Sensible heat)	0.02	0.00	1.14	0.01	5.2	0.02
Q_e (Evaporation)	0.20	0.48	0.44	0.77	56.9	71.5
Q_{bhf} (Bed heat flux)	0.08	0.27	0.16	0.34	22.0	24.4
<i>Total energy</i>						
Q_n	15.84	15.71	6.51	5.51	-	-
Air-water interface	15.84	15.14	6.54	5.65	100	96.3
Water-streambed interface	-0.04	0.22	0.19	0.31	-	3.7

Flux partitioning of energy gains was similar during both study periods. Net radiation was the main energy source accounting for 78% of gains (Table 7.4). Sensible heat transfer was towards the stream channel and accounted for 13% and 14% of all energy gains during 2010 and 2011, respectively. However, condensation was lower in 2011 (3% of gains) than in 2010 (5% of gains) and represented a smaller heat source in 2010. Heat gained at the streambed – water column interface was minimal and the bed heat flux accounting for <2% of all gains during both years. Total heat loss was lower during the 2010 than 2011 melt season (Table 7.4). During 2010, evaporation, net radiation and the stream bed acted as the main energy sinks contributing 57%, 16% and 22% of losses respectively. The amount of energy lost to evaporation and at the streambed-water column interface was greater in 2011 and accounted for 64% and 36% of all energy lost. Sensible heat losses were negligible (<1%) during 2011 (Table 7.4).

Sub-seasonal patterns. In 2010, the latent heat flux acted as both a heat source and heat sink with a clear shift in flux direction apparent as the melt season progressed. Latent heat was predominantly an energy source until day 217 as condensation dominated. Thereafter, latent heat was a sink as evaporation prevailed (Figure 7.4). In 2011, the sub-seasonal shift in flux direction was not as pronounced as for 2010. The highest latent heat gains were on days 180 ($3.33 \text{ MJ m}^{-2}\text{d}^{-1}$) and 167 ($2.59 \text{ MJ m}^{-2}\text{d}^{-1}$) in 2010 and 2011 respectively (i.e. later in the season). The greatest latent heat losses were observed on days 244 ($-2.38 \text{ MJ m}^{-2}\text{d}^{-1}$) and 234 ($-2.53 \text{ MJ m}^{-2}\text{d}^{-1}$) in 2010 and 2011 respectively (i.e. later in the season). During 2010, latent heat contributed frequently >10% of the total daily gains during the early melt season (>40% on day 171). During 2011, the latent heat flux generally made up <10% of total daily heat

gain; however episodic events when the flux contribution >10%, occurred sporadically during the study period (Figure 7.5).

Daily total gains from net radiation declined across both melt seasons, with the highest clear day values in early summer close to the summer solstice on days 188 ($24.67 \text{ MJ m}^{-2}\text{d}^{-1}$) and 177 ($23.33 \text{ MJ m}^{-2}\text{d}^{-1}$) in 2010 and 2011, respectively. Net shortwave radiation acted as an energy source throughout the study period while net longwave radiation was a consistent energy sink (see Figure 7.3). The daily total net radiation flux was negative on two days during the study (calendar days 170 and 245 in 2010); however, these losses were relatively small ($-3.40 \text{ MJ m}^{-2}\text{d}^{-1}$ and $-0.84 \text{ MJ m}^{-2}\text{d}^{-1}$) when compared to average daily total gains. Days when net radiation was an energy sink were characterised by dense low lying cloud cover (i.e. low K_{\downarrow} during the day) and clear night skies (i.e. strong L_{\uparrow} losses). Generally, oscillations in the magnitude of net radiation were inversely related to cloud cover and daily total energy gains ranged between 0 and 94% but generally contributed >60% and rarely less than 50% (Figure 7.5).

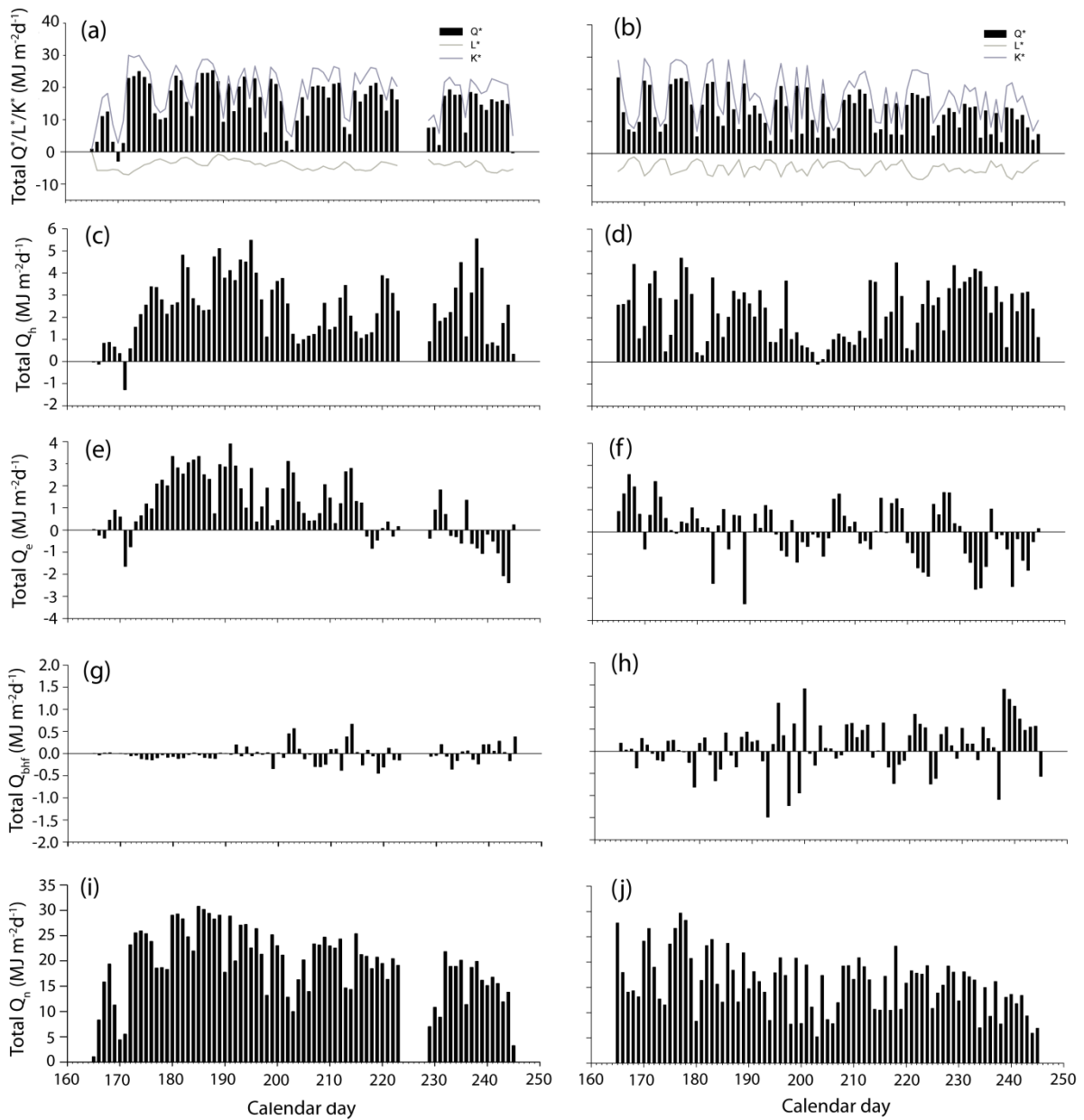


Figure 7.4. Daily total ($\text{MJ m}^{-2}\text{d}^{-1}$) net radiation, net shortwave radiation and net longwave radiation in (a) 2010 and (b) 2011, sensible heat in (c) 2010 and (d) 2011, latent heat in (e) 2010 and (f) 2011, bed heat flux in (g) 2010 and (h) 2011, and daily total energy available for the water column in (i) 2010 and (j) 2011.

The daily total sensible heat flux tracked changes in the temperature gradient between the atmosphere and water column. The flux was a heat source predominantly; however, on days 171 (2010) and 203 (2011) sensible heat was a sink, ($-1.27 \text{ MJ m}^{-2}\text{d}^{-1}$ and $-0.11 \text{ MJ m}^{-2}\text{d}^{-1}$, respectively). These two events coincided with the lowest mean daily temperature records of $1.3 \text{ }^{\circ}\text{C}$ (2010) and 5.8°C (2011). There appeared to be no distinct intra-seasonal dynamic to the sensible heat flux. The proportion of total daily heat gained from sensible heat ranged from 0% to 43%. However, it was generally less than 30% of the total daily energy gain. The highest proportional gains again occurred on days when radiation receipt was lowest (see figure 7.5). As with the latent heat flux, daily gains were proportionally greatest on days of decreased radiation receipt, ranging from <5%, on clear sky days, to 43% on the most overcast days (Figure 7.5).

The bed heat flux tracked changes in mean daily temperature gradients between the bed ($T_{b_{0.40m}}$) and stream. During 2010, the bed heat flux was lower consistently than in 2011 and a clear shift from sink to source was apparent as the melt season progresses (Figure 7.4). However, analysis at the daily time step masks diurnal patterns that illustrate a shift from sink during the day to source during the night. The exception to this is overcast days when the riverbed is a source during both day and night. Due to the small amounts of heat flux at the water column – riverbed interface, contributions are typically <5% to total daily energy gains (Figure 5).

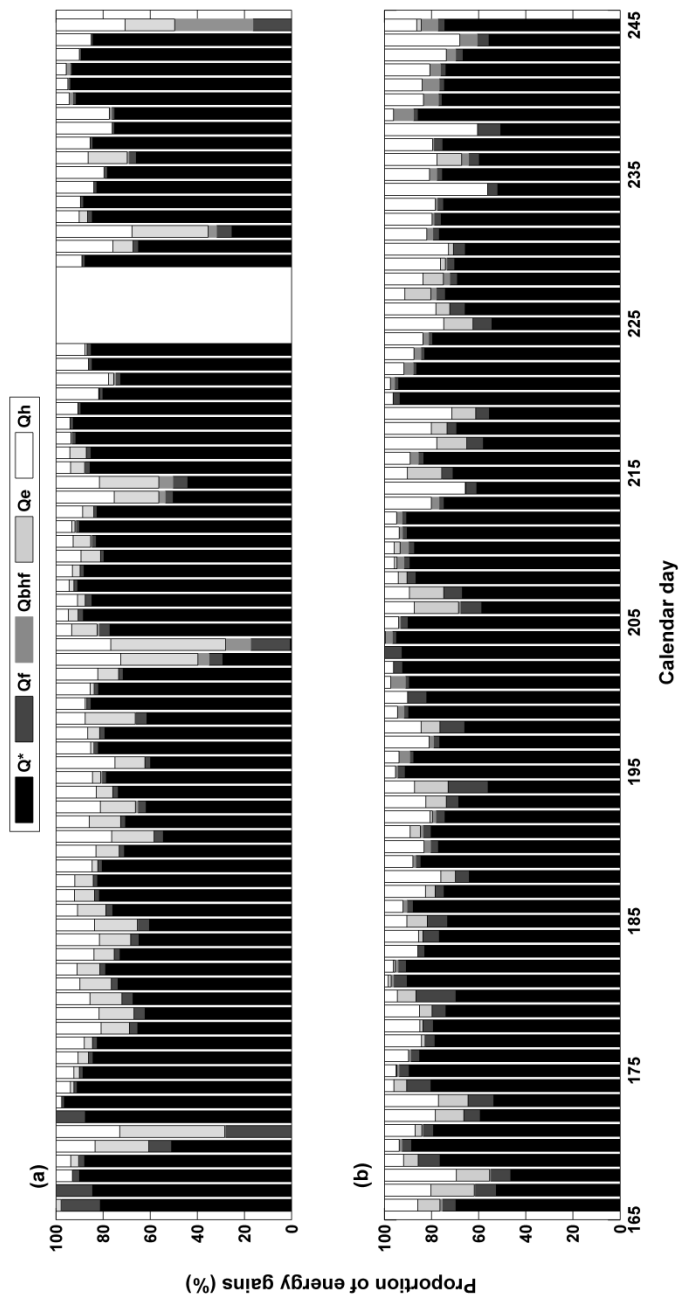


Figure 7.5. Proportion of all energy gains for: (a) the 2010 sampling period; and (b) the 2011 sampling period.

Heat gained from fluid friction rarely exceeded $1.0 \text{ MJ}^2\text{d}^{-1}$ and tracked discharge variability. The highest gains observed in each season ($0.87 \text{ MJ}^2\text{d}^{-1}$ in 2010, and $1.37 \text{ MJ}^2\text{d}^{-1}$ in 2011), were during the period high flows associated with peak snow melt (Figure 7.2). In 2011 gains were higher in the late melt season when a characteristic glacial hydrograph was apparent (Figure 7.2). The proportion that fluid friction contributed to total daily gains ranged from 28 % to 1%, but was generally $<5\%$ (Figure 7.5). The highest proportional gains did not track consistently the days of greatest fluid friction gains, but occurred on days with reduced net radiation receipt (i.e. overcast) and high intensity rain storms.

Energy gains to the water column were always greater than losses but total energy available to the water column declined after the summer solstice. The highest and lowest values for the 2010 season were on days 185 ($30.76 \text{ MJ}^2\text{d}^{-1}$) and 245 ($3.22 \text{ MJ}^2\text{d}^{-1}$), respectively, and for 2011 on days 177 ($29.68 \text{ MJ}^2\text{d}^{-1}$) and 203 ($5.22 \text{ MJ}^2\text{d}^{-1}$). Heat gains at the air water interface dominated the energy exchange process; and the highest (lowest) total energy corresponded to days with the least (most) cloud cover.

7.3.4. Water temperature model

The water temperature simulations, run at 15 minute time steps, provided reasonable predictions of daily mean (T_{mean}) and maximum temperatures (T_{max}). Table 7.5 shows the RMSE and MAE for the whole season, and two sub-seasonal periods; an early season, high flow period and a late season, lower flow period. Simulations across the whole melt season were more accurate, for both maximum and mean daily water temperatures, during 2011 and

RMSE was 0.58°C less for both T_{\max} and T_{mean} in 2011 (Table 7.5). Predictions of T_{\max} were better during the late melt season periods for both 2010 and 2011. T_{mean} predictions were not as accurate as T_{\max} and early season RMSE values were lower than late season during both study years (Table 7.5). Figure 7.6 presents a short (5 day) time series from the two sub-seasonal periods in 2010 and 2011. Nocturnal water temperatures were under-estimated systematically during both years, with differences most pronounced later in the season. In contrast, during early season 2010, systematic over-estimation of maximum daily water temperature occurred. Notably, these errors decreased as snowline altitude increased ($R^2 = 0.48$, $P < 0.001$). T_{mean} errors displayed a significant positive relationship with air temperature during 2010 ($R^2 = 0.4$, $P < 0.001$) and 2011 ($R^2 = 0.30$, $P < 0.001$). Weaker relationships with discharge was also apparent during 2010 ($R^2 = 0.19$, $P < 0.001$).

Table 7.5. Mean absolute error (MAE °C) and root mean square error (RMSE °C) calculated for the simulated stream water temperature.

Period	2010		2011	
	MAE	RMSE	MAE	RMSE
All melt season				
T_{\max}	4.08	2.02	1.98	1.44
T_{mean}	7.50	2.73	4.66	2.15
Days 175-200 <i>(early melt season)</i>				
T_{\max}	4.56	2.13	2.16	1.47
T_{mean}	4.44	2.11	2.49	1.58
Days 220-245 <i>(late melt season)</i>				
T_{\max}	2.56	1.60	1.87	1.31
T_{mean}	7.28	2.70	8.32	2.88

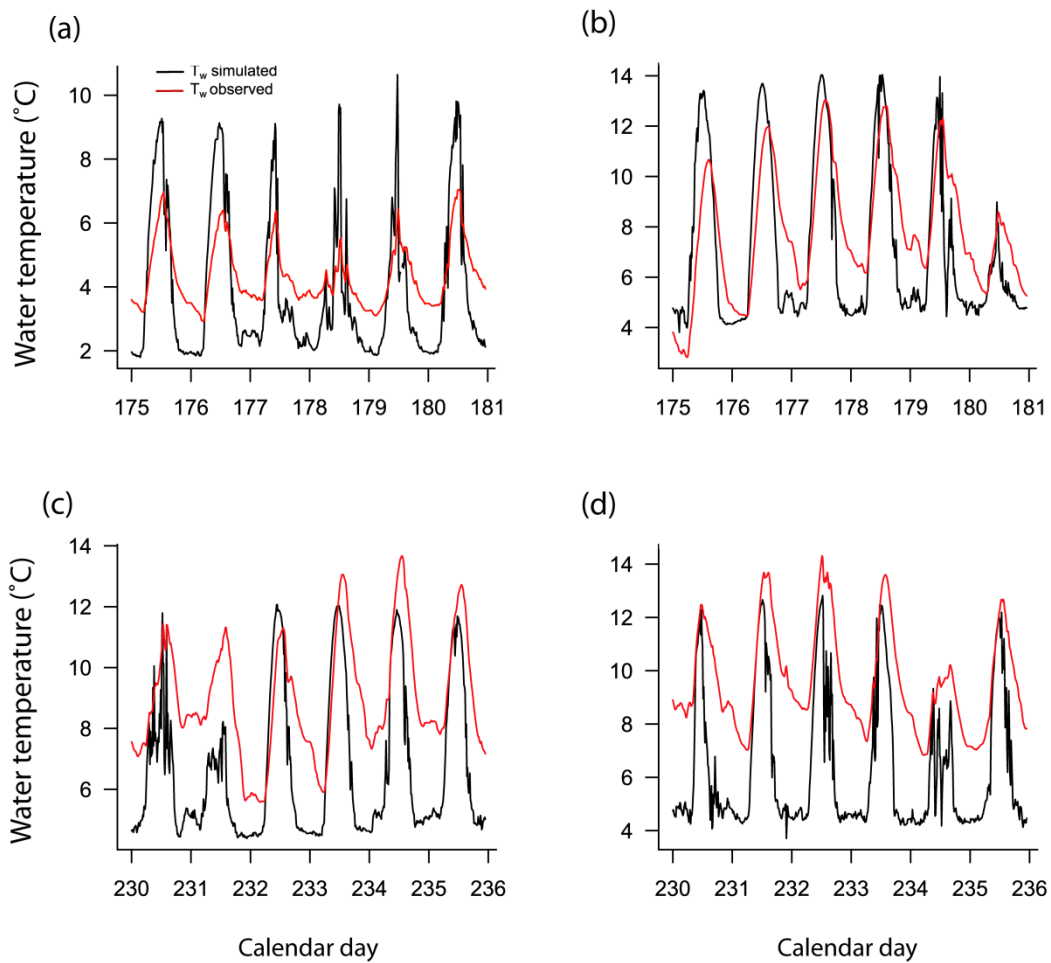


Figure 7.6. Modelled water temperature for selected five day periods during early melt season (a) 2010 and (b) 2011; and late melt season (c) 2010 and (d) 2011.

7.4. Discussion

7.4.1. Thermal dynamics

Seasonal mean water temperatures recorded at site the AWS, on the Taillon stream were similar to those reported previously by Brown & Hannah (2008). However, when compared to studies in other glacier-fed systems, the mean and range of water temperature was greater in the Taillon basin. Uehlinger *et al.* (2003) recorded a lower mean water temperature and range ($<4^{\circ}\text{C}$) during the summer melt season for a glacier-fed river in the Swiss Alps. Chikita *et al.* (2010) also recorded mean daily temperatures of $<4^{\circ}\text{C}$ for an Alaskan stream. These differences are likely due to the larger glaciers ($>10\text{km}^2$) in these other systems mentioned which yield summer discharges (range $\sim 2\text{-}46\text{ m}^3\text{ s}^{-1}$) an order of magnitude greater than those observed in the Taillon basin (range $\sim 0.01 - 0.5\text{ m}^3\text{ s}^{-1}$). This larger glacier flow volume of water has a greater thermal capacity (Poole & Berman 2001) that may explain the cooler, less variable thermal regimes observed in other rivers. This potential glacier scale difference is important when considering the predicted shrinking of the cryosphere (Barnett *et al.* 2005) and subsequent reduction in summer discharges (Jansson *et al.* 2003) as the current thermal patterns observed in the Taillon stream may be considered the future for rivers and streams fed by larger glaciers at present (Milner *et al.* 2009).

The streambed was thermally stable during both melt seasons and had lower (higher) maximum (minimum) temperatures when compared to the water column. However, the vertical gradient of seasonal mean channel bed temperature differed between years. In 2010 a negative gradient was apparent with cooler temperature at depth. Intra-seasonal variability was particularly pronounced in 2010, likely due to increased clear water inputs from the larger snowpack delaying the build up of glacial rock flour at the streambed-water column

interface as observed by Cadbury *et al.*(2008). Nowinski *et al.* (2011) found deposition of fine sediments can alter hydraulic conductivity at a range of temporal scales. Bed temperature differences have been attributed to surface-groundwater interactions and bed substrate properties (Malard *et al.* 2001; Cadbury *et al.* 2008). In the case of the Taillon stream, bed sediments are relatively coarse ($D_{50} = 0.10$ m); and high rates of suspended sediment transport and deposition were documented during both field seasons. The transient nature of the bed, due to infilling of interstitial spaces, along with the large clast sizes has implications for modelling heat fluxes as these both act as heat stores conducting heat to and from the water column at different rates (Westhoff *et al.* 2010).

At the daily time step a number of driver of stream water temperature variability were identified. Prevailing metrological conditions (radiation receipt, air temperature, wind speed and moisture content of the atmosphere) and total stream discharge were directly linked to water temperature (Brown *et al.* 2006a; Cadbury *et al.* 2008). Snow cover (or distance from meltwater source) was also a significant driver as it decreased exposure time of the stream to the atmosphere and increased the thermal capacity of stream water through the generation of cold water runoff (Smith 1975; Brown & Hannah 2008; Cadbury *et al.* 2008). The weaker relationship observed between air temperature and water temperature during 2010 can be attributed to the lower snowline altitude for much of the early season, when radiation receipt is highest, that reduced atmospheric exposure.

7.4.2. Heat exchange processes

In this study the heat budget was dominated by net radiation during both melt seasons which contributed >75% of all energy gains. Similar findings have been reported from open river

channels (Webb & Zhang 1997; Evans *et al.* 1998; Moore *et al.* 2005; Hebert *et al.* 2011) with net radiation contributing >70% of the total heat gain. This is due to high solar radiation receipt, which is primarily a function of cloud cover, riparian cover and topographic shading (Rutherford *et al.* 1997; Isaak & Hubert 2001). With regards to this study, as the site is above the treeline, free from extensive topographic and riparian shading, shortwave radiation gains greatly exceeded longwave radiation emissions. Hannah *et al.* (2004) found that net radiation acted as an energy sink during autumn and winter for a moorland stream in the Scottish Cairngorms. However, due to constraints of access the period of potential autumnal water cooling could not be observed. It is important to note the sub-seasonal variability in net radiation gains but, even under cloudy conditions, daily net radiation gains made ~50% of the total daily heat gain.

Although the evaporative flux was the major source of heat loss (>57%), seasonal losses were exceeded by gains through condensation; hence, the latent heat flux was positive during both field seasons. This is in contrast to other studies when latent heat losses have exceeded gains (Evans *et al.* 1998; Caissie *et al.* 2007; Hannah *et al.* 2008; Hebert *et al.* 2011); however, these studies have been in lower altitude river environments. Interestingly, Webb & Zhang (1997) found condensation gains important in a regulated river reach, directly below the dam, where reservoir releases cooled water temperature. Chikita *et al.* (2010) reported similar results from a glacier-fed stream in Alaska where the latent heat flux was predominantly a heat source and made up ~6% of all energy gained. The sub-seasonal shift of the latent heat flux observed in the Taillon appears to be due to changes in meltwater production and distance from the snowpack. Steep gradients in temperature and humidity during the early summer were maintained by cold melt waters from the snowpack and glacier. The other turbulent heat flux, sensible heat, displayed no sub-seasonal pattern being a consistent

important energy source during both melt seasons. Values were similar to those reported by other authors (Caissie *et al.* 2007; Hebert *et al.* 2011); however, due to the relatively cold water temperature during the summer months temperature gradients between air and water were negative and no oscillation in the flux direction occurred. Proportionally greater gains (24%) were reported by Chikita *et al.* (2010) for the sensible heat flux; but in this study, air-water temperature gradients were greater due to: (i) large amounts of glacier runoff cooling the stream during the warmest summer months; and (ii) warmer air temperature due to the lower latitude.

Heat exchanges at the channel bed- water column interface may be an important component of the energy balance (Webb & Zhang 1999) both as energy sink (Evans *et al.* 1998; Hebert *et al.* 2011) and source (Hannah *et al.* 2004). In this study, heat gains at the channel bed – water column were very small and may be considered insignificant (<1%). During both study periods, the bed heat flux represented an important heat loss (>22%), although the magnitude of loss was small. Fluid friction made a contribution to the energy balance during both years. This was due to the turbulent nature of the stream flow and relatively steep slope; but the flux contribution was notably lower than that observed by both Chikita *et al.* (2010), 38%, and Hannah *et al.* (2004), 24%. This may be due to the relatively incised channel at this study reach. Inter-annual differences in fluid friction may be linked attributed to differences in the flow regime (i.e. snowmelt dominated in 2010 and pluvial/glacier melt dominated in 2011). The more rapid retreat of the transient snowline in 2011 led to the earlier exposure of glacier ice and an efficient drainage network for routing melt waters from the glacier developed by the late melt season (Hannah *et al.* 1999). Hence, higher flows and higher fluid friction energy gains were recorded in 2011.

7.4.3. Modelled water temperature

Reasonable estimates of maximum daily temperature were recorded across both seasons, but in early summer water temperature was consistently overestimated. This was primarily due to increased snowmelt contributions (Smith 1975) and higher stream discharge (Cassie *et al.* 2007), which increased the thermal capacity of the water column (Poole & Berman 2001). Also as the modelling approach was point based (one dimensional), energy advected from upstream was not properly represented (Carrivick *et al.* 2012). Maximum daily temperature predictions for early 2010 were not as accurate for 2011 and were over-estimated systematically. This was a result of the lower snowline altitude during that period which decreased exposure time and increased thermal capacity. The model did not predict mean daily water temperatures as accurately, and during both seasons performance in late melt season was markedly lower than during early summer. A number of processes may have caused the consistent under estimation of nocturnal water temperature. The first is that lateral exchange of surface water between the riparian zone and main channel was not properly quantified and factored into the heat budget (Moore *et al.* 2005). In late afternoon and evening this exchange of water can potentially flux heat into the system (Poole & Berman 2001), thus reducing the rate of change in the total energy flux. Magnusson *et al.* (2012) identified a similar pattern and suggested that infiltration of surface water into the riparian zone, where additional heat is absorbed, then subsequently returned to the main channel accounted for the nocturnal heat exchange increase. Furthermore, negligible differences in discharge between the glacier snout and the AWS gauging station have been recorded (Smith *et al.* 2001), suggesting groundwater surface-water interaction is unlikely, unless gains and losses were balanced, making riparian infiltration-exfiltration a plausible warming mechanism. Second, due to the heterogeneous nature of the river bed sediment size, water-rock clast interactions may not have been properly represented by a single bed heat flux

measurement (Mieier *et al.* 2003). During lower flow periods in the late melt season, when modelled nocturnal temperatures were the least accurate, boulders and large substrate become exposed, above the water column and would equilibrate with the atmosphere and conduct more heat than those submerged (Westhoff *et al.* 2010). Third, diurnal expansion-contraction of the stream network may have caused the main channel to connect-disconnect with slower flowing side channels/ephemeral channels causing the advection of warmer water into the main, glacier-fed channel (Uehlinger *et al.* 2003; Carrivick *et al.* 2012).

7.5. Conclusions

As cryosphere shrinkage is expected to continue, reduced summer discharge and increased stream exposure will result in greater sensitivity of glacier fed streams to climatic change/variability (Vliet *et al.* 2011). This will have significant implications for a range of hydrological and ecological processes and patterns (Webb *et al.* 2008; Woodward *et al.* 2010c). Hence, a detailed understanding of the fundamental controls on stream temperature across a range of environments is urgently required to provide a robust basis for further development of process based models and mitigation scenarios (Garner *et al.* 2012).

This study provides insights into the heat exchange processes operating in an alpine, glacier fed stream using detailed hydro-meteorological records for two summers. The latent heat flux was identified as an important heat source, particularly during the early melt season, when the melting snowpack created steep temperature and humidity gradients between the water and air. However, latent heat also displayed the greatest variability between years, linked to differing snow line altitude and prevailing meteorological conditions. Heat exchanged

between the water column and stream bed was small and suggests that this interface is of reduced importance for warming and cooling the water column. This is in contrast to findings from other stream systems (Evans & Petts 1998, Hannah *et al.* 2008) and is most likely due to the unconsolidated stream bed.

Interestingly the amount of meltwater and distance from source (snowpack) were direct drivers of both stream water temperature and non-radiative surface heat exchange. The systematic over estimation of modelled water temperature during periods of high snow melt, and the weaker relationships with air temperature highlight the important role of water source (i.e. snowpack/glacier ice) and distance from that source for controlling stream temperature. Further development of process based modelling is required to enable accurate prediction of thermal regime responses to climate change in glacier fed streams.

7.6. Chapter summary

In this chapter the point scale energy balance of a glacier-fed stream reach has been quantified, representing the first inter-annual study of the heat exchange processes operating in an alpine stream. In addition to the major heat fluxes (i.e. net radiation and sensible heat), subseasonal changes in watersource dynamics and diurnal contraction/expansion cycles of the channel network are suggested as important processes for warming/cooling the water column. These findings have important implications for the further development of deterministic models in alpine river systems. Future cryospheric, hydrological (inc. water temperature) and ecological change are modelled in Chapter 8 using the climate cascade predictive framework (see Chapter 1, Figure 1.2).

CHAPTER 8

*A future scenario of hydrology, habitat
and biotic patterns for an alpine
glacierized catchment.*

8.1. Introduction

As climate projections suggest a continued warming trend across high altitude and latitude environments (IPCC 2007) many alpine glaciers are expected to disappear, or be significantly reduced, over the next 50 years (Zemp *et al.* 2006). Glacier shrinkage is not only important at the local scale (i.e. headwater alpine river basins), but also at regional/national scales (i.e. macro basin >100,000km²). For example, as little as 1% ice cover can account for 25% of August runoff in downstream lowlands (Huss 2011). Hence, studies have generally focused on predicting river flow patterns in the context of water resources (López-Moreno *et al.* 2008; Bo *et al.* 2010; Viviroli *et al.* 2011; Fatichi *et al.* 2013), with a bias towards anthropogenically altered catchments (e.g. hydro-power schemes).

Alpine aquatic environments are particularly sensitive to climatic change due to the strong linkages between atmospheric forcing, cryospheric processes (i.e. storage and melt cycles) and stream hydrology (Hannah *et al.* 2007). Complex interaction and feedbacks occur between the links of this process chain and operate over a range of time scales from sub-daily to decadal (Jansson *et al.* 2003; Hock *et al.* 2005). For example, long term climate dynamics control glacier storage volume and retention capacity (Hock *et al.* 2005), with increased melt volume expected initially as the climate warms and glaciers recede (Milner *et al.* 2009). However, a reduction in cryospheric mass will lead ultimately to decreased meltwater production and lower stream discharge for glacier fed catchments (Barnett *et al.* 2005). This poses a significant threat to biodiversity as these systems are biological repositories of regional importance (Brown *et al.* 2007a; Jacobsen *et al.* 2012) due to the combination of unique genetic material, taxa and assemblages (Brown *et al.* 2009a; Finn *et al.* 2013).

In Europe, our understanding of alpine catchment hydrology and the potential impacts of future climate change on mountain hydrology is based predominately on research focused on the Alps (Viviroli *et al.* 2011). The limited number of catchment scale hydrological studies which have been carried out in the Pyrénées, have been limited to southern and eastern river basins (Anderton *et al.* 2002; Gallart *et al.* 2002; Lana-Renault *et al.* 2007). These studies have focused mainly on: (i) cryospheric processes, particularly transient snowpack dynamics (Anderton *et al.* 2004; López-Moreno *et al.* 2013); and (ii) catchment model development (e.g. Anderton *et al.* 2002). As yet, in alpine river systems, no modelling studies have used physically based catchment models to link climate driven change and aquatic physicochemical habitat/benthic ecology. However, a recent study from the Waterton-Glacier International Peace Park, N. America, highlighted the potential utility of statistical modelling for predicting the distribution of alpine taxa under climate change scenarios (Muhlfeld *et al.* 2011). Here, the future distribution of an endemic stonefly (*Lednia tumana*) was predicted using maximum entropy modelling and a future scenario of glacier loss.

The ability to project how climatic and hydrological changes will alter benthic habitats and taxa abundances and distributions is important for directing appropriate conservation measures for these threatened ecosystems (Hannah *et al.* 2007). The climate driven process cascade for alpine river ecosystems presented by Hannah *et al.* (2007), and outlined in Figure 1.1, Chapter 1, provides a useful framework for developing modelling strategies specific to alpine river ecosystems. This conceptual model highlights the interconnected nature of climatic, cryospheric and hydrological processes, which in turn control habitat and biotic community characteristics. Figure 8.1 presents a methodological approach for assessment of

hydroecological responses in alpine river catchments based on the climate cascade of Hannah *et al.* (2007). For this approach climate projections can be used to drive simulations of catchment hydrology (i.e. process-based models) or statistical models; the outputs of which provide either: (i) the hydrology/physicochemical habitat variables for predicting biotic responses (e.g. water temperature) or (ii) variables which can be used as a surrogate or proxy for a suite of habitat characteristics (i.e. the habitat template related to glacial runoff (Brown *et al.* 2010b)). However, this approach has yet to be tested for projecting biotic responses in alpine headwater catchments.

The Pyrenean mountain chain is of particular interest from a conservation perspective due to the high levels of micro-endemism within the benthic fauna (Vincon & Ravizza 2001; Brown *et al.* 2009a). Also, due to its southerly location (limit of valley glaciation) and small remnant glaciers, patterns and processes may represent an analogue of future change for the Alps. Hence, the Pyrénées represents an ideal location to test the research framework outlined above.

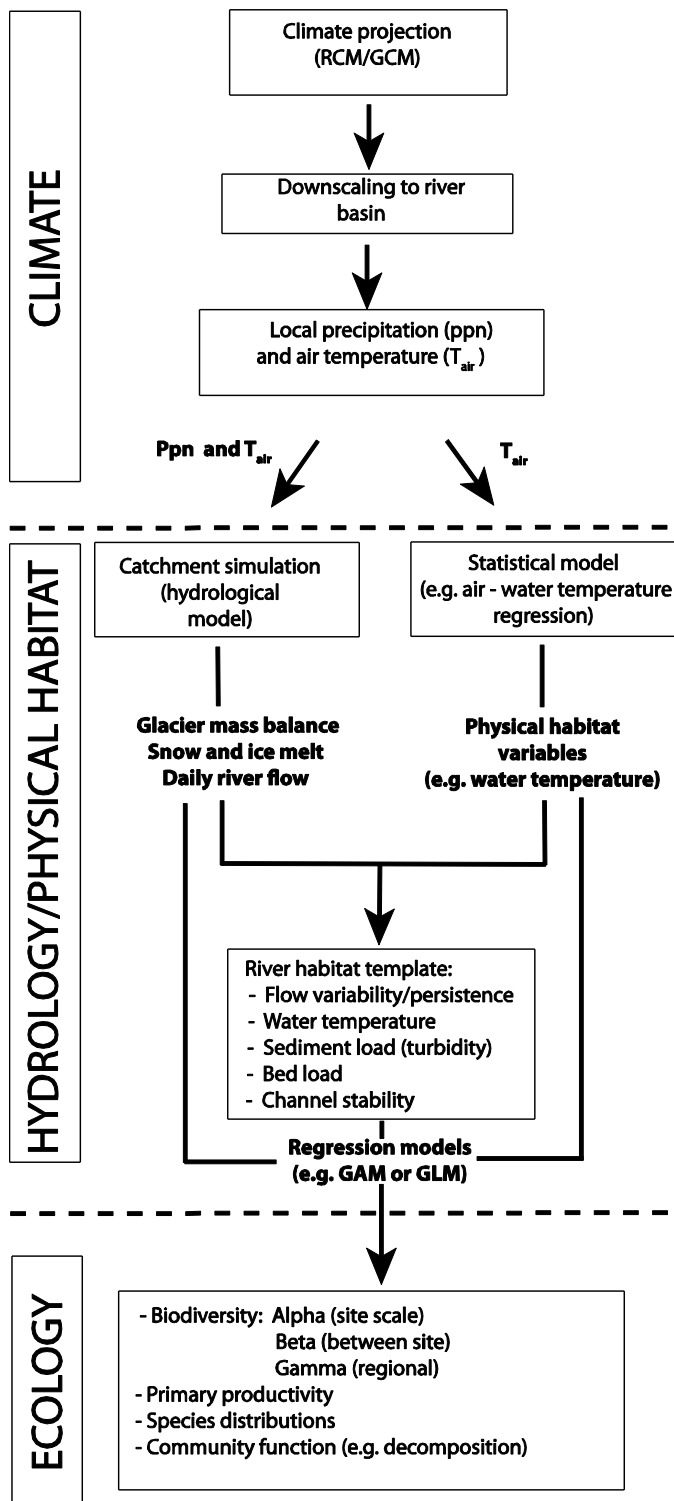


Figure 8.1. Flow diagram displaying scenario modelling framework. Linkages between climate scenarios, simulation/statistical models, and hydrological/habitat/biota output variables.

Given the research gaps outlined above, the aim of this chapter is to identify the hydroecological responses of an alpine glacierized river basin to a future climate scenario (2080 horizon). By employing the research framework outlined in Figure 8.1, a number of objectives are addressed:

- 1) To simulate the impact of projected climate change on cryospheric and hydrological processes, specifically the annual flow regime and changes in meltwater production and timing;
- 2) To model the potential changes in stream water temperature (a master water quality and habitat variable) for sites with contrasting water source dynamics;
- 3) To predict the potential implications of cryospheric change for benthic biodiversity, using Generalized Additive Models (GAMs), and thus provide a first approximation of abundance changes for key taxa.

8.2. Methods

To assess the impact of projected climate change on alpine river ecosystems, the research framework highlighted in Figure 8.1 was adopted. A downscaled climate scenario (RCM:REMO) for the 2080 horizon was used to drive a dynamic catchment hydrological model (TOPKAPI; Ciarapica and Todini, 2002) and a statistical model (air temperature-water temperature regression). A range of hydrological and cryospheric variables (e.g. glacier cover, meltwater production) were derived from the hydrological model (TOPKAPI). Aquatic benthic invertebrate occurrence was then projected based on TOPKAPI outputs. More specific methods and analytical techniques are presented herein.

8.2.1. Field site

The Taillon-Gabiétous catchment is located in the Cirque de Gavarnie, French Pyrénées (43°6'N, 0°10'W). The basin spans an altitudinal range from 1750 m at the lowest gauging station (T3) to 3144 m at the Pic du Taillon (Figure 8.2) and drains an area of 8.8km², of which roughly 3% is covered by glacier ice. On north facing slopes, the permanent snowline is located >2700m (Hannah *et al*, 2000). Two small cirque glaciers are also located on north facing slopes, the Glacier du Taillon (0.09 km²) and the Glacier des Gabiétous (0.07 km²), which feed the Taillon stream and Tourettes stream respectively. The relief is dominated by steep slopes (30-70°) and the underlying geology is composed of sandstone (Marbore sandstone) and limestones (Santonien and Coniacien series). Vegetation was sparse above 2200m and the lower basin (<2100m) was grazed alpine meadow with no canopy cover. Mean daily minimum and maximum air temperatures recorded between 1991 and 2011 at the nearby Gavarnie meteorological station (1390m), were 2.6°C and 12.7°C respectively and mean annual precipitation was 1466mm (Météo France 2011).

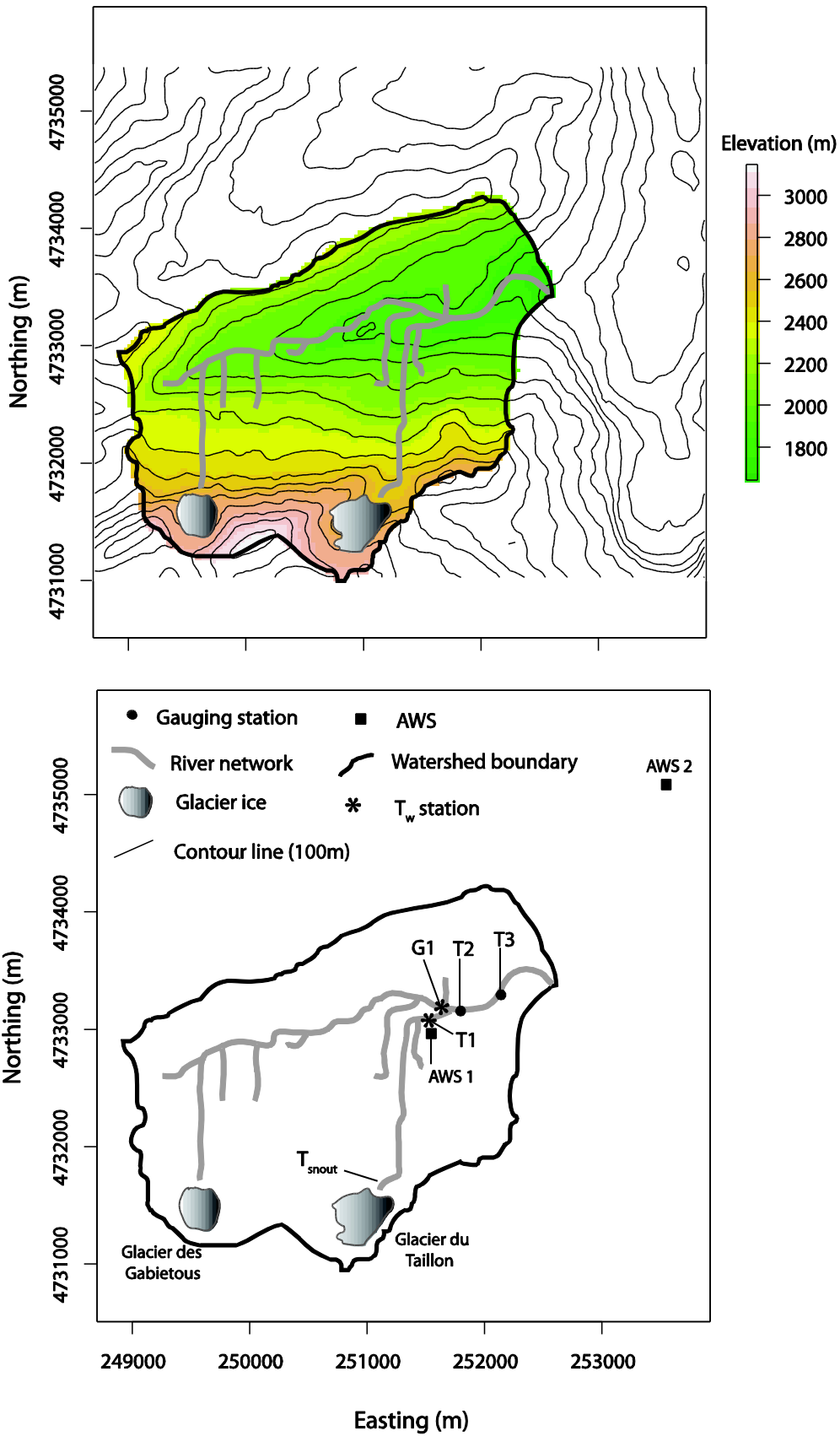


Figure 8.2. Topographic map of the Taillon– Gabiétous study basin with glaciers and extracted river network (top). Location of gauging stations, river temperature stations and automatic weather station (AWS) 1 and AWS 2 (bottom).

8.2.2. Hydro-meteorological variables

Météo France maintains a weather station in Gavarnie approximately 2.5km (~500m decrease in elevation) from the study basin (Figure 8.2: AWS 1). Records of daily total precipitation and daily maximum/minimum air temperatures are available from 1991 to present. The study basin has been instrumented during summer months by a number of research teams from the University of Birmingham (Smith *et al.* 2001; Brown *et al.* 2005). These data were combined with records of air temperature (T_a) and precipitation (ppn) recorded during the melt seasons of 2010/2011 (Figure 8.1: AWS 2) and used to create transfer functions to calibrate data from AWS 1 to the study basin. Data collected between 01/07/2002-01/09/2002, 01/07/2003-01/09/2003, 12/06/2010 – 09/09/10 and 12/06/2011 – 01/09/11 were used for this procedure.

Due to a paucity of discharge records for sites above the treeline in the French Pyrénées, data for calibration and validation of TOPKAPI were limited to flow records collected during this study (2010/2011) and Brown *et al.* (2006) (see Table 8.1). Discharge was recorded at high resolution (15 min), using a Druck pressure transducer and Campbell CR1000 datalogger at site T2 and a Trafag DL/N 70 level logger at T3 (see Chapter 3). Rating curves were created for each site and season (see Appendix 3.1).

Due to the high spatial variability of precipitation in mountainous environments (Viviroli *et al.* 2011) and the significant errors associated with recording snowfall (Savina *et al.* 2012), records were corrected prior to use in the model calibration process. Rainfall was adjusted for wetting loss and evaporation based on methods outlined by Rubel & Hantel (1999). A snowfall correction factor (S_{corr}) was applied based on the gauge type (Rubel & Hantel 1999). S_{corr} was then treated as a calibration parameter and varied by $\pm 10\%$.

8.2.3. Regional climate model

Outputs from the Regional Climate Model (RCM), REMO (Jacob & Podzun 1997), were used in this study. Briefly, REMO is a three dimensional hydrostatic circulation model, based on the numerical weather prediction model (Europa-Model), using a regular longitude–latitude grid in the horizontal and a hybrid vertical coordinate system (Kotlarski *et al.* 2010). Simulations were carried out as part of the EU-FP6 ENSEMBLES project at 25km resolution, using the global ECHAM5 A1B scenario for driving boundary conditions (van der Linden and Mitchell 2009). Data were available from 1961-2080; however, due to limited hydro-meteorological reference data for the study basin, analysis was conducted on the 1991 – 2080 period. Mean daily total precipitation and mean daily air temperature were calculated from the grid cell containing the basin and the surrounding eight grid cells ($n = 9$) to avoid any bias associated with using individual grid cells (Maraun *et al.* 2010).

8.2.4. Bias correction

Although outputs from RCM's are more precise than GCM's, both mean temperature and precipitation are biased when compared to observed data (Chen *et al.* 2011a). Therefore, a change factor method (also termed delta-change approach) was used to adjust the observed temperature and precipitation time series (Akhtar *et al.* 2008; Maraun *et al.* 2010; Chen *et al.* 2011a). RCM data were separated into 20 year periods and then centred around the years 2030, 2050 and 2070. A control period (T_{mref}) 1991 – 2010 was also created to match the observed data set for AWS 1. The change factor method involves modifying the observed historical time series (in this case 1991 -2010), by adding the difference between the future and reference periods as modelled by the RCM.

For mean daily temperature the difference in monthly T_a between the future period i and the modelled reference period ($Tm_{futurei} - Tm_{ref}$), is added to the observed daily time series (Td_{obs}):

$$Td_{futurei} = Td_{obs} + (Tm_{futurei} - Tm_{ref}) \quad (8.1)$$

The daily total precipitation for the future period i ($Pd_{futurei}$) was calculated by multiplying the observed time series Pd_{obs} by the precipitation ratio of reference to future as follows:

$$Pd_{futurei} = Pd_{obs} \times \frac{Pm_{futurei}}{Pm_{ref}} \quad (8.2)$$

8.2.5. Hydrological model

The TOPographic Kinematic APproximation and Integration model (TOPKAPI) is a physically based, distributed rainfall runoff model which employs the kinematic wave approach to simulate channel flow, overland flow and subsurface flow (Ciarapica & Todini 2002). Input information for the model is in raster format and information about topography, land use, soil characteristics, groundwater aquifer depths and glacier size/thickness was obtained from digital elevation models, aerial imagery, land use maps and soil maps (Liu *et al.* 2005). The TOPKAPI model has been adapted recently to improve performance in mountainous river basins (see Ragetti and Pellicciotti (2012) for a detailed description of the melt process representation in TOPKAPI).

Briefly, the main adaptations are: (i) an enhanced temperature index model, based on the work of Pellicciotti *et al.* (2005), for modelling snow and ice melt generation and runoff:

$$M = \begin{cases} TF T + SRF(1 - \alpha)I & T > T_T \\ 0 & T \leq T_T \end{cases} \quad (8.3)$$

where M is the melt rate, α is albedo, I is the incoming shortwave radiation (Wm^2) and T is the air temperature ($^{\circ}\text{C}$). TF (temperature factor) and SRF (shortwave radiation factor) are empirical constants and T_T is the threshold air temperature for melt onset. (ii) the Snow albedo algorithm outlined by Brock *et al.* (2000)

$$\alpha_{snowi} = \alpha_1 - \alpha_2 \log_{10} T_{acci} \quad (8.4)$$

Here α_{snowi} is the albedo of grid cell i on the current day, α_1 and α_2 are empirical constants and T_{acci} cumulated daily positive air temperature; and (iii) a linear reservoir approach to model glacier melt outlined by Hannah and Gurnell (2001).

Table 8.1. Data sets used for calibration and validation of TOPKAPI and the logistic water temperature regression model.

Variable	Site	Date	Data use
Discharge	T3	16/06/10 - 12/06/11	TOPKAPI calibration
	T2	20/06/11 – 09/09/11	TOPKAPI validation
	T2	25/06/03 - 01/09/03	TOPKAPI validation
	T3	27/06/03 - 01/09/03	TOPKAPI validation
Stream water temperature	T1 & G1	02/09/11 - 20/09/12	T _w regression calibration
	T1 & G1	05/09/02 - 01/09/03	T _w regression validation

8.2.6. Logistic air-water temperature regression model

Water temperature is an important physicochemical habitat variable (Webb *et al.* 2008) which controls a range of biological processes; ranging from individual growth rates and fecundity to ecosystem processes such as respiration. Thus, future water temperature projection is key to improving our understanding of how alpine benthic communities will respond to climate change. For sites T1 (Taillon glacier-fed channel) and G1 (Tourettes predominantly groundwater-fed) year round water and air temperature records were available (see Table 8.1). Although these sites are close in space (~200 m), they display markedly different ecological and hydrological characteristics with flows ceasing and the streambed freezing at T1; whereas, at G1 flows are permanent and the streambed remains >0°C (Brown *et al.* 2006b). For both sites, air temperature- water temperature relationships were explained by the S-shaped function outlined by Mohseni *et al.* (1998):

$$T_s = \mu + \frac{\alpha - \mu}{1 + e^{\gamma(\beta - T_a)^2}} \quad (8.5)$$

Where T_s is the simulated water temperature, T_a is the observed air temperature, μ is the minimum water temperature, α is the maximum stream water temperature γ is the steepest slope of the function and β the air temperature at the point of inflection (see Figure 8.3 for the relationship at G1).

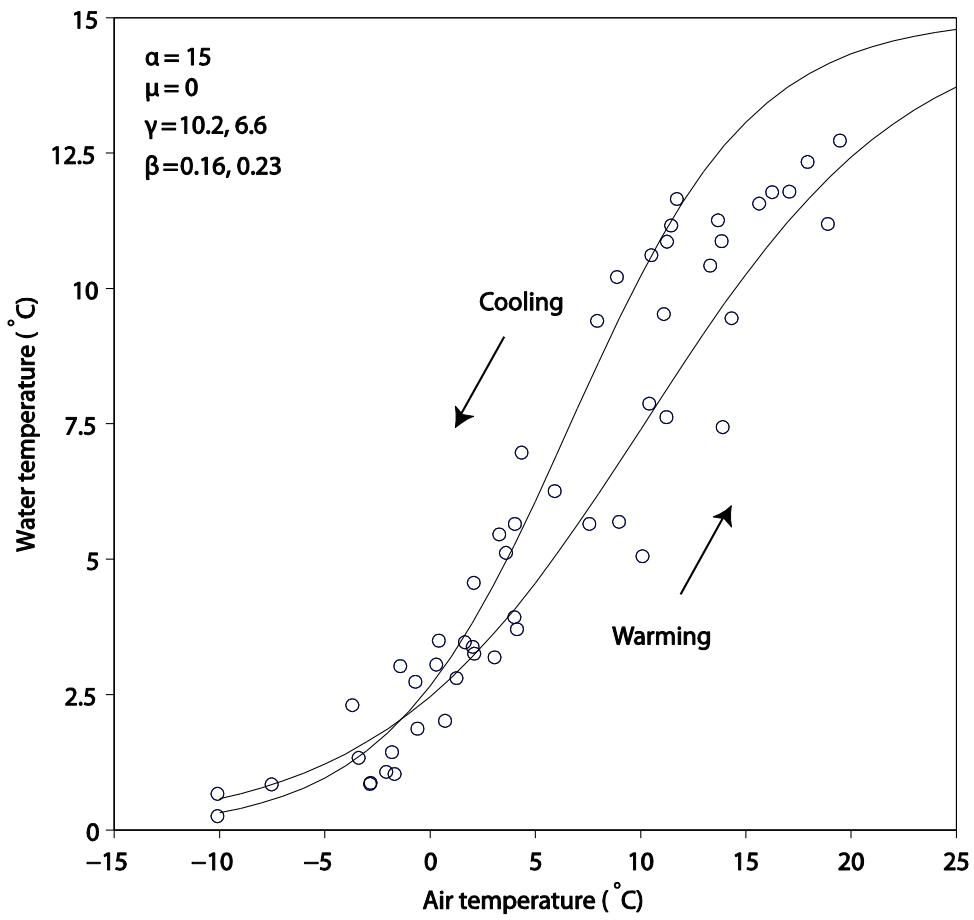


Figure 8.3. Relationship between weekly mean air temperature and water temperature at Site T1. Lines represent logistic functions fitted to data for warming and cooling period to account for hysteresis.

8.2.7. Calibration and validation of models

A suite of model efficiency statistics, following Moriasi *et al.* (2007), was employed to evaluate the performance of simulation runs and optimize the parameter set. The Nash-Sutcliffe coefficient (NS) was calculated as follows:

$$NS = 1 - \frac{\sum_{i=1}^n (Y_i^{obs} - Y_i^{sim})^2}{\sum_{i=1}^n (Y_i^{obs} - Y^{mean})^2} \quad (8.6)$$

Where Y^{obs} and Y^{sim} are the measured and simulated records respectively for n data records. NS values range between -1 and 1 with negative values indicating a model which is a worse predictor than the mean. Model runs with $NS > 0.50$, $PBIAS \pm 25\%$ and $RSR < 0.7$ were considered to represent satisfactory simulations (Moriasi *et al.* 2007)

Percent bias (PBIAS) was calculated as follows

$$PBIAS = \frac{\sum_{i=1}^n (Y_i^{obs} - Y_i^{sim})}{\sum_{i=1}^n (Y_i^{obs})} \quad (8.7)$$

And the root mean square error to observation Stdev ratio (RSR)

$$RSR = \frac{RMSE}{STDEV_{obs}} = \frac{\sqrt{\sum_{i=1}^n (Y_i^{obs} - Y_i^{sim})^2}}{\sqrt{\sum_{i=1}^n (Y_i^{obs} - Y^{mean})^2}} \quad (8.8)$$

TOPKAPI has been tested rigorously in glacierized catchments and parameter sensitivity analysis has been carried out for basins in both Europe (Finger *et al.* 2011) and South

America (Ragetti & Pellicciotti 2012). Hence, the initial range of parameter values was taken from Finger *et al.* (2011); but after 1000 model permutations the range was narrowed considerably. Parameters were then set with smaller increments ($\pm 10\%$) and a further 1000 runs were conducted to identify the final parameter set.

8.2.8. Ecological implications

Following Gibson *et al.* (2005) current and future flow regimes were assessed using the Indicators of Hydrologic Alteration (IHA) (Richter *et al.* 1996). Duration of flow minima and maxima were calculated for the control and the 2061-2080 period. One-way Analysis of Variance (ANOVA) was then used to test for differences between the control and the 2061-2080 period for 1-, 3-, 7-, 30-, and 90-day flow minima and maxima.

As TOPKAPI does not provide residence times for soil water stores, it was not possible to separate robustly slower routed deeper soilwater/groundwater from runoff rapidly routed as overland or near-subsurface flow. Hence, it was not possible to use the water source quantification approach, see Brown (2007), to predict ecological change in response to climate driven changes to cryospheric/hydrological processes. Instead, basin area was calculated for each site from an ASTER DEM (30m resolution), then using current glacier survey data (Association Moraine Pyrénéenne de Glaciologie 2009) and TOPKAPI glacier mass balance outputs, contemporary and future glacier cover in the catchment (GCC) was calculated. This approach, using GCC as the predictor variable, has been used to successfully predict both species diversity and taxa abundances (Rott *et al.* 2006; Füreder 2007; Jacobsen *et al.* 2012).

First, contemporary relationships between the abundance of individual taxa and GCC were developed using abundance data collected over 2 summer melt seasons (see Chapter 1 for sample dates). GLMs with a Poisson distribution corrected for over dispersion were used to

model the relationship between transformed abundance data, $\log_{10}(x+1)$, and GCC. For taxa with significant relationships, regression coefficients were used to identify winners (taxa with negative relationships) and losers (taxa with positive relationships) under the projected scenario of glacier retreat.

To enable a better understanding of the potential changes to biotic communities five taxa representing the key functional strategies displayed in glacial streams (see Chapter 5; Ilg & Castella 2006) were selected for further analysis. (i) *Perla grandis* (Plecoptera: Perlidae), an abundant large bodied predator, (ii) *Rhithrogena* spp. (Ephemeroptera: Heptageniidae), an abundant scraper/collector, (iii) *Leuctra inermis* gr. (Plecoptera: Leuctidae), an abundant shredder, (iv) *Simulium* spp. (Diptera: Simuliidae) an abundant filter feeder, and (v) *Diamesia latitarsis* gr. (Chironomidae: Diptera), a cold stenotherm. For *P. grandis*, *Rhithrogena* spp. and *L. inermis* gr. Generalized Additive Models (GAMs) with a Poisson distribution (corrected for overdispersion) were fitted in R.2.14.1 using the *mgcv* package (Wood 2008). The predictor variable was GCC and the response variable $\log_{10}(\text{abun} + 1)$. For *D. latitarsis* gr., a logarithmic relationship was apparent and a non-linear model was fitted using the *nlme* package (Pinheiro *et al.* 2011) in R.2.14.1. Ecological models were validated against a temporally independent dataset (n=11) taken from Snook (2000) and Brown (2005). Mean error (MA), Pearson's correlation coefficient (r) and coefficient of determination (R^2) were used to assess goodness of fit. Thereafter, the regression models were used to predict future abundances at sites T1 (Taillon glacier-fed), T2 (confluence) and G1 (Tourettes groundwater-fed). Predictions were made for an additional site, T_{snout} located close to the current snout position of the Taillon glacier (Figure 8.2) to provide a broader spectrum of contemporary glacial influence.

8.3. Results

8.3.1. Future temperature and precipitation patterns

The REMO downscaled climate projection for the study region suggest annual air temperature will increase at a rate of $0.05^{\circ}\text{C y}^{-1}$ and will be comparable across all months (Figure 8.4a). For 2021-2040, an annual temperature increase of 0.7°C relative to the control period (1991 -2010) is projected (Table 8.2). A 2.8°C increase is projected for 2061-2080, suggesting warming rates will increase in the latter half of the Century. Differences between summer and winter projected increases in T_a are small ($\leq 0.4^{\circ}\text{C}$) (Table 8.2). The number of months displaying mean air temperatures above freezing is also projected to shift, as during the control period, December (-0.5°C), January (-0.9°C) and February (-0.6°C) are all below 0°C . However, after the 2020 horizon no mean monthly temperatures below 0°C are predicted. For 2061-2080, the mean air temperature of all winter months is predicted to be $\geq 1.6^{\circ}\text{C}$ (Figure 8.4a). Perhaps even more striking is the reduction in the mean number of days below 0C , from 67 during the control period, to 37 for 2061 -2080.

Table 8.2. Predicted seasonal mean change in air temperature and precipitation (relative to 1991-2010) under the A2b scenario for AWS2 (Taillon-Gabiétous basin). Winter = Oct.-March and Summer = April-Sept.

Period	Temperature change			Precipitation change (%)		
	Annual	Winter	Summer	Annual	Winter	Summer
2021-2040	0.7	0.6	0.7	-5	1	-11
2041-2060	1.6	1.4	1.8	-8	-1	-15
2061-2080	2.8	2.7	2.8	-14	-3	-25

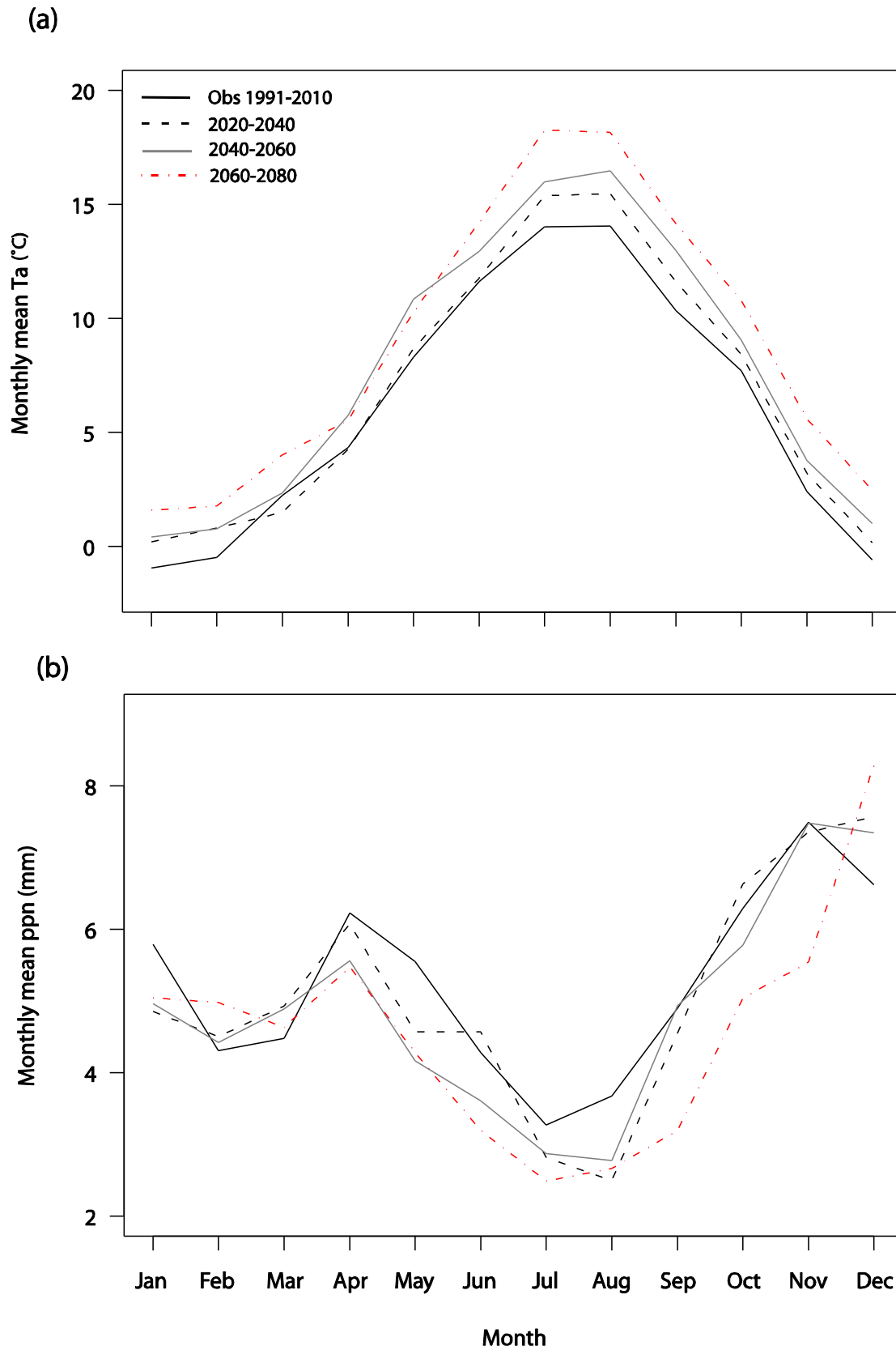


Figure 8.4. Mean annual cycle of observed and downscaled air temperature and precipitation for AWS 2 (Taillon-Gabiétous basin).

A general trend of lower precipitation as the century progresses is projected (Figure 8.4b), with annual precipitation for 2061-2080 14% lower than during the control period (Table 8.2). This trend becomes more complex when the seasonal and monthly changes are considered (Figure 8.4b). Winter precipitation reductions are small ($\leq 4\%$), particularly when compared to summer reductions (25% less precipitation for 2061-2080) and a relative increase is apparent for some winter months (i.e. December, February and March) (Figure 8.4b). Furthermore, a reduction in the proportion of solid state precipitation is also projected (Figure 8.5), with reductions in both solid state precipitation and melt apparent across all elevation bands (Figure 8.6).

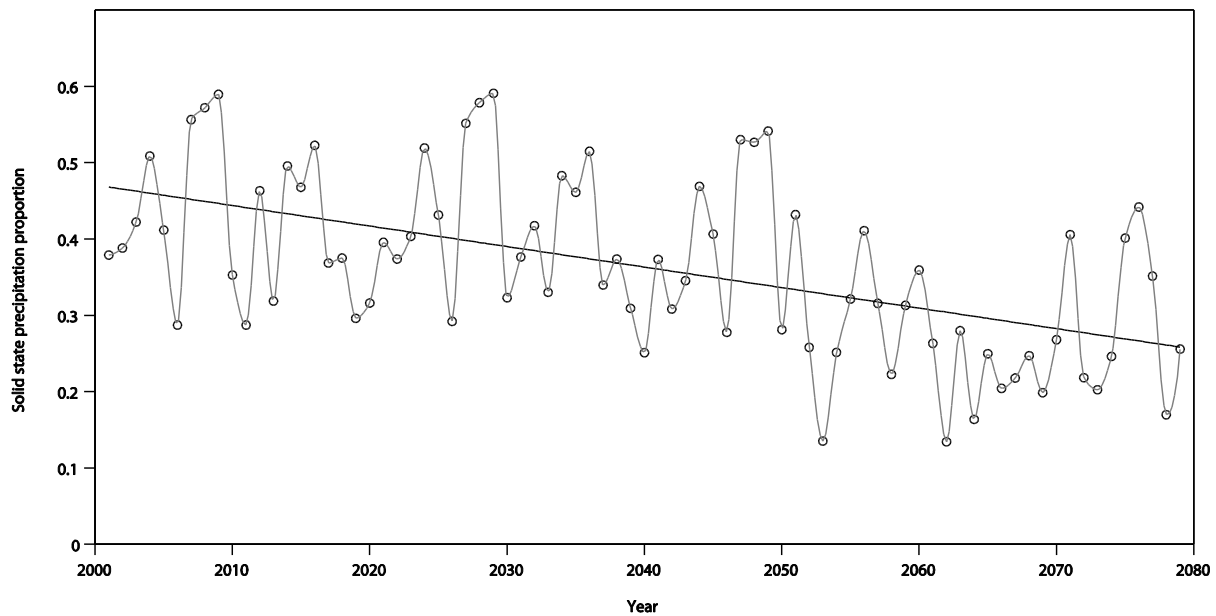


Figure 8.5. The annual proportion of all precipitation that falls as snow (solid state) between 2000 -2080.

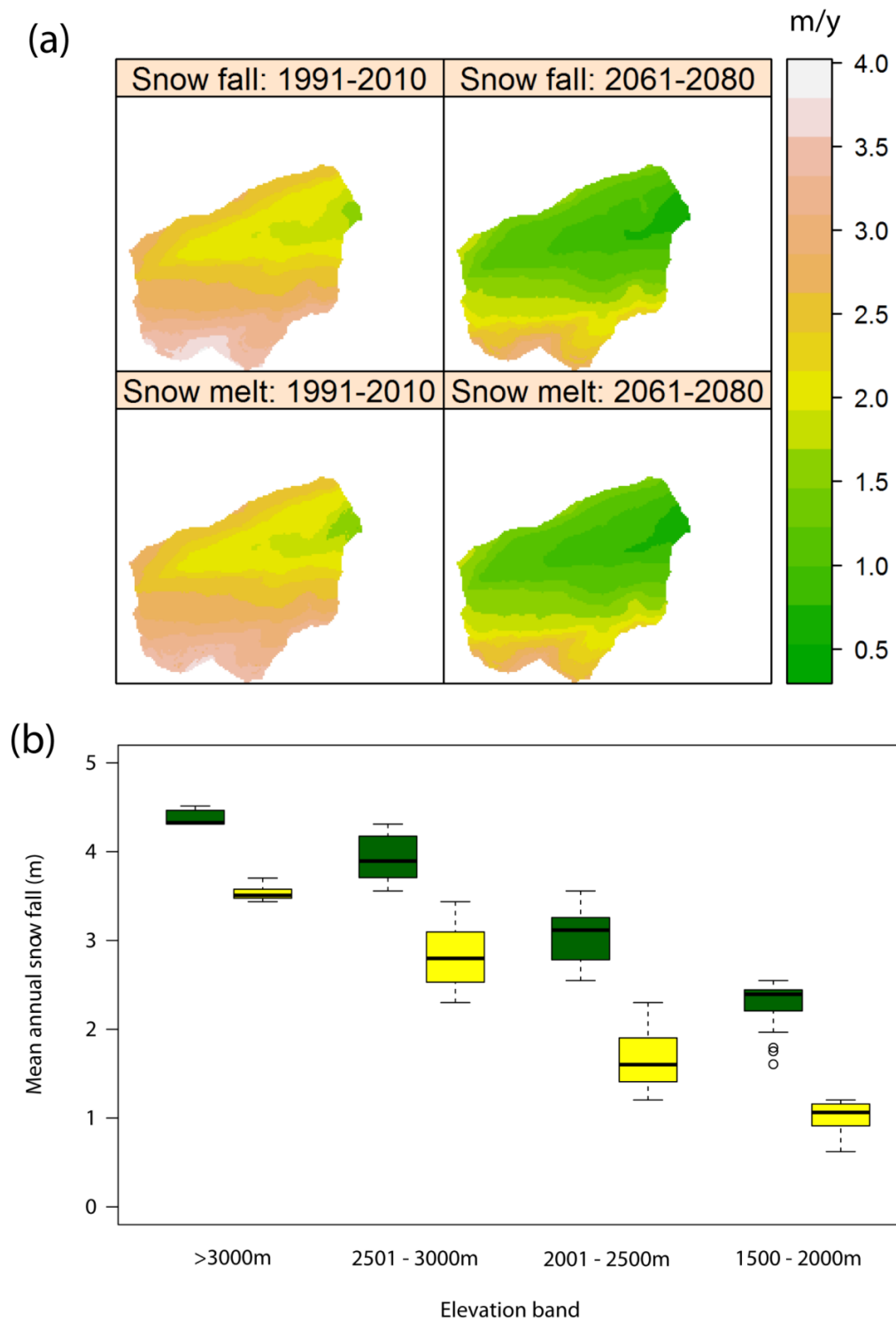


Figure 8.6. (a) Simulated mean annual average snow fall and snow melt for the control period and 2061-2080 period. (b) Mean annual snow fall by elevation for the control period (green boxes) and the 2061-2080 time slice (yellow boxes).

8.3.2. Calibration and validation of TOPKAPI

The final calibrated melt model parameters (Table 8.3) are comparable to those recorded for other glacierized basins (Moore *et al.* 2009; Finger *et al.* 2011; Ragetti & Pellicciotti 2012). Model calibration results represented the timing of the spring meltwater pulse well, as well as flow recession in late summer (Figure 8.7). However, the winter low flow period was underestimated systematically and high flow events in winter and early spring similarly underestimated. From inspection of the calibration and validation summary statistics (mean observed and mean simulated discharge) and the suite of model efficiency metrics (Table 8.4), it is clear that a good fit was achieved for the calibration period. The NS score of 0.77, and the RMSR and PBIAS fulfilled the 'good' model performance criteria outlined by Moriasi *et al.* (2007). For the validation period, the 'best' parameter set produced satisfactory results with as all dates displayed $NS \geq 0.5$ and RMSR and PBIAS within limits outlined by Moriasi *et al.* (2007).

Table 8.3. TOPKAPI melt model parameter descriptions and values for ‘best-fit’ calibration run.

Parameter	Description (units)	Value
S_{corr}	Solid state precipitation correction factor	2.0
TF	Temperature Factor ($\text{m we } ^\circ\text{C}^{-1}\text{h}^{-1}$)	0.01
SRF	Shortwave Radiation Factor ($\text{m we m}^2\text{ W}^{-2}\text{h}^{-1}$)	0.009 5
α_1	First albedo factor	0.8
α_2	Second albedo factor	0.065
T_t	Threshold air temperature for melt ($^\circ\text{C}$)	3
P_t	Threshold temperature for change in precipitation state ($^\circ\text{C}$)	1
K_{ice}	Storage constant for snow melt on glaciers (h)	0.8
K_{snow}	Storage constant for ice melt of glaciers (h)	24
β_{max}	Critical slope for redistribution of snow (\tan°)	32
α_{ice}	Glacier ice albedo	0.3
T_{mod}	Temperature decrease over glacier area ($^\circ\text{C}$)	0.3

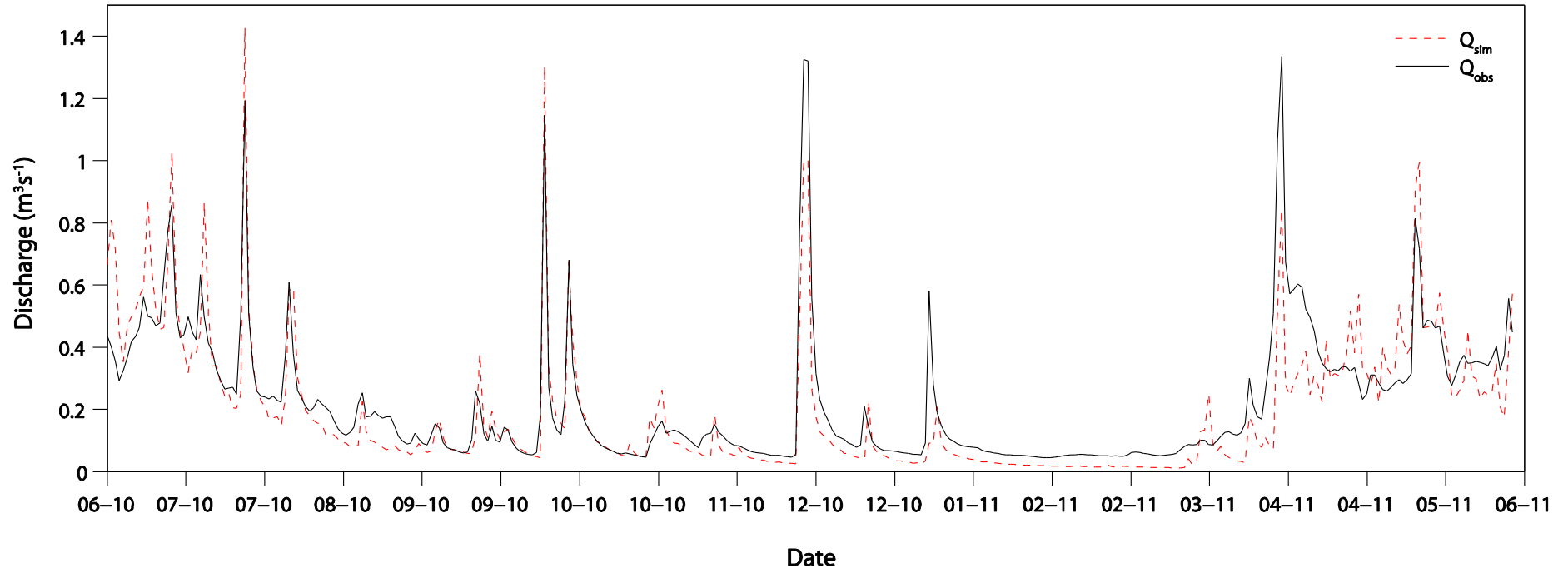


Figure 8.7. Observed and simulated daily discharge for the calibration period (June 2010 –June 2011) at gauge T3 (basin outlet).

Table 8.4. TOPKAPI calibration and validation for the basin outlet, T3 during calibration; and T2 (below the confluence of the Tourrettes and Taillon streams) during validation. Q_o = observed discharge, Q_s simulated discharge, NSE = Nash Sutcliffe coefficient, RMSE = Root mean square error, RMSD = ratio of RMSE to the Stdev

Site	Period	Q _o	Q _s	NSE	RMSD	RMSE	% bias
<i>Calibration</i>							
T3	2010-2011	0.22	0.2	0.77	49.3	0.11	-13.2
	<i>100 best runs</i>	-	-	0.75 (0.01)	49.8 (0.4)	0.11 (0.00)	-14.3 (0.75)
<i>Validation</i>							
T2	Jun-Sep:2002	0.24	0.25	0.63	0.57	0.08	12.7
	Jun-Sep:2003	0.20	0.18	0.54	0.66	0.08	-14.1
	Jun-Sep:2011	0.26	0.26	0.50	0.71	0.08	-8.8

8.3.3. Climate induced hydrological change

Discharge patterns. TOPKAPI simulations using REMO downscaled data indicate, annual mean discharge will decrease for all future time periods (Table 8.4). For the 2020-2041, 2041-60 and 2061 -2080, reductions in mean annual flow are predicted to be 5%, 11% and 16%, respectively. The amplitude of the annual discharge regime is also reduced significantly for 2061-2080 (Figure 8.8), with peak monthly flows ~40% lower than during 1991-2010. The timing of the high flow pulse shifts progressively earlier in the season as the Century progresses, from June (1991 - 2010) to May (post- 2040). However, the timing of the peak daily flow shifts from early summer (DOY = 197) during the control period to autumn/early winter (DOY = 303) for 2061-2080. A reduction in mid-late summer flows (July, August and September) and a marked increase in winter flows are apparent for 2061-2080 (Figure 8.8). Furthermore, the projected increase in baseflow as the Century progresses (e.g. +0.05 m³s⁻¹ for 2061-2080) is due to the consistently higher flows during winter. The reduction in flow

predictability and annual CV are associated with the increasingly pluvial nature of the flow regime (Table 8.5). A significant decrease in the discharge magnitude for the 7 day (ANOVA; $F= 4.8, P <0.05$), 30 day (ANOVA; $F= 11.7, P <0.01$), and 90 day (ANOVA; $F= 23.5, P <0.001$), day maxima is predicted for the 2061-2080 period (Figure 8.9a). Conversely, for the duration of minimum flows, significant increases are predicted for the 1-, 3-, 7-, 30-, and 90-day discharge minima (all ANOVA; $P < 0.01$) from 2061-2080 (Figure 8.9b).

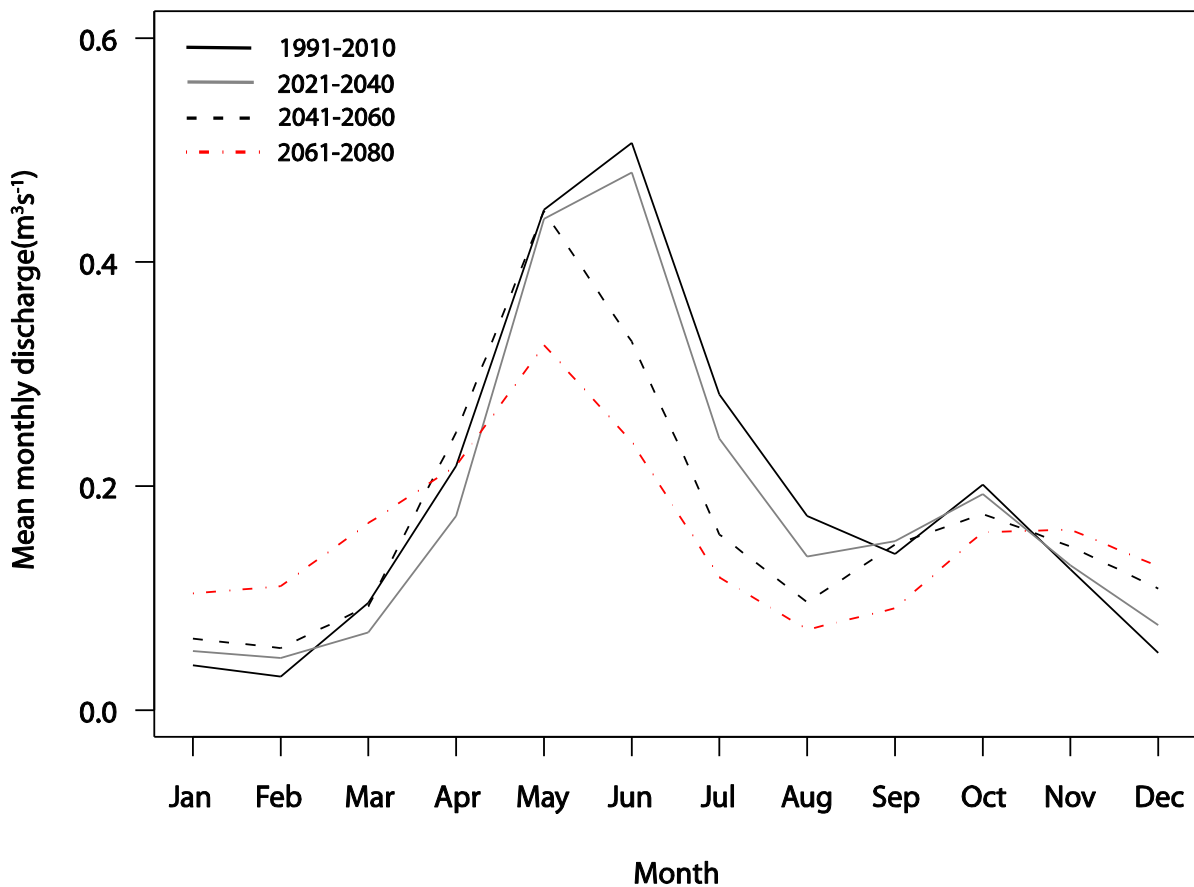


Figure 8.8. Modelled mean annual hydrographs for site T3 for the control period (1991-2010) and future climate periods.

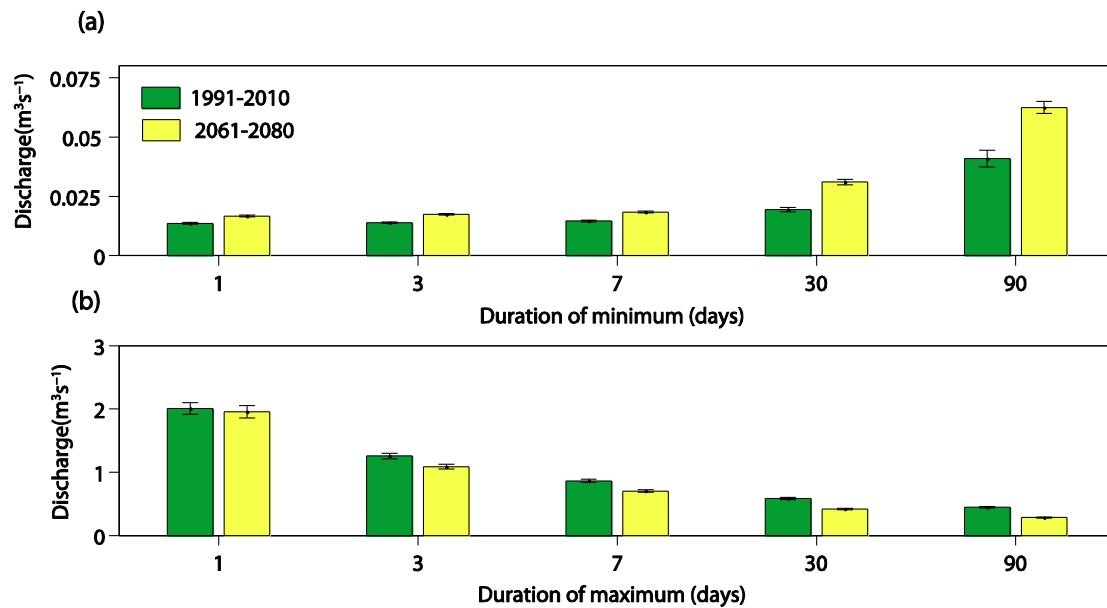


Figure 8.9. One, 3-, 7-, 30-, and 90-day flow minima (a) and maxima (b) simulated for the basin outlet, T3 (mean \pm SE), for the 1991-2010 period (observed climate data used for TOPKAPI simulation) and the 2061-2080 period (REMO RCM projection used for TOPKAPI simulation).

Table 8.5. Flow summary statistics (Mean \pm SD) for the control and future periods. Q_{mean} is mean annual discharge and date max is the mean Julian day when the annual peak flow occurs.

Period	Q_{mean}	% change	Baseflow	Date max	Predictability	Annual CV
1991-2010	0.19 (0.02)	-	0.07 (0.02)	197 (51)	0.48	1.26
2021-2040	0.18 (0.02)	-5	0.08 (0.02)	266 (44)	0.47	1.27
2041-2060	0.17 (0.02)	-11	0.08 (0.02)	269 (49)	0.43	1.28
2061-2080	0.16 (0.03)	-16	0.12 (0.03)	303 (37)	0.41	1.34

Table 8.6. Current and predicted glacier surface areas (km²) and relative change, for the Glacier du Taillon and Glacier des Gabiétous.

Year	Surface area (km ²)		Change relative to 2010 (%)	
	Taillon	Gabiétous	Taillon	Gabiétous
2010	0.09	0.08	-	-
2020	0.09	0.09	0	13
2040	0.02	0.04	-76	-66
2060	0.004	0.01	-95	-86
2080	0.001	0.002	-99	-98

Meltwater dynamics. Total meltwater generation in the Taillon basin is predicted to decline significantly by 2061-80 (ANOVA; $F = 1229$, $P < 0.001$). However, an initial increase for the 2021-40 (+9% relative to the control) is preceded by a large decrease from 2040; -12% for the 2041-60 and -37% for 2061-80. A shift in the timing of peak meltwater generation is apparent for all post 2020 time slices, from June (control period) to May (all projections). The magnitude of this peak increases initially (2020 -2060 projections), then occurs over a shorter time period (post-2040 projections) and decrease significantly post-2061 (Figure 8.10). This pattern is linked to the projected increase in snowmelt during April/May (Figure 8.11a) for 2020-2060; however, after 2060 snowmelt is greater than control period in April. The reduction in late summer flows (i.e. August, September) is linked directly to decreases in flow sourced from ice-melt (Figure 8.11b) due to the reduction in glacier surface area, which for 2061- 2080 is projected to be >95% (i.e. glacier loss) for both the Taillon and Gabiétous glaciers (Table 8.6 and Figure 8.12).

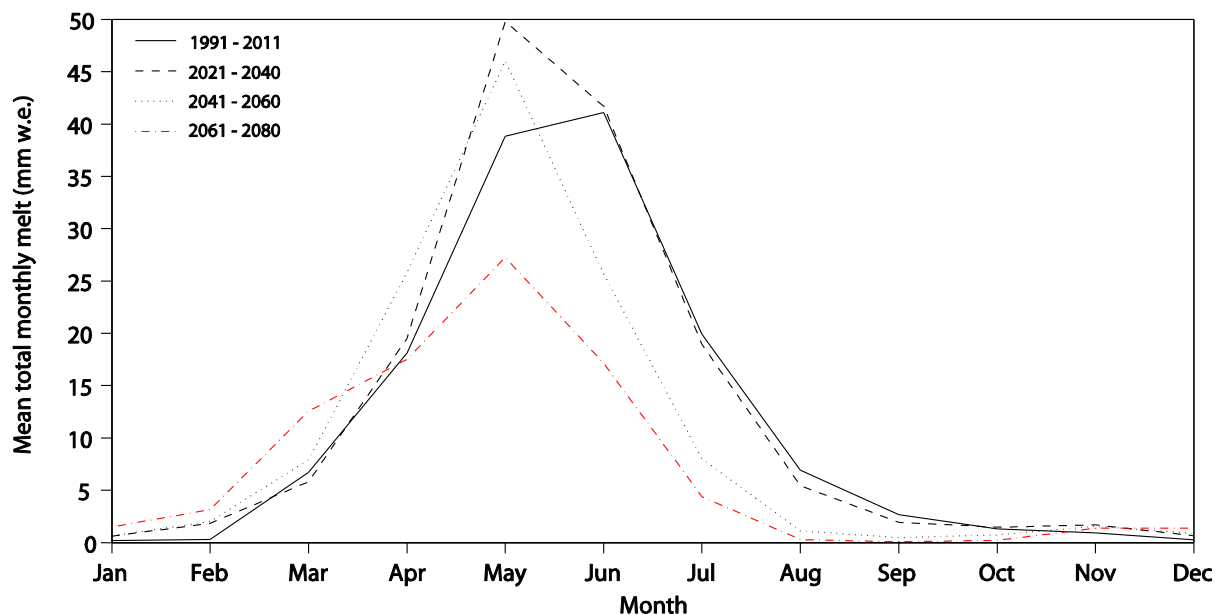


Figure 8.10. Modelled mean monthly total meltwater generation in the Taillon-Gabiétous catchment for the control period (1991-2010) and future climate periods.

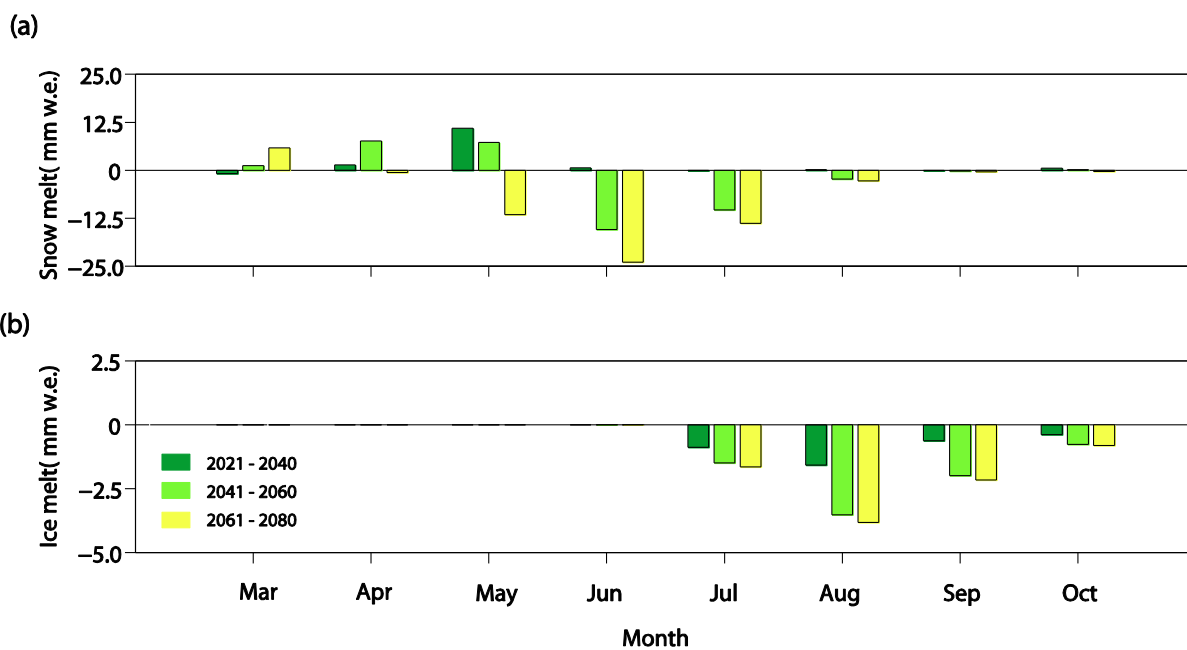


Figure 8.11. Change in modelled mean monthly snowmelt (a) and ice melt (b) for the Taillon-Gabiétous catchment relative to the control period (1991-2010).

8.3.4. Calibration and validation of stream water temperature model

Both the calibration and validation of the water temperature yielded ‘good-fit’ NS values of >0.8 and 0.7 , respectively. RMSE and %bias were satisfactory with <2.0 and 20% , respectively (Table 8.7). Water temperature was higher in 2011 for both G1 (predominately groundwater-fed) and T1 (predominately glacier-fed) but the temperature differences between the two sites were comparable between years (Table 8.8). Mean annual water temperature is projected to increase by 1.5°C and 1.4°C for the 2061-2080 period for sites G1 and T1 respectively. Temperature increase is similar between winter and summer. The most notable change was the number of weeks with sub-zero water temperature (i.e. frozen stream). For site T1, sub-zero water temperature days are projected to reduce from 23.1% during the control to 3.8% for 2061-2080 (Table 8.8, Figure 3.13).

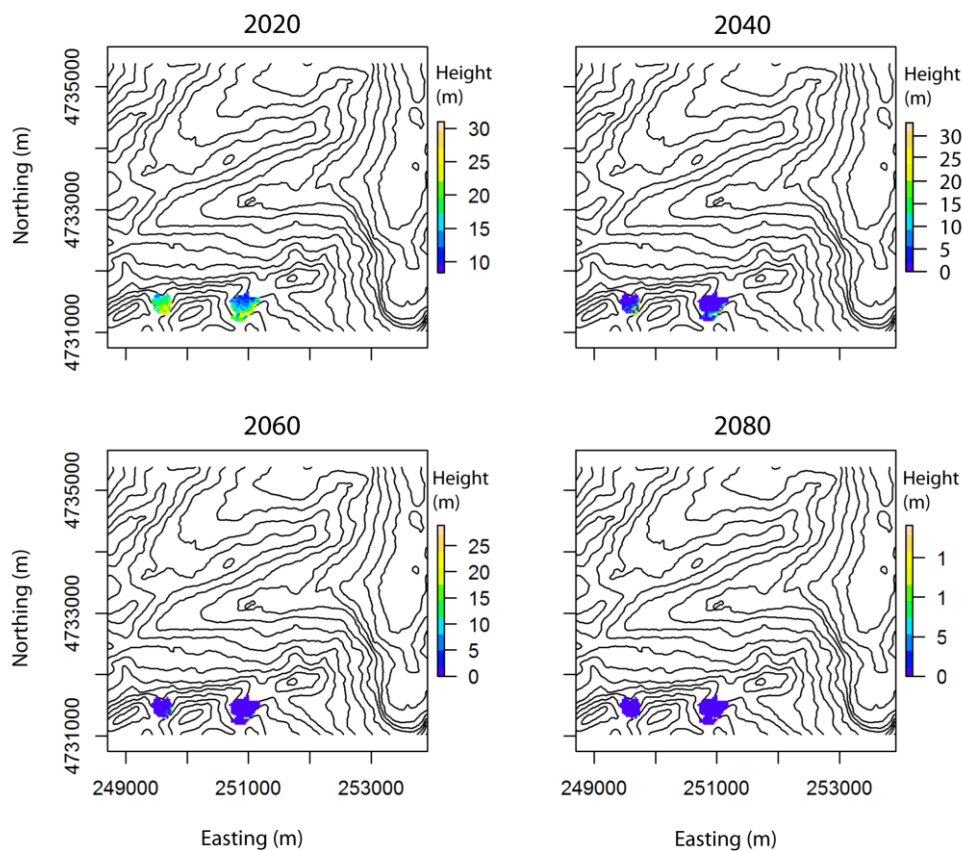
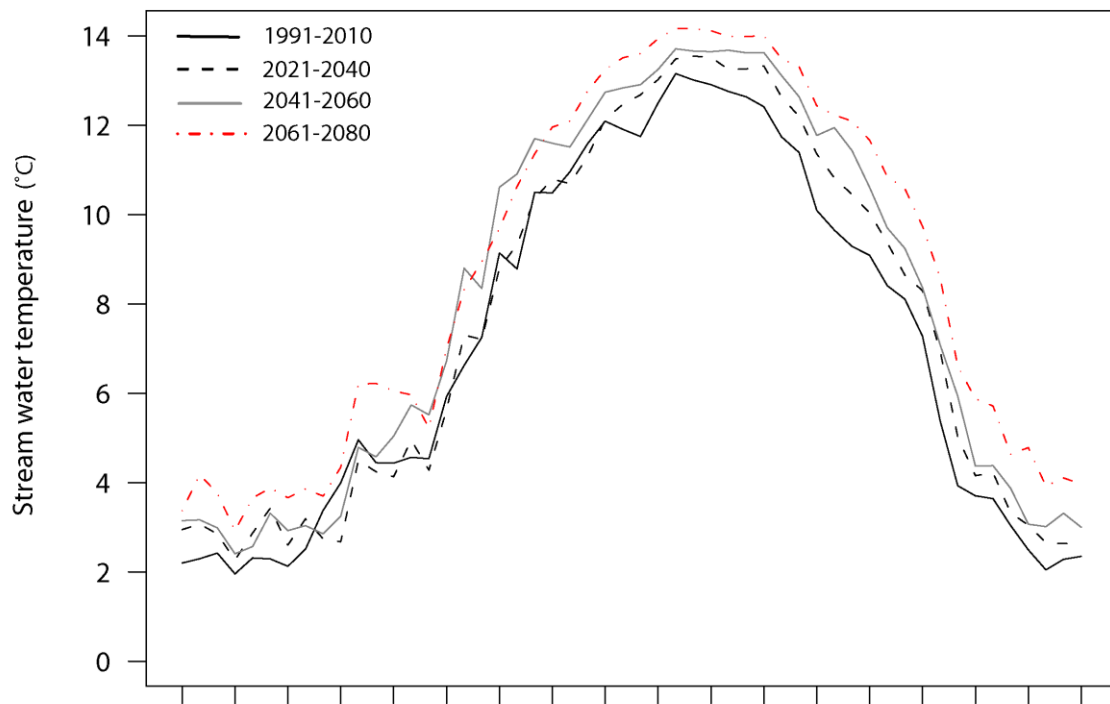


Figure 8.12. Predicted glacier thickness for 2020, 2040, 2060 and 2080 based on REMO RCM climate projections. Solid black lines are 100m contours.

Table 8.7. Calibration and validation results for the air–water temperature logistic regression model and associated model efficiency criteria.

	Site	Period	T_o	T_s	NS	RMSE	% bias
<i>Calibration</i>							
	G1	2011-2012	5.9	4.8	0.8	1.8	19
	T1	2011-2012	3.4	3.7	0.8	1.4	2
<i>Validation</i>							
	G1	2002-2003	4.1	3.6	0.7	1.6	12
	T1	2002-2003	2.1	2.3	0.7	0.9	7

(a)



(b)

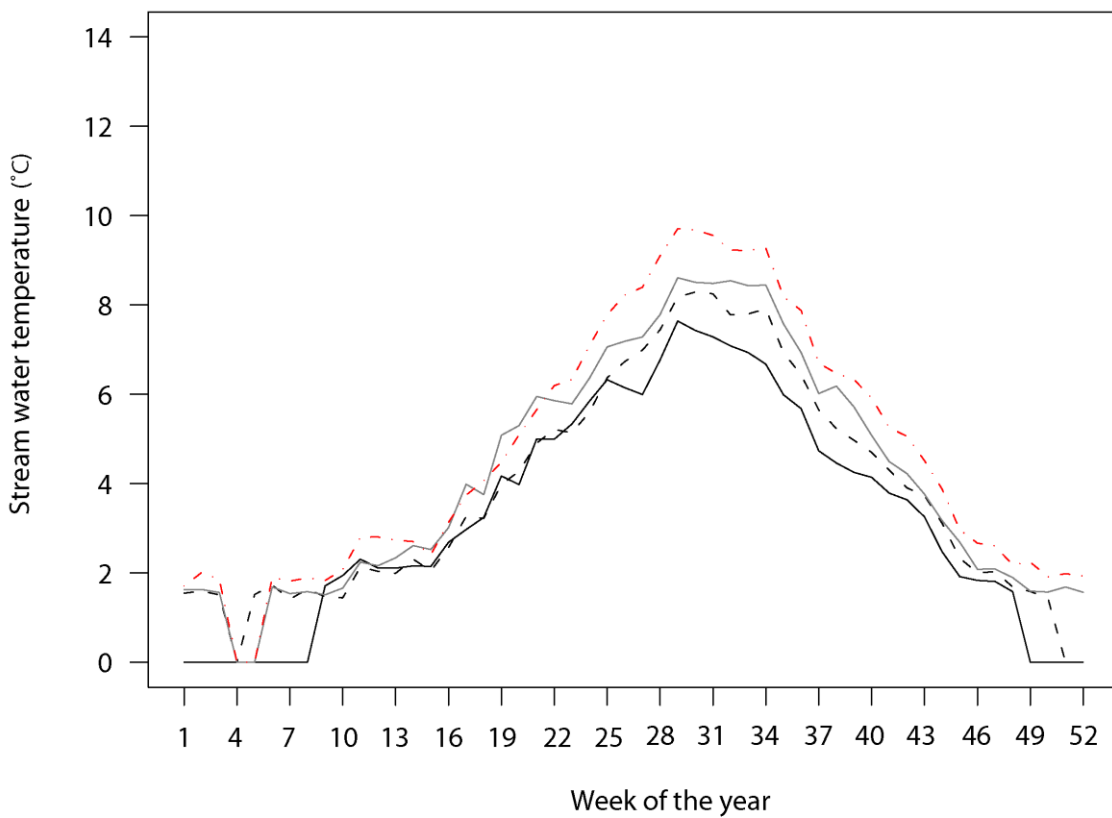


Figure 8.13. Modelled mean weekly water temperatures for: (a) Site G1; and (b) Site T1.

Table 8.8. Summary statistics of water temperature model results for sites C and D. % frozen represents the proportion of weeks when temperatures are predicted to be below 0 °C.

Period	Site G1			Site T1			< 0°C (%)
	Annual T _w	Summer T _w	Winter T _w	Annual T _w	Summer T _w	Winter T _w	
Control	6.2 (4.2)	8.6 (2.7)	3.7 (2.1)	3.3 (2.5)	5.2 (1.7)	1.3 (1.4)	23.1
2021-2040	6.6 (3.6)	9.1 (3.0)	4.2 (2.4)	3.8 (2.5)	5.7 (1.9)	2.0 (1.2)	7.7
2041-2060	7.1 (3.7)	9.7 (2.8)	4.4 (2.5)	4.2 (2.6)	6.3 (1.9)	2.1 (1.2)	3.8
2061-2080	7.7 (3.7)	10.1 (3.1)	5.3 (2.7)	4.7 (2.9)	6.8 (1.4)	2.6 (1.4)	3.8

Table 8.9. Taxa predicted to be ‘winners’ (e.g. range expansion and/or higher abundance) and ‘losers’ (range and abundance reduction) under the post 2040, REMO future climate scenario. Winners and losers were classified as taxa with regression coefficient for GCC > ± 1 S D of the mean.

Winners (+)	Neutral	Losers (-)
<i>Ecdyonurus</i>	Chloroperlidae	<i>Diamesa latitarsis</i> grp
Perlidae	Perlodidae	Empididae
Leuctra	Drusinae	
<i>Microspectra</i>	<i>Diamesa cinerella</i> gr.	
<i>Psychodidae</i>	<i>Baetis</i>	
<i>Rhithrogena</i> spp.	Tipulidae	
<i>Protonemura</i> sp.	<i>Capnioneura</i>	
Simuliidae	<i>Eukiefferiella</i>	
<i>Tvetenia</i>	<i>Orthocladius</i>	
Athericidae		

8.3.5. Ecological responses-taxa abundance changes

Of the 63 taxa, only 21 displayed a significant relationship with glacier cover in the catchment (GCC; Table 8.9). Of these the majority (n = 19) are projected to increase their

range/ abundance (i.e. winners or neutral based on the β coefficient). Only two taxa (*Diamesa latitarsis* grp and Empididae) are predicted to suffer range contractions (Table 8.9). For the regression models of the five key taxa, explanatory power was high generally (all $R^2 > 47\%$; Appendix 8.1) with the models for *P. grandis* and *Simulium* displaying the highest and lowest explanatory R^2 , respectively. Model validation was also reasonable (all $R^2 > 0.5$), with predictions for *Leuctra* spp. and *Diamesa latitarsis* gr. displaying the best and poorest fits respectively (Table 8.10). At all test sites, the general trend is one of increasing abundance, which is pronounced particularly for T_{snout} (post-2030) and T1 (Figure 8.14). The abundance of all taxa, except *Diamesa latitarsis* gr., are projected to increase, or remain unchanged (T2, confluence and G1, groundwater-fed). However, at all sites *Diamesa latitarsis* gr. abundance is projected to decrease, and by 2050 is only present at T_{snout} but in low abundance. Changes in the relative abundance of the five taxa are expected to be minimal for T2 and G1, except for the projected loss of *Diamesa latitarsis* gr. post 2040 (Figure 8.14). However, for T_{snout} and T1, distinct changes in the relative proportions of these key taxa are predicted, with a shift from predominately *Diamesa/Simulium* spp., to abundance of all taxa being comparable to G1 and T2 by 2080.

Table 8.10. Validation results for the taxa abundance – GCC regression models.

Taxa	ME	<i>r</i>	R^2
<i>Perla grandis</i>	-0.36	0.77	0.60
<i>Simulium</i> spp.	0.03	0.85	0.73
<i>Rhithrogena</i> sp.	0.23	0.83	0.72
<i>Leuctra</i> spp.	-0.13	0.88	0.77
<i>Diamesa latitarsis</i> gr.	-0.13	0.72	0.52

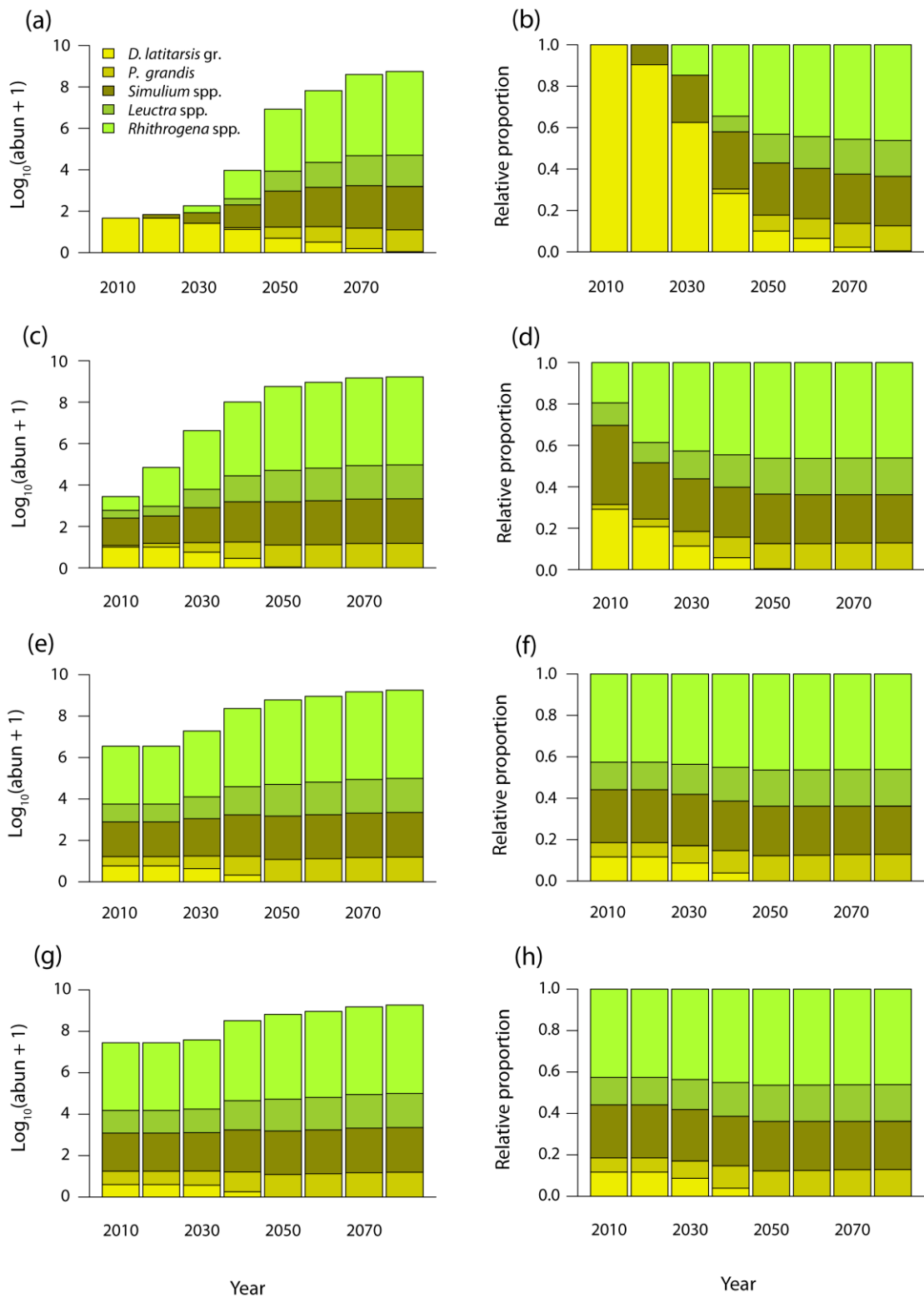


Figure 8.14. GAM and logarithmic regression predictions of the abundance (log_{10}) of key taxa based on REMO RCM projections (2010 – 2080) at sites (a) T_{snout} , (c) T1, (e) T2 and (g) G4. Relative proportion of the five taxa at sites (b) T_{snout} , (d) T1, (f) T2 and (h) G4.

8.4. Discussion

The key aim of this chapter was to identify the hydroecological responses of an alpine, glacierized river to a future scenario of climate-induced hydrological and habitat change. By adopting a suite of modelling approaches, cryospheric, hydrological, physicochemical habitat and ecological change were projected and represent a first approximation of future patterns for the central French Pyrenees. Distinct changes in the hydrological regime by the 2080 horizon were projected, with a shift from a meltwater dominated regime to a more pluvial regime. Water temperature was projected to increase with fewer periods of sub-zero water temperature (i.e. stream frozen). Using hydrological model outputs and known relationship between physicochemical habitat and glacier influence (% glacier cover), GAM and non-linear regression models projected future abundance of key taxa at a number of sites. The range contraction and subsequent loss of the glacial stream specialist (*Diamesa latitarsis* gr.) is projected along with an increase in the abundance of generalist taxa (e.g. *Leuctra* spp. and *Rhithrogena* spp.).

8.4.1. Catchment model calibration and performance

To date catchment scale hydrological studies in the Pyrénées have largely been limited to the Southern and Eastern river basins (Anderton *et al.* 2002; Gallart *et al.* 2002; Lana-Renault *et al.* 2007) and, to the best of the authors knowledge, this study represents the first application of a distributed hydrological model (TOPKAPI) to an alpine, glaciated river catchment in the French Pyrénées. Following the criteria outlined by Moriasi *et al.* (2007), model calibration and validation were ‘good’ and ‘satisfactory’, respectively. Systematic underestimation of the winter low flow period was identified, possibly due to the network of karst springs within the catchment which was not represented in the model (Hannah *et al.* 2000; Smith *et al.* 2001).

These springs are fed via a series of tunnels which transit water within the study area, and also in (out) of the study area from (to) other basins (Parc National des Pyrénées 1991). High flow events in winter and early spring were also underestimated, possibly related to issues modelling runoff associated with rain on snow events, snow drifting and rain gauge record errors ‘under-catch’ associated with hail/sleet storms (Viviroli *et al.* 2011; Savina *et al.* 2012). However, the calibrated parameters appear to be physically- realistic (Table 8.3). The melt parameters, TF and SRF, are comparable to those obtained by Carenzo *et al.* (2009), snow redistribution parameters are comparable to Ragetti and Pellicciotti (2012) and storage constants for the linear reservoir model are similar to Hannah *et al.* (2001) for the Glacier du Taillon.

Model performance, calibration and validation may have been improved if longer historical flow records or glacier mass-balance data were available. A secondary measured variable would have been beneficial as the use of multiple measured variables for calibration and validation have been shown to improve the performance of physically based, distributed hydrological models (Konz & Seibert 2010; Finger *et al.* 2011). The coupling of discharge records and remotely sensed snow cover extent can be particularly useful in remote, data poor, mountain catchments (Finger *et al.* 2011); however, this was not possible for this study due to the small catchment area and the coarse grain size of snow cover extent recorded by the Moderate Resolution Imaging Spectroradiometer (MODIS). Given the data limitations and short calibration and validations periods, the cryospheric and hydrological results presented in this study need to be interpreted with this in mind. However, as calibration parameters were realistic and the TOPKAPI-ETH model is physically based, with key hydrological/cryospheric processes well represented (Fatichi *et al.* 2013), I believe the findings presented give a plausible future scenario.

8.4.2. *Changes in climate and hydrology*

The general trend of lower precipitation, during summer months, and warmer annual air temperature is consistent with predictions from other climatological studies in the Pyrénées. (López-Moreno *et al.* 2008, 2009). It is worth noting that, despite using ensembles of RCM outputs, predictions from other studies on the central Pyrénées are comparable to this study, with winter precipitation change negligible and winter temperature increase of $\sim 3^{\circ}\text{C}$ for the latter part of this century (López-Moreno *et al.* 2008, 2009). The projected reductions in solid precipitation and snow melt at all altitudes are in contrast to simulations for the Alps, where an increase in snowmelt at higher altitudes is projected due to an increase in winter precipitation (e.g. Fatichi *et al.* 2013).

The flow regime of the Taillon-Gabéitous basin is projected to shift from a glacio-nival dominated regime to a more nivo-pluvial regime (Figure 8.8). Following the French natural flow regime classification of Snelder *et al.* (2009), this represents a shift from a type 2 regime (summer peak), which is currently associated with high altitude mountain catchments, towards a type 1 regime (low annual variability), which is associated with lower altitude mountainous catchments. Reductions in discharge magnitude and a progressive shift towards peak flow occurring earlier in the season is in line with predictions for a range of European mountain ranges (Farinotti *et al.* 2012; Finger *et al.* 2012; Fatichi *et al.* 2013). However, unlike the Taillon-Gabéitous basin, catchments with larger valley glaciers are likely to go through an initial period of increased discharge magnitude as glacier mass is rapidly lost then a phase of decreased discharge (Milner *et al.* 2009; Farinotti *et al.* 2012). The loss of glacier ice as a water source is likely to lead to greater year on year flow variability (Jansson *et al.*

2003) as highlighted by the reduction in flow predictability and increase in CV for 2061-2080 (Table 8.5).

8.4.3. Stream temperature model and future predictions

The air temperature - stream water temperature model was successful in predicting weekly air temperatures for both test sites (T1 and G1) with NS values for model validation comparable to those obtained by Mohseni *et al.* (1999) and Van Vliet *et al.* (2011). Projected increases in water temperature for 2061-2080 were similar for both streams (~1.5°C), which is comparable to projections for streams in Pacific Canada (Hague *et al.* 2011) and the Sierra Nevada, USA (Null *et al.* 2013). However, predictions would likely be improved by using both discharge and air temperature (van Vliet *et al.* 2012) or coupling rainfall-runoff models and water temperature models (Null *et al.* 2013), particularly as a recent study identified change in streamflow accounted for 20-40% of the change in the water temperature (Isaak *et al.* 2010).

While many studies have focused on the implications of climatic warming for salmonid survivorship and habitat extent (e.g. Isaak *et al.* 2010, Almodóvar *et al.* 2012), few studies have explored the implications for benthic macroinvertebrates in mountainous regions (but see Sauer *et al.* (2011)). A recent study in the UK projected that in upland areas macroinvertebrate abundance may decline by 21% for every 1°C rise in water temperature (Durance & Ormerod 2007). This is unlikely to be the case in many alpine regions as water temperature is lower than would be expected based on the surface energy balance due to the predominance of cold water sources (i.e. snow and ice) and limited exposure to the atmosphere (Brown & Hannah 2008; Fellman *et al.* 2013). Hence, as water temperature

increases in response to changes in climatic forcing, total macroinvertebrate abundance is likely to increase (Milner *et al.* 2009), but some cold stenotherms may be at risk of extinction (Brown *et al.* 2007a; Muhlfield *et al.* 2011). However, a recent study identified that the thermal tolerance of a range restricted stonefly (*Lednia tumana*) was significantly higher than its observed thermal niche (Treanor *et al.* 2013). This suggests that current distributions of glacier stream specialists may be due to a combination of abiotic conditions and biotic interactions, whereby the former limits superior competitors to sites with lower glacial influence (Flory & Milner 1999).

The proportion of time the stream is frozen is important when considering ecological responses, particularly as benthic taxa will avoid actively stream reaches which freeze-up (Malard *et al.* 2001). In this study, G1 which has numerous groundwater tributary inflows, did not exhibit sub-zero temperature during winter and likely has year round flow permanence (Brown *et al.* 2006b). Annually, T1 displayed a prolonged period of sub-zero water temperature during the control period. Yet, by 2061-2080 a significant reduction (23% to <4%) was observed in sub-zero days. This could potentially lead to an increase in secondary productivity (macroinvertebrate abundance) due to primarily an increase in habitat availability during winter (Lavandier 1974). However, a number of other factors, such as snow cover duration and food availability (i.e. retention of allochthonous material), are also important for determining growth rates and survivorship during winter (Lavandier 1975; Lavandier & Pujol 1975; Schutz *et al.* 2001).

8.4.4. *Ecological predictions and implications*

Following the framework outlined in Figure 8.1, ecological responses to climate change were modelled using GCC, a 'master variable' which determines a number of biologically

important physicochemical habitat parameters (Ilg & Castella 2006). As this modelling approach is not solely based on air temperature like the widely adopted bioclimatic envelope approach (see Thomas *et al.* 2004, Domisch *et al.* 2012), some of the problems associated with single variable ecological modelling are addressed. Most notable is the issue of multiple abiotic factors influencing benthic macroinvertebrate patterns (Ormerod *et al.* 2010). Essentially, the projections outlined herein are based on a dynamic physicochemical habitat template (see Chapter 3) dictated by glacial influence (glacier cover) which strongly controls reach scale benthic macroinvertebrate patterns (Hannah *et al.* 2007; Milner *et al.* 2010). However, the role of geomorphic, biogeographical and biotic interactions are not incorporated and needs to be considered when interpreting these results (Woodward *et al.* 2010a; Jacobsen & Dangles 2012; Weekes *et al.* 2012). This is particularly the case if this approach is adopted to model alpine macroinvertebrate distributions at a larger spatial scale (i.e. inter-basin or inter-region) due to variability in geology, valley segment processes and other macro-basin characteristics.

The abundance of the five focal taxa were projected successfully for sites and dates not used to train the model (Table 8.10) with $R^2 > 0.5$ for all taxa. For the future, particularly post 2040, a significant decline in *D. latitarsis* gr. abundance was projected for all sites, but was most pronounced for T_{snout} , where GCC is $>30\%$ at present. This is not surprising as *D. latitarsis* gr. is a glacial stream specialist which is recorded rarely, and in low abundance, at sites with low glacial influence (Snook & Milner 2001; Rossaro *et al.* 2006). Projected increases in the abundance of generalist taxa (i.e. *Rhithrogena* spp. and *Leuctra* spp.) is viable given the current broad distribution of these taxa at lower altitudes and in non-glaciated river basins (Vincon 1987; Füreder *et al.* 2005; Brittain 2007). The increase in the abundance of the large bodied predator *P. grandis* at sites T1 and T_{snout} is pronounced particularly and also represents a likely scenario as glaciers retreat, leading to the

development of more stable habitat conditions that this taxa requires (Brown *et al.* 2007c). Furthermore, the increase in *Simulium* spp. at T_{snout} and T1 is also plausible as the specific hydraulic requirements of this taxa are a well known control on its distribution (Finelli *et al.* 2002). Thus, the unstable hydraulic conditions of sites with high glacial influence limit colonisation; but, as glaciers recede and habitat conditions become more benign, the availability of suitable habitat for colonisation is increased (Cauvy-Fraunié *et al.* 2013a). At sites which are currently highly glacial, the increase in abundance of taxa associated with lower glacial influence is under the pretext that groundwater contributions are not dependent on aquifer recharge from glacial meltwater (Crossman *et al.* 2011). If this is the case, the loss of predictable melt recharge will likely lead to increased intermittency of summer/autumn flows. This could have implications for future taxa distributions because the trajectory of community change may not be analogous to contemporary patterns identified through space for time substitutions (Johnson & Miyanishi 2008). However, as glacial floodplain subsurface hydrology is complex with potential for multiple flow paths (Roy & Hayashi 2009), it is particularly difficult to predict future patterns (Magnusson *et al.* 2012b).

The projected changes in the relative abundance of the taxa outlined above represents a shift in the dominant functional strategy, particular regarding resource acquisition. The projection in this study suggests an increase in taxa displaying a defined functional feeding strategies (i.e. *P. grandis*: predator, *Simulium* spp.: filter feeder, *Leuctra* spp.: shredder and *Rhithrogena* spp.: grazer/collector). This has been suggested in other studies as a likely ecological scenario as glaciers retreat (Snook & Milner 2002; Füreder 2007). The key driver is the amelioration of habitat conditions (i.e. bed stability and SSC) that is linked to an increase in basal resource availability and diversity. Here, the most important are increases in: (i) autotrophic production, associated with the clearer waters and more stable channels of

reaches with lower glacial influence (Uehlinger *et al.* 2010), and (ii) allochthonous material retention as beds stabilize (Webster *et al.* 1994). However, a likely consequence of the shift towards a more pluvial flow regime is that high flow frequency and magnitude will increase (Middelkoop *et al.* 2001). This has the potential to increase downstream transport of organic matter and increase scour of periphyton growth, thereby reducing food availability for detritivorous macroinvertebrates in low order alpine streams (Small *et al.* 2008).

8.5. Conclusions

The aim of this study was to identify the responses of an alpine, glacierized river ecosystem to a climate change scenario using a conceptual framework first outlined by Hannah *et al.* (2007) and refined for this study (Figure 8.1). Using TOPKAPI, with REMO downscaled and bias-corrected climate projections as input data, a marked reduction in the total magnitude and change in the seasonality of the annual flow regime was projected (Objective 1). These changes are driven primarily by the projected increase in air temperature ($+0.05^{\circ}\text{C y}^{-1}$) which altered a range of interlinked cryospheric processes. First, a decrease in the fraction of precipitation falling as snow led to reduced winter storage and a more pluvial hydrological regime. Second, a decrease in snowpack extent and depth led to an earlier onset and reduced magnitude of the spring melt. Third, the consistent negative mass-balance (due to decreased snow cover of glacier ice) meant a complete loss of ice cover by 2060 was apparent. Thus, late summer flow compensation from glaciers will not occur and the potential for flow intermittency will be increased. An increase in stream water temperature was projected at the predominately groundwater fed site G1 and meltwater fed T1 ($\sim 1.5^{\circ}\text{C}$ by the 2061 -2080 time slice). Furthermore, a marked reduction in the length of time subzero water temperatures occurred was apparent (Objective 2).

Using outputs from the hydrological model as predictor variables, regression models were able to provide a first approximation of the future abundance of key taxa at a number of sites (Objective 3). While an increase in secondary production may be beneficial for insectivorous terrestrial species such as the European dipper (*Cinclus cinclus*) and the Pyrenean Desman (*Galemys pyrenaicus*), the projected replacement of the glacial stream specialist (*Diamesa latitarsis* gr.) by more generalist taxa (e.g. *Leuctra* spp. and *Rhithrogena* spp.) is of major concern.

There are a number of limitations and caveats that need to be considered when interpreting the findings outlined in this Chapter. First, the climate projection was based on a single RCM simulation (REMO with the A1B ECHAM5 driving GCM) and numerous authors have highlighted the uncertainty associated with using single model realisations (Christensen *et al.* 2010; Chen *et al.* 2011a; Fatichi *et al.* 2013). However, the aim of this study was not to assess uncertainty in climate/ hydrological responses but to provide a possible scenario of river ecosystem change under a plausible future climate. Second, the downscaling approach (delta change) did not enable shifts in the occurrence and intensity of extreme events to be considered. This approach may result in an underestimation of projected increases in air temperature as increases in extreme summer heatwaves are not accounted for (Jasper *et al.* 2004). Third, the limited availability of validation data (a common problem in mountainous river basins, Hannah *et al.* 2011), with only one measured variable (discharge) used for the TOPKAPI catchment simulation, can reduce model performance. This issue was highlighted by a Finger *et al.* (2011) where validation against a single variable improved the model performance for the constrained variable but provided poor model performance for the

remaining variables (e.g. glacier mass balance and snow cover). Fourth, for the ecological projections, biotic interactions were not considered and there is an assumption that groundwater will make up the loss of meltwater.

Despite the above limitations and caveats the results presented in this study provide a useful first reference point for this relatively understudied region. Furthermore, the findings provide a proof of concept for the previously untested theoretical framework of Hannah et al (2007), highlighting the potential for its development as a research and management tool to aid scientist, conservationists and river basin managers.

8.6. Chapter summary

In this chapter a future scenario of climate change was used to project changes in cryospheric, hydrological and ecological patterns and processes. The results provide a first approximation of hydroecological change for the relatively understudied Pyrenean alpine zone and a proof-of-concept for a previously untested integrated modelling framework. In the final chapter of this thesis, the findings from Chapters 3-8 are synthesised to provide a comprehensive assessment of potential river ecosystem change in alpine environments.

CHAPTER 9

Synthesis and outlook

9.1. Introduction

The primary aim of this research was to assess the implications of climate-cryosphere change on hydroecological patterns and processes in alpine river systems, and thus enable validation and further development of scientific understanding, monitoring strategies and predictive models. Knowledge gaps and specific objectives were outlined in Chapter 1, and then addressed by the research presented in Chapters 3-8. Relationships between methods for measuring glacial influence were assessed and related to the physicochemical habitat template (Chapter 3). Reach scale community diversity and abundance patterns were used to refine conceptual understanding and further quantify watersource-biodiversity linkages (Chapter 4). Functional diversity/and trait patterns provided a more mechanistic link between cryospheric change and ecological pattern and process (Chapter 5). At a finer spatial scale, climate induced changes in biotic interactions (predation) was investigated experimentally (Chapter 6) and point scale heat exchange process quantified (Chapter 7). Finally, river ecosystem change was modelled for a future climate scenario using a climate cascade framework (Chapter 8). The key research findings are summarised and synthesised in this final chapter, with scientific limitations/caveats highlighted and recommendations for further research proposed.

9.2. Synthesis

Currently, the cryosphere represents the largest store of freshwater on Earth with the predictable annual/diurnal melt cycle important for a range of biogeochemical processes (Hood & Berner 2009), ecological processes (Freimann *et al.* 2013b) and socio-economic practices (Beniston 2012). This frozen water reservoir is sensitive to climatic forcing and, as

climate projections all tend to converge on a warmer future (IPCC 2007), significant changes to meltwater dynamics (Stahl *et al.* 2008) and flow regimes of associated river systems are expected (Barnett *et al.* 2005). To date, the implications of cryospheric loss for sea level rise (Meier *et al.* 2007) and water resources (Beniston 2012) have received significant scientific attention. However, the potential changes to biotic patterns and processes as these systems shift from a largely predictable hydrological regime (due to the dominant role of glacier ice melt), towards an increasingly uncertain, stochastic hydrological future, is becoming an increasing concern (Moore *et al.* 2009). The need to consolidate findings from multiple disciplines (Hannah *et al.* 2007) and develop coherent monitoring strategies/ predictive tools have been highlighted as key research challenges (Milner *et al.* 2009). In this context, research outlined in this thesis has improved understanding of river ecosystem patterns and processes in highly dynamic alpine environments and provided a roadmap for future monitoring and modelling studies in glacierized river systems.

9.2.1. Monitoring for change: the glacial river physicochemical habitat template

In Chapter 3, four methods for quantifying glacial influence, which have been adopted by hydrologists and aquatic ecologists (Ilg & Castella 2006; Brown *et al.* 2007a; Jacobsen & Dangles 2012; Jacobsen *et al.* 2012), were assessed. Three of these methods can be used to define both glacial influence and a physicochemical habitat template which dictates ecological pattern and process. The fourth method, $GI_{I\&C}$, uses the physicochemical habitat to define glacial influence (Ilg & Castella 2006). All these methods can be framed in the context of the climate – hydrology – ecology cascade (Hannah *et al.* 2007), and define glacial influence based on variables at different levels in the process cascade (Figure 9.1). Each approach has advantages and disadvantages as outlined in Chapter 3; however, the choice of method may be constrained by a number of factors including: (i) the research question being

addressed, (ii) the logistical constraints specific to the study region, and (iii) funding limitations.

Despite all the methods being calculated at the reach scale, the three methods based on higher level cryospheric processes (Figure 9.1: GIJ&D, glacier cover and meltwater), described broadly similar physicochemical habitat variables. A distinct harsh – benign gradient running from high – low glacial influence was identified by all three methods (Brown *et al.* 2007b). However, an important distinction between the ‘static’ measures (GI_{J&D}, glacier cover) which are insensitive to spatial heterogeneity and spatially dynamic measures (i.e. meltwater) was highlighted by diurnal flow variability, which was most strongly related to meltwater (Chapter 3). This is due to the ‘static’ measures not accounting for differences in basin geomorphology, in particular differences in drainage patterns and glacial macroform, which dictate the spatial structure of groundwater tributaries and hence the rate groundwater inputs moderate the glacial signal (Weekes *et al.* 2012). This geomorphological influence raises concerns regarding the robustness of meta-analyses or inter-basin studies based on spatiotemporal static measures of glacial influence. Yet, it is important to acknowledge that the meltwater approach is particularly labour intensive (Brown *et al.* 2010b), and while it can account for spatial heterogeneity in basin geomorphology, uncertainty in the hydrograph separation is propagated through the mixing model and characterization of end-members (Soulsby *et al.* 2003).

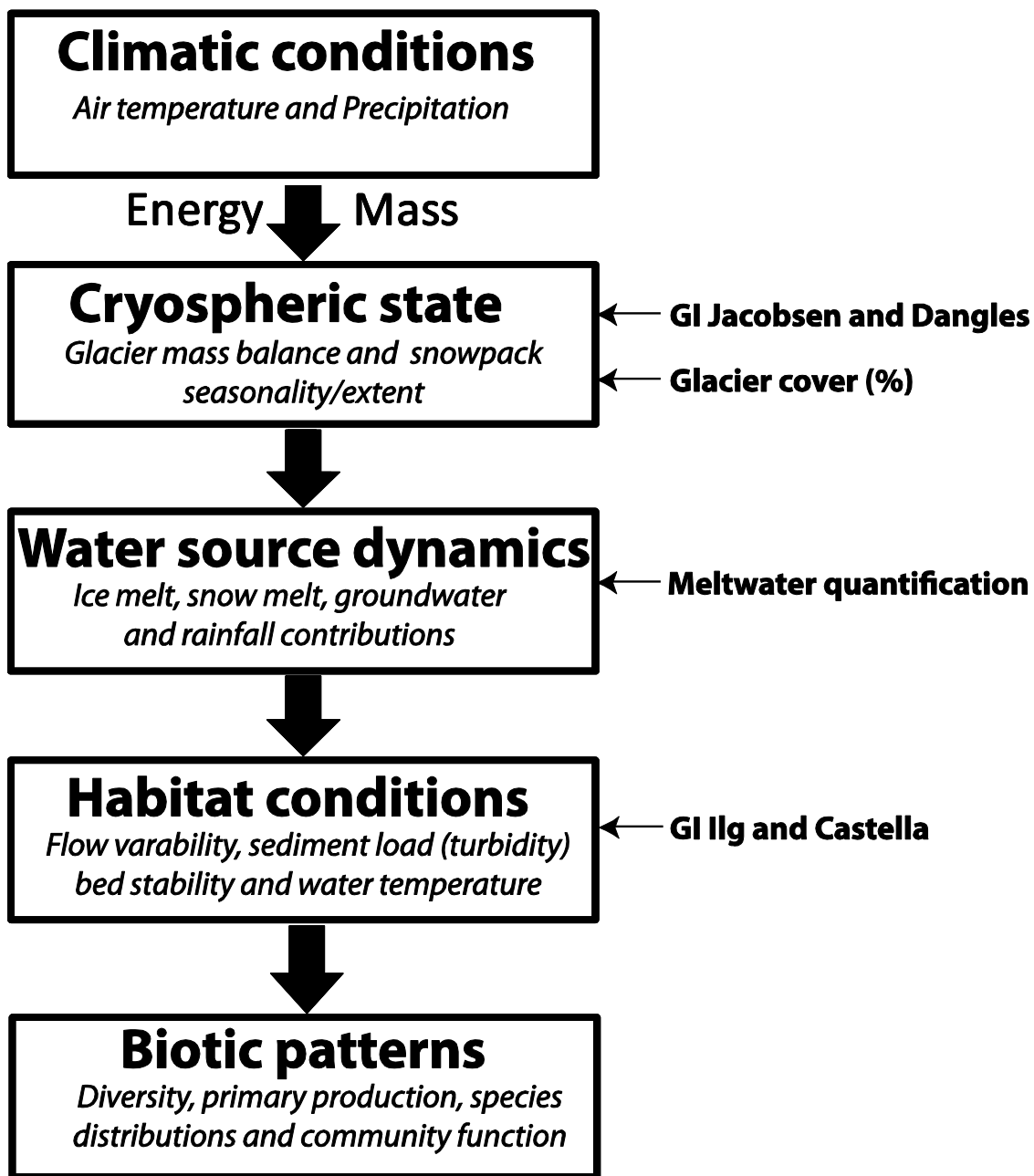


Figure 9.1. The four methods for quantifying glacial influence framed in the context of the climate-hydrology-ecology process cascade.

The use of meltwater and $GI_{I\&C}$, both of which displayed strong concurrence but are labour intensive to calculate, is best suited to answer research question at finer spatial and temporal scales. While these approaches would also be preferable in larger scale studies, the practicality of this is questionable as they are both time consuming and unable to incorporate historical data. Hence, $GI_{J\&D}$ /glacier cover are the only feasible measures for use in large scale, multi-basin studies or for meta-analysis of historical or disparate datasets where few physicochemical parameters were measured. The coupling of static measures with GIS could improve these approaches. For example, river network characterization from satellite imagery and digital terrain models (see Williams *et al.* 2013) could identify the number of tributary inputs, the size of these inputs and distance from the glacial snout. This method is readily accessible and relatively simple as both digital terrain models, see for example the NASA land processes distributed active archive centre (<https://lpdaac.usgs.gov>), and tools for extracting watersheds and river networks, for example Saga (www.saga-gis.org/) and the R statistical environment (R Development Core Team 2012), are freely available and user friendly. Hence, the next step would be to create empirical relationships between the attenuation of the glacial signal and extracted river network parameters for a selection of core test catchments, which could be refined, then applied, to larger scale studies.

A coherent monitoring strategy is required to rigorously and robustly assess the impacts of climate across the broad spectrum of glacial fed river systems (Milner *et al.* 2009). Hence, the ‘filtering’ effect (cf. Poff 1997) that basin lithology appeared to exert on the glacial-physicochemical habitat relationship (Chapter 3) is, from a monitoring perspective, an important finding. Significant differences in SSC and EC were apparent, with ‘soft’ rock streams displaying higher values for both these variables. This highlights the importance that macroscale basin characteristics have on the physicochemical habitat template of alpine river

ecosystems. However, the role of basin geomorphology and glacial macroform were inferred in this study and further work is required to identify the influence these have on the physicochemical habitat template. The conceptual framework of Weekes *et al.* (2012), based on geomorphic processes and morphologies, provides a basis on which to test further the influence of macro-basin characteristics on the glacial influence–habitat template relationship.

9.2.2. *Biodiversity, traits and community assembly*

The harsh-benign physicochemical habitat continuum, running from high to low glacial influence (Chapter 3; (Brown *et al.* 2007b)), is considered as the key control on macroinvertebrate assemblage structure in alpine river systems (Milner *et al.* 2010). Here, deterministic patterns, from low richness/abundance at highly glacial sites, to high richness/abundance at sites of lower glacial influence are expected (Lods-Crozet *et al.* 2001a; Snook & Milner 2001). Recent studies have, however, suggested alpine sites with minimal glacial influence may have lower richness than those with intermediate glacial influence (Füreder 2007; Jacobsen *et al.* 2012), possibly due to increased competitive and trophic interactions. A robust assessment of biodiversity patterns across the full spectrum of glacial influence, defined as meltwater contribution (outlined in Chapter 4), identified unimodal community level responses (e.g. richness and abundance) that were similar across basins of differing geology. These findings suggest that environmental stress/disturbance hypotheses represent a useful theoretical framework for developing predictive models (Shea *et al.* 2004); in essence, meltwater contribution and environmental stress/disturbance can be considered as interchangeable. However, the specific mechanisms maintaining higher diversity at intermediate meltwater sites (e.g. disturbance reduces competition/competitive exclusion) may not adhere

to those outlined in seminal disturbance-diversity papers (Connell 1978; Menge & Sutherland 1987). Fox (2013) suggested that the assumptions of the IDH, particularly those associated with disturbance interrupting competition, are theoretically flawed. Hence, colonisation – competition tradeoffs (see Roxburgh *et al.* 2004, Logue *et al.* 2011), due to the patchiness of refugia and resources at intermediate meltwater sites (i.e. between patch dynamics; cf. Wilson 1994), appears to be the key mechanism driving diversity and abundance peaks in Pyrenean glacial river systems.

To understand better the key drivers of community structure across glacial influence gradient, an assessment of traits and community assembly patterns is required (Mouchet *et al.* 2010; Brown & Milner 2012). The trait analysis (Chapter 5) identified a shift from communities exhibiting resistant and resilient traits (c.f. Füreder 2007), under higher glacial influence, to traits associated with k selected taxa (Pianka 1970) and more stable conditions (Verberk *et al.* 2013) under lower glacial influence. Trait convergence was apparent at higher meltwater sites with communities consisting predominately of dipterans, particularly taxa from the chironomid subfamily Diamesinae. These taxa displayed a specific suite of life history, reproductive and dispersal traits, which are often associated with ‘weedy species’ (Scarsbrook & Townsend 1993), enabling colonisation of this unstable habitat environment (flow variability and unstable channels; see Chapter 3). However, for persistence at such sites, a suite of resistant traits is required, in particular those related to body shape (small/streamlines) and substrate relationship (clinger).

The use of functional diversity indices, coupled with null models (Chapter 5), enabled the community assembly processes operating along the glacial influence gradient to be tested

under a falsification framework. At higher meltwater sites, the ‘harsh’ physicochemical environment acts as a primary filter, inhibited colonisation of other taxa from the regional species pool (Ilg & Castella 2006). As conditions become more benign, limiting similarity (competitive interactions) becomes increasingly important (Paillex *et al.* 2013). Trait divergence (observed/expected functional diversity) at lower meltwater sites was apparent, with the community consisting of predominately competitively superior taxa with a specific suite of traits associated (e.g. large body size and longer generation time). This highlights that limiting similarity/competitive exclusion was an increasingly important assembly process at this lower end of the meltwater spectrum (cf. Mason *et al.* 2012). Interestingly, while trait convergence was greater at high meltwater sites than lower meltwater sites, the highest convergence was recorded at intermediate meltwater sites. This finding was due probably to the dominance of resilient, generalist taxa (similar trait profiles) at intermediate meltwater sites. In particular, taxa displaying traits associated with rapid dispersal/colonization abilities (e.g. *Baetis* spp.) were most abundant. Nevertheless, it is likely that random assembly processes are also operating at the extremes of the spectrum (Thompson & Townsend 2006; Brown & Milner 2012), particular as beta diversity was higher at both high and low meltwater sites (Chapter 4), suggesting the occurrence of rare taxa through chance (re)colonization events (Lepori & Malmqvist 2009).

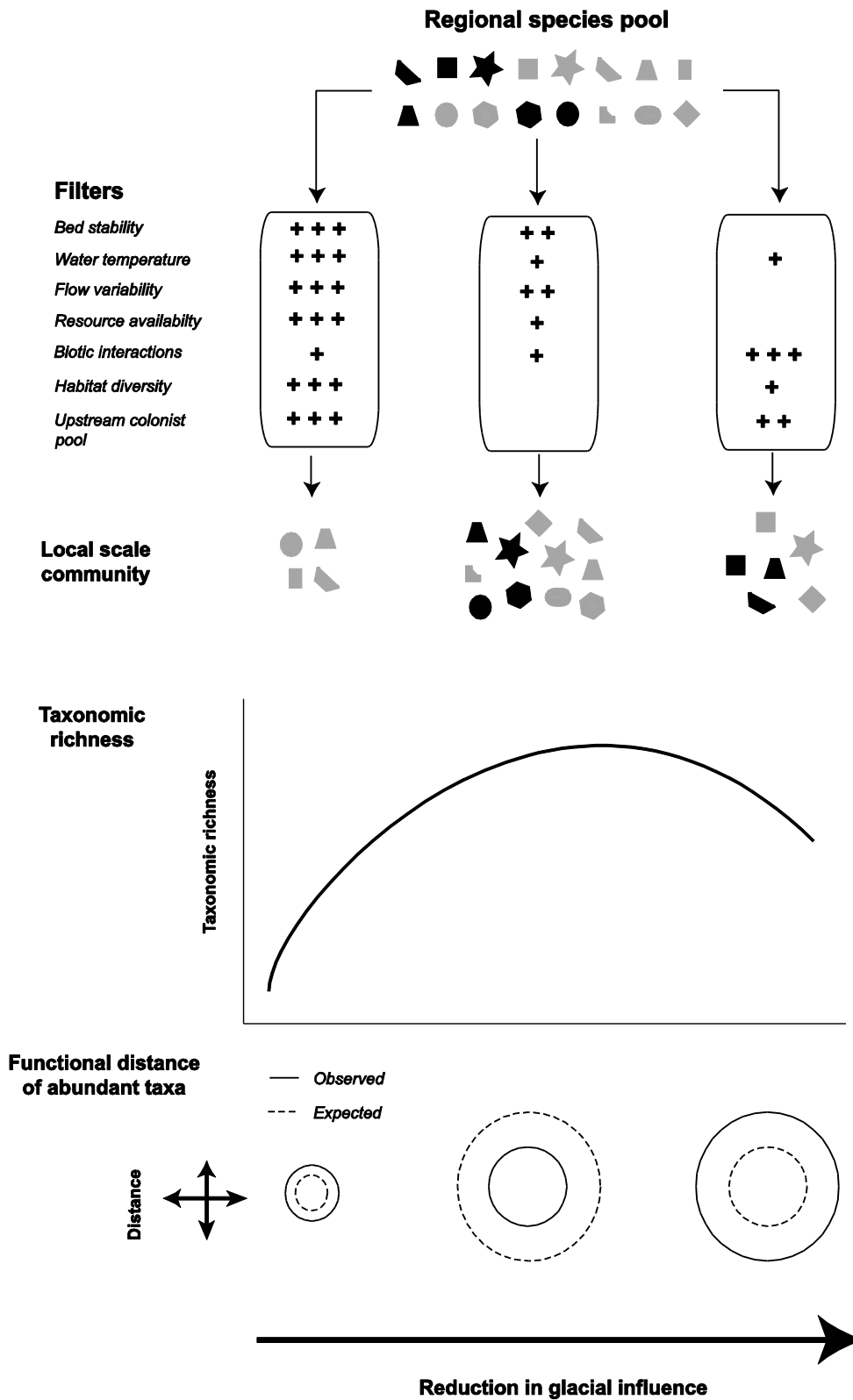


Figure 9.2. A conceptual representation of the abiotic and biotic filters that regulate local taxonomic richness and functional divergence across a gradient of glacial influence. The lowest panel depicts functional divergence of the most abundant taxa in the community, with *observed* (solid lines) representing the actual divergence, and *expected* (dashed line) representing the predicted divergence under a random colonization scenario (i.e. null model).

These findings are conceptualized in Figures 9.2 and 9.3, highlighting the potential changes in habitat, benthic community structure, functional diversity and community assembly processes as glaciers recede. A reduction in habitat harshness (e.g. a decrease in water turbidity and flow variability, and increase in water temperature) can be interpreted in the context of habitat filters (*sensu* Poff 1997) (Figures 9.2). An increased availability and diversity of food resources as glaciers recede is due to greater autotrophic production and increased allochthonous input and retention (Figure 9.3). The unimodal richness and abundance pattern (intermediate peak) is due primarily to a combination of competition-colonization tradeoffs and a reduction in biotic and abiotic filtering at sites of intermediate glacial influence (Figure 9.2). Functional diversity (Rao's QE) increases are largely due to the increase in basal resource diversity and increased trophic height of the food web, which enables more specialist taxa, occupying distinct niches, to colonise at lower meltwater (glacial influence) sites (Figure 9.3).

Community assembly processes and community structure in functional space are highlighted in 9.3c. Under high melt, environmental filtering limits the species pool to a small subset of the regional pool. However, despite low reach scale diversity, stochastic processes mean the most abundant taxa are more separated in niche space than expected under niche filtering. At intermediate levels of glacial influence, despite higher taxon richness and a relative reduction in abiotic filtering, niche filtering is the dominant community assembly process. Here, the most abundant taxa are generalists, with strong instream dispersal (colonization) abilities, hence, are closer together in niche space than expected by neutral models (i.e. trait convergence is apparent). Finally, at lower meltwater, limiting similarity is the dominant assembly mechanisms, with the most abundant taxa spread out in functional space (trait divergence; Figures 9.2 & 9.3); however, the occurrence of rare taxa due to stochastic processes may also be operating.

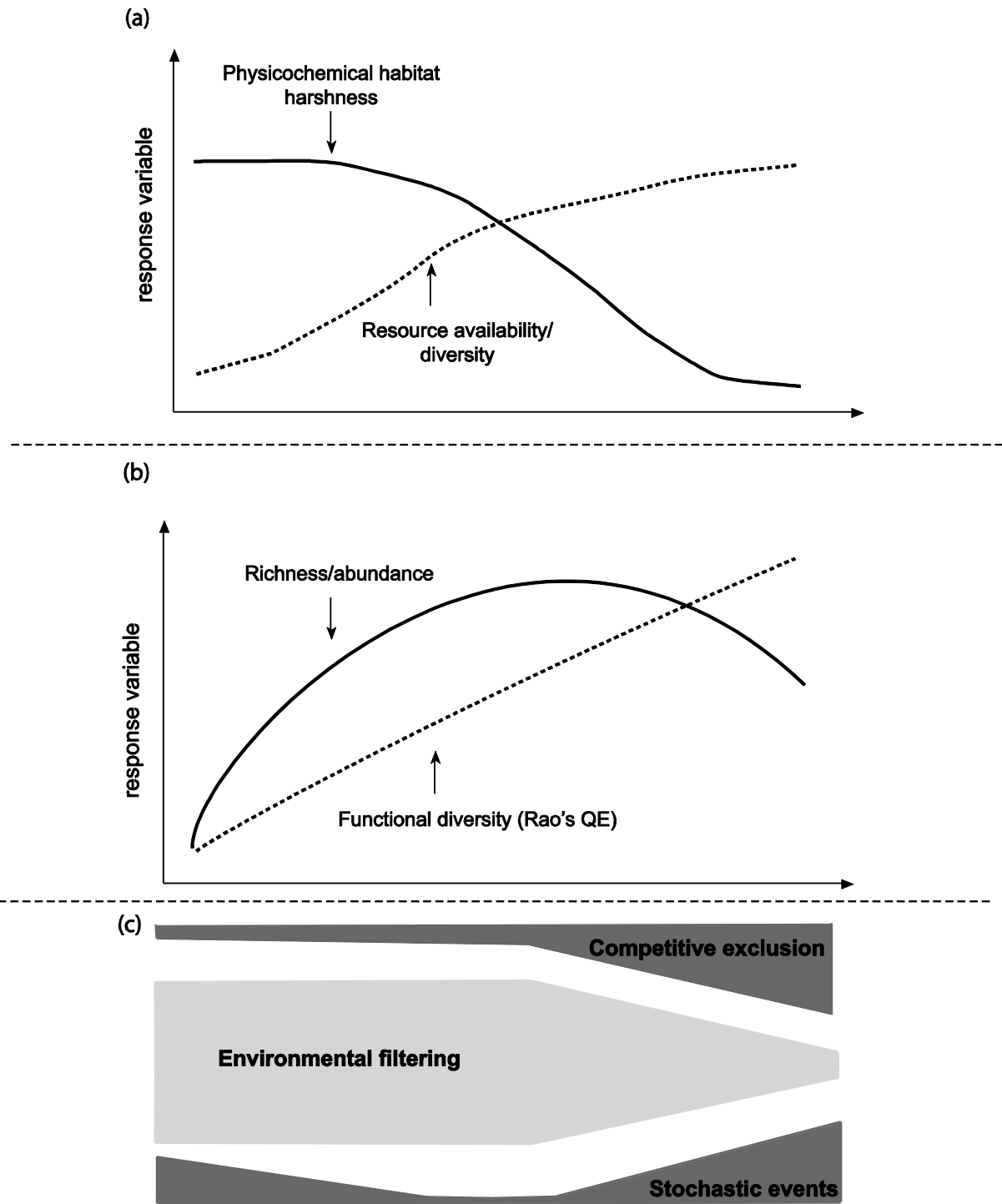


Figure 9.3. A conceptual outline of (a) alpine stream habitat parameters and (b) taxonomic and functional diversity (divergence) along a gradient of glacial influence. (c) The community assembly processes operating along the glacial influence gradient (importance of each process is depicted by the relative thickness of the box).

The interpretations and conceptualization outlined in the previous paragraphs is focused on reach scale diversity and largely ignores the implication of changes in glacier meltwater contributions for basin (beta diversity -between reach) and regional diversity (gamma diversity). Recent studies have highlighted a potential reduction in gamma and beta diversity at both the community (taxonomic; Brown *et al.* 2007; Jacobsen *et al.* 2012) and population (genetic; Finn *et al.* 2013) levels as glacier recede. This study has further validated scenarios of habitat homogenization (loss of spatial heterogeneity in water sourcing and disturbance/stress regimes) and biotic homogenization. A likely scenario of ecological change as glaciers are lost is the replacement of a low diversity, specialist community by a more diverse community, with more generalist taxa (Figure 9.4). While reach scale (α) diversity will increase, both between site (β) and regional (γ) diversity will be reduced.

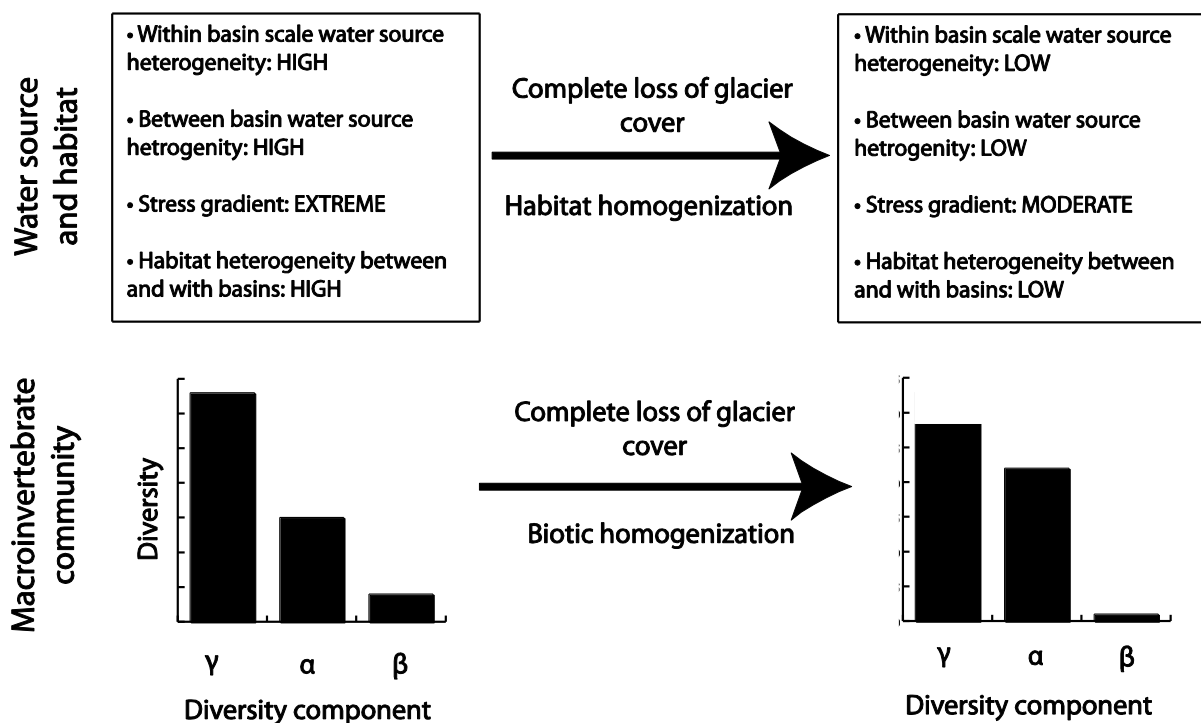


Figure 9.4. Schematic representation of the changes in water source, habitat heterogeneity and biodiversity as glaciers retreat and disappear. Loss of high meltwater habitats and associated specialist taxa reduces gamma diversity (γ). Habitat conditions become more homogenous and benign leading to an increase in reach scale diversity (α) but a reduction in between site diversity (β).

Implications for future monitoring frameworks were highlighted by findings in Chapters 4 and 5. Despite the fact this study was carried out in a single biogeographical region (Vincon & Ravizza 2001), distinct differences in the distributions of individual taxa along the meltwater gradient were apparent between sedimentary and crystalline sites (Chapter 4). However, when assessing community level metrics (e.g. taxonomic richness and EPT richness) geological differences were not apparent. These findings suggest that an indicator taxa approach may not be best suited to identify change in alpine river systems, particularly when attempting to identify a shift from mid to low glacial influence. Trait based approaches would appear to offer a more viable alternative, as they are considered to be insensitive to biogeographic variability (Vandewalle *et al.* 2010) and provide a more mechanistic link between habitat change and taxa distributions (Poff *et al.* 2010). This research highlights that life history and body shape/substrate relationship traits have potential to act as indicators of change in alpine river systems.

9.2.3. Range expansions and biotic interactions

As habitats change in response to climate change, range expansions and contractions of taxa are likely to influence biotic interactions (Gilman *et al.* 2010; Bellard *et al.* 2012). Of particular interest in alpine river systems is the ‘invasion’ of predators into regions where they were previously absent. A number of potential impacts, associated with the climate driven range expansion of *Perla grandis*, on ‘invaded’ first order stream communities were highlighted in Chapter 6. First, increased drift and decreased abundance of *Baetis* spp. were observed in treatment (*P. grandis* present) experimental stream mesocosm channels compared to control channels (*P. grandis* absent). Interestingly, this did not alter the magnitude of the trophic cascade observed in this system despite *Baetis* spp. being the most

abundant grazing taxon. This could be because the invasion was advantageous for some taxa (e.g. chironomids) and a stress for other taxa (i.e. *Baetis* spp.) (Strayer *et al.* 2006). Hence, it appears any reductions in the grazing rates of individual taxa were offset by increases in the grazing rates of others.

Second, new/increased interactions between *P. grandis* and the current top invertebrate predator, *Rhyacophila intermedia*, were identified as *R. intermedia* suffered asymmetrical intraguild predation and appeared to actively avoid *P. grandis*. The apparent increase in trophic height, due to the more generalist predator (*P. grandis*) being able to incorporate other predators into its diet, is likely to result in food webs with a higher link density (König *et al.* 2011; Clitherow *et al.* 2013). Hence, as the climate warms and habitats become more benign, changes in trophic interactions amongst the predator guild and an increase in trophic height is likely (McHugh *et al.* 2010), with implications for food web functioning and stability (Rooney & McCann 2012).

Third community body size was altered in the presence of *P. grandis* with a positive skew to a smaller mean body size apparent. This was due to: (i) other large bodied predators avoiding channels containing *P. grandis*; and (ii) size selective predation and/ or size specific predator avoidance. The alteration of community size spectrum can have ramifications for community stability and ecosystem functioning (Woodward *et al.* 2005). It is, however, difficult to predict how such changes will propagate through the foodweb in alpine systems as changes in interaction strength and omnivory can destabilize and stabilize, respectively (Borrvall *et al.* 2000). Further work is needed to quantify how these changes in body size spectra and trophic interactions will alter alpine aquatic foodweb structure and stability.

9.2.4. Stream temperature dynamics and heat exchange

Cryosphere loss is likely to have a significant impact on alpine stream water temperature (Fellman *et al.* 2013); yet, in Chapter 3 the relationship between glacial influence and water temperature appeared to be modified by other drivers (e.g. basin geomorphology, aspect and water source dynamics). Detailed point scale analysis of stream temperature dynamics presented in Chapter 7 identified a number of important hydrological and meteorological drivers of water temperature variations. Of these, discharge and altitude of the snow line are particularly sensitive to future climate change (Fatichi *et al.* 2013). Decreases in discharge magnitude will reduce the thermal capacity of the water column (Poole & Berman 2001) and a reduction in snow cover extent will increase stream exposure to the atmosphere, while reducing non-glacial cold water inputs (Blaen *et al.* 2013b). Furthermore, distances between streams and glacier margins will be increased with implications for warming rates (Magnusson *et al.* 2012a). Statistical models based on these variables and other meteorological variables (i.e. air temperature) may successfully predict monthly and weekly mean water temperature (van Vliet *et al.* 2012), but the accurate prediction of diurnal temperature dynamics is not possible. This is an issue when considering implications of climate change for salmonids (Isaak *et al.* 2010) and cold stenothermic macroinvertebrates (Domisch *et al.* 2013) as the daily maximum/minimum temperatures, which are biologically more important than mean daily/weekly mean temperature, are not predicted using statistical air temperature – water temperature relationships.

Energy balance or heat budget models reproduce more accurately diurnal temperature variability and are conducive to scenario modelling (e.g. different glacier cover extents or mitigation strategies) (Caissie 2006). However, our understanding of the heat exchange

fluxes in alpine, glacier-fed, river systems is based on a handful of studies, all of which have been carried out over relatively short time periods. Findings presented in Chapter 7 represent the first inter-annual energy balance study for a glacier fed stream and highlight the dominant energy exchange processes (net radiation and sensible heat exchange) and the most variable energy balance component, at both inter annual and sub-seasonal time steps (latent heat). Application of an un-calibrated energy balance model improved physical process understanding and highlighted potential future research directions. Changing water source as the season progressed (i.e. meltwater to groundwater) caused systematic errors in the model suggesting there is a need to represent these hydrological processes in deterministic models. Evening and nocturnal systematic under estimation of water temperature suggested that within channel advective heat transport and wetted channel network expansion/contraction cycles are likely important controls on heat exchange, which also needs to be represented in future models (Carrivick *et al.* 2012).

9.2.5. Modelling river ecosystem change in alpine environments

A framework for predicting alpine river ecosystem responses to climate change (Figure 8.1) was outlined in Chapter 8. Projected cryospheric and hydrological responses were in line with other studies from the Pyrénées (López-Moreno *et al.* 2009) and from other regions (Fatichi *et al.* 2013). A marked reduction in the total magnitude and change in the seasonality of the annual flow regime is likely to have implications for socioeconomic practices (Beniston 2012) and ecological systems (Milner *et al.* 2009). A particular concern is the loss of late summer flow compensation from ice melt as glaciers disappear, coupled with the reduction in transient snowpack size (reduced fraction of precipitation falling as snow). This reduction in precipitation storage pertains to a more unpredictable and precipitation dependent future flow

regime. These predictions have been incorporated into the schematic representation of glacier size and associated runoff magnitude and melt season flow regime presented in Chapter 1 (Figure 9.5). Based on findings outlined in Chapter 8, an additional scenario (D) has been added to the conceptual representation which represents both the loss of glacier cover and a future climate scenario (i.e. 2060-2080). The snow melt discharge peak shifts from June (scenarios A-C) to May and summer low flow is punctuated by high intensity convective storms which only partially recharge alluvial aquifers (Winograd *et al.* 1998), finally in Autumn (October/November) precipitation over high ground falls as rain rather than snow, thus the increase in flow during this period (Figure 9.5).

Using a dose-response relationship model (i.e. glacier cover – taxa abundance relationship), changes in the abundance of taxa representing key groups (i.e. predator, shredder, grazer, filter and cold stenotherm) were simulated based on projected changes in glacier cover (Chapter 8). The model predicted a loss of a cold stenotherm (*Diamesa latitarsis* gr.) from within the Taillon-Gabiétous basin by 2070. The replacement of glacier stream specialists (i.e. cold stenotherms) by more generalist shredding, grazing and filtering taxa (e.g. *Leuctra* spp., *Rhithrogena* spp. and *Simulium* spp.) is a key finding. While an increase in secondary production may be beneficial for insectivorous terrestrial species such as the European dipper (*Cinclus cinclus*) and Pyrenean Desman (*Galemys pyrenaicus*), the predicted replacement of the glacial stream specialist adds weight to previous suggestions of reduced gamma and beta diversity as glaciers recede (Brown *et al.* 2007a; Jacobsen *et al.* 2012; Finn *et al.* 2013). The effect of changes in macroinvertebrate structure on ecosystem functioning is still largely unknown and a key research gap which needs to be addressed (Khamis *et al.* 2013; Appendix A).

The findings synthesised above highlight important considerations and caveats regarding the application and interpretation of the climate-hydrology-ecology predictive framework (Figure 1.2.; Figure 8.1). First, the potential filtering effect of macro-basin properties needs to be considered when linking the water source to physicochemical habitat characteristics (Figure 9.6). Second, the feedback mechanisms within the biodiversity/ biotic component of the process chain need to be considered, some of which were highlighted in Chapter 6. It is likely that a range of other biotic feedbacks will occur in synergy (Bellard *et al.* 2012) such as changes in phenology, metabolic rates, fecundity and growth rates (Figure 9.6). These biotic changes are likely to have significant impacts on both biodiversity and network stability (e.g. phenological mismatches; Durant *et al.* 2007) and ecosystem functioning (e.g. changes in allometric scaling could alter resource turnover rates; Woodward *et al.* 2010) Thus, the modelling results in Chapter 8 and synthesis above must be interpreted with some caution.

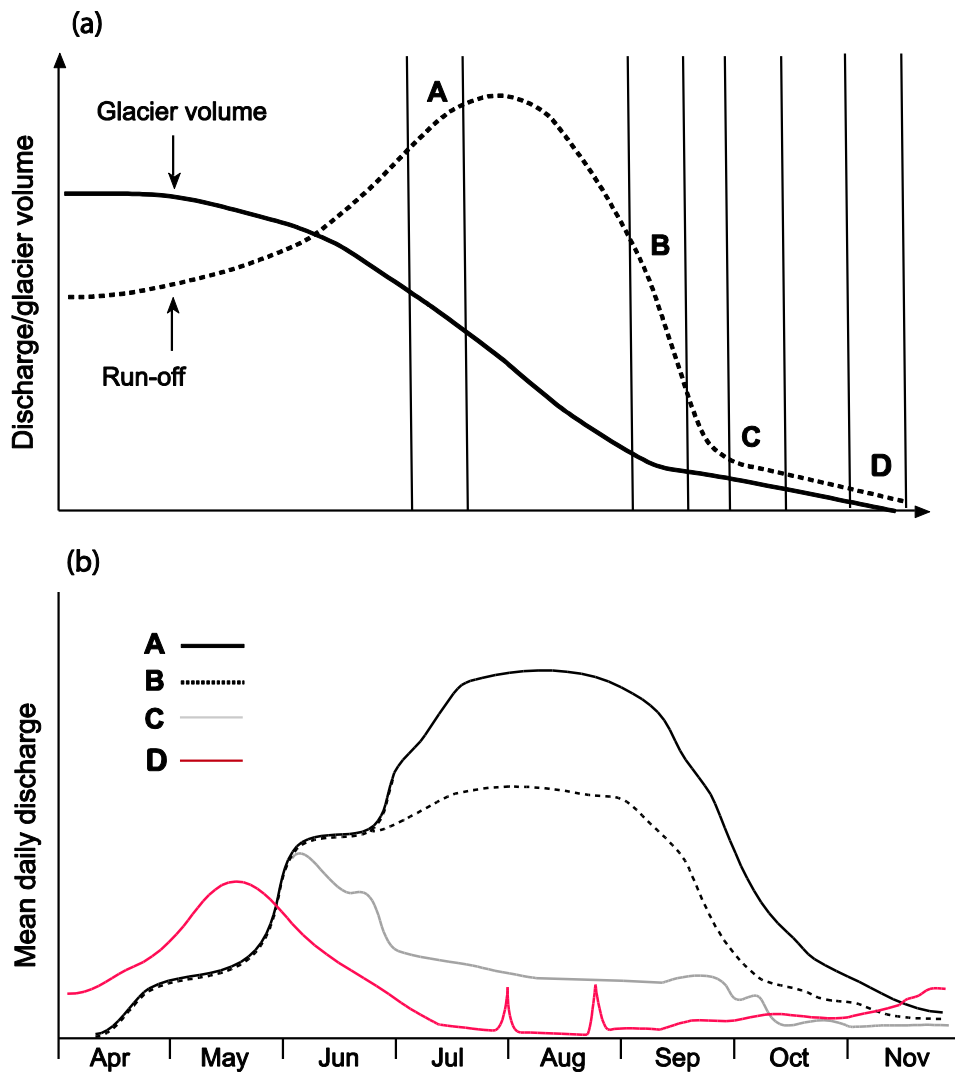


Figure 9.5. (a) Hypothetical responses of runoff magnitude to changes in glacier volume and (b) smoothed glacial melt season flow regimes associated with four stages along a continuum of glacier retreat. Scenario D represents glacier loss and a future climate scenario (e.g. post 2050).

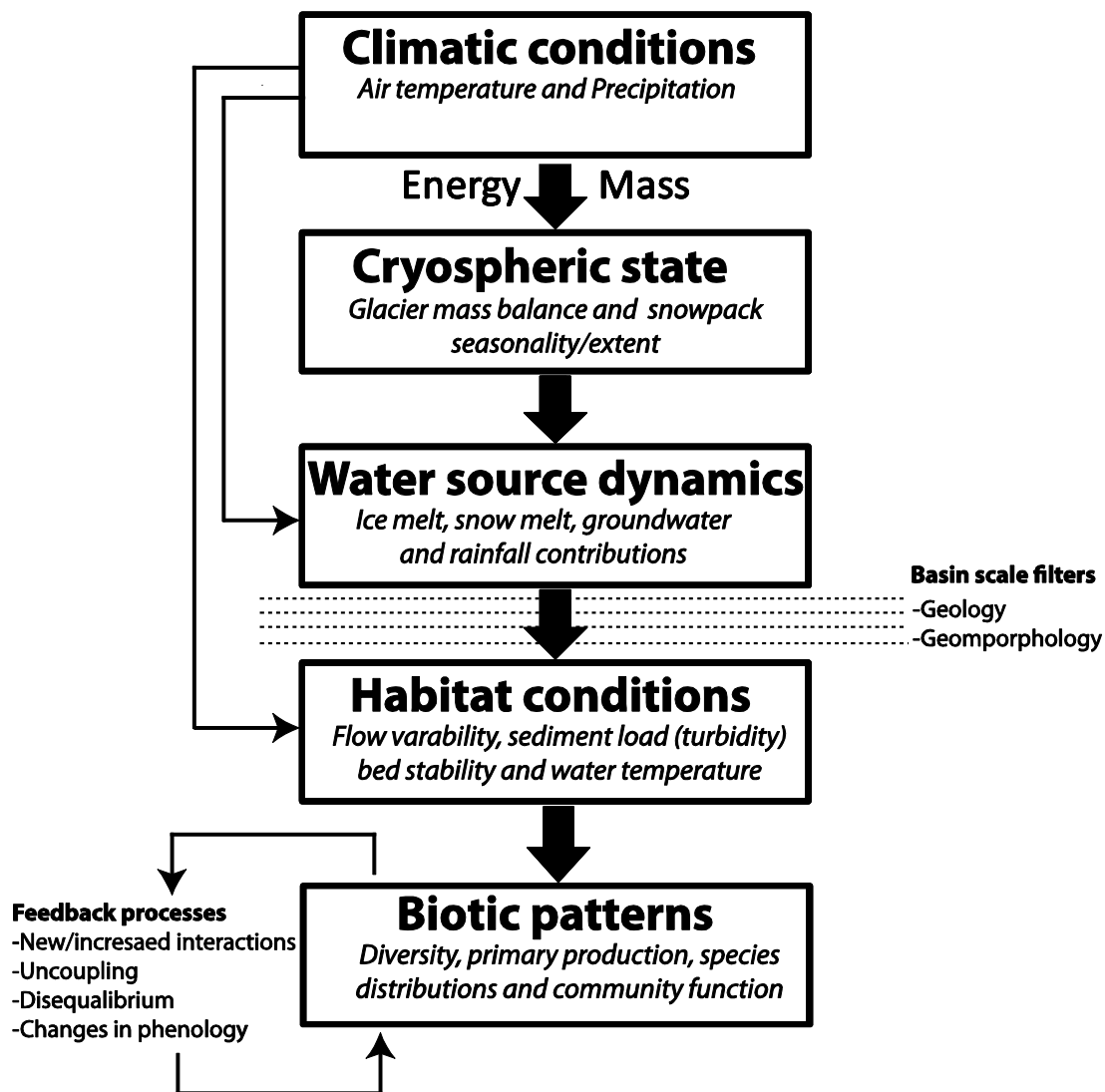


Figure 9.6. A modified conceptual representation of the linkages between climate-hydrology –ecology. The filtering effect of macro-basin characteristic and potential biotic feedback mechanisms are now highlighted.

9.3. Further research avenues

There is significant scope for further research in alpine river systems to improve monitoring strategies and predictive models. There is also potential for testing ecological theory due to the relatively simple communities and steep environmental gradients. In this section specific research avenues identified by, or specifically relevant to the results chapters will be highlighted.

- There is an urgent need to improve understanding of the relationships between biodiversity and ecosystem functioning in alpine systems (khamis *et al.* 2013; Appendix A). This will likely need to involve work at the microbial level, as recent research (e.g. Freimann *et al.* 2013a) has highlighted the potential for microbial communities to buffer the potential impacts of loss of glacier runoff on ecosystem functioning.
- Further validation of the climate cascade predictive framework is required in other glacierized river basins, particularly given that as it was developed (Hannah *et al.* 2007) and tested (this thesis) in a single Pyrenean river basin. Hence, the transferability of this approach is still largely unknown and given the diverse range of glacierized river systems (e.g. Arctic, equatorial, temperate mountain and lowland coastal) this represents a future research imperative. However, future study catchments need to be carefully selected with the following data prerequisites: (i) comprehensive historical flow records; (ii) glacier mass balance data; and (iii) historical ecological records. A robust assessment, as such, will highlight the utility of the climate cascade predictive framework as a potential tool for river basin managers to better plan and direct future conservation measures.

- A more rigorously test of the trait based monitoring approach (outlined in Chapter 5) is required to assess fully its potential as a tool for identifying environmental change in alpine river systems. This would require analysis of biological trait-glacial influence relationships to be extended to incorporate multiple biogeographical regions and covering a latitudinal gradient. Ideally, field sampling should include Arctic, temperate alpine, equatorial (i.e. Andes) and also island (e.g. Iceland and New Zealand) sites to incorporate the range of glacier types and associated hydrological regimes along with the reduced species pool associated with islands. It may also be useful to refine trait databases for alpine taxa. In particular, a shift to focus on traits more specific to alpine environments (e.g. freeze tolerance) and work to improve trait resolution for dipteran taxa would be beneficial.
- Further work is required to test the ‘filtering’ effect of macro-basin scale properties and valley segment/reach scale geomorphic processes on the glacier melt – physicochemical habitat and glacier melt – biodiversity relationships. In particular the importance of channel processes (e.g. colluvial/alluvial), which can vary at the within basin scale, need to be assessed (Weekes *et al.* 2012). This will need to involve two approaches potentially: (i) long(er) term monitoring to identify how a certain basin/valley/reach type will respond to observed changes in glacier influence (retreat); and (ii) large scale meta-analysis and synthesis of currently published disparate data sets, to isolate potential filtering effect on glacier–habitat–biodiversity relationships.
- The links between meltwater contribution-river habitat–biodiversity was explored in Chapter 4 and the role of stress/disturbance was highlighted as a key driver of

community and population level diversity and abundance patterns. However, there remains a distinct need to undertake paired catchment studies to compare similar streams (i.e. comparable altitude, discharge, slope and geology) with and without glacial influence (Füreder *et al.* 2005). This will enable the effects of downstream increases in stream size, water temperature and size of the upstream colonist pool to be separated from those associated with changes in meltwater contribution.

- To understand better the mechanisms driving richness and abundance peaks at sites of intermediate glacial influence, an experimental approach could be adopted to isolate the colonisation and community succession dynamics. For example, recording colonisation rates (substrate baskets) and drift rates at monitoring sites across the gradient of glacier influence (Death 1996; Winterbottom *et al.* 1997) could improve understanding of coexistence mechanisms operating (e.g. colonization-competition tradeoffs). Furthermore, disturbance of patches (substrate baskets) could be manipulated in a controlled experiment to create a gradient of successional states. This would contribute also to general ecological theory as empirical tests of meta-community theory and coexistence mechanisms are limited (Roxburgh *et al.* 2004; Logue *et al.* 2011).
- Current knowledge of connectance foodwebs in alpine river systems is based on findings from highly glacial (Clitherow *et al.* 2013) and non glacial stream reaches (Lavandier & Decamps 1984). Thus, it would be useful to construct foodwebs for reach scale communities covering the full spectrum of glacial influence; from highly glacial to groundwater fed (no glacial influence) reaches. This would improve our understanding of how these ecological networks are likely to respond as glacier

recede and disappear. Furthermore, it will improve our understanding of resource overlap and apparent completion in these systems enabling corroboration of community assembly processes identified using null model approaches.

- It is becoming increasingly clear that space for time substitutions do not provide a sufficient basis for predicting the future effects of climate change on stream water temperature in glacier fed systems due to basin specific controls on thermal regimes (Chapter 3; Moore *et al.* 2009, Blaen *et al.* 2013). Thus, further work on the energy balance of glacial fed streams is required to improve process understanding and refine deterministic stream temperature models to enable more robust prediction of change. As highlighted in this thesis (Chapter 7) the role of in stream heat advection and glacial river network expansion cycles in warming and cooling the stream both need to be quantified. Higher spatial resolution sampling using Distributed Temperature Sensors (DTS) may provide a useful insight into the importance of this processes and whether it needs to be incorporated in the development of future deterministic models. The logistical constraints of high alpine field work may, however, be an issue for installation of DTS. This would need careful consideration but with sufficient funding a helicopter could be used for installation and retrieval.
- The impacts of multiple predators on prey behaviour and community structure have been highlighted (Sih *et al.* 1998). Further work investigating the impacts of potential range expansions of both invertebrate (e.g. *P. grandis*), and vertebrate predators (e.g. *Calotriton asper* and *Salmo trutta*), would be useful for unravelling the synergistic effects of (novel) biotic interactions and climate change (Gilman *et al.* 2010). A factorial experimental approach would enable the potential impacts of decoupling

(e.g. *P. grandis* and *S. trutta*) and novel interactions (e.g. *C. asper* and *S. trutta*) on alpine biodiversity to be assessed.

9.4. Concluding remarks

This thesis has improved our understanding of the process connections (i.e. cryosphere-watersource-habitat-biota) operating in alpine river ecosystems. Potential filters (e.g. macro-scale basin properties) and feedbacks (e.g. novel biotic interactions) to this chain of interlinked processes have also been highlighted and thus need careful consideration when making inferences regarding projected hydroecological change in these systems. As both empirical observation and statistical modelling point towards a loss of beta and gamma diversity, primarily due to habitat homogenization and extinctions, there is a distinct need for more coherent monitoring strategies. Findings presented in this thesis provide a first ‘testbed’ for use and interpretations of the multiple methods for quantifying environmental change in glacier-fed river systems, which can hopefully facilitate a more unified approach to monitoring in alpine river systems. In addition, the potential utility of functional trait profiles for detecting future change had been raised but requires testing over multiple biogeographical regions.

Finally, the climate cascade conceptual framework (Hannah *et al.* 2007) has the potential to be a particularly useful tool for scenario testing alpine river ecosystem change. A first approximation of both hydrological and ecological patterns was derived from large scale atmospheric circulation patterns and represents a distinct step forward, as previously predictions have been based on conceptual models and inference from observational data (Milner *et al.* 2009). Refinement of this predictive tool is now required to both highlight

priority habitats for conservation (i.e. those with sufficient ice mass to buffer against climate change), and enable more informed management strategies to be devised for threatened alpine river ecosystems (Khamis *et al.* 2013).

REFERENCES

- Adam JC, Hamlet AF, Lettenmaier DP (2009) Implications of global climate change for snowmelt hydrology in the twenty-first century. *972*, 962–972.
- Akhtar M, Ahmad N, Booij MJ (2008) The impact of climate change on the water resources of Hindukush – Karakorum – Himalaya region under different glacier coverage scenarios. *Journal of Hydrology*, **355**, 148–163.
- Allan D (1982) Feeding habits and prey consumption of three setipalpiid stoneflies (Plecoptera) in a mountain stream. *Ecology*, **63**, 26–34.
- Allan JD, Flecker AS, McClintock NL (1987) Prey size selection by carnivorous stoneflies. *Limnology and Oceanography*, **32**, 864–872.
- Almodóvar A, Nicola GG, Ayllón D, Elvira B (2012) Global warming threatens the persistence of Mediterranean brown trout. *Global Change Biology*, **18**, 1549–1560.
- Anderson MJ, Crist TO, Freestone AL, Sanders NJ (2011) Navigating the multiple meanings of beta diversity: a roadmap for the practicing ecologist. *Ecology Letters*, **14**, 19–28.
- Anderson SP, Drever JI, Frost C, Holden P (2000) Chemical weathering in the foreland of a retreating glacier. *Geochimica et Cosmochimica Acta*, **64**, 1173–1189.
- Anderton SP, Latron J, White SM, Llorens P, Gallart F, Salvany C, O’Connell PE (2002) Internal evaluation of a physically-based distributed model using data from a Mediterranean mountain catchment. *Hydrology and Earth System Sciences*, **6**, 67–84.
- Anderton SP, White SM, Alvera B (2004) Evaluation of spatial variability in snow water equivalent for a high mountain catchment. *Hydrological Processes*, **18**, 435–453.
- Araújo MB, Luoto M (2007) The importance of biotic interactions for modelling species distributions under climate change. *Global Ecology and Biogeography*, **16**, 743–753.
- Association Moraine Pyrénéenne de Glaciologie (2009) *Les glaciers des Pyrénées françaises Rapport d’ étude 2008-09*. Association Moraine Pyrénéenne de Glaciologie: Luchons, France (www.moraine.fr.st).
- Bady P, Doledec S, Fesl C, Gayraud S, Bacchi M, Scholl F (2005) Use of invertebrate traits for the biomonitoring of European large rivers: the effects of sampling effort on genus richness and functional diversity. *Freshwater Biology*, **50**, 159–173.
- Barnett TP, Adam JC, Lettenmaier DP (2005) Potential impacts of a warming climate on water availability in snow-dominated regions. *Nature*, **438**, 303–309.
- Del Barrio G, Creus J, Puigdefabregas J (1990) Thermal seasonality of the high mountain belts of the Pyrenees. *Mountain Research and Development*, **10**, 227–233.
- Barry S, Welsh AH (2002) Generalized additive modelling and zero inflated count data. *Ecological Modelling*, **157**, 179–188.

- Bechara J., Moreau G, Hare L (1993) The impact of brook trout (*Salvelinus fontinalis*) on an experimental stream benthic community : the role of spatial and size refugia. *Journal of Animal Ecology*, **62**, 451–464.
- Beche L a., Mcelravy EP, Resh VH (2006) Long-term seasonal variation in the biological traits of benthic-macroinvertebrates in two Mediterranean-climate streams in California, U.S.A. *Freshwater Biology*, **51**, 56–75.
- Bellard C, Bertelsmeier C, Leadley P, Thuiller W, Courchamp F (2012) Impacts of climate change on the future of biodiversity. *Ecology Letters*, **15**, 365–377.
- Beniston M (2012) Impacts of climatic change on water and associated economic activities in the Swiss Alps. *Journal of Hydrology*, **412-413**, 291–296.
- Beniston M, Diaz HF, Bradley RS (1997) Climatic change at high elevation sites: an overview. *Climatic Change*, **36**, 233–251.
- Benjamin JR, Fausch KD, Baxter C V (2011) Species replacement by a nonnative salmonid alters ecosystem function by reducing prey subsidies that support riparian spiders. *Oecologia*, **167**, 503–12.
- Benyahya L, Caissie D, Satish MG, El-jabi N (2012) Long-wave radiation and heat flux estimates within a small tributary in Catamaran Brook (New Brunswick, Canada). *Hydrological Processes*, **484**, 475– 484.
- Biggs BJJ, Gerbeaux P (1993) New Zealand Journal of Marine and Freshwater Research Periphyton development in relation to macro-scale (geology) and micro-scale (velocity) limiters in two gravel bed rivers, New Zealand. *New Zealand Journal of Marine and Freshwater Research*, **27**, 37–41.
- Blaen PJ, Hannah DM, Brown LE, Milner AM (2013a) Water source dynamics of high Arctic river basins. *Hydrological Processes*.
- Blaen PJ, Hannah DM, Brown LE, Milner AM (2013b) Water temperature dynamics in High Arctic river basins. *Hydrological Processes*, **27**, 2958–2972.
- Bo T, Fenoglio S, López-Rodríguez MJ, Tierno de Figueroa JM (2008) Trophic behavior of two Perlidae species (Insecta, Plecoptera) in a river in Southern Spain. *International Review of Hydrobiology*, **93**, 167–174.
- Bo T, Fenoglio S, López-Rodríguez MJ, Tierno de Figueroa JM, Grenna M, Cucco M (2010) Do predators condition the distribution of prey within micro habitats? An experiment with Stoneflies (Plecoptera). *International Review of Hydrobiology*, **95**, 285–296.
- Bonada N, Dolédec S, Statzner B (2007) Taxonomic and biological trait differences of stream macroinvertebrate communities between mediterranean and temperate regions: implications for future climatic scenarios. *Global Change Biology*, **13**, 1658–1671.
- Bongers T, Ferris H (1999) Nematode community structure as a bioindicator in environmental monitoring. *Trends in Ecology & Evolution*, **14**, 224–228.

- Borrvall C, Ebenman B, Jonsson T (2000) Biodiversity lessens the risk of cascading extinction in model food webs. *Ecology Letters*, **3**, 131–136.
- Botta-Dukát Z (2005) Rao's quadratic entropy as a measure of functional diversity based on multiple traits. *Journal of Vegetation Science*, **16**, 533–540.
- Bottazzi E, Bruno MC, Pieri V, Sabatino ADI, Silveri L (2011) Spatial and seasonal distribution of invertebrates in Northern Apennine rheocene springs. *Journal of Limnology*, **70**, 77–92.
- Bowen I (1926) The ratio of heat losses by conduction and by evaporation from any water surface. *Physics Review*, **27**, 779–787.
- Brittain JE (2007) Mayflies, biodiversity and climate change. In: *International advances in the ecology, zoogeography and systematics of mayflies and stoneflies* (eds: Hauer FR, Stanford JA, Newell RL), pp1–14. University of California Publications in Entomology, vol. 1.
- Brock BW, Arnold NS (2000) A spreadsheet-based (Microsoft Excel) point surface energy balance model for glacier and snow melt studies. *Earth Surface Processes and Landforms*, **25**, 649–658.
- Brock BW, Willis IC, Sharp MJ (2000) Measurement and parameterisation of albedo variations at Haut Glacier d'Arolla, Switzerland. *Journal of Glaciology*, **46**, 675–688.
- Brodeur RD (1998) Prey selection by age-0 walleye pollock, *Theragra chalcogramma*, in nearshore waters of the Gulf of Alaska. *Environmental Biology of Fishes*, **51**, 175–186.
- Brookshire ENJ, Dwire KA (2003) Controls on patterns of coarse organic particle retention in headwater streams. *Journal of the North American Benthological Society*, **22**, 17–34.
- Brown GW (1969) Predicting temperatures of small streams. *Water Resources Research*, **5**, 68–75.
- Brown GH (2002) Glacier meltwater hydrochemistry. *Applied Geochemistry*, **17**, 855–883.
- Brown LE (2005) Hydroecological response of alpine streams to dynamic watersource contributions. PhD Thesis, University of Birmingham, UK.
- Brown LE, Cooper L, Holden J, Ramchunder SJ (2010a) A comparison of stream water temperature regimes from open and afforested moorland, Yorkshire Dales, northern England. *Hydrological Processes*, **24**, 3206–3218.
- Brown LE, Céréghino R, Compin A (2009a) Endemic freshwater invertebrates from southern France: Diversity, distribution and conservation implications. *Biological Conservation*, **142**, 2613–2619.
- Brown LE, Edwards FK, Milner AM, Woodward G, Ledger ME (2011) Food web complexity and allometric scaling relationships in stream mesocosms: implications for experimentation. *The Journal of Animal Ecology*, **80**, 884–95.

- Brown LE, Hannah DM (2008) Spatial heterogeneity of water temperature across an alpine river basin. *Hydrological Processes*, **22**, 954–967.
- Brown LE, Hannah DM, Milner AM (2003) Alpine stream habitat classification : an alternative approach incorporating the role of dynamic water source contributions. *Arctic, Antarctic, and Alpine Research*, **35**, 313–322.
- Brown LE, Hannah DM, Milner AM (2005) Spatial and temporal water column and streambed temperature dynamics within an alpine catchment: implications for benthic communities. *Hydrological Processes*, **19**, 1585–1610.
- Brown LE, Hannah DM, Milner AM (2006a) Hydroclimatological influences on water column and streambed thermal dynamics in an alpine river system. *Journal of Hydrology*, **325**, 1–20.
- Brown LE, Hannah DM, Milner AM (2006b) Short communication thermal variability and stream flow permanency in an alpine river system. *River Research and Applications*, **501**, 493–501.
- Brown LE, Hannah DM, Milner AM (2006c) Thermal variability and stream flow permanency in an alpine river system. *River Research and Applications*, **22**, 493–501.
- Brown LE, Hannah DM, Milner AM (2007a) Vulnerability of alpine stream biodiversity to shrinking glaciers and snowpacks. *Global Change Biology*, **13**, 958–966.
- Brown LE, Hannah DM, Milner AM, Soulsby C, Hodson AJ, Brewer MJ (2006d) Water source dynamics in a glacierized alpine river basin (Taillon-Gabiétous, French Pyrénées). *Water Resources Research*, **42**, W08404.
- Brown LE, Milner AM (2012) Rapid loss of glacial ice reveals stream community assembly processes. *Global Change Biology*, **18**, 2195–2204.
- Brown LE, Milner AM, Hannah DM (2007b) Hydroecology of alpine rivers. In: *Hydroecology and Ecohydrology: Past, Present and Future* (eds: Wood PJ, Hannah DM, Sadler JP), pp339–360. John Wiley and Sons: Hoboken, NJ.
- Brown LE, Milner AM, Hannah DM (2007c) Groundwater influence on alpine stream ecosystems. *Freshwater Biology*, **52**, 878–890.
- Brown LE, Milner AM, Hannah DM (2009b) ARISE: a classification tool for Alpine River and Stream Ecosystems. *Freshwater Biology*, **54**, 1357–1369.
- Brown LE, Milner AM, Hannah DM (2010b) Predicting river ecosystem response to glacial meltwater dynamics: a case study of quantitative water sourcing and glaciality index approaches. *Aquatic Sciences*, **72**, 325–334.
- Buisson L, Grenouillet G (2009) Contrasted impacts of climate change on stream fish assemblages along an environmental gradient. *Diversity and Distributions*, **15**, 613–626.

- Buse A (1973) Goodness of fit in generalized least squares estimation. *The American Statistician*, **27**, 106–108.
- Buyse J (1993) *Los tresmiles del Pirineo*. Ediciones Martin Roca SA, Barcelona.
- Bücher A, Dessens J (1991) Secular trend of surface temperature at an elevated observatory in the Pyrenees. *Journal of Climate*, **4**, 859–868.
- Cadbury SL, Hannah DM, Milner AM, Pearson CP, Brown LE (2008) Stream temperature dynamics within a New Zealand glacierized river basin. *River Research and Applications*, **89**, 68–89.
- Cadbury SL, Milner AM, Hannah DM (2011) Hydroecology of a New Zealand glacier-fed river: linking longitudinal zonation of physical habitat and macroinvertebrate communities. *Ecohydrology*, **4**, 520–531.
- Cadotte MW, Carscadden K, Mirotchnick N (2011) Beyond species: functional diversity and the maintenance of ecological processes and services. *Journal of Applied Ecology*, **48**, 1079–1087.
- Caissie D (2006) The thermal regime of rivers: a review. *Freshwater Biology*, **51**, 1389–1406.
- Caissie D, Satish MG, El-jabi N (2005) Predicting river water temperatures using the equilibrium temperature concept with application on Miramichi River catchments (New Brunswick, Canada). *Hydrological Processes*, **19**, 2137–2159.
- Caissie D, Satish M, Eljabi N (2007) Predicting water temperatures using a deterministic model: Application on Miramichi River catchments (New Brunswick, Canada). *Journal of Hydrology*, **336**, 303–315.
- Calvet M (2004) The Quaternary glaciation of the Pyrenees. *Developments in Quaternary Sciences*, **2**, 119–128.
- Campbell Grant EH, Lowe WH, Fagan WF (2007) Living in the branches: population dynamics and ecological processes in dendritic networks. *Ecology letters*, **10**, 165–75.
- Cantonati M, Füreder L, Gerecke R, Jüttner I, Cox EJ (2012) Crenic habitats, hotspots for freshwater biodiversity conservation: toward an understanding of their ecology. *Freshwater Science*, **31**, 463–480.
- Cardinale BJ, Hillebrand H, Charles DF (2006) Geographic patterns of diversity in streams are predicted by a multivariate model of disturbance and productivity. *Journal of Ecology*, **94**, 609–618.
- Carenzo M, Pellicciotti F, Rimkus S, Burlando P (2009) Assessing the transferability and robustness of an enhanced temperature-index glacier-melt model. *Journal of Glaciology*, **55**, 258–274.

- Carrivick JL, Brown LE, Hannah DM, Turner AGD (2012) Numerical modelling of spatio-temporal thermal heterogeneity in a complex river system. *Journal of Hydrology*, **414-415**, 491–502.
- Castella E, Adalsteinsson H, Brittain JE, *et al.* (2001) Macrobenthic invertebrate richness and composition along a latitudinal gradient of European glacier-fed streams. *Freshwater Biology*, **46**, 1811–1831.
- Cauvy-Fraunié S, Andino P, Espinosa R, Calvez R, Anthelme F, Jacobsen D, Dangles O (2013a) Glacial flood pulse effects on benthic fauna in equatorial high-Andean streams. *Hydrological Processes*.
- Cauvy-Fraunié S, Condom T, Rabatel a., Villacis M, Jacobsen D, Dangles O (2013b) Technical Note: Using wavelet analyses on water depth time series to detect glacial influence in high-mountain hydrosystems. *Hydrology and Earth System Sciences Discussions*, **10**, 4369–4395.
- Chase JM, Abrams PA, Grover JP, *et al.* (2002) The interaction between predation and competition: a review and synthesis. *Ecology Letters*, **5**, 302–315.
- Chen J, Brissette FP, Leconte R (2011a) Uncertainty of downscaling method in quantifying the impact of climate change on hydrology. *Journal of Hydrology*, **401**, 190–202.
- Chen IC, Hill JK, Ohlemüller R, Roy DB, Thomas CD (2011b) Rapid range shifts of species associated with high levels of climate warming. *Science*, **333**, 1024–1026.
- Chessel D, Dufour AB, Thioulouse J (2004) The ade4 package - I: One-table methods. *R News*, **4**, 5–10.
- Chesson P, Huntly N (1997) The role of harsh and fluctuating conditions in the dynamics of ecological communities. *American Naturalist*, **150**, 519–553.
- Chevenet F, Dolédec S, Chessel D (1994) A fuzzy coding approach for the analysis of long-term ecological data. *Freshwater Biology*, **31**, 295–309.
- Chikita KA, Kaminaga RYO, Kudo I, Kim Y (2010) Parameters determining water temperature of a proglacial stream: the Phelan creek and Gulkana glacier, Alaska. *River Research and Applications*, **26**, 995–1004.
- Christensen JH, Kjellstrom E, Giorgi F, Lenderink, G., Rummukainen M (2010) Weight assignment in regional climate models. *Climate Research*, **44**, 179–194.
- Christophersen N, Hooper RP (1992) Multivariate analysis of stream water chemical data: the use of principal components analysis for the end-member mixing problem. *Water Resources Research*, **28**, 99–107.
- Ciarapica L, Todini E (2002) TOPKAPI: a model for the representation of the rainfall-runoff process at different scales. *Hydrological Processes*, **16**, 207–229.

- Clitherow LR, Carrivick JL, Brown LE (2013) Food web structure in a harsh glacier-fed river. *PloS One*, **8**, e60899.
- Collier KJ, Quinn JM (2003) Land-use influences macroinvertebrate community response following a pulse disturbance. *Freshwater Biology*, **48**, 1462–1481.
- Comte L, Grenouillet G (2013) Do stream fish track climate change? Assessing distribution shifts in recent decades. *Ecography*.
- Connell JH (1978) Diversity in tropical rain forests and coral reefs. *Science*, **199**, 1302–1310.
- Cox JG, Lima SL (2006) Naiveté and an aquatic-terrestrial dichotomy in the effects of introduced predators. *Trends in Ecology & Evolution*, **21**, 674–80.
- Crossman J, Bradley C, Boomer I, Milner AM (2011) Water flow dynamics of groundwater-fed streams and their ecological significance in a glacierized catchment. *Arctic, Antarctic, and Alpine Research*, **43**, 2011.
- Céréghino R (2006) Ontogenetic diet shifts and their incidence on ecological processes: a case study using two morphologically similar stoneflies (Plecoptera). *Acta Oecologica*, **30**, 33–38.
- Death RG (1996) The effect of patch disturbance on stream invertebrate structure: the influence of disturbance history community. *Oecologia*, **108**, 567–576.
- Death RG (2010) Disturbance and riverine benthic communities: what has it contributed to general ecological theory? *River Research and Applications*, **25**, 15–25.
- Debelmas J (1974) *Géologie de la France*. Doin.
- Diaz HF, Grosjean M, Graumlich L (2003) Climate variability and change in high elevation regions: past, present and future. *Climatic Change*, **2001**, 1–4.
- Dickson NE, Carrivick JL, Brown LE (2012) Flow regulation alters alpine river thermal regimes. *Journal of Hydrology*, **464-465**, 505–516.
- Dirzo R, Raven PH (2003) Global state of biodiversity loss. *Annual Review of Environment and Resources*, **28**, 137–167.
- Dolédec S, Chessel D, Ter Braak CJF, Champely S (1996) Matching species traits to environmental variables: a new three-table ordination method. *Environmental and Ecological Statistics*, **3**, 143–166.
- Dolédec S, Phillips N, Scarsbrook M, Riley RH, Townsend CR (2006) Comparison of structural and functional approaches to determining landuse effects on grassland stream invertebrate communities. *Journal of the North American Benthological Society*, **25**, 44–60.

- Domisch S, Araújo MB, Bonada N, Pauls SU, Jähnig SC, Haase P (2013) Modelling distribution in European stream macroinvertebrates under future climates. *Global Change Biology*, **19**, 752–62.
- Dray S, Legendre P (2008) Testing the species traits-environment relationships: the fourth-corner problem revisited. *Ecology*, **89**, 3400–3412.
- Dupias G (1985) *Vegetation des Pyrenees*. CNRS, Toulouse.
- Durance I, Ormerod SJ (2007) Climate change effects on upland stream macroinvertebrates over a 25-year period. *Global Change Biology*, **13**, 942–957.
- Durant JM, Hjermann DØ, Ottersen G, Stenseth NC (2007) Climate and the match or mismatch between predator requirements and resource availability. *Climate Research*, **33**, 271–283.
- Dyurgerov MB, Meier MF (2000) Twentieth century climate change: evidence from small glaciers. *PNAS*, **97**, 1406 – 1411.
- Dziöck F, Gerisch M, Siegert M, Hering I, Scholz M, Ernst R (2011) Reproducing or dispersing? Using trait based habitat templet models to analyse Orthoptera response to flooding and land use. *Agriculture, Ecosystems & Environment*, **145**, 85–94.
- Déry SJ, Hernández-Henríquez M a, Owens PN, Parkes MW, Petticrew EL (2012) A century of hydrological variability and trends in the Fraser River Basin. *Environmental Research Letters*, **7**, 1–10.
- Díaz AM, Alonso MLS, Gutiérrez MRV-A (2008) Biological traits of stream macroinvertebrates from a semi-arid catchment: patterns along complex environmental gradients. *Freshwater Biology*, **53**, 1–21.
- Díaz S, Cabido M (2001) Vive la différence: plant functional diversity matters to ecosystem processes. *Trends in Ecology & Evolution*, **16**, 646–655.
- Edington JM, Hildrew AG (1995) *A revised key to the caseless caddis larvae of the British Isles with notes on their ecology*. Freshwater Biological Association.
- Elliott JM (2003) A comparative study of the functional response of four species of carnivorous stoneflies. *Freshwater Biology*, **48**, 191–202.
- Emmerson MC, Raffaelli D (2004) Predator-prey body size, interaction strength and the stability of a real food web. *Journal of Animal Ecology*, **73**, 399–409.
- Engler R, Randin CF, Thuiller W, *et al.* (2011) 21st century climate change threatens mountain flora unequally across Europe. *Global Change Biology*, **17**, 2330–2341.
- Evanno G, Castella E, Antoine C, Paillat G, Goudet J (2009) Parallel changes in genetic diversity and species diversity following a natural disturbance. *Molecular Ecology*, **18**, 1137–44.

- Evans EC, Mcgregor GR, Petts GE (1998) River energy budgets with special reference to river bed processes. *Hydrological Processes*, **12**, 575–595.
- Faith DP, Norris RH (1989) Correlation of environmental variables with patterns of distribution and abundance of common and rare freshwater macroinvertebrates. *Biological Conservation*, **50**, 77–98.
- Farinotti D, Usselman S, Huss M, Bauder A, Funk M (2012) Runoff evolution in the Swiss Alps: projections for selected high-alpine catchments based on ENSEMBLES scenarios. *Hydrological Processes*, **26**, 1909–1924.
- Fatichi S, Rimkus S, Burlando P, Bordoy R, Molnar P (2013) Elevational dependence of climate change impacts on water resources in an alpine catchment. *Hydrology and Earth System Sciences Discussions*, **10**, 3743–3794.
- Feio MJ, Poquet JM (2011) Predictive models for freshwater biological assessment: statistical approaches, biological elements and the Iberian peninsula experience: a review. *International Review of Hydrobiology*, **96**, 321–346.
- Fellman JB, Nagorski S, Pyare S, Vermilyea AW, Scott D, Hood E (2013) Stream temperature response to variable glacier coverage in coastal watersheds of Southeast Alaska. *Hydrological Processes*.
- Fenoglio S, Bo T, Pessino M, Malacarne G (2007) Feeding of *Perla grandis* nymphs (Plecoptera: Perlidae) in an Apennine first order stream (Rio Berga, NW Italy). *Ann. Soc. Entomol. Fr.*, **43**, 221–224.
- Fenoglio S, Bo T, Tierno de Figueroa JM, López-Rodríguez MJ, Malacarne G (2008) A comparison between local emergence patterns of *Perla grandis* and *Perla marginata* (Plecoptera, Perlidae). *Hydrobiologia*, **607**, 11–16.
- Finelli C, Hart D, Merz R (2002) Stream insects as passive suspension feeders: effects of velocity and food concentration on feeding performance. *Oecologia*, **131**, 145–153.
- Finger D, Heinrich G, Gobiet A, Bauder A (2012) Projections of future water resources and their uncertainty in a glacierized catchment in the Swiss Alps and the subsequent effects on hydropower production during the 21st century. *Water Resources Research*, **48**, W025.
- Finger D, Pellicciotti F, Konz M, Rimkus S, Burlando P (2011) The value of glacier mass balance, satellite snow cover images, and hourly discharge for improving the performance of a physically based distributed hydrological model. *Water Resources Research*, **47**, W07519.
- Finn DS, Khamis K, Milner AM (2013) Loss of small glaciers will diminish beta diversity in Pyrenean streams at two levels of biological organization. *Global Ecology and Biogeography*, **22**, 40–51.
- Finn DS, Poff NL (2008) Emergence and flight activity of alpine stream insects in two years with contrasting winter snowpack. *Arctic, Antarctic, and Alpine Research*, **40**, 638–646.

- Flory EA, Milner AM (1999) The role of competition in invertebrate community development in a recently formed stream in Glacier Bay National Park, Alaska. *Aquatic Ecology*, **33**, 175–184.
- Flynn DFB, Gogol-Prokurat M, Nogeire T, *et al.* (2009) Loss of functional diversity under land use intensification across multiple taxa. *Ecology letters*, **12**, 22–33.
- Forrester G., Dudley TL, Grimm NB (1999) Trophic interactions in open systems: effects of predators and nutrients on stream food chains. *Limnology and Oceanography*, **44**, 1187–1197.
- Fox JW (2013) The intermediate disturbance hypothesis should be abandoned. *Trends in Ecology & Evolution*, **28**, 86–92.
- Freimann R, Bu H, Findlay SEG, Robinson CT (2013a) Response of lotic microbial communities to altered water source and nutritional state in a glaciated alpine floodplain. *Limnology and Oceanography*, **58**, 951–965.
- Freimann R, Bürgmann H, Findlay SE, Robinson CT (2013b) Bacterial structures and ecosystem functions in glaciated floodplains: contemporary states and potential future shifts. *The ISME journal*.
- Friberg N, Bergfur J, Rasmussen J, Sandin L (2013) Changing Northern catchments: Is altered hydrology, temperature or both going to shape future stream communities and ecosystem processes? *Hydrological Processes*, **27**, 734–740.
- Füreder L (2007) Life at the edge: habitat condition and bottom fauna of alpine running waters. *International Review of Hydrobiology*, **92**, 491–513.
- Füreder L (2012) Melting biodiversity. *Nature Climate Change*, **2**, 318–319.
- Füreder L, Schutz C, Burger R, Wallinger M (1998) High Alpine streams as models for ecological gradients. *IAHS Publication*, **248**, 387–394.
- Füreder L, Schutz C, Wallinger M, Burger R (2001) Physico-chemistry and aquatic insects of a glacier-fed and a spring-fed alpine stream. *Freshwater Biology*, **46**, 1673–1690.
- Füreder L, Wallinger M, Burger R (2005) Longitudinal and seasonal pattern of insect emergence in alpine streams. *Aquatic Ecology*, **39**, 67–78.
- Füreder L, Welter C, Jackson JK (2003) Dietary and stable isotope ($\delta^{13}\text{C}$, $\delta^{15}\text{N}$) analyses in alpine stream insects. *International Review of Hydrobiology*, **88**, 314–331.
- Gallardo B, Gascón S, García M, Comín FA (2009) Testing the response of macroinvertebrate functional structure and biodiversity to flooding and confinement. **68**, 315–326.
- Gallart F, Llorens P, Latron J, Regúes D (2002) Hydrological processes and their seasonal controls in a small Mediterranean mountain catchment in the Pyrenees. *Hydrology and Earth System Sciences*, **6**, 527–537.

- Garamszegi LZ (2006) Comparing effect sizes across variables: generalization without the need for Bonferroni correction. *Behavioral Ecology*, **17**, 682–687.
- Garner G, Hannah D, Malcolm I, Sadler J (2012) Inter-annual variability in spring- summer stream water temperature, microclimate and heat exchanges: a comparison of forest and moorland environments. In: *Hydrology for a changing world*, pp01–08. British Hydrological Society.
- Gellatly AF, Parkinson R (1994) Rockfalls and glacier contraction: Cirque de Troumouse ,French Pyrénées. *Pirineos*, **33**, 143–144.
- Genereux D (1998) Quantifying uncertainty in tracer-based hydrograph separations. *Water Resources Research*, **34**, 915–919.
- Gerisch M, Agostinelli V, Henle K, Dziöck F (2012) More species, but all do the same: contrasting effects of flood disturbance on ground beetle functional and species diversity. *Oikos*, **121**, 508–515.
- Gibson CA, Meyer JL, Poff NL, Hay LE, Georgakakos A (2005) Flow regime alterations under changing climate in two river basins: implications for freshwater ecosystems. *River Research and Applications*, **21**, 849–864.
- Gilman SE, Urban MC, Tewksbury J, Gilchrist GW, Holt RD (2010) A framework for community interactions under climate change. *Trends in Ecology & Evolution*, **25**, 325–331.
- Gomez D, Sese JA, Villar L (2003) The vegetation of the alpine zone in the Pyrenees. In: *Alpine biodiversity in Europe*, Ecological Studies, Vol. 167 (eds: L. Nagy, G. Grabherr, C. Korner and D.B.A. Thompson), pp 85–92. Springer-Verlag, Berlin.
- González Trueba JJ, Moreno RM, Martínez De Pisón E, Serrano E (2008) The Holocene “Little Ice Age” glaciation and current glaciers in the Iberian Peninsula. *The Holocene*, **18**, 551–568.
- Gotelli NJ, McCabe DJ (2002) Species co-occurrence: a meta-analysis of J. M. Diamond’s assembly rules model. *Ecology*, **83**, 2091.
- Grabherr G, Gottfried M, Pauli H (2000) GLORIA: A Global Observation Research Initiative in Alpine Environments. *Mountain Research and Development*, **20**, 190–191.
- Graf W, Waringer J, Pauls SU (2009) A new feeding group within larval Drusinae (Trichoptera: Limnephilidae): the *Drusus alpinus* Group sensu Schmid , 1956, including larval descriptions of *Drusus franzi* Schmid, 1956, and *Drusus alpinus* (Meyer-Dur, 1875). *Zootaxa*, **62**, 53 – 62.
- Gray JS (1989) Effects of environmental stress on species rich assemblages. *Biological Journal of the Linnean Society*, **37**, 19–32.
- Grunewald K, Scheithauer J (2010) Europe’s southernmost glaciers: response and adaptation to climate change. *Journal of Glaciology*, **56**, 129–142.

- Götzenberger L, de Bello F, Bråthen KA, *et al.* (2012) Ecological assembly rules in plant communities—approaches, patterns and prospects. *Biological Reviews*, **87**, 111–27.
- Hague MJ, Ferrari MR, Miller JR, Patterson DA, Russell GL, Farrell a. P, Hinch SG (2011) Modelling the future hydroclimatology of the lower Fraser River and its impacts on the spawning migration survival of sockeye salmon. *Global Change Biology*, **17**, 87–98.
- Hallet B, Hunter L, Bogen J (1996) Rates of erosion and sediment evacuation by glaciers: a review of field data and their implications. *Global and Planetary Change*, **12**, 213–235.
- Hannah DM, Brown LE, Milner AM (2007) Integrating climate – hydrology – ecology for alpine river systems. *Aquatic Conservation: Marine and Freshwater Ecosystems*, **17**, 636–656.
- Hannah DM, Demuth S, van Lanen HAJ, *et al.* (2011) Large-scale river flow archives: importance, current status and future needs. *Hydrological Processes*, **25**, 1191–1200.
- Hannah DM, Gurnell AM (2001) A conceptual, linear reservoir runoff model to investigate melt season changes in cirque glacier hydrology. *Journal of Hydrology*, **246**, 123–141.
- Hannah DM, Gurnell AM, Mcgregor GR (1999) A methodology for investigation of the seasonal evolution in proglacial hydrograph form. *Hydrological Processes*, **13**, 2603–2621.
- Hannah DM, Gurnell AM, Mcgregor GR (2000) Spatio-temporal variation in microclimate, the surface energy balance and ablation over a cirque glacier. *International Journal of Climatology*, **20**, 733–758.
- Hannah DM, Malcolm IA, Bradley C (2009) Seasonal hyporheic temperature dynamics over riffle bedforms. *Hydrological Processes*, **23**, 2178–2194.
- Hannah DM, Malcolm IA, Soulsby C, Youngson AF (2008) A comparison of forest and moorland stream microclimate, heat exchanges and thermal dynamics. *Hydrological Processes*, **22**, 919–940.
- Hannah DM, Malcolm IA, Youngson AF (2004) Heat exchanges and temperatures within a salmon spawning stream in the Cairngorms, Scotland: seasonal and sub-seasonal dynamics. *River Research and Applications*, **20**, 635–652.
- Hebert C, Caissie D, Satish MG, El-Jabi N (2011) Study of stream temperature dynamics and corresponding heat fluxes within Miramichi River catchments (New Brunswick, Canada). *Hydrological Processes*, **25**, 2439–2455.
- Heino J (2005) Functional biodiversity of macroinvertebrate assemblages along major ecological gradients of boreal headwater streams. *Freshwater Biology*, **50**, 1578–1587.
- Heino J, Virkkala R, Toivonen H (2009) Climate change and freshwater biodiversity: detected patterns, future trends and adaptations in northern regions. *Biological Reviews*, **84**, 39–54.

- Hellmann JJ, Prior KM, Pelini SL (2012) The influence of species interactions on geographic range change under climate change. *Annals of the New York Academy of Sciences*, **1249**, 18–28.
- Herschy R (1985) *Stream Flow Measurements*. Elsevier Applied Science: Oxford.
- Hieber M, Robinson CT, Uehlinger URS, Ward J V (2005) A comparison of benthic macroinvertebrate assemblages among different types of alpine streams. *Freshwater Biology*, **50**, 2087–2100.
- Hintze JL, Nelson RD (1998) Violin plots: a box plot-density trace synergism. *The American Statistician*, **52**, 181–184.
- Hock R, Jansson P, Braun LN (2005) Modelling the Response of Mountain Glacier Discharge to Climate Warming. In: *Global change in mountain regions (a state of knowledge overview)* (eds: Huber U, Bugmann H, Reasoner M), pp 243–252. Dordrecht, Springer.
- Holt RD, Lawton JH (1994) The ecological consequences of shared natural enemies. *Annual Review of Ecology and Systematics*, **25**, 495–520.
- Hood E, Berner L (2009) Effects of changing glacial coverage on the physical and biogeochemical properties of coastal streams in southeastern Alaska. *Journal of Geophysical Research*, **114**, G03001.
- Hughes AR, Byrnes JE, Kimbro DL, Stachowicz JJ (2007) Reciprocal relationships and potential feedbacks between biodiversity and disturbance. *Ecology letters*, **10**, 849–64.
- Huryn A, Wallace J (2000) Life history and production of stream insects. *Annual Review of Entomology*, **45**, 83–110.
- Huss M (2011) Present and future contribution of glacier storage change to runoff from macroscale drainage basins in Europe. *Water Resources*, **47**, 1–14.
- Ilg C, Castella E (2006) Patterns of macroinvertebrate traits along three glacial stream continuums. *Freshwater Biology*, **51**, 840–853.
- IPCC (2007) The physical sciences basis. In Contribution of Working Group I to the Fourth Assessment Report of the Intergovernmental Panel on Climate Change (eds: M. Parry, O. Canziani, J. Palutkof, P. Van der Linden, & C. Hanson). Cambridge, UK.
- Isaak D, Hubert W (2001) A hypothesis about factors that affect maximum summer stream temperatures across montane landscapes. *Journal of the American Water Resources Association*, **37**, 351–366.
- Isaak DJ, Luce CH, Rieman BE, *et al.* (2010) Effects of climate change and wildfire on stream temperatures and salmonid thermal habitat in a mountain river network. *Ecological Applications*, **20**, 1350–1371.

- Jacob D, Podzun R (1997) Sensitivity studies with the regional climate model REMO. *Meteorology and Atmospheric Physics*, **63**, 119–129.
- Jacobsen D, Dangles O (2012) Environmental harshness and global richness patterns in glacier-fed streams. *Global Ecology and Biogeography*, **21**, 647–656.
- Jacobsen D, Milner AM, Brown LE, Dangles O (2012) Biodiversity under threat in glacier-fed river systems. *Nature Climate Change*, **2**, 361–364.
- Janssen P, Heuberger P (1995) Calibration of process-oriented models. *Ecological Modelling*, **83**, 55–66.
- Jansson P, Hock R, Schneider T (2003) The concept of glacier storage: a review. *Journal of Hydrology*, **282**, 116–129.
- Jasper K, Calanca P, Gyalistras D, Fuhrer J (2004) Differential impacts of climate change on the hydrology of two alpine river basins. *Climate Research*, **26**, 113–129.
- Jefferies MJ, Lawton JH (1984) Enemy free space and the structure of ecological communities. *Biological Journal of the Linnean Society*, **23**, 269–286.
- Johnson SL (2004) Factors influencing stream temperatures in small streams: substrate effects and a shading experiment. *Canadian Journal of Fisheries and Aquatic Sciences*, **61**, 913–923.
- Johnson EA, Miyanishi K (2008) Testing the assumptions of chronosequences in succession. *Ecology letters*, **11**, 419–31.
- Kaushal SS, Likens GE, Jaworski NA, *et al.* (2010) Rising stream and river temperatures in the United States. *Frontiers in Ecology and the Environment*, **8**, 461–466.
- Kelson K, Wells SG (1989) Geologic influences on fluvial hydrology and bedload transport in small mountainous watersheds, northern New Mexico, U.S.A. *Earth Surface Processes and Landforms*, **14**, 671–690.
- Khamis K, Hannah DM, Hill M, Brown LE, Castella E, Milner AM (2013) Alpine aquatic ecosystem conservation policy in a changing climate. *Environmental Science & Policy*, .
- Kikvidze Z, Michalet R, Brooker RW, Cavieres LA, Lortie CJ, Pugnaire FI, Callaway RM (2011) Climatic drivers of plant–plant interactions and diversity in alpine communities. *Alpine Botany*, **121**, 63–70.
- Knighton AD (1980) Longitudinal changes in size and sorting of stream-bed material in four English rivers. *Geological Society of America Bulletin*, **91**, 55.
- Knispel S, Castella E (2003) Disruption of a longitudinal pattern in environmental factors and benthic fauna by a glacial tributary. *Freshwater Biology*, **49**, 604–618.
- Knispel S, Sartori M, Brittain JE (2006) Egg development in the mayflies of a Swiss glacial floodplain. *Journal of the North American Benthological Society*, **25**, 430–443.

- Kondoh M (2001) Unifying the relationships of species richness to productivity and disturbance. *Proceedings of the Royal Society of London. Series B: Biological Sciences*, **268**, 269–71.
- Konz M, Seibert J (2010) On the value of glacier mass balances for hydrological model calibration. *Journal of Hydrology*, **385**, 238–246.
- Kotlarski S, Paul F, Jacob D (2010) Forcing a distributed glacier mass balance model with the Regional Climate Model REMO. Part I: climate model evaluation. *Journal of Climate*, **23**, 1589–1606.
- Kratz KW (1996) Effects of stoneflies on local prey populations: mechanisms of impact across prey density. *Ecology*, **77**, 1573–1585.
- Kulakowski D, Bebi P, Rixen C (2011) The interacting effects of land use change, climate change and suppression of natural disturbances on landscape forest structure in the Swiss Alps. *Oikos*, **120**, 216–225.
- König T, Kaufmann R, Scheu S (2011) The formation of terrestrial food webs in glacier foreland: Evidence for the pivotal role of decomposer prey and intraguild predation. *Pedobiologia*, **54**, 147–152.
- Körner C (2007) The use of “altitude” in ecological research. *Trends in Ecology & Evolution*, **22**, 569–74.
- Lake PS (2000) Disturbance, patchiness, and diversity in streams. *Journal of the North American Benthological Society*, **19**, 573–592.
- Lake PS (2013) Resistance, Resilience and Restoration. *Ecological Management & Restoration*, **14**, 20–24.
- Lammers RB, Pundsack JW, Shiklomanov AI (2007) Variability in river temperature, discharge, and energy flux from the Russian pan-Arctic landmass. *Journal of Geophysical Research*, **112**, G04S59.
- Lana-Renault N, Latron J, Regüés D (2007) Streamflow response and water-table dynamics in a sub-Mediterranean research catchment (Central Pyrenees). *Journal of Hydrology*, **347**, 497–507.
- Lancaster J (1990) Predation and drift of lotic macroinvertebrates during colonization. *Oecologia*, **85**, 48–56.
- Larsen S, Pace G, Ormerod SJ (2011) Experimental effects of sediment deposition on the structure and function of macroinvertebrate assemblages in temperate streams. *River Research and Applications*, **267**, 257–267.
- Latron J, Anderton S, White SUE, Llorens P, Gallart F (2003) Seasonal characteristics of the hydrological response in a Mediterranean mountain research catchment (Vallcebre, Catalan Pyrenees): field investigations and modelling. In: *Hydrology of the Mediterranean and Semiarid Regions*. (eds: Servat E, Wajdi N, Leduc C, Shakeel A),

- pp106–110. International Association of Hydrological Sciences (IAHS), Proceedings of an International Symposium, IAHS 278; Montpellier, France: International Association of Hydrological Sciences.
- Lavandier P (1974) The ecology of a high mountain stream in the Pyrénées: I. Physical conditions (In French). *Annales de Limnologie*, **10**, 173–220.
- Lavandier P (1975) Cycle biologique et production de *Capnioneura brachyptera* D.(Plécoptères) dans un ruisseau d'altitude des Pyrénées centrales. *Annales de Limnologie*, **11**, 145–156.
- Lavandier P, Céréghino R (1995) Use and partition of space and resources by two coexisting *Rhyacophila* species (Trichoptera) in a high mountain stream. *Hydrobiologia*, **300**, 157–162.
- Lavandier P, Decamps H (1984) Estaragne. In: *Ecology of European Rivers* (Ed: B Whitton), pp 237-264, Blackwell Scientific Publications, Oxford.
- Lavandier P, Pujol J-Y (1975) Cycle biologique de *Drusus rectus* (Trichoptera) dans les Pyrénées centrales: Influence de la température et de l'enneigement. *Annales de Limnologie*, **11**, 255–262.
- Lavergne S, Mouquet N, Wilfried T, Ophélie R (2010) Biodiversity and climate change : integrating evolutionary and ecological responses of species and communities. *Annual Review of Ecology, Evolution, and Systematics*, **41**, 321–350.
- Leach JA, Moore RD (2010) Above-stream microclimate and stream surface energy exchanges in a wildfire-disturbed riparian zone. *Hydrological Processes*, **24**, 2369–2381.
- Ledger ME, Harris RML, Milner AM, Armitage PD (2006) Disturbance, biological legacies and community development in stream mesocosms. *Oecologia*, **148**, 682–691.
- Lencioni V (2004) Survival strategies of freshwater insects in cold environments. *Journal of Limnology*, **63**, 45–55.
- Lencioni, V, Rossaro B (2005) Microdistribution of chironomids (Diptera: Chironomidae) in Alpine streams: an autoecological perspective. *Hydrobiologia*, **533**, 61–76.
- Lepori F, Malmqvist B (2009) Deterministic control on community assembly peaks at intermediate levels of disturbance. *Oikos*, **118**, 471–479.
- Ligeiro R, Hughes RM, Kaufmann PR, *et al.* (2013) Defining quantitative stream disturbance gradients and the additive role of habitat variation to explain macroinvertebrate taxa richness. *Ecological Indicators*, **25**, 45–57.
- van der Linden P, Mitchell JFB. (2009) ENSEMBLES: Climate change and its impacts: Summary of research and results from the ENSEMBLES project, technical report, Met Off. Hadley Cent, Exeter, UK

- Liu Z, Martina ML V, Todini E (2005) Flood forecasting using a fully distributed model : application of the TOPKAPI model to the Upper Xixian Catchment. *Hydrology and Earth System Sciences*, **9**, 347–364.
- Lloyd NJ, Mac Nally R, Lake PS (2005) Spatial autocorrelation of assemblages of benthic invertebrates and its relationship to environmental factors in two upland rivers in southeastern Australia. *Diversity and Distributions*, **11**, 375–386.
- Lods-Crozet B, Castella E, Cambin D, Ilg C, Knispel S, Mayor-Simeant H (2001a) Macroinvertebrate community structure in relation to environmental variables in a Swiss glacial stream. *Freshwater Biology*, **46**, 1641–1661.
- Lods-Crozet B, Lencioni V, Olafsson JS, *et al.* (2001b) Chironomid (Diptera: Chironomidae) communities in six European glacier-fed streams. *Freshwater Biology*, **46**, 1791–1809.
- Logue JB, Mouquet N, Peter H, Hillebrand H (2011) Empirical approaches to metacommunities: a review and comparison with theory. *Trends in Ecology & Evolution*, **26**, 482–91.
- Lowney CL (2000) Stream temperature variation in regulated rivers: evidence for a spatial pattern in daily minimum and maximum magnitudes. *Water Resources*, **36**, 2947–2955.
- López-Moreno JI, Beniston M, García-Ruiz JM (2008) Environmental change and water management in the Pyrenees: facts and future perspectives for Mediterranean mountains. *Global and Planetary Change*, **61**, 300–312.
- López-Moreno JI, Goyette S, Beniston M (2009) Impact of climate change on snowpack in the Pyrenees: horizontal spatial variability and vertical gradients. *Journal of Hydrology*, **374**, 384–396.
- López-Moreno JI, Pomeroy JW, Revuelto J, Vicente-Serrano SM (2013) Response of snow processes to climate change: spatial variability in a small basin in the Spanish Pyrenees. *Hydrological Processes*, **27**, 2637–2650.
- MacArthur RH, Wilson E. (1967) *The theory of island biogeography*. Princeton University Press.
- MacDonald RJ, Boon S, Byrne JM, Silins U (2013) A comparison of surface and subsurface controls on summer temperature in a headwater stream. *Hydrological Processes*, n/a–n/a.
- Mackey R, Currie D (2001) The diversity – disturbance relationship: is it generally strong and peaked? *Ecology*, **82**, 3479–3492.
- Magnusson J, Jonas T, Kirchner JW (2012a) Temperature dynamics of a proglacial stream: Identifying dominant energy balance components and inferring spatially integrated hydraulic geometry. *Water Resources Research*, **48**, 1–16.

- Magnusson J, Kobierska F, Huxol S, Hayashi M, Jonas T, Kirchner JW (2012b) Melt water driven stream and groundwater stage fluctuations on a glacier forefield (Dammagletscher, Switzerland). *Hydrological Processes*.
- Malard F, Mangin A, Uehlinger U, Ward J V (2001) Thermal heterogeneity in the hyporheic zone of a glacial floodplain. *Canadian Journal of Fisheries and Aquatic Sciences*, **1335**, 1319–1335.
- Malard F, Tockner K, Ward J V (2000) Physico-chemical heterogeneity in a glacial riverscape. *Landscape Ecology*, **15**, 679–695.
- Malard F, Uehlinger U, Zah R, Tockner K (2006) Flood-Pulse and riverscape dynamics in a braided glacial river. *Ecology*, **87**, 704–716.
- Malcolm IA, Hannah DM, Donaghy MJ, Soulsby C, Youngson AF (2004) The influence of riparian woodland on the spatial and temporal variability of stream water temperatures in an upland salmon stream. *Hydrology and Earth System Sciences*, **8**, 449–459.
- Mantua N, Tohver I, Hamlet A (2010) Climate change impacts on streamflow extremes and summertime stream temperature and their possible consequences for freshwater salmon habitat in Washington State. *Climatic Change*, **102**, 187–223.
- Maraun D, Wetterhall F, Ireson A., *et al.* (2010) Precipitation downscaling under climate change: Recent developments to bridge the gap between dynamical models and the end user. *Review of Geophysics*, **48**, 1–34.
- Mason NWH, de Bello F, Mouillot D, Pavoine S, Dray S (2013) A guide for using functional diversity indices to reveal changes in assembly processes along ecological gradients. *Journal of Vegetation Science*, **24**, 794–806.
- Mason NWH, Lanoiselée C, Mouillot D, Wilson JB, Argillier C (2008) Does niche overlap control relative abundance in French lacustrine fish communities? A new method incorporating functional traits. *The Journal of Animal Ecology*, **77**, 661–9.
- Mason NWH, Mouillot D, Lee WG, Wilson JB (2005) Functional richness, functional evenness and functional divergence: the primary components of functional diversity. *Oikos*, **111**, 112–118.
- Mason NWH, Richardson SJ, Peltzer DA, de Bello F, Wardle DA, Allen RB (2012) Changes in coexistence mechanisms along a long-term soil chronosequence revealed by functional trait diversity. *Journal of Ecology*, **100**, 678–689.
- Matthaei CD, Uehlinger U, Frutiger A (1997) Response of benthic invertebrates to natural versus experimental disturbance in a Swiss prealpine river. *Freshwater Biology*, **37**, 61–77.
- Mayor SJ, Cahill JF, He F, Sólymos P, Boutin S (2012) Regional boreal biodiversity peaks at intermediate human disturbance. *Nature communications*, **3**, 1142.

- Mccabe DJ, Gotelli NJ (2000) Effects of disturbance frequency, intensity, and area on assemblages of stream macroinvertebrates. *Oecologia*, **124**, 270–279.
- McCabe DJ, Hayes-Pontius EM, Canepa A, Berry KS, Levine BC (2012) Measuring standardized effect size improves interpretation of biomonitoring studies and facilitates meta-analysis. *Freshwater Science*, **31**, 800–812.
- McGill BJ, Enquist BJ, Weiher E, Westoby M (2006) Rebuilding community ecology from functional traits. *Trends in Ecology & Evolution*, **21**, 178–85.
- McHugh PA, McIntosh AR, Jellyman PG (2010) Dual influences of ecosystem size and disturbance on food chain length in streams. *Ecology letters*, **13**, 881–90.
- McPeck MA (1990) Determination of species composition in the Enallagma damselfly assemblages of permanent lakes. *Ecology*, **71**, 83–98.
- Meier W, Bonjour C, Wu A, Reichert P (2003) Modeling the Effect of Water Diversion on the Temperature of Mountain Streams. *Journal of Environmental Engineering*, **129**, 755–764.
- Meier MF, Dyurgerov MB, Rick UK, *et al.* (2007) Glaciers dominate eustatic sea-level rise in the 21st century. *Science*, **317**, 1064–7.
- Mellor CJ (2012) Arctic water source dynamics, stream habitat and biodiversity in a changing climate: a field-based investigation in Swedish Lapland. PhD Thesis, University of Birmingham, UK.
- Menezes S, Baird DJ, Soares AMVM (2010) Beyond taxonomy : a review of macroinvertebrate trait-based community descriptors as tools for freshwater biomonitoring. *Journal of Applied Ecology*, **47**, 711–719.
- Menge BA, Sutherland JP (1976) Species diversity gradient: synthesis of the roles of predation, competition, and temporal heterogeneity. *American Naturalist*, **110**, 351–369.
- Menge BA, Sutherland JP (1987) Community regulation: variation in disturbance, competition and predation in relation to environmental stress and recruitment. *The American Naturalist*, **130**, 730–757.
- Micheli F, Halpern BS (2005) Low functional redundancy in coastal marine assemblages. *Ecology Letters*, **8**, 391–400.
- Middelkoop H, Daamen K, Gellens D, *et al.* (2001) Impact of climate change on hydrological regimes and water resources management in the Rhine basin. *Climatic Change*, **49**, 105–128.
- Milner AM, Brittain JE, Brown LE, Hannah DM (2010) Water Sources and Habitat of Alpine Streams. In: *Alpine Waters* (ed: Bundi U), pp175–191. Springer, Berlin.

- Milner AM, Brittain JE, Castella E, Petts GE (2001) Trends of macroinvertebrate community structure in glacier-fed rivers in relation to environmental conditions: a synthesis. *Freshwater Biology*, **46**, 1833–1847.
- Milner AM, Brown LE, Hannah DM (2009) Hydroecological response of river systems to shrinking glaciers. *Hydrological Processes*, **77**, 62–77.
- Milner AM, Petts GE (1994) Glacial rivers: physical habitat and ecology. *Freshwater Biology*, **32**, 295–307.
- Miyake Y, Nakano S (2002) Effects of substratum stability on diversity of stream invertebrates during baseflow at two spatial scales. *Freshwater Biology*, **47**, 219–230.
- Mohseni O, Erickson TR, Stefan HG (1999) Sensitivity of stream temperatures in the United States to air temperatures projected under a global warming scenario. *Water Resources Research*, **35**, 3723–3733.
- Mohseni O, Stefan HG, Erickson TR (1998) A nonlinear regression model for weekly stream temperatures. *Water Resources Research*, **34**, 2685–2692.
- Monaghan KA, Milner AM (2009) Effect of anadromous salmon redd construction on macroinvertebrate communities in a recently formed stream in coastal Alaska. *Journal of the North American Benthological Society*, **28**, 153–166.
- Montori A (1992) Alimentacion de las larvas de triton pirenaico, *Euproctus asper*, en el prepirineo de la Cerdana, Espana. *Amphibia-Reptilia*, **13**, 157–167.
- Moog O (ed) (1995) *Fauna Aquatica Austriaca*. Bundesministerium für Land-und Forstwirtschaft. Wasserwirtschaftskataster Wien.
- Moore RDD (2003) Introduction to salt dilution gauging for streamflow measurement : Part 1. *Watershed Management Bulletin*, **7**, 20–23.
- Moore RD, Fleming SW, Menounos B, *et al.* (2009) Glacier change in western North America: influences on hydrology, geomorphic hazards and water quality. *Hydrological Processes*, **61**, 42–61.
- Moore RD, Sutherland P, Gomi T, Dhakal A (2005) Thermal regime of a headwater stream within a clear-cut, coastal British Columbia, Canada. *Hydrological Processes*, **19**, 2591–2608.
- Moriasi DN, Arnold JG, Liew MW Van, Bingner RL, Harmel RD, Veith TL (2007) Model evaluation guidelines for systematic quantification of accuracy in watershed simulations. *Watershed Simulations*, **50**, 885–900.
- Mouchet M, Guilhaumon F, Villéger S, Mason NWH, Tomasini J-A, Mouillot D (2008) Towards a consensus for calculating dendrogram-based functional diversity indices. *Oikos*, **117**, 794–800.

- Mouchet MA, Villéger S, Mason NWH, Mouillot D (2010) Functional diversity measures: an overview of their redundancy and their ability to discriminate community assembly rules. *Functional Ecology*, **24**, 867–876.
- Muhlfeld CC, Giersch JJ, Hauer FR, *et al.* (2011) Climate change links fate of glaciers and an endemic alpine invertebrate. *Climatic Change*, **106**, 337–345.
- Mérigoux S, Dolédec S (2004) Hydraulic requirements of stream communities: a case study on invertebrates. *Freshwater Biology*, **49**, 600–613.
- Müller-Liebenau I (1969) Revision der europäischen Arten der Gattung *Baetis* LEACH, 1815 (Insecta, Ephemeroptera). *Gewasser und Abwasser* 48/49. Göttingen.
- Naeem S, Wright JP (2003) Disentangling biodiversity effects on ecosystem functioning: deriving solutions to a seemingly insurmountable problem. *Ecology Letters*, **6**, 567–579.
- Nakagawa S (2004) A farewell to Bonferroni: the problems of low statistical power and publication bias. *Behavioral Ecology*, **15**, 1044–1045.
- Nelson ML, Rhoades CC, Dwire KA (2011) Influence of bedrock geology on water chemistry of slope wetlands and headwater streams in the Southern Rocky Mountains. *Wetlands*, **31**, 251–261.
- Nogues-Bravo D, Araujo MB, Errea MP, Martinez-Rica JP (2007) Exposure of global mountain systems to climate warming during the 21st Century. *Global environmental change*, **17**, 420–428.
- Nolte U, Hoffmann T (1992) Fast life in cold water: *Diamesa incallida* (Chironomidae). *Ecography*, **15**, 25–30.
- Nowinski JD, Cardenas MB, Lightbody AF (2011) Evolution of hydraulic conductivity in the floodplain of a meandering river due to hyporheic transport of fine materials. *Geophysical Research Letters*, **38**, L01401.
- Null SE, Viers JH, Deas ML, Tanaka SK, Mount JF (2013) Stream temperature sensitivity to climate warming in California's Sierra Nevada: impacts to coldwater habitat. *Climatic Change*, **116**, 149–170.
- Nylin S, Gotthard K (1998) Plasticity in life-history traits. *Annual Review of Entomology*, **43**, 63–83.
- Ohmura A (2012) Enhanced temperature variability in high-altitude climate change. *Theoretical and Applied Climatology*, **110**, 499–508.
- Oksanen J, Blanchet FG, Kindt R, *et al.* (2012) vegan: community ecology. R package version 2.0-5. Available at: <http://CRAN.R-project.org/package=vegan>.
- Ormerod SJ, Dobson M, Hildrew AG, Townsend CR (2010) Multiple stressors in freshwater ecosystems. *Freshwater Biology*, **55**, 1–4.

- Ormerod SJ, Tyler SJ (1991) Exploitation of prey by a river bird, the dipper *Cinclus cinclus* (L.), along acidic and circumneutral streams in upland Wales. *Freshwater Biology*, **25**, 105–116.
- Paillex A, Dolédec S, Castella E, Mérigoux S, Aldridge DC (2013) Functional diversity in a large river floodplain: anticipating the response of native and alien macroinvertebrates to the restoration of hydrological connectivity. *Journal of Applied Ecology*, **50**, 97–106.
- Parc National des Pyrénées (1991) Gouffres du Versant Français du Taillon (Gavarnie, Haute Pyrénées). Document Scientifique du Parc National des Pyrénées **27**, 159 pp., Tarbes, France.
- Parker SM, Huryn AD (2011) Effects of natural disturbance on stream communities: a habitat template analysis of arctic headwater streams. *Freshwater Biology*, **56**, 1342–1357.
- Parkinson R, Gellatly A (1991) Soil formation on holocene moraines in the Cirque de Tromouse, Pyrenees. *Pirineos*, **69**, 69–82.
- Parmesan C (2006) Ecological and evolutionary responses to recent climate change. *Annual Review of Ecology, Evolution, and Systematics*, **37**, 637–671.
- Pauli H, Gottfried M, Reiter K, Klettner C, Grabherr G (2007) Signals of range expansions and contractions of vascular plants in the high Alps: observations (1994–2004) at the GLORIA master site Schrankogel, Tyrol, Austria. *Global Change Biology*, **13**, 147–156.
- Pavoine S, Vallet J, Gachet S, Dufour AB, Hervé D (2009) On the challenge of treating various types of variables: application for improving the measurement of functional diversity. *Oikos*, **118**, 391–402.
- Peckarsky BL (1982) Aquatic insect predator-prey relations. *BioScience*, **32**, 261–266.
- Peckarsky BL (1983) Biotic interactions or abiotic limitations? A model of lotic community structure. In: *Dynamics of lotic ecosystems*. (eds: Fontaine TD, Bartell SM), pp 303–323. Ann Arbor Science, Michigan.
- Peckarsky BL (1985) Do predaceous stoneflies and siltation affect the structure of stream insect communities colonizing enclosures? *Canadian Journal of Zoology*, **63**, 1519–1530.
- Peckarsky BL (1996) Alternative predator avoidance syndromes of stream-dwelling mayfly larvae. *Ecology*, **77**, 1888–1905.
- Peckarsky BL, Cowan CA (1995) Microhabitat and activity periodicity of predatory stoneflies and their mayfly prey in a western Colorado stream. *Oikos*, **74**, 513–521.
- Peckarsky BL, Horn SC, Statzner B (1990) Stonefly predation along a hydraulic gradient: a field test of the harsh—benign hypothesis. *Freshwater Biology*, **24**, 181–191.
- Peckarsky BL, Kerans BL, Taylor BW, McIntosh AR (2008) Predator effects on prey population dynamics in open systems. *Oecologia*, **156**, 431–440.

- Peckarsky BL, Penton MA (1989) Mechanisms of prey selection by stream-dwelling stoneflies. *Ecology*, **70**, 1203–1218.
- Pellicciotti F, Brock B, Strasser U, Burlando P, Funk M, Corripio J (2005) An enhanced temperature-index glacier melt model including the shortwave radiation balance: development and testing for Haut Glacier d’Arolla, Switzerland. *Journal of Glaciology*, **51**, 573–587.
- Petchey OL, Evans KL, Fishburn IS, Gaston KJ (2007) Low functional diversity and no redundancy in British avian assemblages. *The Journal of Animal Ecology*, **76**, 977–85.
- Petchey OL, Gaston KJ (2002) Functional diversity (FD), species richness and community composition. *Ecology Letters*, **5**, 402–411.
- Pfankuch D (1975) *Stream Reach Inventory and Channel Stability Evaluation*. United States Department of Agriculture Forest Service, Region 1, Missoula, MT, U.S.A.
- Pianka ER (1970) On *r*- and *K*-Selection. *American Naturalist*, **104**, 592–597.
- Pickett STA, Kolasa J, Armesto JJ, Collins SL (1989) The ecological concept of disturbance and its expression at various hierarchical levels. *Oikos*, **54**, 129.
- Pinheiro J, Bates D, DebRoy S, Sarkar D (2011) nlme: linear and nonlinear mixed effects models. R package version 3.1-102.
- Poff NL (1997) Landscape filters and species traits: towards mechanistic understanding and prediction in stream ecology. *Journal of the North American Benthological Society*, **16**, 391–409.
- Poff NL, Olden JD, Vieira NKM, Finn DS, Simmons MP, Kondratieff BC (2006) Functional trait niches of North American lotic insects: traits-based ecological applications in light of phylogenetic relationships. *Journal of the North American Benthological Society*, **25**, 730–755.
- Poff NL, Pyne MI, Bledsoe BP, Cuhaciyan CC, Carlisle DM (2010) Developing linkages between species traits and multiscaled environmental variation to explore vulnerability of stream benthic communities to climate change. *Journal of the North American Benthological Society*, **29**, 1441–1458.
- Polis GA, Myers CA, Holt RD (1989) The ecology and evolution of intraguild predation : potential competitors that eat each other. *Annual Review of Ecology and Systematics*, **20**, 297–330.
- Polis G, Sears A, Huxel G, Strong D, Maron J (2000) When is a trophic cascade a trophic cascade? *Trends in Ecology & Evolution*, **15**, 473–475.
- Poole GC, Berman CH (2001) An ecological perspective on in-stream temperature: natural heat dynamics and mechanisms of human-caused thermal degradation. *Environmental Management*, **27**, 787–802.

- Post D (2002) The long and short of food-chain length. *Trends in Ecology & Evolution*, **17**, 269–277.
- Puey N (2010) Ecology of the benthic macroinvertebrates in the lower Ebro River: community characterization, population dynamics and bioaccumulation of pollutants in response to environmental factors. PhD Thesis. University of Barcelona, Spain.
- Quilty E, Moore RD (2007) Measuring stream temperature. *Watershed Management Bulletin*, **10**, 25–30.
- R Development Core Team (2012) R: A language and environment for statistical computing. R Foundation for Statistical Computing, Vienna, Austria. ISBN 3-900051-07-0, URL <http://www.R-project.org/>.
- Ragetti S, Pellicciotti F (2012) Calibration of a physically based, spatially distributed hydrological model in a glacierized basin: On the use of knowledge from glaciometeorological processes to constrain model parameters. *Water Resources Research*, **48**, 1–20.
- Rao CR (1982) Diversity and dissimilarity coefficients: a unified approach. *Theoretical Population Biology*, **21**, 24–43.
- Richards C, Johnson LB, Host GE (1996) Landscape-scale influences on stream habitats and biota. *Canadian Journal of Fisheries and Aquatic Sciences*, **53**, 295–311.
- Richards J, Moore R, Forrest A (2012) Late-summer thermal regime of a small proglacial lake. *Hydrological Processes*, **26**, 2687–2695.
- Richter BD, Baumgartner J V, Powell J, Braun DP (1996) A method for assessing hydrologic alteration within ecosystems. *Conservation Biology*, **10**, 1163–1174.
- Robinson CT, Tockner K, Burgherr P (2002) Seasonal patterns in macroinvertebrate drift and seston transport in streams of an alpine glacial flood plain. *Freshwater Biology*, **47**, 985–993.
- Rooney N, McCann KS (2012) Integrating food web diversity, structure and stability. *Trends in Ecology & Evolution*, **27**, 40–6.
- Rossaro B (1980) Description of some unknown larvae of the *Diamesa* genus and corrections to previous descriptions (Diptera, Chironomidae). *Archiv für Hydrobiologie*, **90**, 298–308.
- Rossaro B, Lencioni V, Boggero A, Marziali L (2006) Chironomids from southern alpine running waters: ecology, biogeography. *Hydrobiologia*, **562**, 231–246.
- Rott E, Cantonati M, Füreder L, Pfister P (2006) Benthic Algae in High Altitude Streams of the Alps – a Neglected Component of the Aquatic Biota. *Hydrobiologia*, **562**, 195–216.
- Roxburgh SH, Shea K, Wilson J. (2004) The intermediate disturbance hypothesis: path dynamics and mechanisms of species coexistence. *Ecology*, **85**, 359–371.

- Roy JW, Hayashi M (2009) Multiple , distinct groundwater flow systems of a single moraine – talus feature in an alpine watershed. *Journal of Hydrology*, **373**, 139–150.
- Rubel F, Hantel M (1999) Correction of daily rain gauge measurements in the Baltic sea drainage basin. *Nordic Hydrology*, **30**, 191 – 208.
- Rutherford JC, Blackett S, Blackett C, Saito L, Colley RJD (1997) Predicting the effects of shade on water temperature in small streams in small streams. *New Zealand Journal of Marine and Freshwater Research*, **31**, 707–721.
- Del Río M, Rico I, Serrano E, Tejado JJ (2012) GPR Prospection in the Ossoue Glacier (Pyrenees). In: *14th International Conference on Ground Penetrating Radar (GPR)* pp684–688, Shanghai, China.
- Sable KA, Wohl E (2006) The relationship of lithology and watershed characteristics to fine sediment deposition in streams of the Oregon coast range. *Environmental management*, **37**, 659–70.
- Sauer J, Domisch S, Nowak C, Haase P (2011) Low mountain ranges: summit traps for montane freshwater species under climate change. *Biodiversity and Conservation*, **20**, 3133–3146.
- Savina M, Schäppi B, Molnar P, Burlando P, Sevruk B (2012) Comparison of a tipping-bucket and electronic weighing precipitation gage for snowfall. *Atmospheric Research*, **103**, 45–51.
- Scarsbrook MR, Townsend CR (1993) Stream community structure in relation to spatial and temporal variation: a habitat templet study of two contrasting New Zealand streams. *Freshwater Biology*, **29**, 395–410.
- Scherrer SC, Appenzeller C, M. Laternser (2004) Trends in Swiss alpine snow days – the role of local and large scale climate variability. *Geophys. Res. Lett.*, **31**.
- Schutz C, Wallinger M, Burger R, Füreder L (2001) Effects of snow cover on the benthic fauna in a glacier-fed stream. *Freshwater Biology*, **46**, 1691–1704.
- Serrat D, Ventura J (1993) Glaciers of the Pyrenees, Spain and France. In: *Satellite Image Atlas of Glaciers of the world*. (eds: Williams RS, Ferrigno JG), pp E49–E61. US Geological Survey Professional Paper 1386-E-2.
- Sese J, Perrandez J V, Villar L (1999) La flora alpinade de los Pirineos. Unpatrimonio singular. In: *Espacios Naturales Protegidos del Pirineo* (ed: Villar L), pp 57–76. Zaragoza, Ecología y cartografía. Consejo de Protección la Naturaleza de Aragón.
- Shea K, Roxburgh SH, Rauschert ESJ (2004) Moving from pattern to process: coexistence mechanisms under intermediate disturbance regimes. *Ecology Letters*, **7**, 491–508.
- Shurin JB, Borer ET, Seabloom EW, Blanchette CA, Cooper D (2002) A cross-ecosystem comparison of the strength of trophic cascades. *Ecology Letters*, **5**, 785–791.

- Sih A, Bolnick DI, Luttbeg B, *et al.* (2010) Predator-prey naïveté, antipredator behavior, and the ecology of predator invasions. *Oikos*, **119**, 610–621.
- Sih A, Englund G, Wooster D (1998) Emergent impacts of multiple predators on prey. *Trends in Ecology & Evolution*, **13**, 350–355.
- Small MJ, Doyle MW, Fuller RL, Manners RB (2008) Hydrologic versus geomorphic limitation on CPOM storage in stream ecosystems. *Freshwater Biology*, **53**, 1618–1631.
- Smith K (1975) Water temperature variations within a major river system. *Nordic Hydrology*, **6**, 155–169.
- Smith BPG (1999) Water source and storage areas within a small alpine catchment in the French Pyrenees. PhD thesis. University of Birmingham, Birmingham, UK.
- Smith BPG, Hannah DM, Gurnell AM (2001) A hydrogeomorphological context for ecological research on alpine glacial rivers. *Freshwater Biology*, **46**, 1579–1596.
- Smith H, Wood PJ, Gunn J (2003) The influence of habitat structure and flow permanence on invertebrate communities in karst spring systems. *Hydrobiologia*, **510**, 53–66.
- Smithson MJ (2011) Workshop on: Noncentral Confidence Intervals and Power Analysis. Department of Psychology, Australian National University, Canberra, Australia. (Available from: <http://psychology3.anu.edu.au/people/smithson/details/CIstuff/CI.html>).
- Snelder TH, Lamouroux N, Leathwick JR, Pella H, Sauquet E, Shankar U (2009) Predictive mapping of the natural flow regimes of France. *Journal of Hydrology*, **373**, 57–67.
- Snook DL (2000) Macroinvertebrate communities in alpine glacier-fed streams: The Taillon catchment in the French Pyrenees. PhD Thesis. University of Birmingham, UK.
- Snook DL, Milner AM (2001) The influence of glacial runoff on stream macroinvertebrate communities in the Taillon catchment, French Pyrénées. *Freshwater Biology*, **46**, 1609–1623.
- Snook DL, Milner AM (2002) Biological traits of macroinvertebrates and hydraulic conditions in a glacier-fed catchment (French Pyrenees). *Archiv für Hydrobiologie*, **153**, 245–271.
- Somero GN (2010) The physiology of climate change: how potentials for acclimatization and genetic adaptation will determine “winners” and “losers”. *The Journal of Experimental Biology*, **213**, 912–20.
- Soulsby C, Chen M, Ferrier RC, Helliwell RC, Jenkins A, Harriman R (1998) Hydrogeochemistry of shallow groundwater in an upland Scottish catchment. *Hydrological Processes*, **12**, 1111–1127.

- Soulsby C, Petry J, Brewer M, Dunn S, Ott B, Malcolm I (2003) Identifying and assessing uncertainty in hydrological pathways: a novel approach to end member mixing in a Scottish agricultural catchment. *Journal of Hydrology*, **274**, 109–128.
- Southwood TR. (1977) Habitat, the templet for ecological strategies? *Journal of Animal Ecology*, **46**, 336–365.
- Sponseller R., Benfield E., Valett H. (2001) Relationships between land use , spatial scale and stream macroinvertebrate communities. *Freshwater Biology*, **46**, 1409–1424.
- Srivastava D, Kumar A, Verma A, Swaroop S (2012) Characterization of suspended sediment in meltwater from glaciers of Garhwal Himalaya. *Hydrological Processes*.
- Stahl K, Moore RD, Shea JM, Hutchinson D, Cannon AJ (2008) Coupled modelling of glacier and streamflow response to future climate scenarios. *Water Resources*, **44**, 1–13.
- Statzner B, Dolédec S, Hugueny B (2004) Biological trait composition of European stream invertebrate communities : assessing the effects of various trait filter types. *Ecography*, **4**, 470–488.
- Statzner B, Hildrew AG, Resh VH (2001) Species traits and environmental constraints: entomological research and the history of ecological theory. *Annual Review of Ecology, Evolution, and Systematics*, **46**, 291–316.
- Stevenson RJ (1997) Scale-dependent determinants and consequences of benthic algal heterogeneity. *Journal of the North American Benthological Society*, **16**, 248–262.
- Stewart IT (2009) Changes in snowpack and snowmelt runoff for key mountain regions. *Hydrological Processes*, **94**, 78–94.
- Stone RD (1987) The activity patterns of the Pyrenean desman (*Galemys pyrenaicus*) (Insectivora: Talpidae), as determined under natural conditions. *Journal of Zoology*, **213**, 95–106.
- Strayer DL, Eviner VT, Jeschke JM, Pace ML (2006) Understanding the long-term effects of species invasions. *Trends in Ecology & Evolution*, **21**, 645–51.
- Suecker JK, Ryan JN, Kendall C, Jarrett RD (2000) Determination of hydrologic pathways during snowmelt for alpine/subalpine basins, Rocky Mountain National Park, Colorado. *Water Resources Research*, **36**, 63-75.
- Suhling I, Suhling F (2013) Thermal adaptation affects interactions between a range-expanding and a native odonate species. *Freshwater Biology*, **58**, 705–714.
- Tachet H, Richoux P, Bournard M, Usseglio-Polatera P (2000) *Invertébrés d'eau douce. Systematique, Biologie, Ecologie*. Paris, CNRS Publishers.
- Theurer F, Koos K, Miller W (1984) *Instream water temperature model*. Instream Flow Information Paper 16. US Fish and Wildlife Service. FWS/OBS.84/15/v.p.

- Thomas CD, Cameron A, Green RE, *et al.* (2004) Extinction risk from climate change. *Nature*, **427**, 145–8.
- Thompson K, Petchey OL, Askew AP, Dunnett NP, Beckerman AP, Willis AJ (2010) Little evidence for limiting similarity in a long-term study of a roadside plant community. *Journal of Ecology*, **98**, 480–487.
- Thompson R, Townsend C (2006) A truce with neutral theory: local deterministic factors , species traits and dispersal limitation together determine. *Journal of Animal Ecology*, **75**, 476–484.
- Tierno de Figueroa JM, López-Rodríguez MJ, Lorenz A, Graf W, Schmidt-Kloiber A, Hering D (2010) Vulnerable taxa of European Plecoptera (Insecta) in the context of climate change. *Biodiversity and Conservation*, **19**, 1269–1277.
- Tonkin J, Death RG (2012) Consistent effects of productivity and disturbance on diversity between landscapes. *Ecosphere*, **3**, 1–19.
- Townsend C, Doledec S, Scarsbrook M (1997a) Species traits in relation to temporal and spatial heterogeneity in streams: a test of habitat templet theory. *Freshwater Biology*, **37**, 367–387.
- Townsend CR, Dolédec S, Scarsbrook M (1997b) Species traits in relation to temporal and spatial heterogeneity in streams: a test of habitat templet. *Freshwater Biology*, **37**, 367–387.
- Townsend CR, Hildrew AG (1994) Species traits in relation to a habitat templet for river systems. *Freshwater Biology*, **31**, 265–275.
- Townsend CR, Ross M, Mcintosh AR (1998) Disturbance, resource supply, and food-web architecture in streams. *Ecology Letters*, **1**, 200–209.
- Townsend CR, Scarsbrook MR, Dolédec S (1997c) The intermediate disturbance hypothesis , refugia , and biodiversity in streams. *Limnology and Oceanography*, **42**, 938–949.
- Treanor HB, Giersch JJ, Kappenman KM, Muhlfeld CC, Webb MAH (2013) Thermal tolerance of meltwater stonefly *Lednia tumana* nymphs from an alpine stream in Waterton–Glacier International Peace Park, Montana, USA. *Freshwater Science*, **32**, 597–605.
- Trexler JC, Loftus WF, Perry S (2005) Disturbance frequency and community structure in a twenty-five year intervention study. *Oecologia*, **145**, 140–52.
- Uehlinger U, Malard F, Ward J V. (2003) Thermal patterns in the surface waters of a glacial river corridor (Val Roseg, Switzerland). *Freshwater Biology*, **48**, 284–300.
- Uehlinger U, Robinson CT, Hieber M, Zah R (2010) The physico-chemical habitat template for periphyton in alpine glacial streams under a changing climate. *Hydrobiologia*, **657**, 107–121.

- Vanak AT, Gompper ME (2010) Interference competition at the landscape level: the effect of free-ranging dogs on a native mesocarnivore. *Journal of Applied Ecology*, **47**, 1225–1232.
- Vandewalle M, Bello F, Berg MP, *et al.* (2010) Functional traits as indicators of biodiversity response to land use changes across ecosystems and organisms. *Biodiversity and Conservation*, **19**, 2921–2947.
- Verberk WCEP, Noordwijk CGE Van, Hildrew AG (2013) Delivering on a promise: integrating species traits to transform descriptive community ecology into a predictive science. *Freshwater Science*, **32**, 531–547.
- Vincon G (1987) Etude hydrobiologique de la vallée d' Ossau (Pyrénées- Atlantiques II . Le milieu et la structure du peuplement benthique. *Annales de Limnologie*, **3**, 225–243.
- Vincon G, Ravizza C (2001) Leuctridae (Plecoptera) of the Pyrenees. *Annales de Limnologie*, **37**, 293–322.
- Viviroli D, Archer DR, Buytaert W, *et al.* (2011) Climate change and mountain water resources: overview and recommendations for research, management and policy. *Hydrology and Earth System Sciences*, **15**, 471–504.
- van Vliet MTH, Ludwig F, Zwolsman JJG, Weedon GP, Kabat P (2011) Global river temperatures and sensitivity to atmospheric warming and changes in river flow. *Water Resources Research*, **47**.
- van Vliet MTH, Yearsley JR, Franssen WHP, Ludwig F, Haddeland I, Lettenmaier DP, Kabat P (2012) Coupled daily streamflow and water temperature modelling in large river basins. *Hydrology and Earth System Sciences*, **16**, 4303–4321.
- Ward J V (1994) Ecology of alpine streams. *Freshwater Biology*, **32**, 277–294.
- Waringer J, Graf W, Pauls SU, Previsic A, Kucinic M (2010) A larval key to the Drusinae species (Trichoptera: Limnephilinae) of Austria , Germany, Switzerland and the dinaric western Balkan. *Denisia*, **29**, 383–406.
- Warton D, Hui K. (2011) The arcsine is asinine: the analysis of proportions in ecology. *Ecology*, **92**, 3–10.
- Webb BW (1996) Trends in stream and river temperature. *Hydrological Processes*, **10**, 205–226.
- Webb BW, Hannah DM, Moore RD, Brown LE, Nobilis F (2008) Recent advances in stream and river temperature research. *Hydrological Processes*, **22**, 902–918.
- Webb BW, Walling DE (1997) Complex summer water temperature behaviour below a UK regulating reservoir. *Regulated Rivers: Research and Management*, **13**, 463–477.
- Webb BW, Zhang Y (1997) Spatial and seasonal variability in the components of the river heat budget. *Hydrological Processes*, **11**, 79–101.

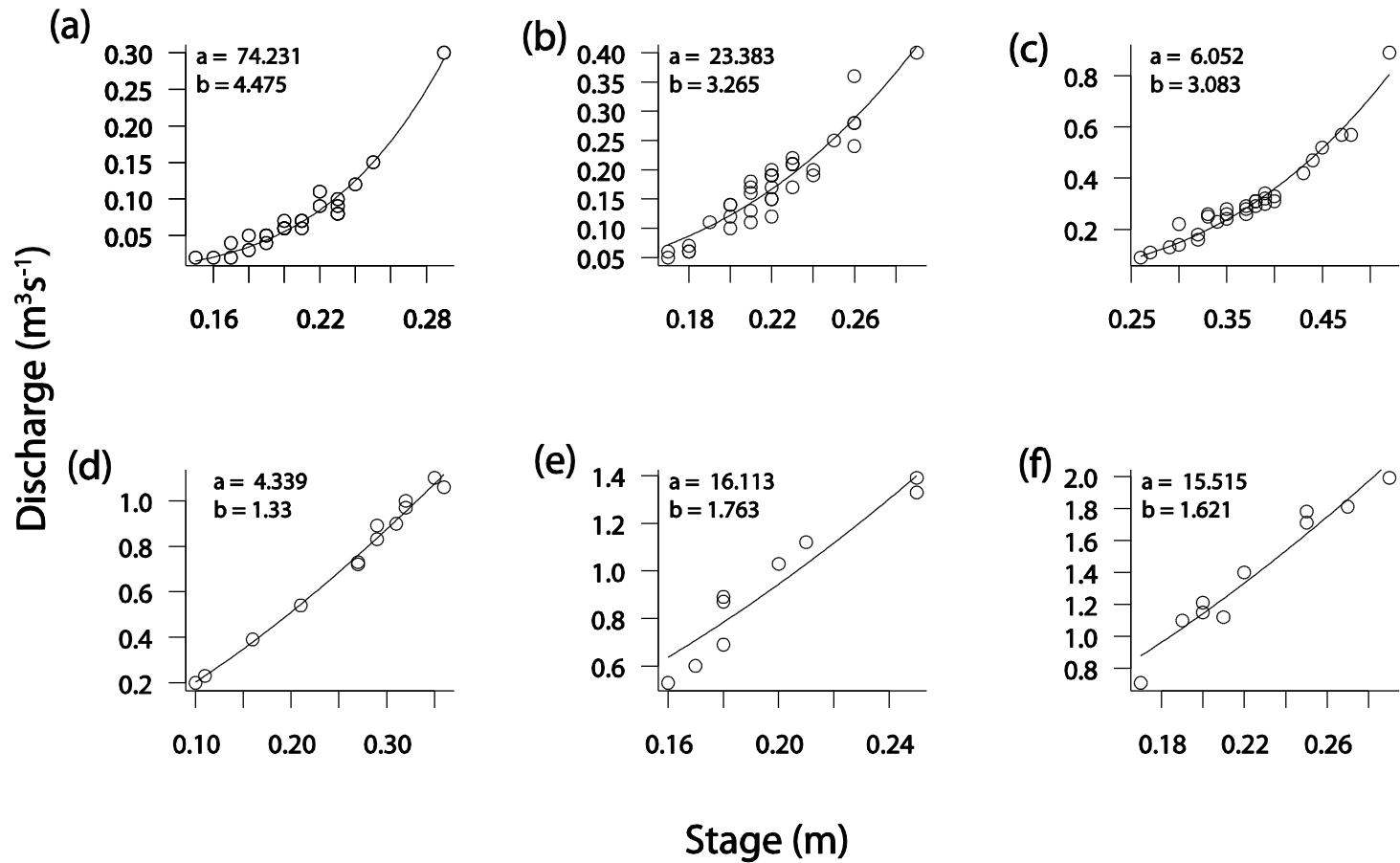
- Webb BW, Zhang Y (1999) Water temperatures and heat budgets in Dorset chalk water courses. *Hydrological Processes*, **13**, 309–321.
- Webster JR, Covich AP, Tank JL, Crockett T V (1994) Retention of coarse organic particles in streams in the southern Appalachian Mountains. *Journal of the North American Benthological Society*, **13**, 140–150.
- Weekes AA, Torgersen CE, Montgomery DR, Woodward A, Bolton SM (2012) A process-based hierarchical framework for monitoring glaciated alpine headwaters. *Environmental management*, **50**, 982–97.
- Westhoff MC, Bogaard TA, Savenije HHG (2010) Quantifying the effect of in-stream rock clasts on the retardation of heat along a stream. *Advances in Water resources*, **33**, 1417–1425.
- Williams BS, D'Amico E, Kastens JH, Thorp JH, Flotemersch JE, Thoms MC (2013) Automated riverine landscape characterization: GIS-based tools for watershed-scale research, assessment, and management. *Environmental Monitoring and Assessment*, **185**, 7485–99.
- Williams MW, Losleben M V, Hamann HB (2002) Alpine areas in the Colorado front range as monitors of climate change and ecosystem response. *American Geographical Society*, **92**, 180–191.
- Wilson JB (1994) The intermediate disturbance hypothesis of species coexistence is based on patch dynamics. *New Zealand Journal of Ecology*, **18**, 176–181.
- Winograd IJ, Riggs AC, Coplen TB (1998) The relative contributions of summer and cool-season precipitation to groundwater recharge, Spring Mountains, Nevada, USA. *Hydrogeology Journal*, **6**, 77–93.
- Winterbottom J, Orton S, Hildrew A (1997) Field experiments on the mobility of benthic invertebrates in a southern English stream. *Freshwater Biology*, **38**, 37–47.
- Wissinger S, Mcgrady J (1993) Intraguild predation and competition between larval dragonflies : direct and indirect effects on shared prey. *Ecology*, **74**, 207–218.
- Wood SN (2006) *Generalized additive models: An introduction with R*. Chapman and Hall.
- Wood SN (2008) Fast stable direct fitting and smoothness selection for generalized additive models. *Journal of the Royal Statistical Society: Series B*, **70**, 495–518.
- Woodward GUY, Benstead JP, Beveridge OS, *et al.* (2010a) Ecological Networks in a Changing Climate. *Advances In Ecological Research*, **42**.
- Woodward G, Dybkjaer JB, Ólafsson JS, Gíslason GM, Hannesdóttir ER, Friberg N (2010b) Sentinel systems on the razor's edge: effects of warming on Arctic geothermal stream ecosystems. *Global Change Biology*, **16**, 1979–1991.

- Woodward G, Ebenman B, Emmerson M, Montoya JM, Olesen JM, Valido A, Warren PH (2005) Body size in ecological networks. *Trends in Ecology & Evolution*, **20**, 402–409.
- Woodward G, Hildrew AG (2001) Invasion of a stream food web by a new top predator. *Journal of Animal Ecology*, **70**, 273–288.
- Woodward G, Hildrew AG (2002a) The impact of a sit-and-wait predator: separating consumption and prey emigration. *Oikos*, **3**, 409–418.
- Woodward G, Hildrew AG (2002b) Body-size determinants of niche overlap and intraguild predation within a complex food web. *Journal of Animal Ecology*, **71**, 1063–1074.
- Woodward G, Perkins DM, Brown LE (2010c) Climate change and freshwater ecosystems: impacts across multiple levels of organization. *Philosophical Transactions of the Royal Society B: Biological Sciences*, **365**, 2093–106.
- Wooster D, Sih A (1995) A review of the drift and activity responses of stream prey to predator presence. *Oikos*, **73**, 3–8.
- Wright JF (1974) Some factors affecting the distribution of *Crenobia alpina* (Dana), *Polycelis felina* (Dalyell) and *Phagocata vitta* (Dugès) (Platyhelminthes) in Caernarvonshire, North Wales. *Freshwater Biology*, **4**, 31–59.
- Wright JC, Elorral RM (1967) Heat budget studies on the Madison River, Yellowstone National Park. *Limnology and Oceanography*, **12**, 578–583.
- Xenopoulos MA, Lodge DM, Alcamo J, Marker M, Schulze K, Van Vuurens DP (2005) Scenarios of freshwater fish extinctions from climate change and water withdrawal. *Global Change Biology*, **11**, 1557–1564.
- Yang LH, Rudolf VHW (2010) Phenology, ontogeny and the effects of climate change on the timing of species interactions. *Ecology letters*, **13**, 1–10.
- Young RG, Quarterman AJ, Eyles RF, Smith RA, Bowden WB (2005) Water quality and thermal regime of the Motueka River: Influences of land cover, geology and position in the catchment. *New Zealand Journal of Marine and Freshwater Research*, **39**, 37–41.
- Younus M, Hondzo M, Engel BA (2000) Stream temperature dynamics in upland agricultural watersheds. *Journal of Environmental Engineering*, **126**, 518–526.
- Zah R, Burgherr P, Bernasconi S., Uehlinger U (2001) Stable isotope analysis of macroinvertebrates and their food sources in a glacier stream. *Freshwater Biology*, **46**, 871–882.
- Zemp M, Haeberli W, Hoelzle M, Paul F (2006) Alpine glaciers to disappear within decades? *Geophysical Research Letters*, **33**, 6–9.
- Zuur AF, Ieno EN, Elphick CS (2010) A protocol for data exploration to avoid common statistical problems. *Methods in Ecology and Evolution*, **1**, 3–14.

- Zuur AF, Ieno EN, Walker N, Saveliev AA, Smith G. (2009) *Mixed effects models and extensions in ecology with R*. Springer, New York.
- Zwart H (1986) The variscan geology of the Pyrenees. *Tectonophysics*, **129**, 9–27.
- Zwick P (2004) Key to the west palaeartic genera of stoneflies (Plecoptera) in the larval stage. *Limnologica*, **34**, 315–348.
- Zwick P, Vinçon G (2009) Contribution to the knowledge of Pyrenean stoneflies (Insecta : Plecoptera). *Annales de Limnologie*, **29**, 47–57.

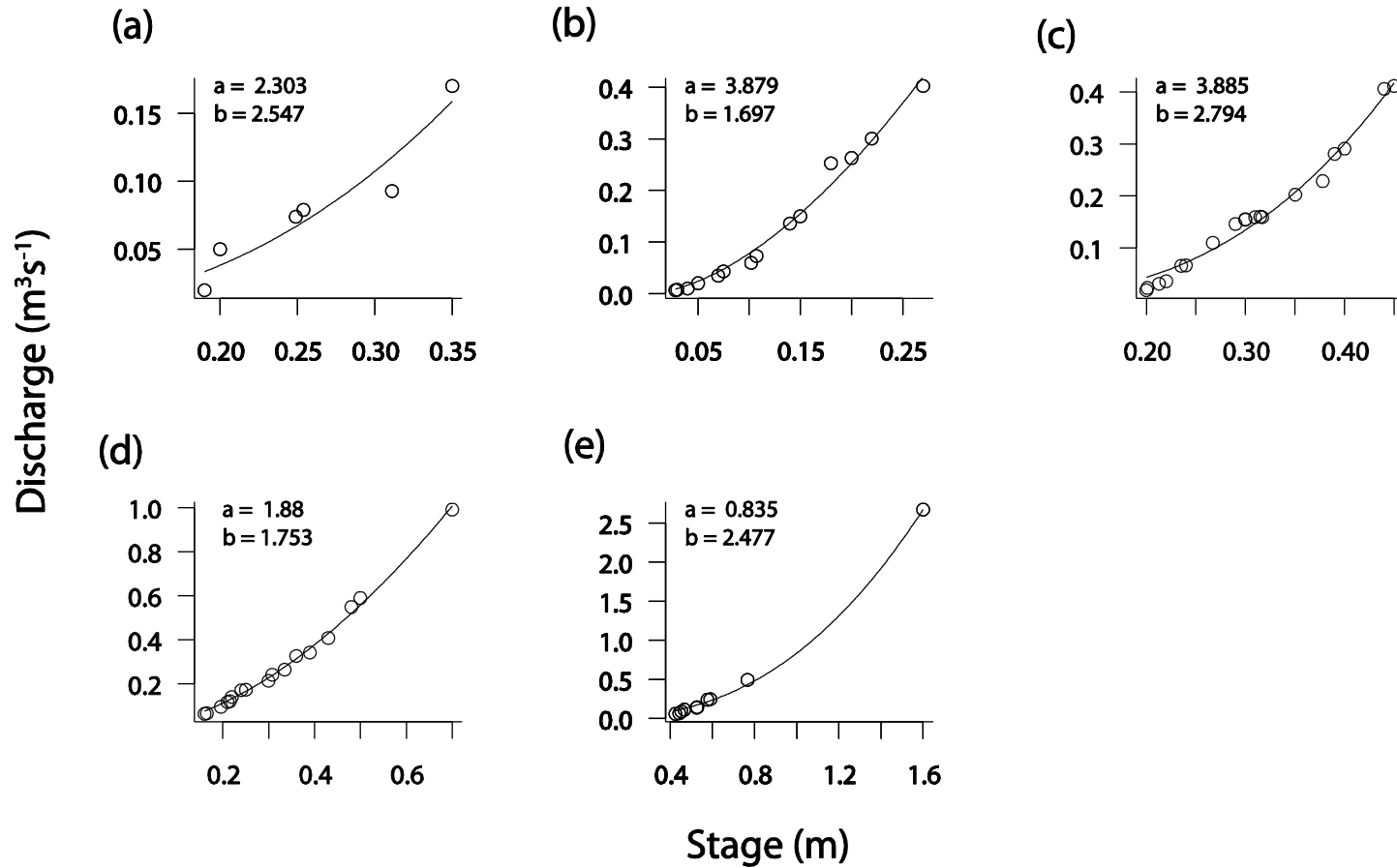
Appendix 3.1

Rating curves for all gauging stations during the 2010 field season; (a) G4 pre-flood, (b) G4 post-flood (c), T3, (d) T4, (d) O3, (e) Taillon basin outlet. Regression coefficients are displayed in each panel (all curves are of the form: $y = ax^b$).



Appendix 3.1 cont.

Rating curves for all gauging stations during the 2010 field season; (a) G4 pre-flood, (b) G4 post-flood (c), T3, (d) T4, (d) O3, (e) Taillon basin outlet. Regression coefficients are displayed in each panel (all curves are of the form: $y = ax^b$).



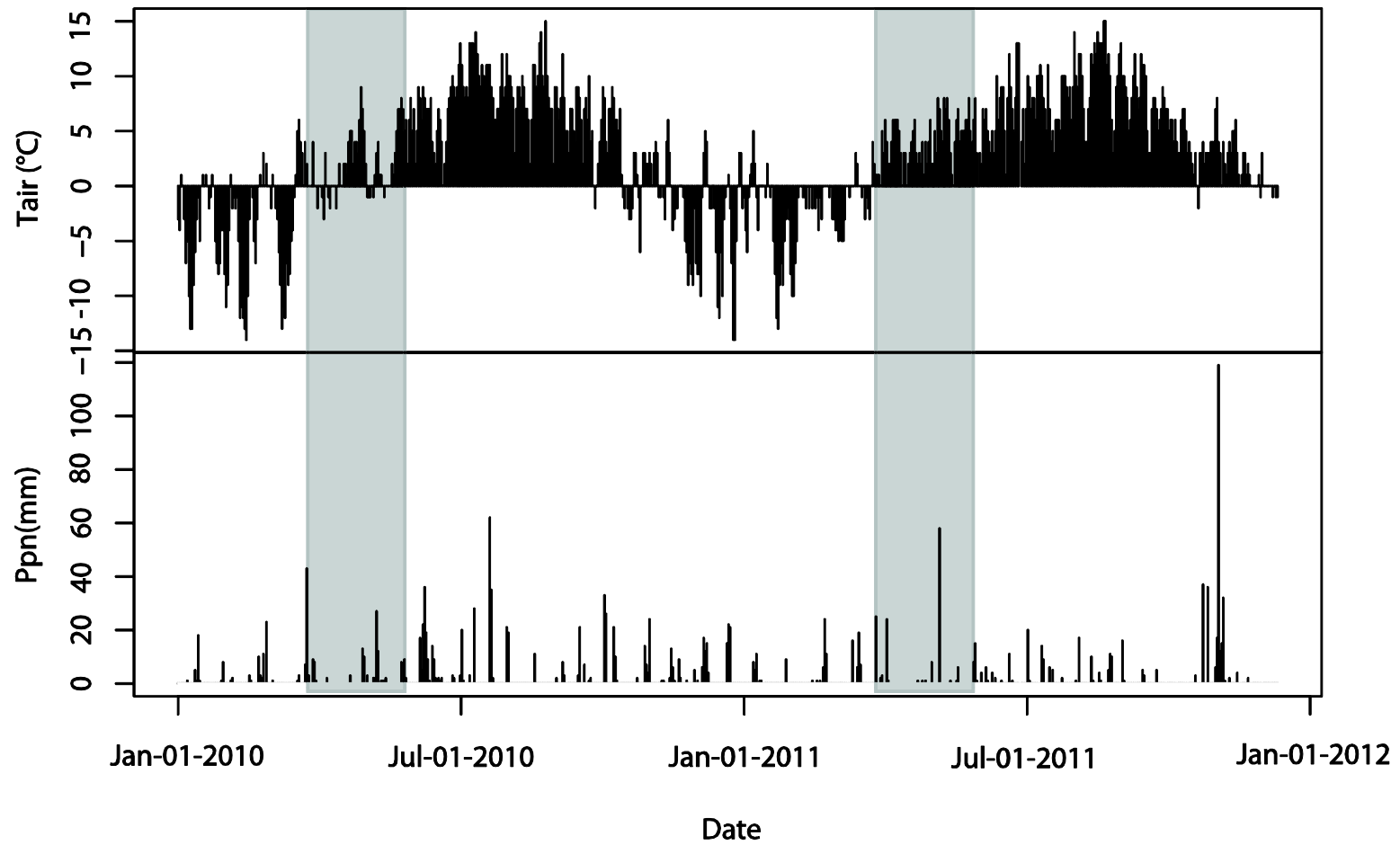
Appendix 3.2

Mean hydrograph separation uncertainty estimates for each site during the 2010 and 2011 field seasons. Following Genereux (1998) uncertainty (95% confidence) ,was proportioned between the end members (Melt: Meltwater and GW: Groundwater) and the errors associated with analysis (River). SD is displayed in parentheses.

Site	2010					2011				
	Uncertainty		Source of uncertainty (%)			Uncertainty		Source of uncertainty (%)		
			Melt	GW	River			Melt	GW	River
G1	0.12	(0.01)	10.36	87.90	1.75	0.09	(0.04)	53.93	45.51	0.56
G2	0.28	(0.02)	0.85	98.23	0.92	0.25	(0.04)	2.39	96.69	0.92
G3	0.31	(0.03)	0.57	98.55	0.89	0.25	(0.05)	2.34	96.74	0.92
G4	0.38	(0.03)	0.25	98.91	0.84	0.37	(0.01)	0.43	98.70	0.87
O1	0.21	(0.04)	28.51	71.15	0.35	0.05	(0.02)	48.26	51.14	0.60
O2	0.40	(0.06)	1.91	97.73	0.36	0.29	(0.07)	0.49	98.69	0.82
O3	0.38	(0.02)	2.38	97.25	0.36	0.35	(0.09)	0.26	98.93	0.81
T1	0.10	(0.04)	19.93	78.53	1.54	0.08	(0.01)	51.01	48.08	0.91
T2	0.19	(0.03)	3.36	95.78	0.86	0.11	(0.03)	26.83	72.29	0.88
T3	0.16	(0.06)	5.73	92.87	1.40	0.11	(0.01)	21.82	77.08	1.10
T4	0.26	(0.05)	1.23	97.81	0.96	0.14	(0.02)	12.25	86.74	1.01
T5	0.24	(0.03)	1.46	97.56	0.98	0.16	(0.03)	9.83	89.31	0.85
V1	-		-	-	-	0.10	(0.04)	51.16	47.55	1.29
V2	0.29	(0.04)	0.54	95.31	4.15	0.23	(0.03)	1.85	96.22	1.93
V3	0.31	(0.04)	0.41	95.45	4.14	0.26	(0.04)	0.93	97.16	1.92
V4	0.38	(0.01)	0.08	95.80	4.12	0.30	(0.01)	0.26	97.84	1.89
VHS	0.29	(0.06)	0.69	95.16	4.15	0.27	(0.03)	0.67	97.41	1.91

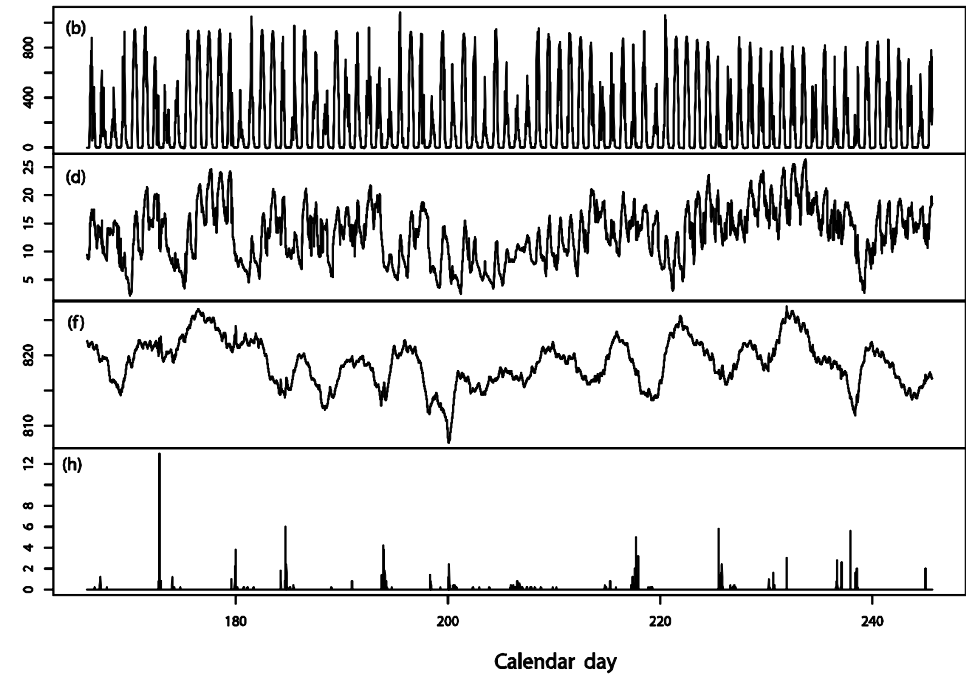
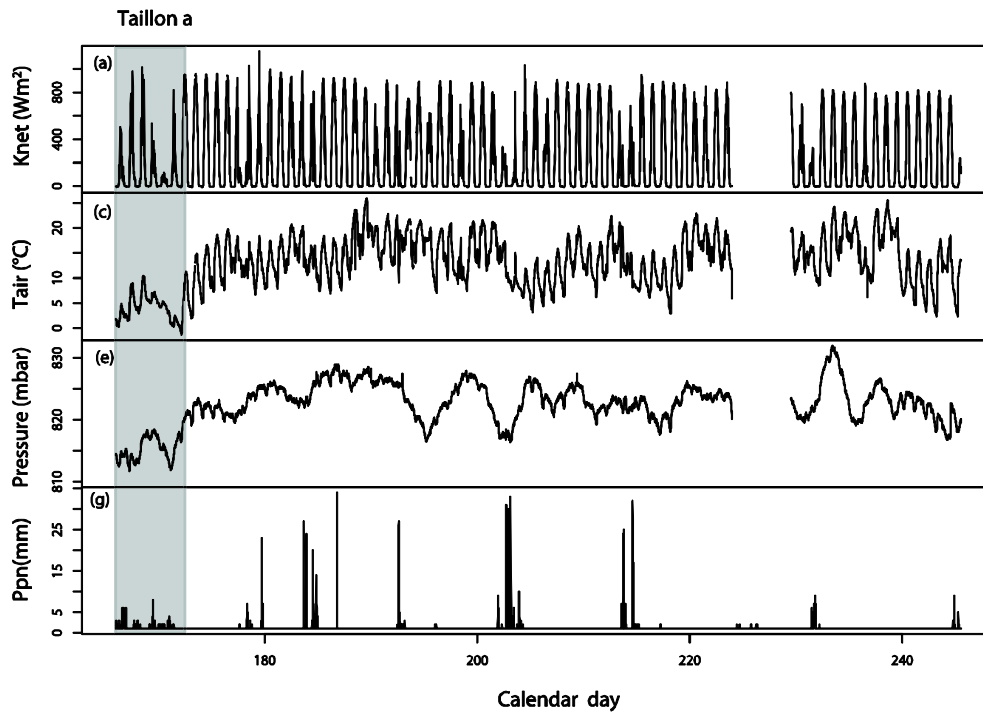
Appendix 3.3

Daily mean air temperature and daily total precipitation records for the Gavarnie MeteoFrance station. The spring periods prior to the 2010 and 2011 summer field campaigns are highlighted.



Appendix 3.4

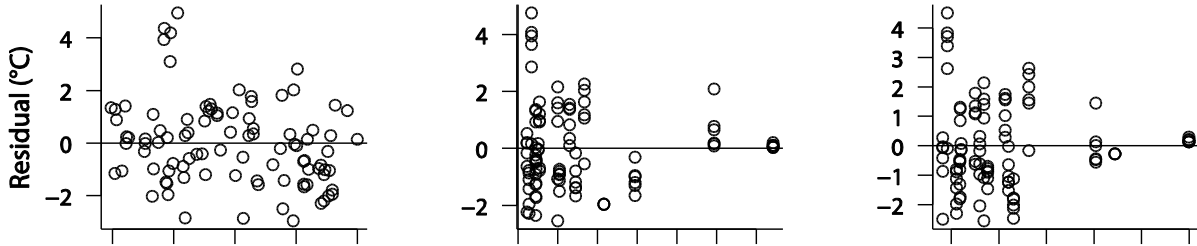
Time series of meteorological variable recorded as the AWS located in the Taillon basin with the ‘cold’ Taillon hydrochemistry sampling period highlighted. Net shortwave radiation for (a) 2010 and (b) 2011; air temperature for (c) 2010 and (d) 2011; atmospheric pressure for (e) 2010 and (f) 2011; and precipitation for (g) 2010 and (h) 2011. All records are 15min averages except precipitation which are 15min totals.



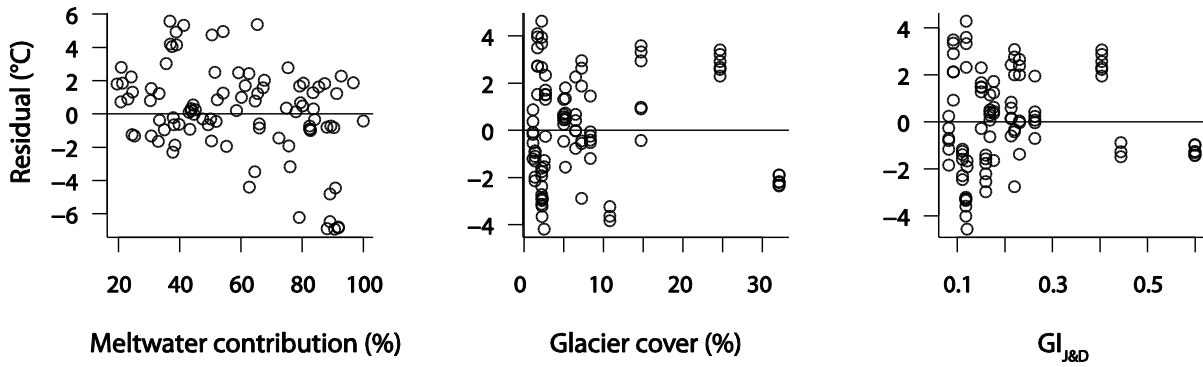
Appendix 3.5

Residuals from the Linear mixed models for (a) minimum water temperature and (b) mean water temperature.

(a)



(b)



Appendix 4.1

Study site locations and reach scale physicochemical characteristics (T_w = water temperature, PFAN = Pfankuch Index, SSC = suspended sediment concentration and EC = electrical conductivity). Subscript _s denotes hillslope channels.

Site	Basin	Altitude (m)	Width (m)	Depth (cm)	T_w mean (°C)	T_w range (°C)	pH	EC ($\mu\text{S cm}^{-1}$)	SSC (mg L^{-1})	PFAN	Meltwater (%)
Ne1	Néous	2200	2.2	13.5	7.3	13.0	8.5	18.0	10.8	42	87
Ne3	Néous	1720	2.8	15.6	7.7	7.4	8.3	23.0	4.6	32	47
O1	Ossoue	2250	5.1	9.2	7.1	11.2	8.2	38.0	57.7	44	99
O2	Ossoue	2005	4.1	13.8	8.0	6.5	8.2	74.0	6.3	40	65
O3	Ossoue	1870	7.7	13.0	9.1	8.5	8.3	80.0	2.1	34	59
O _s 1	Ossoue	2350	0.7	1.6	9.3	17.5	8.1	80.0	5.1	32	0
O _s 2	Ossoue	1820	8.8	6.1	10.4	16.5	8.5	107.0	4.2	30	0
G1	Taillon	2080	1.2	9.0	9.7	10.8	8.3	91.0	14.1	50	92
G2	Taillon	2030	3.2	11.2	8.4	6.5	8.4	113.0	3.8	38	61
G3	Taillon	1900	1.9	10.2	11.2	14.2	8.4	130.0	4.2	38	56
G4	Taillon	1860	2.5	8.0	11.6	6.8	8.6	172.0	3.9	32	43
T1	Taillon	2560	5.5	10.3	0.8	3.2	9.0	55.0	212.3	54	89
T2	Taillon	2150	3.3	8.9	9.1	13.5	8.8	98.0	90.0	44	87
T3	Taillon	1870	2.7	5.3	8.9	11.3	8.8	120.0	43.2	40	82
T4	Taillon	1860	2.3	13.8	9.8	9.8	8.6	132.0	40.0	38	75
T _s 1	Taillon	2030	0.6	4.4	9.5	3.3	7.5	176.0	4.4	30	0
T _s b	Taillon	1930	0.4	1.6	12.7	15.7	8.4	231.0	5.2	32	0
Tr2	Tromouse	1750	5.5	12.5	7.8	8.1	8.3	170.0	4.8	30	20
V1	Vignemale	2250	3.7	8.9	2.9	NA	8.7	62.0	11.9	48	90

Site	Basin	Altitude (m)	Width (m)	Depth (cm)	T _w mean (°C)	T _w range (°C)	pH	EC (μS cm ⁻¹)	SSC (mg L ⁻¹)	PFAN	Meltwater (%)
V3	Vignemale	1980	8.1	13.8	6.7	7.8	8.2	95.0	5.9	38	23
V4	Vignemale	1820	14.9	15.8	8.6	9.6	8.0	96.0	5.8	36	21
VHS	Vignemale	2150	6.0	11.8	4.6	2.8	8.5	69.0	15.9	34	24
V _S 1	Vignemale	2150	1.6	4.7	3.7	0.6	8.6	105.0	2.1	32	0
V _S 2	Vignemale	1980	2.2	4.8	7.7	1.5	7.9	48.0	1.4	30	0
V _S 3	Vignemale	1800	0.7	12.5	6.3	0.3	7.0	133.0	2.4	34	0

Appendix 4.2

Mantel tests results for regression model residuals and distance between sites(m). The test determines if the Euclidean distance matrices for each variable are correlated and the significance calculated from 999 permutations.

Response variable	Mantel r	P
Total density	-0.07	0.78
Taxonomic richness	-0.01	0.46
EPT richness	0.02	0.45
Predator proportion	0.07	0.21
Evenness	0.05	0.25
Beta diversity	-0.07	0.74
Trichoptera proportion	0.06	0.68
Ephemeroptera proportion	0.04	0.41
Plecoptera proportion	0.03	0.37
Diptera proportion	0.05	0.44
<i>R. evoluta</i> density	-0.04	0.45
<i>B. alpinus</i> density	0.07	0.52
<i>Protonemura</i> density	0.05	0.71
<i>D. latitarsis</i> density	-0.07	0.73

Appendix 4.2

Mantel tests results for regression model residuals and distance between sites(m). The test determines if the Euclidean distance matrices for each variable are correlated and the significance calculated from 999 permutations.

Response variable	Mantel r	P
Total density	-0.07	0.78
Taxonomic richness	-0.01	0.46
EPT richness	0.02	0.45
Predator proportion	0.07	0.21
Evenness	0.05	0.25
Beta diversity	-0.07	0.74
Trichoptera proportion	0.06	0.68
Ephemeroptera proportion	0.04	0.41
Plecoptera proportion	0.03	0.37
Diptera proportion	0.05	0.44
<i>R. evoluta</i> density	-0.04	0.45
<i>B. alpinus</i> density	0.07	0.52
<i>Protonemura</i> density	0.05	0.71
<i>D. latitarsis</i> density	-0.07	0.73

Appendix 4.3

Analysis of deviance results for geology as an interaction term in the regression models. A significant increase in deviance implies geology is an important explanatory variable.

Response variable	Deviance Δ	<i>P</i>
Total density	21.7	<0.001
Taxonomic richness	4.3	0.72
EPT richness	2.1	0.34
Predator proportion	0.2	0.90
Evenness	0.1	0.91
Beta diversity	0.6	0.003
Trichoptera proportion	0.2	0.06
Ephemeroptera proportion	0.3	0.36
Plecoptera proportion	0.2	0.44
Diptera proportion	1.1	0.09
<i>R. evoluta</i> density	57.3	<0.001
<i>B. alpinus</i> density	0.4	0.61
<i>Protonemura</i> density	0.2	0.72
<i>D. latitarsis</i> density	28.6	<0.001

Appendix 5.1

Trait list for the most common taxa (n = 51). Coding follows Tachet (2002) except Chironomidae which have been adapted from Snook (2000).

Taxa	Maximal size (mm)					Life cycle			Aquatic stages				Reproduction						Dispersal			Resistance			Respiration						
	<2.5	2.5-5.0	5.0-10.0	10.0-20.0	20.0-30.0	Semivoltine	Univoltine	Multivoltine	Egg	Larvae	Pupa	Adult	Ovoviviparity	Egg free	Egg cement	Clutch cement	Clutch free	Clutch vegetation	Clutch terrestrial	Asexual	Aq passive	Aq active	Aerial passive	Aerial active	Eggs	Diapause	None	Tegument	Gills	Plastron	Spiracle
<i>Agapetus</i>	0	0	3	0	0	1	2	1	3	3	3	0	0	0	0	3	0	0	0	0	1	2	1	1	0	0	3	3	0	0	0
<i>Amphinemura</i>	0	1	3	0	0	0	3	0	3	3	0	0	0	0	3	0	0	0	0	2	2	0	1	1	1	0	3	2	0	0	
<i>Apatania</i>	0	0	1	3	0	2	3	0	3	3	3	0	0	0	0	3	0	0	3	3	2	0	2	0	2	2	3	2	0	0	
<i>Arcynopteryx</i>	0	0	0	3	1	3	0	0	3	3	0	0	0	0	0	3	0	0	0	2	2	0	1	3	0	0	3	0	0	0	
<i>Athericidae</i>	0	0	0	0	3	0	3	1	0	3	0	0	0	0	0	0	0	0	3	0	1	0	1	0	0	1	0	1	0	0	
<i>Baetis</i>	0	0	3	1	0	0	3	2	3	3	0	0	0	0	1	3	0	0	0	3	2	1	3	2	0	2	1	2	0	0	
<i>Blepharicera</i>	0	0	3	0	0	0	3	0	2	3	2	0	0	0	0	0	3	0	0	2	1	0	1	0	2	0	1	3	0	0	
<i>Capnianeura</i>	0	1	3	0	0	2	1	0	3	3	0	0	1	0	3	0	0	0	0	2	2	0	1	0	3	1	3	0	0	0	
<i>Chaetopterygini</i>	0	0	0	3	0	0	3	0	3	3	3	0	0	0	0	3	0	0	1	0	1	0	2	0	2	1	2	2	0	0	
<i>Chloroperla</i>	0	0	3	0	0	1	2	0	3	3	0	0	0	0	3	0	0	0	0	3	2	0	1	0	3	1	3	0	0	0	
<i>Crenobia</i>	0	0	0	2	3	0	3	0	3	3	0	3	0	0	0	2	0	0	0	1	2	0	0	3	0	0	3	0	0	0	

	<2.5	2.5-5.0	5.0-10.0	10.0-20.0	20.0-30.0	Semivoltine	Univoltine	Multivoltine	Egg	Larvae	Pupa	Adult	Ovoviviparity	Egg free	Egg cement	Clutch cement	Clutch free	Clutch vegetation	Clutch terrestrial	Asexual	Aq passive	Aq active	Aerial passive	Aerial active	Eggs	Diapause	None	Tegument	Gills	Plastron	Spiracle
<i>Diamesa</i>	0	2	3	0	0	0	1	3	1	2	3	0	0	0	0	2	1	0	2	0	2	1	1	1	0	0	3	3	0	0	0
<i>Dicranota</i>	0	0	1	3	2	0	3	0	2	2	0	0	0	1	0	0	1	0	0	0	2	1	0	1	0	0	2	0	0	0	3
<i>Drusus discolor</i>	0	0	0	3	0	1	3	0	3	3	3	0	0	0	0	3	0	0	1	0	3	2	0	2	0	0	1	3	2	0	0
<i>Drusus rectus</i>	0	0	0	3	0	1	3	0	3	3	3	0	0	0	0	3	0	0	1	0	3	2	0	2	0	0	1	3	2	0	0
<i>Ecdymurus</i>	0	0	0	3	0	1	3	0	3	3	0	0	0	0	1	3	0	0	0	0	3	1	1	3	2	1	2	1	3	0	0
<i>Elmis</i>	0	3	0	0	0	1	3	0	3	3	0	2	0	0	0	3	0	0	0	0	2	1	0	2	0	0	3	1	3	3	0
<i>Empididae</i>	0	0	3	0	0	0	3	2	0	2	3	0	0	0	0	0	0	0	3	0	1	1	0	3	0	0	1	1	0	0	1
<i>Esolus</i>	0	3	0	0	0	1	3	0	3	3	0	2	0	0	0	3	0	0	0	0	2	1	0	2	0	0	3	1	3	3	0
<i>Eukiefferiella</i>	0	1	3	0	0	0	1	3	0	3	3	0	0	0	0	2	1	0	2	0	2	1	1	1	0	1	3	3	1	0	0
<i>Hydreanea</i>	0	3	0	0	0	1	3	0	3	3	0	2	0	0	0	3	0	0	0	0	2	1	0	2	0	0	3	0	0	3	0
<i>Hydropsyche</i>	0	0	1	3	1	2	2	0	3	3	3	0	0	0	0	3	0	0	0	0	3	2	1	3	0	0	3	2	3	0	0
<i>Isoperla</i>	0	0	1	3	0	2	3	0	3	3	0	0	0	0	1	2	0	0	0	0	2	2	0	2	1	0	3	3	0	0	0
<i>Leuctra</i>	0	0	3	1	0	1	3	0	3	3	0	0	0	0	3	0	0	0	0	0	2	2	0	1	1	0	3	3	0	0	0
<i>Limonidae</i>	0	0	2	3	0	0	3	1	2	1	0	0	0	1	0	1	0	0	0	0	0	1	2	1	0	0	3	1	0	0	3
<i>Micrasema</i>	0	1	3	0	0	1	2	0	3	3	3	0	0	0	0	2	0	0	0	0	0	1	1	2	0	0	3	3	2	0	0
<i>Micropsectra</i>	0	2	3	0	0	0	2	3	0	3	3	0	1	0	0	1	3	0	0	0	1	1	3	1	1	0	3	3	1	0	0
<i>Nemoura</i>	0	1	3	0	0	2	2	0	3	3	0	0	0	0	3	0	0	0	0	0	2	2	0	2	0	1	3	3	0	0	0
<i>Oligocheata</i>	1	1	1	1	1	0	0	2	3	3	0	3	0	0	0	3	0	0	0	2	1	0	0	0	0	0	1	3	0	0	0
<i>Orthocladius</i>	0	2	3	0	0	0	3	2	1	2	3	0	0	0	0	2	1	0	2	0	2	1	1	1	0	0	2	3	1	0	0
<i>Pachyleuctra</i>	0	0	0	3	0	3	1	0	3	3	0	0	0	0	3	0	0	0	0	0	1	1	0	1	1	1	0	3	0	0	0
<i>Parametrioctenus</i>	0	2	3	0	0	0	1	3	1	2	3	0	0	0	0	2	1	0	2	0	2	1	1	1	0	0	3	3	1	0	0
<i>Paratrichocladius</i>	0	3	1	0	0	0	3	2	1	2	3	0	0	0	0	2	1	0	2	0	2	1	1	1	0	0	2	3	1	0	0

Appendix 5.1: Cont.

Taxa	Substrate relationship					Diet							Functional feeding group					Body form			Case			
	Flier	Swimmer	Crawler	Burrower	interstitial	Clinger	Microorganisms	FPOM	CPOM	Algae	Macrophyte	Dead invertebrates	Invertebrates	Scrapper	Shredder	Collector/Deposit feeder	Filter feeder	Piercer	Predator	Streamlined	Cylindrical	Other	No case	Case
<i>Agapetus</i>	0	0	2	0	0	1	0	1	0	5	0	0	0	3	0	0	0	0	0	0	2	1	3	0
<i>Amphinemura</i>	0	0	5	0	1	1	0	1	2	1	0	0	0	0	3	1	0	0	0	1	0	2	3	0
<i>Apatania</i>	0	0	5	0	0	0	0	1	1	4	1	0	1	3	0	1	0	0	0	0	2	1	3	0
<i>Arcynopteryx</i>	0	0	5	0	0	0	1	1	0	1	0	0	5	0	0	0	0	0	2	1	0	2	3	0
<i>Athericidae</i>	0	0	5	0	2	0	0	0	0	0	0	0	5	0	0	0	0	3	0	0	2	1	3	0
<i>Baetis</i>	0	3	4	0	1	0	0	2	2	5	1	0	0	3	0	1	0	0	0	2	2	0	3	0
<i>Blepharicera</i>	0	0	1	0	0	4	0	0	0	5	0	0	0	3	0	0	0	0	0	1	0	2	3	0
<i>Capnianeura</i>	0	0	5	1	1	0	0	1	2	0	2	0	0	0	3	0	0	0	0	2	1	1	3	0
<i>Chaetopterygini</i>	0	0	5	0	0	0	0	1	3	1	2	0	1	0	3	0	0	0	0	0	2	1	0	3
<i>Chloroperla</i>	0	0	5	1	1	0	0	1	1	1	1	0	5	0	3	0	0	0	1	2	1	1	3	0
<i>Crenobia</i>	0	0	4	0	1	0	0	0	0	0	0	1	3	0	0	0	0	0	4	0	0	3	3	0
<i>Diamesa</i>	0	0	1	0	1	3	0	2	0	4	0	0	0	3	0	2	0	0	0	0	2	0	3	0
<i>Dicranota</i>	0	0	3	0	2	0	0	1	0	0	0	0	3	0	0	0	0	0	3	0	2	1	3	0
<i>Drusus discolor</i>	0	0	5	0	0	0	1	0	1	1	2	0	2	0	0	1	2	0	2	0	2	1	0	3
<i>Drusus rectus</i>	0	0	5	0	0	0	1	0	1	3	2	0	1	2	0	3	0	0	0	0	2	1	0	3

	Flier	Swimmer	Crawler	Burrower	interstitial	Clinger	Microorganisms	FPOM	CPOM	Algae	Macrophyte	Dead invertebrates	Invertebrates	Scrapper	Shredder	Collector/Deposit feeder	Filter feeder	Piercer	Predator	Streamlined	Cylindrical	Other	No case	Case
<i>Ecdynurus</i>	0	1	5	0	0	0	0	2	0	3	0	0	0	3	0	1	0	0	0	3	0	0	3	0
<i>Elmis</i>	1	0	4	0	0	0	0	1	0	3	0	0	0	2	0	3	0	0	0	0	0	3	3	0
<i>Empididae</i>	0	0	2	1	1	0	0	0	0	0	0	0	5	0	0	0	0	0	3	0	2	1	3	0
<i>Esolus</i>	1	0	4	0	0	0	0	1	0	3	0	0	0	2	0	3	0	0	0	0	0	3	3	0
<i>Eukiefferiella</i>	0	0	1	0	1	0	0	3	0	2	0	0	0	2	0	2	0	0	2	0	2	0	2	2
<i>Hydreanea</i>	1	0	4	0	0	0	0	1	0	3	0	0	0	3	0	1	0	0	0	0	0	3	3	0
<i>Hydropsyche</i>	0	0	2	0	0	1	0	2	1	3	0	0	3	0	0	0	3	0	1	0	2	1	3	0
<i>Isoperla</i>	0	0	4	0	0	0	0	1	0	1	0	0	5	0	2	0	0	0	3	2	0	1	3	0
<i>Leuctra</i>	0	0	5	2	1	0	0	1	1	2	2	1	0	1	3	1	0	0	0	0	2	1	3	0
<i>Limonidae</i>	0	0	1	5	0	0	0	3	0	2	0	0	1	3	0	2	0	0	0	0	2	1	3	0
<i>Micrasema</i>	0	0	3	0	0	1	0	1	2	2	1	0	1	0	0	1	3	0	0	0	2	1	0	3
<i>Micropsectra</i>	0	0	2	0	1	0	0	3	0	2	0	0	0	1	0	2	0	0	0	0	2	0	2	2
<i>Nemoura</i>	0	0	5	0	1	0	0	1	2	1	0	0	0	0	3	0	0	0	0	0	2	1	3	0
<i>Oligocheata</i>	0	0	0	1	1	0	1	2	0	2	0	0	0	3	0	1	0	0	0	0	3	0	3	0
<i>Orthocladius</i>	0	0	1	1	1	1	0	2	0	2	0	0	1	3	0	1	1	0	0	0	2	0	3	2
<i>Pachyleuctra</i>	0	0	5	2	0	0	0	2	2	3	1	0	0	1	3	1	0	0	0	1	0	2	3	0
<i>Parametriocnemus</i>	0	0	2	0	2	0	0	3	0	2	0	0	0	1	0	2	0	0	0	0	2	0	3	2
<i>Paratrichocladius</i>	0	0	1	1	1	1	0	2	0	2	0	0	1	3	0	1	1	0	0	0	2	0	3	2
<i>Parorthocladius</i>	0	0	1	1	1	1	0	2	0	2	0	0	1	3	0	1	1	0	0	0	2	0	3	2
<i>Tanypodinae</i>	0	3	2	1	1	0	0	0	1	1	0	0	5	1	0	1	0	0	3	0	2	0	2	2
<i>Perla</i>	0	0	5	0	0	0	0	0	1	0	0	0	5	0	0	0	0	0	3	1	0	2	3	0
<i>Perlodes</i>	0	0	5	0	0	0	0	0	1	1	0	0	5	0	1	0	0	0	3	1	0	2	3	0

	Flier	Swimmer	Crawler	Burrower	interstitial	Clinger	Microorganisms	FPOM	CPOM	Algae	Macrophyte	Dead invertebrates	Invertebrates	Scrapper	Shredder	Collector/Deposit feeder	Filter feeder	Piercer	Predator	Streamlined	Cylindrical	Other	No case	Case
<i>Plectrocnemias</i>	0	0	2	0	0	2	0	1	0	1	0	0	3	0	0	0	3	0	3	0	2	1	3	0
<i>Polycelis</i>	0	0	4	0	1	0	0	0	0	0	0	1	3	0	0	0	0	0	4	0	0	3	3	0
<i>Prosimulium</i>	0	0	2	0	1	4	0	2	0	1	0	0	0	0	0	1	3	0	0	0	2	1	3	0
<i>Protonemura</i>	0	0	5	0	1	0	0	1	2	1	0	0	0	0	3	0	0	0	0	0	2	1	3	0
<i>Pseudodiamesa</i>	0	0	2	0	1	0	0	1	0	2	0	0	2	1	0	1	0	0	2	0	2	0	3	0
<i>Rheocricotopus</i>	0	0	1	0	2	0	0	3	0	2	0	0	0	2	0	2	0	0	2	0	2	0	2	2
<i>Rhithrogena</i>	0	1	5	0	1	0	1	1	2	3	1	0	0	3	0	1	0	0	0	3	0	0	3	0
<i>Rhyacophila</i>	0	2	3	0	0	2	0	0	1	1	0	0	5	0	0	0	0	0	3	1	2	0	3	0
<i>Simulium</i>	0	0	2	0	1	4	0	3	0	1	0	0	1	0	0	1	3	0	0	0	2	1	3	0
<i>Siphonoperla</i>	0	0	5	1	1	0	1	1	2	1	1	0	5	0	3	0	0	0	1	2	1	1	3	0
<i>Synorthocladius</i>	0	0	1	1	1	1	0	2	0	2	0	0	1	3	0	1	1	0	0	0	2	0	3	2
<i>Tanytarsinii</i>	0	0	2	0	1	0	0	3	0	2	0	0	0	1	0	2	0	0	0	0	2	0	3	2
<i>Tipula</i>	0	0	2	0	1	0	0	1	0	2	2	0	1	0	2	1	0	0	2	0	2	1	3	0
<i>Tvetenia</i>	0	0	1	1	1	1	0	2	0	2	0	0	1	3	0	1	1	0	0	0	2	0	3	2

Appendix 5.2

Correlations (RV coefficients) between all the biological traits recorded. Only significant correlations ($P < 0.05$) are displayed. P -values were estimated via a permutation procedure with 999 repeats.

	Size	Number of generations	Aquatic stages	Reproduction	Dispersal	Resistance	Respiration	Substrate relationship	Diet	Functional feeding	Body form
Number of generations	0.19										
Aquatic stages	0.14	0.34									
reproduction	-	0.20	0.34								
Dispersal	0.13	0.26	0.21	0.12							
Resistance	-	-	-	-	0.10						
Respiration	0.10	-	-	-	0.11	-					
Substrate relationship	0.21	0.37	0.25	0.14	0.26	-	-				
Diet	0.25	0.16	0.09	0.15	0.22	-	-	0.16			
Functional feeding	0.17	0.15	0.15	0.29	0.22	0.13	0.10	0.17	0.65		
Body form	0.12	0.40	0.54	0.17	0.23	0.19	-	-	-	-	
Case construction	-	-	0.25	0.11	-	0.10	-	-	-	-	0.19

Appendix 5.3

Logistic regression results for the occurrence of selected traits in response to meltwater proportion. All *P* values are corrected to control for the false discovery rate (FDR) associated with multiple statistical test (* = $P < 0.05$, ** = $P < 0.01$, *** = $P < 0.001$).

Trait	Modality	t	Deviance	<i>P</i>	Response
Maximal body size	20–40 mm	-3.28	0.39	**	↓
	10–20 mm	-3.59	0.35	**	↓
	2.5-5.0 mm (<i>Resil</i>)	3.17	0.34	**	↑
	Small (<10mm) ¹ (<i>Resil</i>)	3.91	0.38	**	↑
Voltinism	Multivoltine (<i>Resil</i>)	4.44	0.47	***	↑
	Semivoltine Clutch terrestrial (<i>Resil</i>)	-3.09	0.32	**	↓
Reproduction		2.79	0.28	*	↑
Dissemination	Aquatic active	-5.69	0.58	***	↓
	Aquatic passive	3.03	0.28	**	↑
Resistance	Eggs (<i>Resis</i>)	-3.55	0.36	**	↓
	None	3.04	0.28	**	↑
Substrate relationship	Crawler	-4.78	0.50	***	↓
	Clinger (<i>Resis</i>)	3.12	0.35	**	↑
Diet	Inverts	-5.34	0.61	***	↓
	FPOM	3.77	0.38	***	↑
	Algae/diatoms	3.44	0.33	**	↑
Functional feeding group	Predator	-4.66	0.55	***	↓
	Collector/deposit feeder	5.23	0.53	***	↑
	Scraper	2.99	0.27	**	↑
Body form	Other	-3.58	0.41	**	↓
	Cylindrical (<i>Resis</i>)	3.03	0.29	**	↑
Current velocity	< 50 ms	-5.12	0.52	***	↓

Appendix 6.1.

Length – mass regression equations. All equations are in the form $f(x) = \ln A + B \ln x$, where A and B are constants, x body length (mm) and $f(x)$ is body mass (mg).

Taxa regression relationship		ln(A)	B	Taxa in channels	Reference
<i>Nemoura</i>	<i>cinerea</i>	-6.265	3.588	<i>Protonemura</i> sp.	Giustini <i>et al.</i> (2008)
<i>Amphinemura</i>	spp	-5.9	3.32	<i>Amphinemura</i> sp.	Burgherr & Meyer (1997)*
<i>Chloroperla</i>	spp	-5.80	2.67	<i>Chloroperla</i> sp.	Burgherr & Meyer (1997)*
<i>Paraleptophlebia</i>	<i>submarginata</i>	-5.386	2.872	<i>Habroleptiodes</i> sp	Giustini <i>et al.</i> (2008)
<i>Ecdyonurus</i>	<i>helveticus</i>	-5.015	2.90	<i>Ecdyonurus</i> sp.	Giustini <i>et al.</i> (2008)
<i>Baetis</i>	spp.	-5.429	2.689	<i>Baetis</i> spp.	Giustini <i>et al.</i> (2008)
<i>Rhyacophila</i>	sp.	-4.615	2.48	<i>Rhyacophila</i> spp.	Benke (1999)
Orthoclaudiinae		-6.214	2.254	Orthoclaudiinae	Benke (1999)
<i>Plectrocnemia</i>	<i>conspersa</i>	2.58	2.80	<i>Plectrocnemia</i> sp.	Hildrew (1978)*
<i>Stenelmis</i>	spp.	-4.509	2.48	<i>Elmis/ Esolus</i> sp.	Benke (1999)
<i>Dugesia</i>	<i>tigrina</i>	-4.721	2.145	<i>Polycelis</i> sp.	Benke (1999)
Empididae		-5.221	2.546	Psycodidae	Benke (1999)
<i>Diamesa</i>	spp.	-6.231	2.602	Diamesinae	Nolte (1990)*
Naididae		-7.957	2.1	Oligochaeta	Finogenova (1984)*
<i>Brachycentrus</i>	<i>etowahensis</i>	-5.991	3.443	<i>Micrasema</i> sp.	Benke (1999)
<i>Pedicia</i>	spp.	-8.947	2.851	Pediciidae	Benke (1999)
		-			
<i>Simulium</i>	Sp.	4.5009	2.074	<i>Simulim</i> sp	Meyer (1989)*
Tanypodinae		-5.571	2.411	Tanypodinae	Benke (1999)

*In Stead *et al.* (2003)

Stead TK, Schmid-Araya JM, Hildrew AG (2003) All creatures great and small: patterns in the stream benthos across a wide range of metazoan body size. *Freshwater Biology*, **48**, 532–547.

Benke AC, Huryn AD, Smock LA, Wallace JB (1999) Length-mass relationships for freshwater macroinvertebrates in North America with particular reference to the Southeastern United States. *Journal of the North American Benthological Society*, **18**, 308–343.

Giustini M, Miccoli FP, Luca G, Cicolani B (2008) Length–weight relationships for some plecoptera and ephemeroptera from a carbonate stream in central Apennine (Italy). *Hydrobiologia*, **605**, 183–191.

Taxa	FFG	C1	C2	C3	C4	T1	T2	T3	T4
Limoniidae	Pre					8	8		
Tipulidae	Pre*	8		8					8
Misc taxa									
<i>Polycelis</i> sp.	Pre	38					8		15
Oligochaeta	Shr	8	15		8	15	23	8	
Collembola	Shr	8						8	

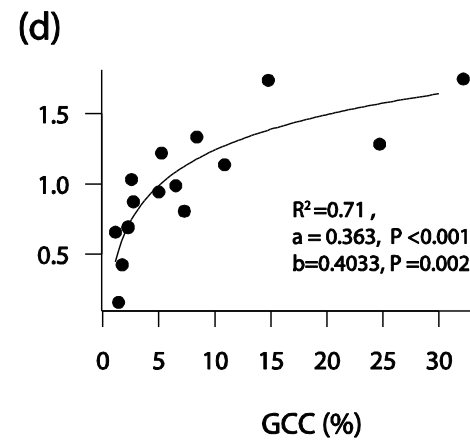
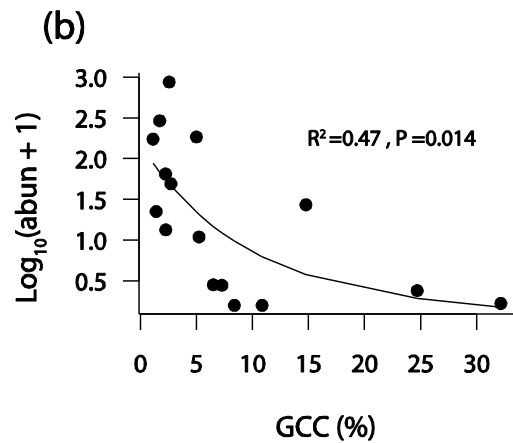
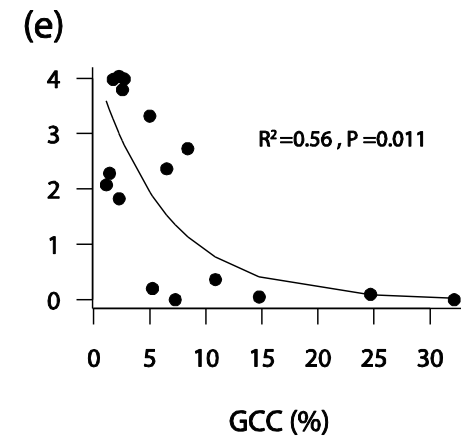
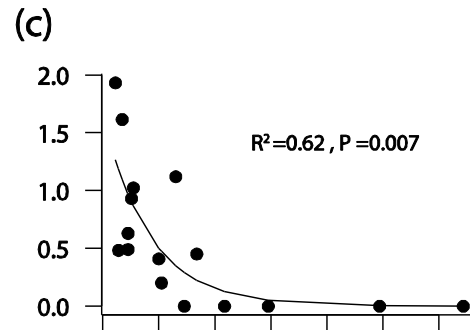
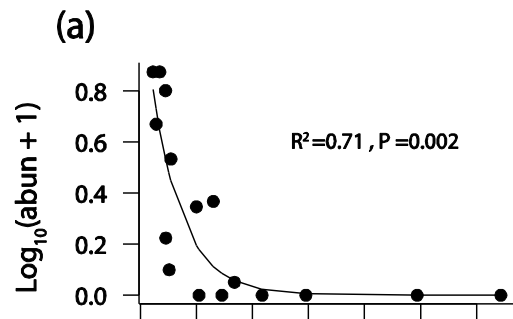
Appendix 6.3.

Mean \pm SE macroinvertebrate drift (ind. 24hr⁻¹) recorded from the control and treatment channels for: (i) date A (10-11 July); (ii) date B (18-19 July); and (iii) date C (26-27 July).

Taxa	Control channels (ind 24hr ⁻¹)			Treatment channels (ind 24hr ⁻¹)		
	Date A	Date B	Date C	Date A	Date B	Date C
Ephemeroptera						
<i>Habroleptoides</i> sp.					0.3 (0.1)	
<i>Baetis alpinus</i>	14.5 (2.6)	11.5 (1.3)	13.0 (1.2)	18.0 (1.8)	16.3 (0.7)	19.5 (2.1)
<i>Baetis gemellus</i>	4.3 (1.0)	1.8 (0.2)	4.0 (0.8)	8.0 (0.8)	4.0 (0.2)	6.0 (0.8)
<i>Baetis muticus</i>	0.3 (0.1)	1.0 (0.2)		2.5 (0.3)	1.5 (0.1)	0.0 (0.0)
<i>Ecdynourus</i> sp.						0.3 (0.1)
Plecoptera						
<i>Protonemura</i> sp.	1.3 (0.2)	2.8 (0.2)	1.3 (0.2)	2.0 (0.5)	2.3 (0.1)	1.5 (0.3)
Trichoptera						
<i>Micrasema</i> sp.	1.8 (0.4)	2.0 (0.5)	2.0 (0.5)	3.3 (0.4)	4.3 (0.2)	2.8 (0.8)
<i>Agapetus fuscipies</i>				0.5 (0.1)	0.3 (0.1)	
<i>Plectrocnemia</i> sp.				0.3 (0.1)	0.3 (0.1)	
<i>Rhyacophila intermedia</i>		0.5 (0.1)	0.5 (0.1)	0.8 (0.1)	0.8 (0.1)	1.8 (0.1)
Coleoptera						
<i>Elmis</i> sp.	0.8 (0.1)	2.3 (0.4)	0.5 (0.3)	0.8 (0.2)	2.5 (0.5)	0.5 (0.3)
<i>Elodes</i> sp.		0.3 (0.1)			0.3 (0.1)	
<i>Esolus</i> sp.	0.3 (0.1)			0.3 (0.1)	1.0 (0.2)	0.3 (0.1)
Diptera						
Ceratopogonidae				0.3 (0.1)		0.3 (0.1)
Diamesinae	1.5 (0.4)	3.8 (1.2)		2.5 (0.1)	1.3 (0.1)	0.3 (0.1)
<i>Dixa</i> sp.		0.3 (0.1)				0.5 (0.1)
Limoniidae	0.3 (0.1)					
Orthoclaadiinae	0.8 (0.4)	0.8 (0.2)	2.8 (0.6)	3.3 (0.6)	1.8 (0.3)	3.5 (0.6)
<i>Prosimulium</i> sp.				0.0 (0.0)	0.3 (0.1)	
Psychodidae				0.5 (0.3)	0.3 (0.1)	
<i>Simulium</i> sp.		2.5 (0.3)	3.8 (0.7)	0.0 (0.0)	3.0 (0.2)	4.5 (0.9)
Tanypodiinae				0.3 (0.1)	0.3 (0.1)	0.3 (0.1)
Thaumaleidae				0.3 (0.1)		
Tipulidae		0.3 (0.1)				
Misc taxa						
Oligochaeta						0.3 (0.1)
<i>Polycelis</i> sp.			1.5 (0.5)	0.5 (0.3)		0.3 (0.5)

Appendix 8.1

GAM models based on glacier cover in the catchment and (a) *P. grandis* (b) *Simulium* spp. (c) *Leuctra* spp. (d) *D. Latitarsis* gr., and *Rhithrogena* spp.



Available online at www.sciencedirect.com

ScienceDirect

journal homepage: www.elsevier.com/locate/envsci

Alpine aquatic ecosystem conservation policy in a changing climate

K. Khamis ^a, D.M. Hannah ^a, M. Hill Clarvis ^{b,*}, L.E. Brown ^c,
E. Castella ^d, A.M. Milner ^{a,e}

^a School of Geography, Earth and Environmental Science, University of Birmingham, Birmingham B15 2TT, UK

^b Research Group on Climate Change and Climate Impacts, University of Geneva, CH-1227 Geneva, Switzerland

^c School of Geography/water@leeds, University of Leeds, Woodhouse Lane, Leeds LS2 9JT, UK

^d Institut F.A. Forel and Institute for Environmental Sciences, University of Geneva, CH-1227 Geneva, Switzerland

^e Institute of Arctic Biology, University of Alaska, Fairbanks, AK 99775, USA

article info

Article history:

Received 26 June 2013

Received in revised form

7 October 2013

Accepted 7 October 2013

Available online xxx

Keywords:

Adaptation

Climate change

Conservation

Headwaters

Pyrenees

European Alps

Glaciers, River, Stream

abstract

Freshwater ecosystems are often of high conservation value, yet many have been degraded significantly by direct anthropogenic impacts and are further threatened by global environmental change. Traditionally, conservation science and policy has promoted principles based on preservation and restoration paradigms, which are linked to assumptions of stationarity and uniformitarianism. Adaptation requires new approaches based on flexibility, iterativity, non-linearity, and redundancy. Many high alpine river networks represent near natural, pristine river systems and important biodiversity 'hotspots' of European freshwater fauna. However, there remains a lack of guidance on alpine river conservation strategies under a changing climate at EU, regional and local levels. A critical evaluation of current conservation and adaptation principles and governance frameworks was undertaken with relation to predicted climate change impacts on freshwater ecosystems. Case studies are presented from two alpine zones in mainland Europe (the Pyrenees and the Swiss Alps). The complexity of climate change impacts on hydrological regimes, habitat and biota from both case study regions suggests that current legislative and policy mechanisms, which frame conservation approaches, need to be realigned. In particular, a shift in focus from species-centric approaches to more holistic ecosystem functioning conservation is proposed. A methodological approach is set out that may help conservationists and resource managers to both prioritise their efforts, and better predict future habitat and biotic responses to set ecological baseline conditions. Due to the complexity and limited potential for preventative intervention in these systems, conservation strategies should focus on: (i) the maintenance and enhancement of connectivity within and between alpine river basins and (ii) the control and reduction of additional anthropogenic stressors.

2013 Elsevier Ltd. All rights reserved.

1. Introduction

The physicochemical template of freshwater ecosystems is highly diverse, both between (e.g. wetlands, rivers, lakes) and

within biotypes (Brown et al., 2003), supporting habitats and species of high conservation value (Wilcox and Thurow, 2006). However, many of these systems, particularly in lowland or populated areas, have been significantly degraded by global

* Corresponding author. Tel.: +41 0 76 227 2468.

E-mail address: Margot.Hill@unige.ch (M.H. Clarvis).

1462-9011/\$ – see front matter # 2013 Elsevier Ltd. All rights reserved.

<http://dx.doi.org/10.1016/j.envsci.2013.10.004>